LATE PLEISTOCENE GLACIAL AND ENVIRONMENTAL HISTORY OF THE SKAGIT VALLEY, WASHINGTON AND BRITISH COLUMBIA

by

Jon L. Riedel

B.Sc. (Geography and Biology), University of Wisconsin – LaCrosse, 1982

M.Sc. (Geography), University of Wisconsin – Madison, 1987

Licensed Geologist, State of Washington, since 1998

THESIS SUBMITTED IN PARTIAL FULFILLMENT OF
THE REQUIREMENTS FOR THE DEGREE OF

DOCTOR OF PHILOSOPHY

In the Department of
Earth Sciences

© Jon L. Riedel 2007

SIMON FRASER UNIVERSITY

Summer 2007

All rights reserved. This work may not be
reproduced in whole or in part, by photocopy
or other means, without permission of the author.

Approval

Name:	**Jon L. Riedel**
Degree:	**Doctor of Philosophy**
Title of Thesis:	**Late Pleistocene Glacial and Environmental History of Skagit Valley, Washington and British Columbia**

Examining Committee:

Chair: **Dr. John J. Clague**
Senior Supervisor

Dr. Brent C. Ward
Supervisor

Dr. Ralph A. Haugerud
Supervisor

Dr. Rolph Mathewes
Internal Examiner

Dr. Douglas Clark
External Examiner

Date Defended/Approved: June 12, 2007

SFU SIMON FRASER UNIVERSITY
LIBRARY

Declaration of Partial Copyright Licence

The author, whose copyright is declared on the title page of this work, has granted to Simon Fraser University the right to lend this thesis, project or extended essay to users of the Simon Fraser University Library, and to make partial or single copies only for such users or in response to a request from the library of any other university, or other educational institution, on its own behalf or for one of its users.

The author has further granted permission to Simon Fraser University to keep or make a digital copy for use in its circulating collection (currently available to the public at the "Institutional Repository" link of the SFU Library website <www.lib.sfu.ca> at: <http://ir.lib.sfu.ca/handle/1892/112>) and, without changing the content, to translate the thesis/project or extended essays, if technically possible, to any medium or format for the purpose of preservation of the digital work.

The author has further agreed that permission for multiple copying of this work for scholarly purposes may be granted by either the author or the Dean of Graduate Studies.

It is understood that copying or publication of this work for financial gain shall not be allowed without the author's written permission.

Permission for public performance, or limited permission for private scholarly use, of any multimedia materials forming part of this work, may have been granted by the author. This information may be found on the separately catalogued multimedia material and in the signed Partial Copyright Licence.

While licensing SFU to permit the above uses, the author retains copyright in the thesis, project or extended essays, including the right to change the work for subsequent purposes, including editing and publishing the work in whole or in part, and licensing other parties, as the author may desire.

The original Partial Copyright Licence attesting to these terms, and signed by this author, may be found in the original bound copy of this work, retained in the Simon Fraser University Archive.

Simon Fraser University Library
Burnaby, BC, Canada

Revised: Summer 2007

Abstract

Drainage patterns established in the Tertiary in the North Cascades were reorganized to accommodate southern drainage of Cordilleran Ice Sheet meltwater. Repeated continental glaciation rendered the Skagit an interconnected valley, with meltwater routes opening it to the Fraser and Okanogan watersheds, and linking it to a drainage system around the east margin of the Puget lobe of the ice sheet.

Alpine glaciers from two major tributaries blocked Skagit valley during the late Wisconsin Evans Creek stade, creating glacial lakes Concrete and Skymo. Organic material from lake sediments provides the first radiometric constraint on the beginning of the Evans Creek stade in the Cascades about 25,040 ^{14}C yr BP. Sediments and macrofossils at the Cedar Grove section define two advances of Baker alpine glaciers during this stade, separated by warmer and wetter climate at 20,310 ^{14}C yr BP. During colder parts of the Evans Creek stade macrofossils indicate treeline was as much as 1200 ± 150 m lower than present, which corresponds to a mean July temperature depression of approximately 7 ± 1°C. Glacier equilibrium line altitudes (ELA) during the cold periods were depressed 730-970 m below the modern glaciation threshold.

Skagit valley alpine glaciers advanced several times to positions 5-10 km below valley heads between 12, 200 and 9,975 ^{14}C yr BP. ELA depression during these advances vary from 340 ± 100 m to 590 ±75 m, with greater depression in maritime western tributaries. Skagit ELA depression values are about 200 m less than reported for the southern North Cascades during the Sumas stade. The effect of the Cordilleran Ice Sheet on precipitation likely caused ELAs to be higher in the Skagit valley than in the southern North Cascades.

Keywords: glaciers; late Pleistocene; geochronology; equilibrium line altitude; North Cascades; Skagit valley; moraines; macrofossils

Dedication

I dedicate this thesis to the many Riedels and Ploens that made it possible. In particular, it is for my mother, Bernice Ploen Riedel, whose journey through life has been far more difficult than mine. Through the great depression, World War II, and a long illness, she has taught me lessons of love, humility, and perseverance.

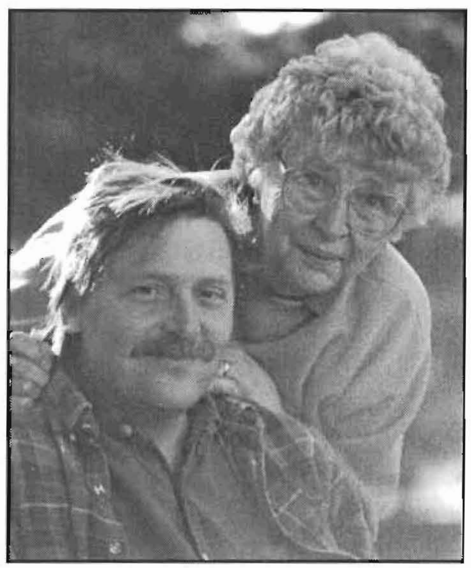

Acknowledgements

Few people reach their goals without the support and guidance of others. This research would not have been possible without the patient, informed supervision of my senior advisor, Dr. John J. Clague. His encouragement led me to attempt and stick with this project while continuing with a full-time job and raising a family. Juggling these three large, slippery balls would not have been possible without the support of my partner and my employer. My wife, Sarah Welch, supported this effort from the very beginning and provided assistance with editing and preparation of the final document. I extend thanks to Bruce Freet, Jack Oelfke, and Bill Paleck for allowing me to maintain my career with the National Park Service while in a Ph.D. program.

I also want to thank the other members of my supervisory committee, Dr. Brent Ward of Simon Fraser University and Dr. Ralph Haugerud of the U.S. Geological Survey. I am fortunate to have been associated with such excellent geologists and people. Many other geologists contributed to the success of this project, including Dr. Rowland Tabor, Dr. Kevin Scott, Dr. Johannes Koch, Dr. John Stone, and Dave Tucker. I am grateful to Dr. Linda Brubaker, Alecia Spooner, and Alice Telka for identification of macrofossils. Alice, in particular, has done a tremendous amount of work in support of this research.

I acknowledge the staff of the Department of Earth Sciences and the Office of Graduate Studies for their support and patience. In particular, I want to thank Tarja Vaisanen, Glenda Pauls, Wendy Bourke, and Matt Plotnikoff. Field assistance was provided by friends, family, and colleagues, including my brother Tom Riedel, brother-in-law Dan Goska, Jeanna Wenger, Mike Larrabee, Stephen Dorsch, Rob Burrows, Dan Heidal, and Bob Mierendorf. Mike, Jeannie, and Steve also patiently assisted me in the use of geographic information systems.

Funding for this project came from several sources, including Simon Fraser University, the Natural Sciences Engineering and Research Council of Canada, the Skagit Environmental Endowment Commission, and the U.S. National Park Service.

Table of Contents

List of Figures

List of Tables

Chapter 1: Introduction

My motivation for choosing this research project is two-fold. First, as our species continues to alter the very foundations of life on this planet, we need to know how Earth's climate system functions. Detailed studies of climate change in sensitive mountain systems are an important component of global climate change data sets. Second, as the human population increases by a quarter-million people each day, development encroaches upon hazardous mountain environments. Rapid population growth in Skagit County, Washington, underscores the need to understand the surficial geology of this rugged mountain landscape. Bringing these motivations together is the realization that very important geologic information about past climate change is being lost to development and erosion.

Mountain regions are important for the study of climate change because they contain glaciers, steep environmental gradients, and diverse plant and animal habitats. Alpine glaciers provide key information on climate change because of their short lag times, steep balance gradients, and distribution along strong climatic gradients (Porter, 1977; Clark and Bartlein, 1995; Clague et al., 1997; Hodge et al., 1997). Widespread glacial and periglacial landforms and deposits also influence geologic hazards and groundwater availability.

The North Cascade Range is distinct from the Cascades south of Snoqualmie Pass for several reasons, not the least of which are its greater height and breadth (McKee, 1972). These features impart strong climate gradients controlled by elevation and distance from the Pacific Ocean. Rapid changes in temperature and precipitation have affected the extent of glaciation and the pattern of vegetation throughout the Quaternary Period. Spatial diversity in glacial and environmental responses to climate changes provides an opportunity to understand regional and global patterns of change during the late Pleistocene. These factors, along with a paucity of Quaternary research in the North Cascades, make Skagit valley an ideal place to study climate change and landscape evolution by analyzing glacial landforms, sediments, and macrofossils.

Research objectives

My overarching goal for this project was to develop a detailed history of late Pleistocene glaciation in the Skagit valley, an 8000 km^2 watershed in northern Washington and southernmost British Columbia. I focused on the Fraser Glaciation, which spans the period 30,000 - 10,000 radiocarbon years ago (approximately coincident with marine oxygen isotope stage 2).

Unusual drainage features and repeated glaciation of Skagit valley led me to study the influence of proglacial drainage of the Cordilleran Ice Sheet on stream patterns and geomorphology. Dr. Haugerud and I began this research in the mid 1990s. My understanding of the Quaternary geology and Ralph's knowledge of the regional geology led us to examine the geomorphologic evolution of the Skagit valley. High-resolution digital elevation models, network analysis, and a conceptual model allowed me to achieve several specific objectives (Chapter 2):

- assess how the Cordilleran Ice Sheet affected the development of the region's drainage patterns and geomorphology at the local scale,
- determine if Skagit River is an antecedent stream superimposed across the topography and geologic structure of the North Cascade Range, and
- link proglacial ice sheet drainage through the North Cascades via Skagit River to other regional Pleistocene drainage systems in southern British Columbia and Puget Lowland.

Evidence collected in this study shows that glacial lakes Skymo and Concrete formed behind ice and drift dams from two tributary alpine glaciers on the floor of Skagit valley during the Evans Creek stade of the Fraser Glaciation. The lake sediments span more than 8,000 years, and contain abundant macrofossils identified by Alice Telka and Alecia Spooner. These data helped reach three research objectives (Chapters 3 and 4):

- develop a detailed radiometric chronology of the Evans Creek stade,
- identify Evans Creek stade plant and insect communities, and
- analyze changes in macrofossil abundance and diversity to understand patterns of climate variability during the Evans Creek stade.

I used the distribution of glacial and lacustrine sediments, glacial landforms, and ice physics to reconstruct two alpine glacier systems that developed at the beginning of the Fraser Glaciation, and five smaller alpine glaciers that formed at the end of this glaciation. I was able to obtain limited age control on four of the terminal moraines deposited during the Sumas stade using tephra, radiocarbon, and beryllium 10 surface exposure ages determined by Dr. John Stone at the University of Washington. Despite the limited age-control, I was able to address several specific objectives (Chapter 5):

- examine the efficacy of two different approaches for estimating glacier equilibrium line altitude (ELA),
- measure ELA depression from the modern glaciation threshold for three alpine glacier advances during the Fraser Glaciation, and
- assess regional patterns of ELA depression to understand the magnitude and spatial and temporal variability of climate change during the Fraser Glaciation.

Thesis overview

The thesis comprises four main chapters. Chapter 2 discusses the geologic evolution of the Skagit River watershed. Skagit valley contains a number of unusual drainage elements, including long, interconnected valleys, barbed tributaries, under-fit streams, and low elevation, mid-valley divides. Quantitative analysis of connectivity between valleys draining through mountain divides, aerial photographs, and a field-verified, process-form model were used to assess the impact of continental glaciation on the drainage and geomorphology of the North Cascades. I present evidence that Skagit River is not an antecedent stream superimposed across the geologic and structural grain of the North Cascades (Waitt, 1977). The south-flowing Cordilleran Ice Sheet repeatedly blocked northward drainage in the region and ultimately breached a major regional drainage divide at Skagit Gorge. This event led to the capture of upper Skagit River, which formerly drained north to Fraser River, by lower Skagit River. Elimination of the Skagit Gorge divide doubled the size of the Skagit watershed and created a meltwater corridor leading from south-central British Columbia to Puget Sound and the Pacific Ocean (Riedel et al., 2007).

Chapter 3 presents the first detailed chronology of the Evans Creek stade in the Cascades. I present evidence from the Cedar Grove site along Skagit River that the Evans Creek stade began about 25,040 ^{14}C yr BP, and from the Big Boy site 5 km upstream that it ended about 16,400 ^{14}C yr BP.

Chapter 4 describes plant and animal macrofossils recovered from Evans Creek stade deposits at the Big Boy section on Skagit River and the Skymo section on Ross Lake. Rich assemblages from both sites provide evidence that Skagit valley contained a diverse mixture of lowland and alpine species. Subalpine forest grew along the shores of glacial Lake Skymo in upper Skagit valley, providing evidence that treeline was as much as 1200 ± 150 m lower than present during the Evans Creek stade. Changes in macrofossil abundance and diversity after 20,770 ^{14}C yr BP and after 17,570 ^{14}C yr BP indicate that climate during the Evans Creek stade varied between cold-dry and cold-moist, confirming millennial-scale climate variability during the Fraser Glaciation (Grigg and Whitlock, 2002).

Chapter 5 investigates the magnitude of climate change during the Evans Creek and Sumas stades of the Fraser Glaciation by determining equilibrium line altitudes of glaciers. I compared reconstructed ELA values to modern glaciation threshold to determine ELA depression. I examined spatial patterns of climate change by comparing ELA depression along east-west and north-south climate gradients. These data provide evidence that the Cordilleran Ice Sheet exerted a strong influence on local climate in Skagit valley during the Sumas stade, keeping glacial ELAs several hundred metres higher than in the southern North Cascades (Porter et al., 1983).

The final chapter is a brief synthesis of this research. It includes discussion of results in the context of the development of our understanding of the last ice age and recommendations for future research.

Chapter 2: Geomorphology of a Cordilleran ice sheet drainage network through breached divides in the North Cascades mountains of Washington and British Columbia

Published under the authorship of Riedel, J.L.,
Haugerud, R.A., and Clague, J.J., 2007. Geomorphology, in press.

Abstract

The Skagit River valley in northern Washington and southern British Columbia contains long interconnected valleys, barbed tributaries, underfit streams, and low-elevation mid-valley divides. Quantitative measures of connectivity between valleys draining through breached mountain divides, aerial photographs, and a field-verified, process-form model were used to assess the impact of continental glaciation on the drainage pattern and geomorphology of the watershed. Structural control on drainage patterns and intense, repeated continental glaciation rendered the Skagit an interconnected valley, with meltwater routes connecting it to the Fraser and Okanagan watersheds. Divide elimination by drainage of large proglacial lakes led to several hundred metres of erosion at 10 breached divides. Other geomorphic effects of recurrent continental glaciation include the bisection of a major mountain valley, divide migration of as much as 50 km, erosion of canyons 15-30 km downstream of breached divides, and deposition of exceptionally large alluvial fans at canyon mouths. Drainage patterns established in the Tertiary were reorganized to accommodate southern drainage of glacial meltwater trapped in mountain valleys at the southern margin of the Cordilleran Ice Sheet. The Skagit basin is now a regional focus for drainage to Puget Sound from the northernmost North Cascades and parts of southern interior British Columbia. The key to establishing this system was the elimination of a regional divide in what is now Skagit Gorge, which resulted in the capture of the upper Skagit valley by the lower Skagit River. Patterns of drainage modification caused by continental glaciation in the Skagit basin are similar to those in other mountain areas. The Skagit's interconnected valleys are similar to the great through-valleys of Scotland, transmountain valleys of British Columbia, and ice portals of Scandinavia.

Keywords: Glaciation; Cordilleran ice sheet; drainage patterns; geomorphology

Introduction

For more than a century, geologists working on several continents have recognized the impact of glaciation on the development of drainage networks. Willis (1888), Suess (1888), and Penck (1905) first suggested that glacial erosion breached divides and rearranged drainage patterns. Subsequent work in mountainous regions has focused on divide elimination by glacial ice or meltwater erosion from alpine glaciers and continental ice sheets.

Alpine glaciers make minor modifications to drainage patterns through the processes of cirque headwall migration and excavation of ice sheds between adjacent valleys (Linton, 1967; Waitt, 1975). Processes that lead to divide breaching include abrasion, plucking, and exfoliation of bedrock associated with cirque and trough formation.

Mountain ice sheets have broadened and deepened passes and, in some cases, linked two valleys that were initially separated by a high divide (Flint, 1971, p. 141). Such interconnected valleys have been referred to as trans-range valleys in British Columbia (Kerr, 1936), through-valleys in Scotland (Dury, 1953), and ice portals in Scandinavia (Suess, 1888). They formed by divide elimination associated primarily with drainage of proglacial lakes (Dury, 1953; Mathews, 1968). Drainage reversals caused by proglacial lake drainage took place frequently during ice sheet glaciation of southern British Columbia (Fulton, 1969; Clague, 1981; Mathews, 1991) and northern Washington (Waitt and Thorson, 1983).

The objectives of this chapter are to document proglacial drainage of the Cordilleran Ice Sheet in the North Cascades in Washington and British Columbia, and to assess the impact of this process on the area's geomorphology and drainage patterns at local and regional scales. This contribution provides a framework for understanding the pattern of retreat of the Cordilleran Ice Sheet, important new data for reconstructing the hydrology of the ice sheet, and a detailed geomorphic model to apply to ice sheet drainage in other mountainous regions.

My study focuses on the Skagit River watershed (Figure 2-1) for several reasons. First, the area has three major hydrologic divides that separate flow into the Fraser, Columbia, and Puget Sound watersheds. A regional divide trending west to east across the range is a barrier to southward expansion of the Cordilleran Ice Sheet and meltwater drainage (Figure 2-2). Second, this area has been repeatedly glaciated by the Cordilleran Ice Sheet, which flowed into the region from the north, up several major valleys. The thick, temperate, fast-moving ice sheet maintained high water and ice discharges capable of producing considerable geomorphic change (Booth, 1987). Third, drainage patterns in the area have many peculiar features, including long interconnected valleys, breached hydrologic divides, reversed dendritic segments, underfit streams, barbed tributaries, bisected valleys, and low-elevation mid-valley divides occupied by lakes and wetlands. Formation of these features has been the subject of debate in the literature. Fourth, Skagit River is the only stream that cuts across the structure and topography of the North Cascades (Figures 2-1 and 2-2).

Pre-glacial drainage patterns

The drainage evolution of the North Cascades reflects several major elements of the region's geologic history (Tabor et al., 1989; Haugerud et al., 1994; Tabor and Haugerud, 1999), including (i) Late Cretaceous-earliest Tertiary orogeny with high-grade regional metamorphism, (ii) Eocene strike-slip faulting, basin development, and magmatism, (iii) Oligocene to recent construction of the Cascade Magmatic Arc, and (iv) Pleistocene glaciation. Primary stream networks have dendritic, trellis, radial, and rectangular drainage patterns (Figure 2-2), whereas at a local scale, first- and second-order streams flowing down steep valley walls display a pervasive parallel pattern (Zernitz, 1932). Dendritic drainage patterns are generally thought to form on gentle regional slopes (Zernitz, 1932), and several large, north-draining dendritic networks possibly developed prior to rapid uplift of the region in the late Miocene.

Rocks comprising the Skagit crest and parts of the North Cascades and Pacific crests were at depths of up to 30 km during Late Cretaceous and earliest Tertiary time, and record subsequent uplift of these areas (Tabor et al., 1989). Orogeny included strong northwest-southeast elongation and large-magnitude strike-slip movement on northwest-trending faults. Most third-order and higher subsequent streams follow this regional trend (Figure 2-1), including Cascade River (Entiat Fault), Granite Creek (Ross Lake Fault Zone), Goodell Creek, Big Beaver Creek, and upper Lost River/East Fork Pasayten River.

Eocene extension led to north-northwest-trending, right-lateral strike-slip faulting, basin development, local uplift, and volcanism. Radial stream patterns were established in the Eocene by volcanoes over the Golden Horn Batholith (Figure 2-1). Basins formed in western Washington during the Eocene and were filled with the Chuckanut, Chumstick, and Swauk formations, which include sediment derived from the Omineca Belt several hundred kilometres to the northeast

(Johnson, 1984). This evidence indicates that there was no regional north-south Cascade divide similar to the Pacific crest in the Eocene.

Recent thermochronometric (U-Th/He) research has identified two major periods of regional uplift and exhumation in the North Cascades, one between 45 and 36 Ma and a second between 11 and 2 Ma, with uplift locally continuing to the present (Reiners et al., 2002). Cascade arc volcanism and associated deformation likely had several lasting effects on North Cascades drainage. Regional uplift on a north-south axis initiated formation of the Pacific crest divide by 11 Ma ago. Minor arc-parallel extension established faults of probable early Miocene age that extend in a northeast-southwest direction through the Skagit watershed. The faults control the trend of several large valleys, including upper Skagit valley between Sumallo River and Klesilkwa Creek, upper Lightning Creek in Manning Park, and possibly Skagit Gorge (Figures 2-1 and 2-2). Cascade arc volcanism and uplift locally created radial drainage and may have contributed to the development of the North Cascades crest divide over the crystalline core of the range. Elements of radial drainage associated with centers of Cascade arc volcanism include the upper Nooksack, Chilliwack, and Little Beaver valleys (Figures 2-1 and 2-2).

The North Cascades and Pacific crests were established before the time Columbia River basalt flows drowned the mouths of several east-draining North Cascades valleys, including Methow valley (Waters, 1939; Barksdale, 1941). The basalts were deposited over broad erosion surfaces of Miocene age on the western and southern margins of the Columbia and interior British Columbia plateaus (Waters, 1939; Mathews, 1964). Similar erosion surfaces that slope to the north have been described in the upper Skagit valley (Mathews, 1968; Haugerud, 1985).

The Skagit drainage patterns developed in a temperate, wet climate. Annual precipitation currently exceeds 4 m in western parts of the basin. Streams and glaciers have deeply incised valleys, creating local relief of up to 2500 m. Higher precipitation on the west slope of the North Cascades and lower base levels of west-draining streams favour growth of west-flowing drainage networks and easterly migration of drainage divides (Mathews, 1968).

Resistant bedrock exposed by rapid uplift and exhumation, together with complex geologic structures, have created multiple, modern drainage divides (Figure 2-2). Primary regional divides include the Pacific crest (see C-C' in Figure 2-2) and what I refer to informally as the Skagit crest (B-B'). A third regional divide, the North Cascades crest (A-A'), trends west to east through the region and is of particular importance in this study because it separates south-draining Skagit and Methow valleys from north-flowing Chilliwack, Silverhope, and Pasayten valleys.

Continental glaciers originating in British Columbia inundated the Skagit region from the north several times during the Pleistocene (Waitt and Thorson, 1983; Clague, 1989). Deposits in Puget Lowland to the west indicate that the area was covered by continental ice sheets at least six times in the middle to late Pleistocene (Easterbrook et al., 1988; Booth et al., 2004). Tipper (1971), Waitt and Thorson (1983), Ryder (1989), and others have noted that ice sheets formed in British Columbia repeatedly through the Pleistocene. Ryder (1989) reported two potential continental glaciations at higher elevations near Cathedral Peaks in the British Columbia-Washington boundary area (Figure 2-1). The effects of erosion during multiple ice sheet glaciations are evident in many mountain valleys and passes in the North Cascades, particularly those that trend north-south, parallel to regional flow of the ice sheet. Examples include the broad upper Skagit and lower Pasayten valleys. Most recently, the Skagit River watershed was inundated by the south-flowing Cordilleran Ice Sheet during Vashon stade of the Fraser Glaciation, which reached its climax about 14,500 ^{14}C yr BP (Armstrong et al., 1965; Porter and Swanson, 1998).

Methods

I used two approaches to evaluate the effects of the Cordilleran Ice Sheet on development of the drainage network in the North Cascades. I applied Haynes' (1977) method for assessing glacial drainage pattern modification, and used a field-verified, process-form model to identify and link geological and morphological features created by drainage of proglacial lakes dammed by the ice sheet.

Haynes (1977) applied graph theory developed by Kansky (1963) for transportation networks to quantitatively evaluate modification of drainage patterns. Modification is referenced to connectivity between large mountain valleys, and is defined by α and β values:

$$\alpha = \frac{E - V + G}{2V-5} \times 100\% \qquad (1)$$

where V = number of stream junctions (nodes), E = number of stream segments (links), and G = number of separate subbasins, and

$$\beta = \frac{E}{V} \qquad (2)$$

Alpha and beta values are determined by marking and counting links and nodes on a drainage network map (Figure 2-3). As noted by Haynes (1977), a perfectly dendritic drainage network has an α value of 0 and a β value of < 1. In applying this technique, I define stream segments to include valleys through breached divides that have clearly been modified by meltwater erosion, resulting in divide lowering and migration. Therefore, the focus is on regional-scale drainage modifications and connectivity between 3rd order and larger streams, not minor local changes. Calculating α and β values for the upper Skagit area provides an independent, quantitative assessment of glacial drainage impacts and a comparison of the degree of drainage modification in the Skagit to that in other areas (Table 2-1).

My primary method for identifying effects of the Cordilleran Ice Sheet on the evolution of the Skagit drainage network is a conceptual process-form model initially developed by Riedel and Haugerud (1994) and presented in a more detailed form in Figure 2-4. The model is based on three key aspects of the geology and geologic history of the region: (i) regional drainage to the north, toward the source of the Cordilleran Ice Sheet; (ii) ice dams formed by the ice sheet in these valleys; and (iii) proglacial lakes deep enough to overtop mountain divides.

Abundant geomorphic evidence verifies these features of the process-form model. Waitt and Thorson (1983) and Booth (1987) have provided the most detailed reconstructions of the Cordilleran Ice Sheet in the upper Skagit River basin. They estimate that ice surface elevations at the last glacial maximum were 2000-2500 m. Most passes in the upper Skagit watershed are lower than 1500 m in elevation and thus could be crossed by proglacial water confined in steep mountain valleys. Mathews (1968) and Waitt (1977) suggested that the ice sheet flowed into the upper Skagit valley from the north and northeast during the Fraser Glaciation. North-flowing streams were blocked as the ice advanced, and large proglacial lakes developed in the Chilliwack, Silverhope, Similkameen/Pasayten, and Ashnola valleys. The ice sheet also blocked drainage in these valleys as it downwasted and retreated to the north during deglaciation. Proglacial lake deposits have also been recognized throughout southern British Columbia (Mathews, 1944; Armstrong and Tipper, 1948; Fulton, 1969; Tipper, 1971; Eyles and Clague, 1991; Goff, 1993; Ward and Thomson, 2004) and in northern Washington (Bretz, 1913; Mackin, 1941; Thorson, 1980; Waitt and Thorson, 1983).

I used the process-form model to guide my search for depositional and erosional landforms within 13,000 km^2 of mountainous terrain along the International Boundary between Mt. Baker on the west and the Okanagan Highlands on the east (Figure 2-1). Shaded relief DEMs, aerial photographs, large-scale topographic maps, geologic maps, field surveys, and well logs were used to identify features formed by glacial meltwater drainage. A limitation of this approach is that erosion has obliterated late Tertiary and all but the most recent Pleistocene deposits in these valleys. Therefore, my analysis is based largely on events and landforms dating to the end of the last ice sheet glaciation.

Divide migration was measured on 1:24,000-scale U.S. and 1:20,000-scale Canadian topographic maps from the location of a breached divide along the valley floor to the location of the modern divide (Table 2-2). Divide elevation change was measured from the modern divide to the floor of the lowest nearby mountain pass that has not been breached by meltwater but has similar bedrock and aspect (Figure 2-5). In the case of the Skagit River, divide change was measured as the difference in elevation between Jasper Pass and Sunshine valley. Values for divide erosion should be considered maximum, first-order approximations because of the uncertainty of original, preglaciation pass elevations. They include the combined effects of ice and meltwater erosion.

Results

Drainage connectivity

I identified 53 links and 49 nodes between the Skagit and adjacent watersheds (Figure 2-3), yielding an α value of 5.7 and a β value of 1.1 (Table 2-1). Upper Skagit valley is better connected to adjacent major valleys than lower Skagit valley because it has seven links to the Fraser and Okanagan valleys. Links with the Fraser include Chilliwack Pass, Klesilkwa Pass, and the Nicolum valley (Figure 2-2). Links with the Okanagan valley include Snass and Skaist passes, Lightning Lakes, and Holman Pass. Several divides are on valley floors at elevations of a few hundred metres above sea level and are the primary links between large interior valleys (Figure 2-2; Table 2-2). Baker and Sauk valleys, which are lower Skagit tributaries, each have one breached divide. All other lower Skagit tributaries head in high cirques and passes that were not breached by proglacial lake outlet erosion.

Geomorphic evidence of proglacial lake drainage

Geomorphic evidence of meltwater drainage across divides in the upper Skagit valley is presented from west to east, along the North Cascades, Pacific, and Skagit crests. A deep, narrow notch cuts across Chilliwack Pass, which is 160 m lower than adjacent passes on the divide between Chilliwack and Baker valleys (Figure 2-2). The notch is bedrock-walled, and its floor is partially covered by talus. Chilliwack Pass was a relatively minor route for proglacial drainage, and divide migration at the pass is only 800 m (Table 2-1). To the south toward Skagit valley, Pass Creek flows in a deep canyon with a large alluvial fan at its junction with Baker valley. Where the two streams meet, the larger Baker River is forced to the opposite side of the valley and has a braided pattern.

Two passes on the Chilliwack-Silverhope divide bear evidence of proglacial drainage modification (Figures 2-2, 2-6, and 2-7). Post Creek drains into Chilliwack River through a pronounced V-shaped valley, whereas Hicks Creek to the east has a U-shaped cross-section typical of glacial valleys. The modern divide between the two valleys, unlike adjacent passes located along ridges, is the bottom of a deep valley. Further, Post Creek heads at a knickpoint within this valley just east of Greendrop Lake. Divide migration toward Silverhope Creek and lengthening of Post Creek at the expense of Hicks Creek is 5.9 km. Erosion of the divide, estimated from the lowest pass to the south that was not breached, is 620 m (Table 2-2).

Two passes in upper Tulameen valley carried meltwater from proglacial lakes to the south into Skagit River (Figures 2-2, 2-6 and 2-7). Snass and Skaist creeks are deep canyons cut across the combined Pacific and North Cascades crests and show evidence of having been modified by water. Snass Pass, the lower of the two outlets, has an elevation of 1470 m asl, and the divide at the head of Skaist Creek is 1520 m asl.

The upper part of the Snass meltwater outlet is a narrow V-shaped canyon with a flat, gravel-covered floor. The canyon does not head in a cirque as do most other major valleys in the area, but rather opens into Tulameen valley as a narrow canyon. Divide migration from the present divide at Snass Pass to the former regional divide is ~ 4.5 km. East Snass Creek, the former valley head, cascades into the over-deepened, narrow canyon as a hanging valley. Divide lowering associated with proglacial lake drainage, measured from adjacent Punchbowl Pass, is 320 m. At its junction with Skagit valley, the outlet valley has gravel terraces 40 m above present river level that grade into a massive coarse gravel deposit known as Rhododendron Flats (Figure 2-7).

The valley of Skaist Creek has a similar geomorphology to that of Snass Creek, including a cirque-less valley head, a long canyon across a regional divide, and a large gravel deposit at its junction with Skagit valley at Cayuse Flats (Figure 2-7). Captain Grant Creek and other tributaries enter Skaist Creek at sharp angles and display a reversed dendritic drainage pattern. These streams once drained northward, but were captured and their flow reversed when divides were lowered an estimated 220 m (Table 2-2). The head of Skaist valley opens into Tulameen valley at an elevation of 1517 m asl and is a secondary outlet for drainage of the Tulameen's eastern tributaries. Meltwater erosion of the outlet has resulted in 7.6 km of northward divide migration and lengthening of Skaist Creek.

Two other drainage routes through breached divides cut across the Pacific crest farther south (Figures 2-2 and 2-6). The lowest of the breached divides between Similkameen and Skagit valleys is Lightning Lakes, which, at 1220 m asl, is 100 m lower than the Holman Pass and Hidden Lakes outlets (Table 2-2). Lightning Creek flows south through a breached former divide near the International Boundary, which I informally refer to as Hozomeen Pass (Figures 2-2, 2-5, and 2-8). This pass is a steep bedrock canyon, in contrast to a higher, ice-scoured pass directly to the east. Divide migration, from Hozomeen Pass to the modern low divide at Lightning Lakes, is 5 km.

Proglacial drainage from Similkameen valley to Skagit valley bisected Freezeout valley downstream of the breached divide at Hozomeen Pass (Figure 2-8). Upper Freezeout valley now drains south down Lightning Creek, and the former lower half of the valley containing Hozomeen Lake is beheaded. Prior to Pleistocene glaciation, Freezeout Creek drained west from the Pacific crest directly to Skagit valley. Other Skagit tributaries to the south were unaffected by Cordilleran Ice Sheet drainage but still follow this pattern (e.g., Three Fools, Devil's, and Ruby creeks; Figure 2-1).

Meltwater also cut a 200-m-deep canyon along Lightning Creek that ends in a large alluvial fan at Skagit River (Figures 2-8 and 2-9). The fan is at least 23 m thick at its apex and is composed mainly of large cobbles and small boulders. Rapid deposition of the fan forced Skagit River to the west side of the valley and temporarily dammed it. A large kettle lake indicates that the fan formed during one or more large floods that transported icebergs derived from the retreating Cordilleran Ice Sheet.

Meltwater flowed from proglacial lakes in Okanagan River tributaries via Lost River to Methow valley (Figures 2-2 and 2-10). It cut a steep bedrock canyon across the divide between the Pasayten (Okanagan) and Methow watersheds, leading to divide migration of 12 km (Table 2-2), which significantly changed the drainage pattern in this area. Drainage diversion produced a reversed dendritic pattern in the headwaters of Lost River, where a branch of the upper East Fork Pasayten River was captured by Methow River (Figure 2-10). Ptarmigan and Johnny creeks were once part of the north-flowing, dendritic, Pasayten River drainage network, but are now barbed tributaries of Lost River. Downstream of the breached divide, Lost River flows in a deep bedrock canyon that is much deeper than the valley of adjacent Robinson Creek. Lost River deposited a huge alluvial fan at its junction with Methow valley, forcing Methow River to the opposite valley wall. Based on well-log data, the fan is at least 50 m thick and is composed mainly of cobble gravel and boulders as large as 2 m diameter.

Holman Pass was a secondary outlet for a proglacial lake in Pasayten valley (Figures 2-2 and 2-6; Table 2-2). The outlet was probably active only during later stages of the Fraser Glaciation when ice advanced to block the West Fork Pasayten valley. Meltwater cut an impressive 30-km-long, V-shaped canyon down Canyon Creek to its junction with Skagit River.

Ashnola River is a tributary of Similkameen River east of Pasayten valley (Figure 2-2). Several lines of evidence indicate that water from a proglacial lake crossed Ashnola Pass and drained southeast down Lake Creek to the Methow and Columbia rivers. The North Cascades crest is breached at Ashnola Pass, and the headwaters of Lake Creek extend into Ashnola valley, with divide migration of 1.2 km and divide lowering of 260 m (Table 2-2). A long canyon extends from the outlet of Fawn Lake at Ashnola Pass through the breached divide to the mouth of the valley, where it ends in a large alluvial fan.

At all of the sites examined, breached, U-shaped, north-facing valleys are connected through breached divides to south-facing, V-shaped canyons. Modern divides at proglacial drainage outlets are located on valley floors and are marked by swamps or chains of lakes.

Geomorphic evidence indicates that upper Skagit valley and the Skagit crest were also affected by proglacial lake drainage. Six of the outlets described above lead into Skagit valley, and early Fraser Glaciation lake deposits have been identified in the upper part of the valley. Other geomorphic evidence includes barbed tributaries, reversed dendritic drainage patterns (Sumallo River and Klesilkwa Creek), a long canyon (Skagit Gorge), and thick gravel fills at the mouth of Skagit Gorge and the head of the Skagit River delta (Drost and Lombard, 1978). Skagit River tributaries in Skagit Gorge are deeply incised, and a series of bedrock benches extends from the mouths of Stetattle Creek to Ruby Creek (Figure 2-11). The benches are 300-400 m above the floor of Skagit valley at the upper end of the gorge. Striations and erratics indicate that the benches and the inner walls of the Skagit Gorge have been glaciated. From the Diablo Lake overlook, Skagit Gorge is clearly seen to be a narrow canyon cut into the bottom of a U-shaped valley. A 5-km-long bench on the south flank of Sourdough Mountain slopes 10-15° north-northeast (Figure 2-11), opposite the direction of flow of Skagit River. Stetattle and Thunder creeks are large tributaries that enter lower Skagit valley as deep, narrow canyons. Other tributaries, such as Goodell Creek, enter as U-shaped hanging valleys.

Most of the breached divides discussed above lead into the Skagit valley and, combined with the other geomorphic evidence, indicate that the former North Cascades crest was breached in Skagit Gorge. Divide lowering, estimated from nearby Jasper Pass (1270 m asl) to the modern low divide between the Fraser and Skagit valleys at Sunshine Valley, is 690 m (Table 2-2). Divide migration from the gorge to Sunshine valley is 50 km (Figure 2-7).

Discussion

Drainage connectivity

My research supports Haynes' (1977) findings that ice sheet glaciation breaches divides and modifies dendritic drainage patterns. A β value for the Skagit River basin of 1.1 indicates that multiple divides are breached, and the α value of 5.7 places the Skagit among the most altered drainage networks studied by Haynes (Table 2-1). The α value is less than reported for western Scotland and Greenland, but is higher than the value for the adjacent Coast Mountains.

There are four reasons for the relatively high Skagit α value. First, the Skagit basin experienced many ice sheet glaciations, each of which probably caused considerable landscape change. Second, north-draining valleys in the region were ideal sites for proglacial lakes to form during repeated advances of south-flowing ice sheets. The primary drainage route for the large, deep proglacial lakes that formed in these valleys was the Skagit River. Third, watersheds with mixed lithologies and strong structural control on drainage, such as the Skagit, are predisposed to higher alpha values because complex geology tends to inhibit development of dendritic drainage patterns. Structural control on the location of breached divides and interconnected valleys in the Skagit basin is strong, because nearly every breached divide is located near a late Cretaceous, Eocene, or mid-Tertiary fault (Figure 2-1). These faults were exploited by glaciers and streams, providing pathways that facilitated connection of the upper Skagit basin to adjacent valleys (Figure 2-1). Fourth, unlike the Coast Mountains of British Columbia, which have alpha values

<3 (Haynes, 1977) the North Cascades were not a source area for the Cordilleran Ice Sheet. Invasion of the Skagit basin by an allochthonous ice sheet dammed valleys, breached divides, and interrupted drainage. In contrast, Coast Mountains were source areas for the ice sheet and offered direct routes for ice and meltwater to the Pacific Ocean, and they retain more of their pre-glacial drainage patterns.

Depositional evidence

Proglacial lake deposits in tributary valleys and outwash fans at outlet canyon mouths confirm that a regional drainage system was operating at the end of the last glaciation. The depositional record of proglacial lakes is fragmentary and deposits have not been examined systematically, but the existence of these lakes during advance and retreat phases of the last glaciation has been confirmed in most large valleys in the region.

Saunders et al. (1987) presented evidence for damming of the lower Chilliwack valley during a resurgence of the Cordilleran Ice Sheet late in the Fraser Glaciation (Figures 2-2 and 2-6). Reported lake sediments deposited at elevations below the elevation of Chilliwack Pass, but confirm that the valley was dammed by the ice sheet. Divide lowering of 160 m and divide migration of 800 m at Chilliwack Pass, and the deep canyon and extensive fan at the mouth of Pass Creek, attest to the considerable geomorphic effect of meltwater draining across mountain divides.

Goff (1993) identified several levels of glacial Lake Silverhope between 60 and 1020 m asl in Silverhope valley (Figure 2-7). He also described a Gilbert-type delta with topset beds at 920 m asl in the middle of the valley that prograded to the south, toward Skagit valley. Goff (1993) linked the draining of this lake to a jökulhaup that deposited the Post Creek fan in Chilliwack valley to the west (Clague and Luternauer, 1982). The divide between Post and Hicks creeks is 530 m higher than Klesilkwa Pass, the lowest pass in the Silverhope watershed. For water to flow over Hicks Pass into Post Creek, Klesilkwa Pass must have been blocked by ice in Skagit valley. Goff (1993) suggested that a proglacial lake in Silverhope valley drained south via Klesilkwa Pass to Skagit River when the lake was at 760 m asl and lower. If correct, the lake depth at Klesilkwa Pass at this lake stage was about 180 m.

Holmes (1965) described late Fraser Glaciation glacial lake strand lines at 1310 m asl in lower Pasayten valley (Figures 2-2 and 2-6). Several passes in the Pasayten and adjacent watersheds are much lower than this (Table 2-2). Depending on the location of the ice sheet margin and lake level, water could have drained to the west and south into the Skagit River or to the southeast into Methow River.

Mathews (1968) suggested that a large amount of meltwater flowed from Similkameen valley through Lightning Lakes into Skagit valley. The evidence he cited includes large outwash terraces sloping west toward Skagit valley and the deep, narrow, V-shaped Lightning Lakes canyon, which has a floor 40 m lower than adjacent hanging tributary valleys with U-shaped cross-sections. The breached divide at Hozomeen Pass, bisected Freezeout Creek valley, and Lightning Creek alluvial fan support Mathews' (1968) conclusions.

Erosional evidence

Erosion at proglacial lake outlets during multiple ice sheet glaciations lowered divides and shifted them northward. Amounts of divide lowering and migration differ due to variable rock resistance, ice and water discharge, original divide height, and the length of time a particular divide was crossed by glaciers or meltwater. For example, Chilliwack Pass was a relatively minor meltwater route and the divide migrated only 800 m during the Pleistocene. In contrast, Hozomeen Pass was a major meltwater route located along the Hozomeen Fault; the divide migrated 5 km from the pass to Lightning Lakes during the Pleistocene (Figure 2-7; Table 2-2). Secondary drainage of smaller proglacial lakes across mountain passes occurred at many other locations not discussed in this paper. For example, Waitt (1979) identified similar meltwater features at Windy Pass and Robinson Pass along the North Cascades crest.

Net divide lowering along primary meltwater routes is 500-700 m, which is several hundred metres more than along secondary routes (Table 2-2). Many divides along primary drainage routes have been eliminated. Assuming that divide breaching commenced ~2.5 Ma ago with the onset of late Cenozoic Northern Hemisphere glaciation (Ruddiman and Wright, 1987), the average local rate of erosion is 200-300 m/Ma, which is comparable to regional geologic estimates (Tribe, 2002; Tucker, 2004). It is also broadly consistent with thermochronometric estimates of exhumation, which range from 200 m/Ma through most of the Oligocene to 1 km/Ma in the late Miocene (Reiners et al., 2002).

Breaching of divides and drainage reversal produced barbed tributaries with elbows of capture at several locations. Elbows of capture are sharp turns in a stream course where tributaries join a trunk stream (Dury, 1953; Bishop, 1995). Examples include the junctions of Ptarmigan and Johnny creeks with Lost River and the junction of upper Sumallo River with Skagit River

(Figures 2-7 and 2-10). Elbows of capture are commonly misidentified (Bishop, 1995), but they can provide a means of rapidly assessing potential locations of drainage changes over large areas.

Modern divides between some large valleys are long, flat valley floors with chains of lakes or swamps. Examples include the swamp at Klesilkwa Pass between Silverhope and Skagit rivers, Lightning Lakes between Skagit and Similkameen rivers, and Hidden Lakes between Similkameen and Methow rivers. The position of each of these divides could change in the event of a landslide or renewed glaciation. Several low passes are located along major faults, such as Klesilkwa Pass along the Ross Lake Fault (Figures 2-1 and 2-2), where fault movement weakened rocks.

Other prominent features created by proglacial drainage from the Cordilleran Ice Sheet are 15- to 30-km-long canyons downstream of breached divides and large alluvial fans at canyon mouths. Canyons occur along Skagit Gorge, Lightning Creek, Canyon-Ruby Creek, Canyon Creek, Lost River, and Lake Creek (Figure 2-1). Large gravel fans are present at all canyon mouths and typically displace larger trunk streams to opposite sides of the valleys.

Proglacial lake drainage modified pre-existing dendritic, trellis, and other drainage patterns. The changes are most pronounced north of the North Cascades crest. Dendritic drainage patterns are reversed in upper Skagit and Pasayten valleys, creating barbed or fish-hook tributaries (Bishop, 1995) that are not structurally controlled. Continental glaciation has had little impact on radial drainage patterns, which are restricted to higher mountain areas. Elements of Eocene and Miocene radial stream patterns have survived significant erosion in upper Skagit valley near the Mt. Rahm volcanics and near the Golden Horn Batholith. The Tertiary Ross Lake and Pasayten faults and northeast-striking faults of Miocene age were exploited by meltwater to form primary drainage links between the Skagit and adjacent Fraser and Okanagan watersheds. Lowering of divides along these faults has enhanced the rectangular drainage pattern in upper Skagit valley (Figures 2-1 and 2-7). At the regional scale, drainage rearrangement by glaciation has merged different stream patterns, such as the trellis pattern in lower Skagit valley with dendritic and rectangular patterns in upper Skagit valley.

Skagit Gorge is the only canyon that cuts across the structural and topographic grain of the former North Cascades and modern Skagit crests (Figures 2-1 and 2-2). The gorge is morphologically similar to other breached divides with steep gradients, steep, planar sidewalls, and no valley spurs (Figure 2-11). Bedrock benches in Skagit Gorge are similar to other breached regional divides. For example, Dury (1953) noted similar features, which he termed *rock knobs*, at the breached divide near the Callop defile in northwest Scotland. I interpret the Skagit Gorge bench system to be a remnant of the former North Cascades crest that has been strongly altered by glacier ice and meltwater erosion. This erosion has obscured the exact location of the breached divide within the 17-km-long gorge.

The north-sloping feature at the east end of Sourdough Mountain (Figure 2-11) is similar to erosion surfaces described by Mathews (1968), Haugerud (1985), and others in the upper Skagit region. Mathews (1968) noted the existence of a mature erosion surface above 1800 m asl near Lightning Lake that slopes gently to the northeast. He tentatively correlated it with similar features on the east slope of the North Cascades and the British Columbia interior that are covered by Miocene basalt flows (Waters, 1939; Mathews, 1964, 1968). If my interpretations of the modified drainage networks and erosion surface are correct, remnants of north-directed drainage have survived for more than 10 million years in this region.

Considering this evidence, I suggest that repeated overflow of proglacial lakes at the southern margin of the Cordilleran Ice Sheet breached the North Cascades crest at Skagit Gorge, causing lower Skagit River to capture upper Skagit River and its tributaries (Figures 2-7 and 2-11). Thunder Creek was once the headwaters of the north-draining upper Skagit system, which flowed to Fraser River via Klesilkwa Pass or Sunshine Valley (Figure 2-7). Both of these routes follow regional faults and provide low elevation links between the Fraser and Skagit valleys. Capture of this drainage by lower Skagit River resulted in a large drop in base level and incision of lower Thunder Creek and other Skagit tributaries entering Skagit Gorge. The importance of divide elimination at this site is highlighted by the 50 km of divide migration from Skagit Gorge to Sunshine Valley and by an estimated 700 m of divide lowering (Table 2-2).

Timing of drainage rearrangements

The high connectivity of the upper Skagit drainage network suggests that Skagit River drained Cordilleran Ice Sheet meltwater from parts of southern interior British Columbia to the Pacific Ocean. This proglacial meltwater drainage system operated during advance and retreat phases of the Fraser Glaciation, as well as during earlier glaciations. During early advance and late retreat stages of the Fraser Glaciation, Glacial Lake Quilchena drained south from Thompson Valley into Tulameen River, via an outlet at 1010 m asl (Figure 2-7; Fulton, 1969). When the ice sheet terminus was farther south, the ice sheet dammed other western Okanagan and eastern

Fraser tributaries, including Similkameen and Tulameen rivers (Holmes, 1965; Mathews, 1968). Proglacial lakes then drained into Skagit valley via Skaist and Snass creeks, Klesilkwa Pass, and Lightning Lakes across divides with elevations between 580 and 1520 m asl. The breached divide at Skagit Gorge provided a direct, low-elevation route for meltwater through the mountains to the Pacific Ocean via several outlets, including lower Skagit valley, Darrington, and Barlow Pass (Figure 2-2). When the lower Skagit and Darrington outlets were blocked during advanced stages of glaciation, Barlow Pass at 700 m asl was the southernmost outlet for drainage of a large area. Water flowing through this corridor entered a major ice-marginal channel and flowed around the southern margin of the Puget lobe of the Cordilleran Ice Sheet to the Pacific Ocean via Chehalis River (Booth and Hallet, 1993). Estimates of water discharge for the Puget lobe should therefore include meltwater routed through the Skagit watershed from the Fraser and Okanagan watersheds.

Determining when divides were first breached and this drainage system was first established is problematic in the absence of exposed late Tertiary and early Pleistocene deposits. Divide breaching probably began during initial ice-sheet glaciation. Initial breaching at an outlet led to higher discharge through the outlet, which led to higher rates of erosion, establishing a positive feedback loop. Through such a mechanism, master meltwater routes were established for each watershed. Divide cutting and canyon formation were rapid because of large hydraulic heads and large water fluxes in many valleys. For example, with a late Fraser Glaciation lake at 1310 m asl in Pasayten valley (Holmes, 1965), water depths through Hozomeen Pass exceeded 40 m. Many of the canyons, including Skagit Gorge, existed before the latest advance of the Cordilleran Ice Sheet, as indicated by the presence of glacial striations on lower canyon walls. The regional ice sheet drainage system was probably established during initial ice-sheet glaciation of the area, late in the Pliocene or early in the Pleistocene. Presented with similar evidence, Dury (1953) came to the same conclusion about the great through-valleys in the Scottish Highlands.

North-directed, dendritic stream patterns and Miocene erosion surfaces that penetrate deeply into the mountains indicate that the North Cascades crest was established by 11 Ma (Reiners et al., 2002). Survival of landscape features of this age is remarkable because denudation estimates since this time range from 1 to 5 km (Reiners et al., 2003). Rapid erosion by streams and valley glaciers appears to have maintained basic drainage patterns through millions of years of rapid uplift until they were modified by continental glaciation.

Alteration of pre-glacial mountain divides

Divide elimination connected otherwise isolated mountain valleys (Flint, 1971) and altered regional drainage divides. The Pacific crest is breached at Holman, Hozomeen, Lost, Snass, and Skaist passes; and the North Cascades crest is breached at Chilliwack, Lost River, and Ashnola passes (Figure 2-2). The North Cascades crest was the focus of divide breaching because valleys draining north from it were blocked for extended periods by the southward-advancing and northward-retreating ice sheet.

I propose that, prior to continental glaciation, the North Cascades crest followed the high, resistant peaks of the Chelan Mountains terrane in a northwest-southeast direction, parallel to the topographic and structural grain of the North Cascades (A-B-B'-A' in Figure 2-2; Figure 2-12A). From Cascade Pass, it followed the modern trend of the Pacific crest to the east to the Methow-Okanagan divide. Breaching of the North Cascades crest at Skagit Gorge led to divide migration north into less resistant rocks of the Hozomeen and Methow terranes (Figure 2-12C). The Skagit crest is left as a remnant of the North Cascades crest within the crystalline core of the range. A tendency for progressive eastward divide migration because of the pronounced climatic asymmetry across the North Cascades was inferred by Mathews (1968) and Reiners et al. (2003). My results underscore the importance of northward divide migration caused by proglacial drainage associated with continental glaciation.

Conclusion

From at least the Miocene until initial continental glaciation in the late Pliocene, a regional drainage divide that I informally term the "North Cascades crest" separated flow south into Puget Sound and along Methow and Columbia rivers from flow north to Fraser and Okanagan rivers (Figures 2-2 and 2-12). Continental glaciation reorganized this drainage network by forcing drainage to the south. Reversal of drainage led to divide elimination, divide migration of tens of kilometres, creation of relict dendritic drainage patterns and barbed tributaries, enhancement of rectangular drainage patterns, erosion of long canyons downstream of breached divides, beheading and bisection of major mountain valleys, and deposition of large alluvial fans at canyon mouths. These changes established a regional drainage system linking Skagit valley with parts of the Okanagan and Fraser watersheds. The key event in the establishment of this system was breaching of the North Cascades crest at Skagit Gorge. Once the divide was breached, parts of the Okanagan and Fraser valleys were opened to the Pacific Ocean via Skagit valley (Figures 2-2 and 2-12). Capture of the upper Skagit watershed by lower Skagit River indicates that Skagit River is not an antecedent stream superimposed across the structure and topography of the crystalline core of the North Cascades as suggested by Waitt (1977).

The concepts developed in this paper can be used to assess the impact of ice sheet glaciation on drainage development in other mountain areas. Situations where ice sheets advanced into mountainous terrain may have undergone drainage changes similar to those described in this paper. Glacial diversion should be considered along with beheading, stream capture, and tectonic diversion as processes of drainage diversion (Bishop, 1995). Other areas in western North America where this analysis could be applied include the Okanagan, Fraser, and Columbia valleys and their tributaries.

Meltwater diversion in the Skagit River watershed created a landscape similar to that of other mountain ranges that experienced a similar style of glaciation. Breached divides in the North Cascades are similar to wind gaps found in the White and Green mountains of New England. The interconnected Skagit-Okanagan-Fraser valleys strongly resemble the great through-valleys in Scotland, trans-range valleys in British Columbia, and the ice portals of Scandinavia.

Acknowledgements

This research was supported by the U.S. National Park Service, U.S. Geological Survey, and the Natural Sciences and Engineering Research Council of Canada. I thank Mike Larrabee and Jeanna Wenger of the National Park Service for drafting figures.

Figures

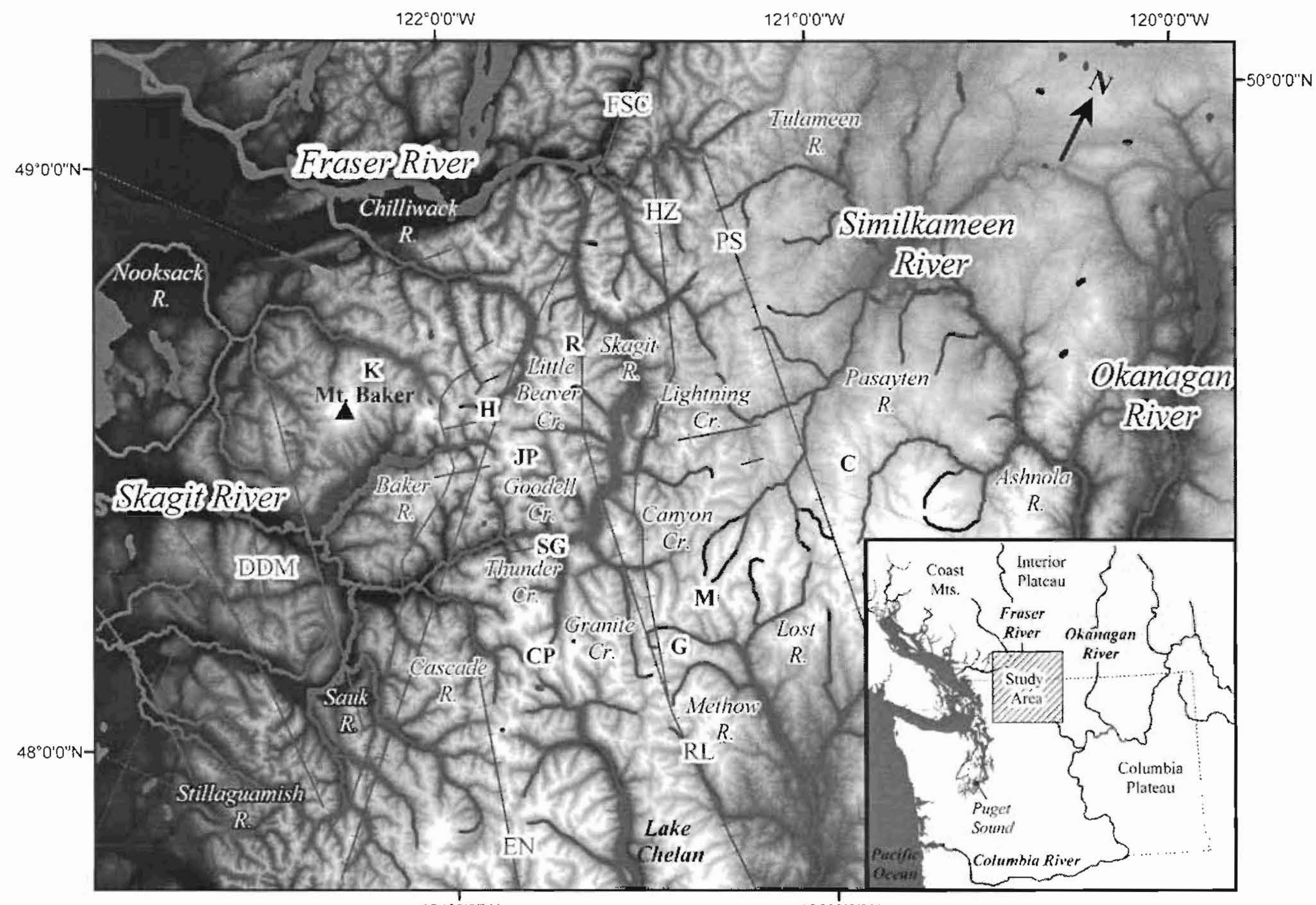

Figure 2-1. **Drainage pattern and major faults of the Skagit region. Faults include Fraser-Straight Creek (FSC), Entiat (EN), Ross Lake (RL), Hozomeen (HZ), Darrington-Devil's Mountain (DDM), and Pasayten (PS). Other locations discussed in the paper include Cascade Pass (CP), Cathedral Peaks (C), Monument Peak Batholith (M), Golden Horn Batholith (G); and Mt. Rahm (R), Hannegan (H), and Kulshan (K) volcanic rocks.**

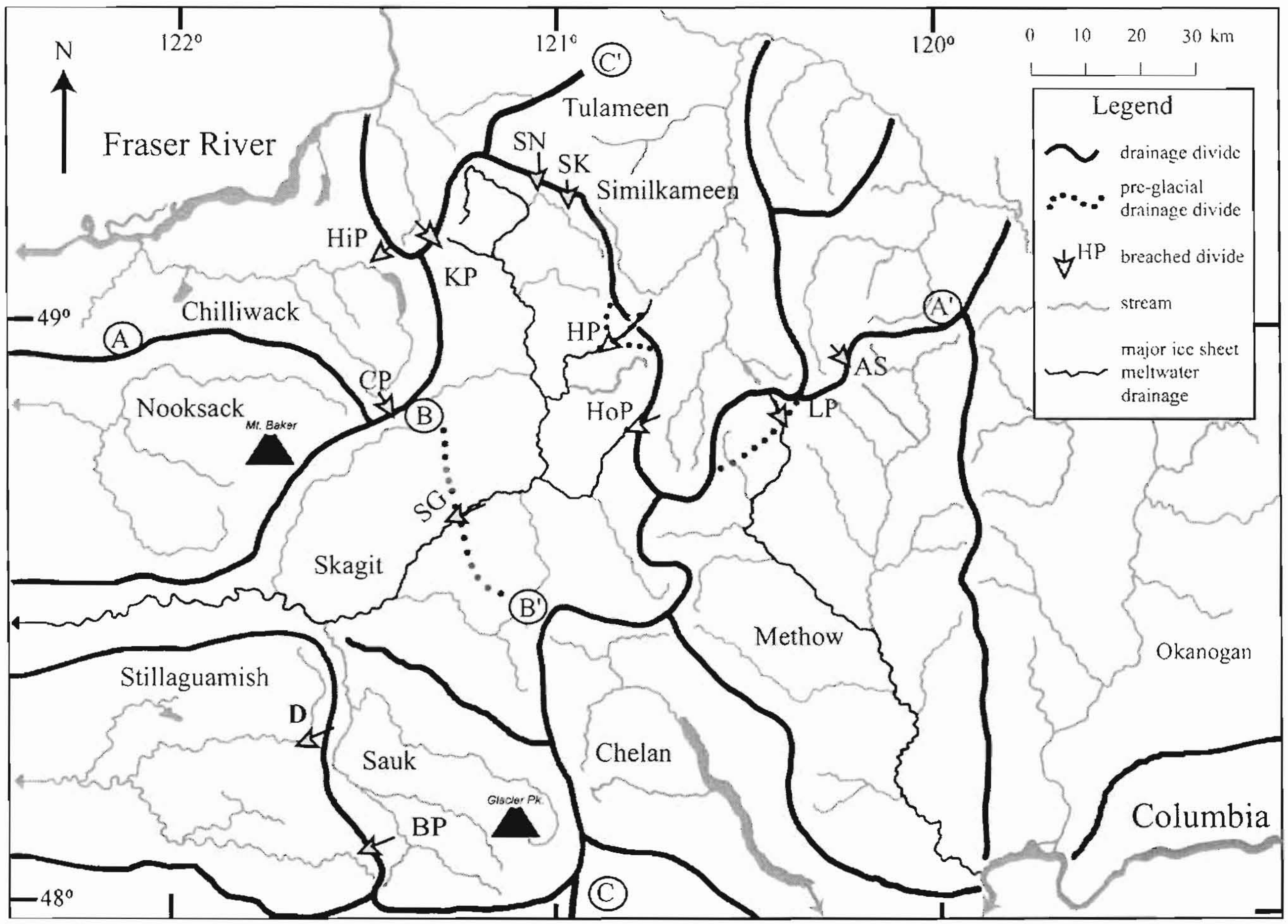

Figure 2-2. **Breached divides of the Skagit region: Chilliwack Pass (CP), Hicks Pass (HiP), Klesilkwa Pass (KP), Snass Pass (SN), Skaist Pass (SK), Hozomeen Pass (HP), Holman Pass (HoP), Lost River Pass (LP), Ashnola Pass (AS), Skagit Gorge (SG), Darrington (D), and Barlow Pass (BP). A-A' = North Cascades crest, B-B' = Skagit crest, C-C' = Pacific crest.**

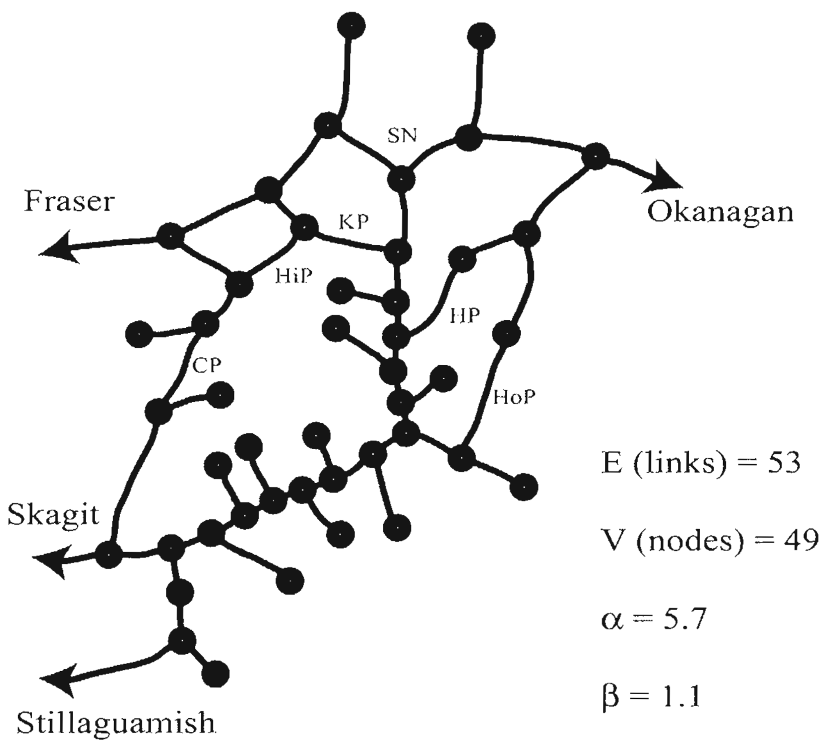

Figure 2-3. Skagit River drainage connectivity; nodes (arrows and dots) include stream junctions while links (lines) are through breached divides and along faults. Note the large number of links between valleys in the upper watershed, where Skagit River has breached divides with the Fraser (3) and Okanagan (4) watersheds.

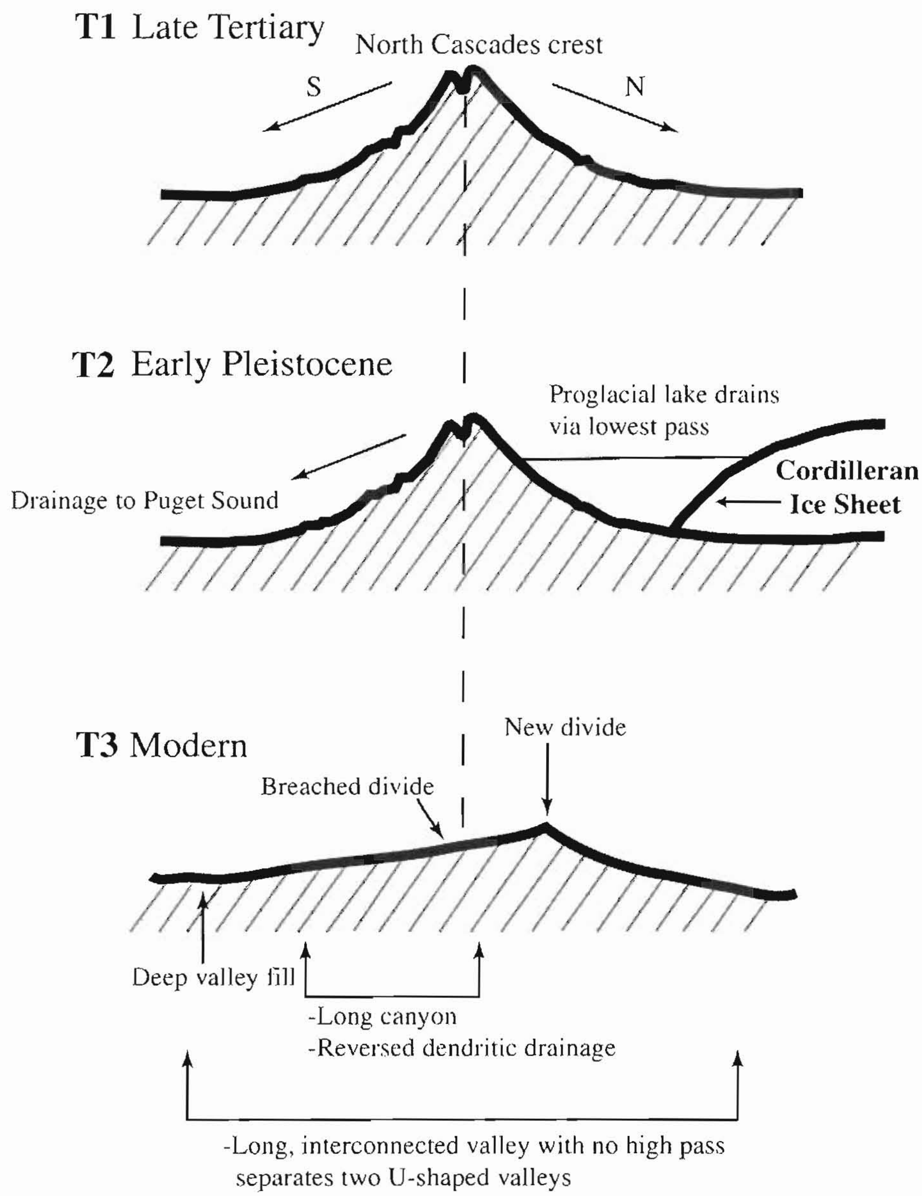

Figure 2-4. Process-form model illustrating the geomorphic effects of Cordilleran Ice Sheet drainage across the North Cascades crest.

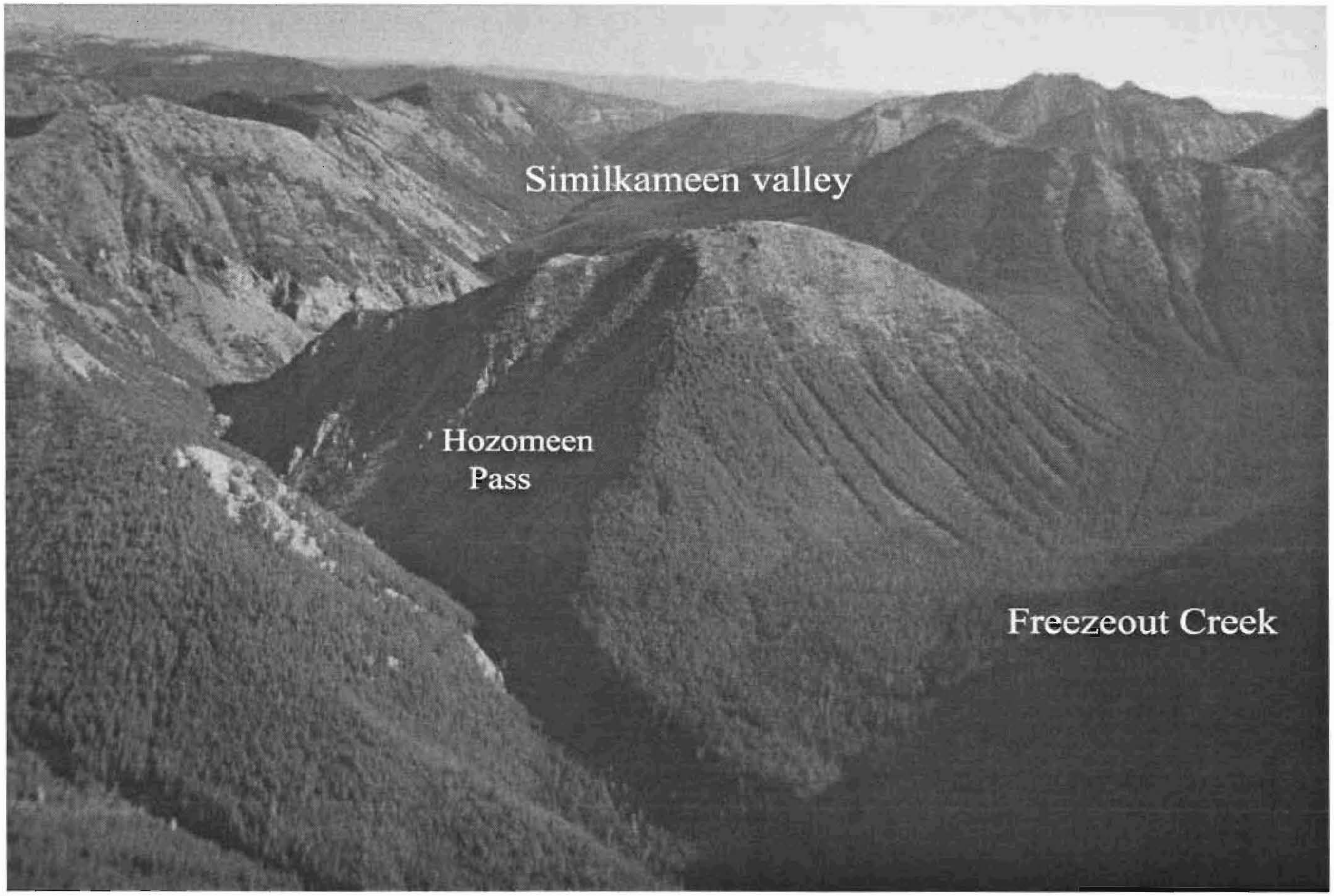

Figure 2-5. View northeast over the breached divide at Hozomeen Pass into Similkameen valley. Note the contrast between the meltwater-modified Hozomeen Pass and the glacially modified pass to the east.

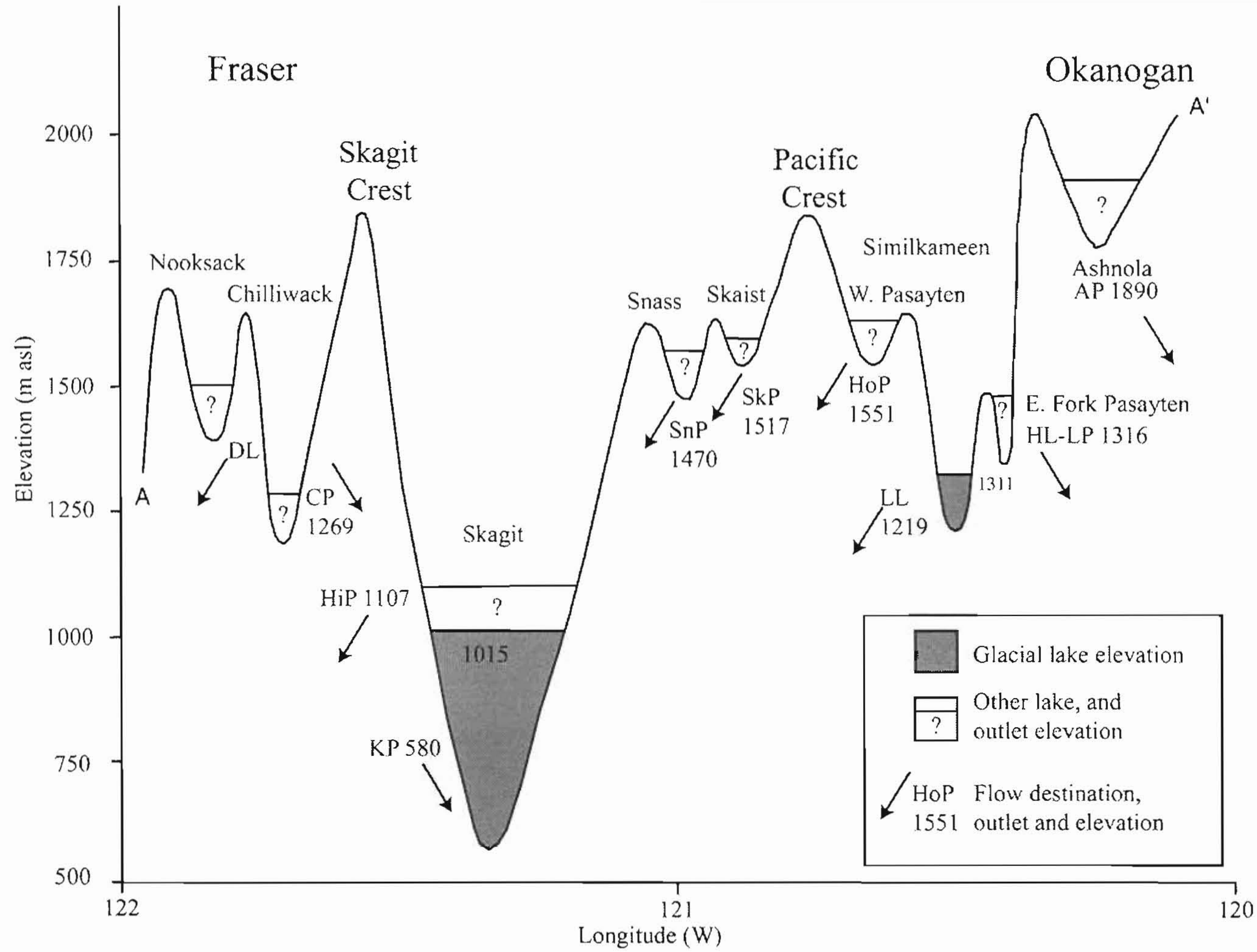

Figure 2-6. Topographic cross-section along the modern North Cascades crest (A-A', Fig. 2-2) showing locations of breached divides and proglacial lake and outlet elevations (data from Holmes, 1965; and Goff, 1993).

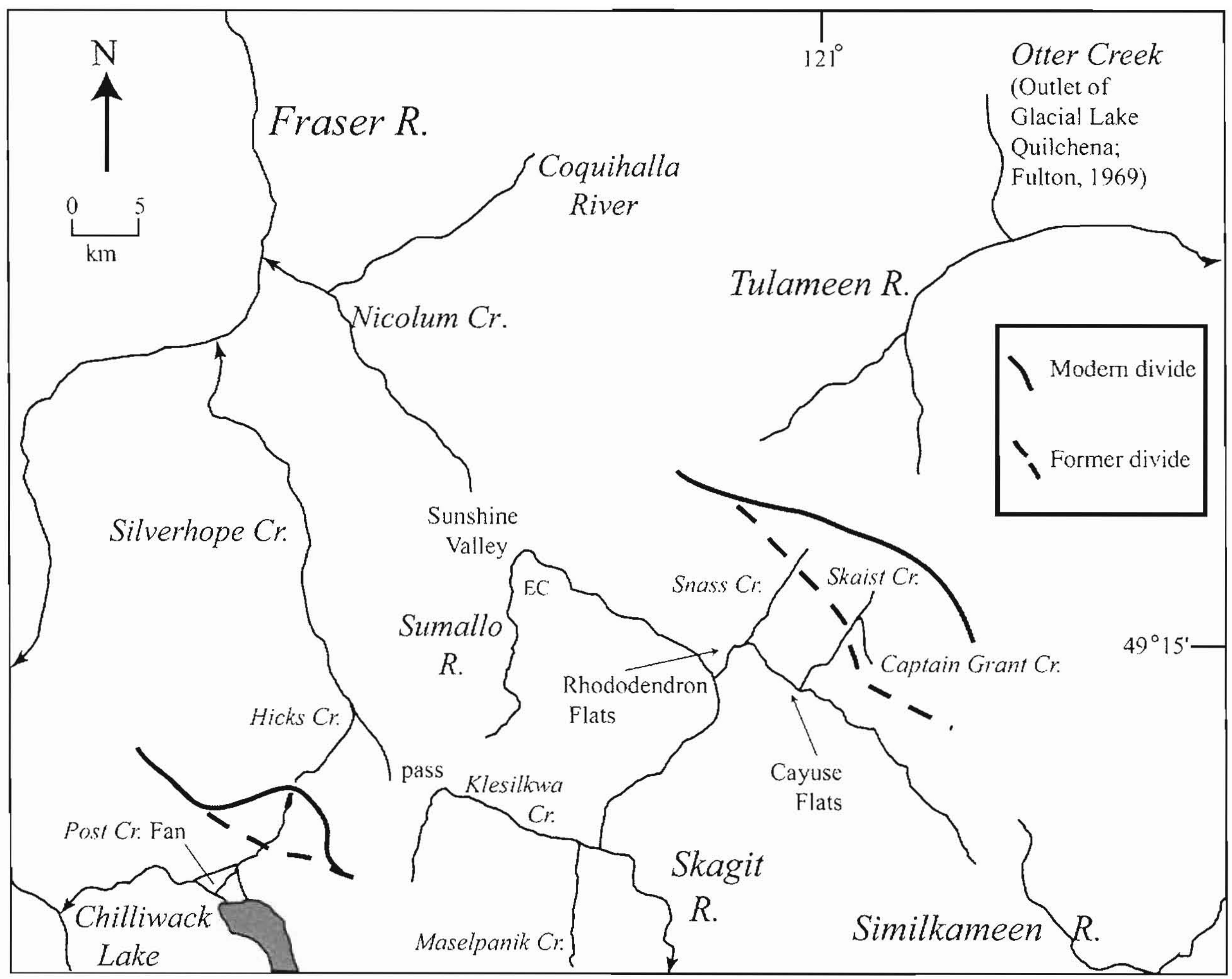

Figure 2-7. **Drainage pattern and divide changes in the upper Skagit River watershed. The Otter Creek outlet to Glacial Lake Quilchena (Fulton, 1969) links Skagit River to glacial drainage systems outside the North Cascades. Note elbow of capture (EC), which suggests that upper Summalo River once flowed northwest.**

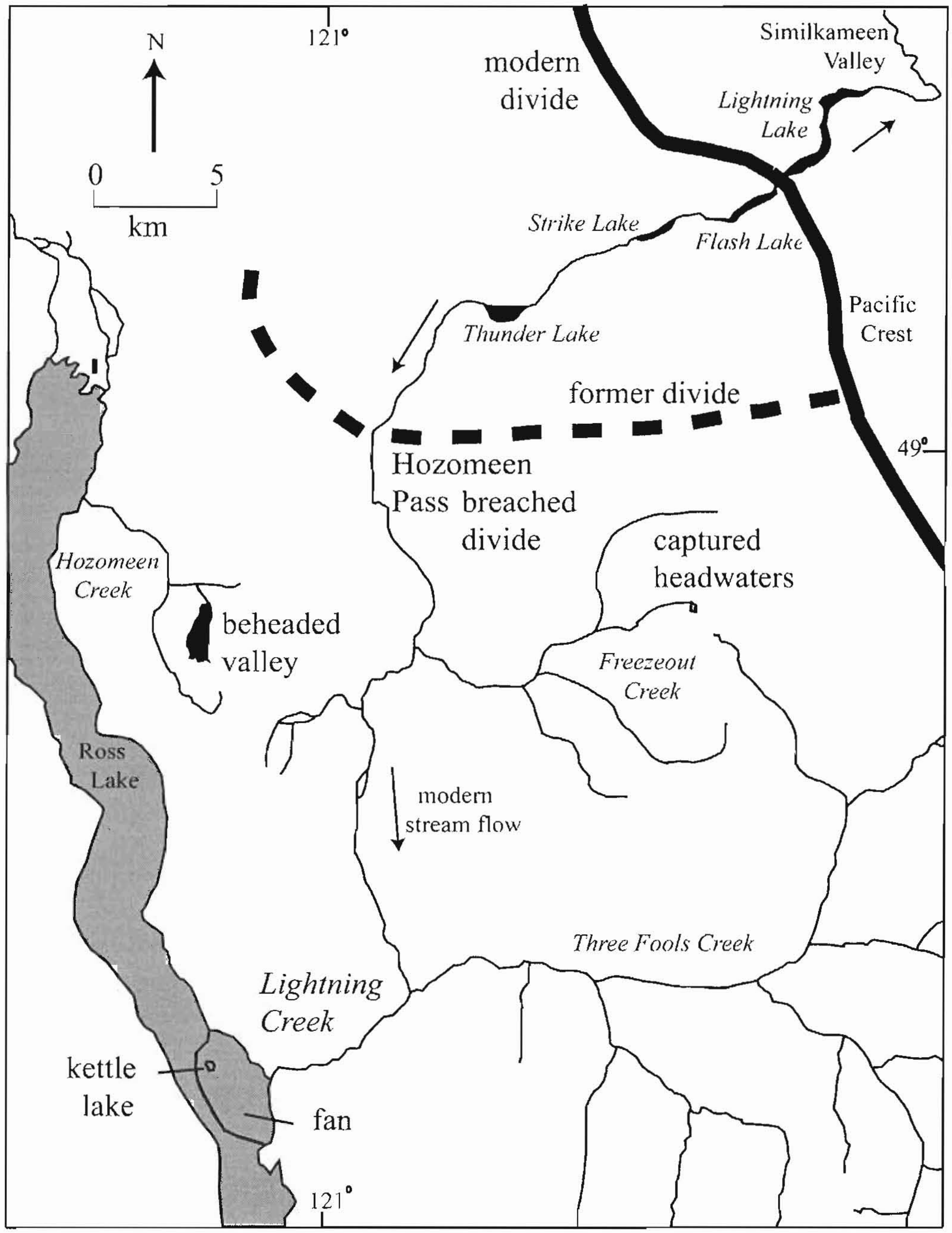

Figure 2-8. Drainage pattern and divide changes in the upper Lightning Creek area. Note breached divide at Hozomeen Pass. Erosion by proglacial meltwater bisected Freezeout Creek and beheaded Hozomeen Creek. Upper Freezeout Creek became connected to Three Fools Creek along the trace of the Hozomeen Fault.

Figure 2-9. The Lightning Creek fan in Skagit valley was deposited by meltwater flowing from the Okanagan valley. The fan is much larger than other tributary fans in the area and was deposited rapidly at the end of the last glaciation.

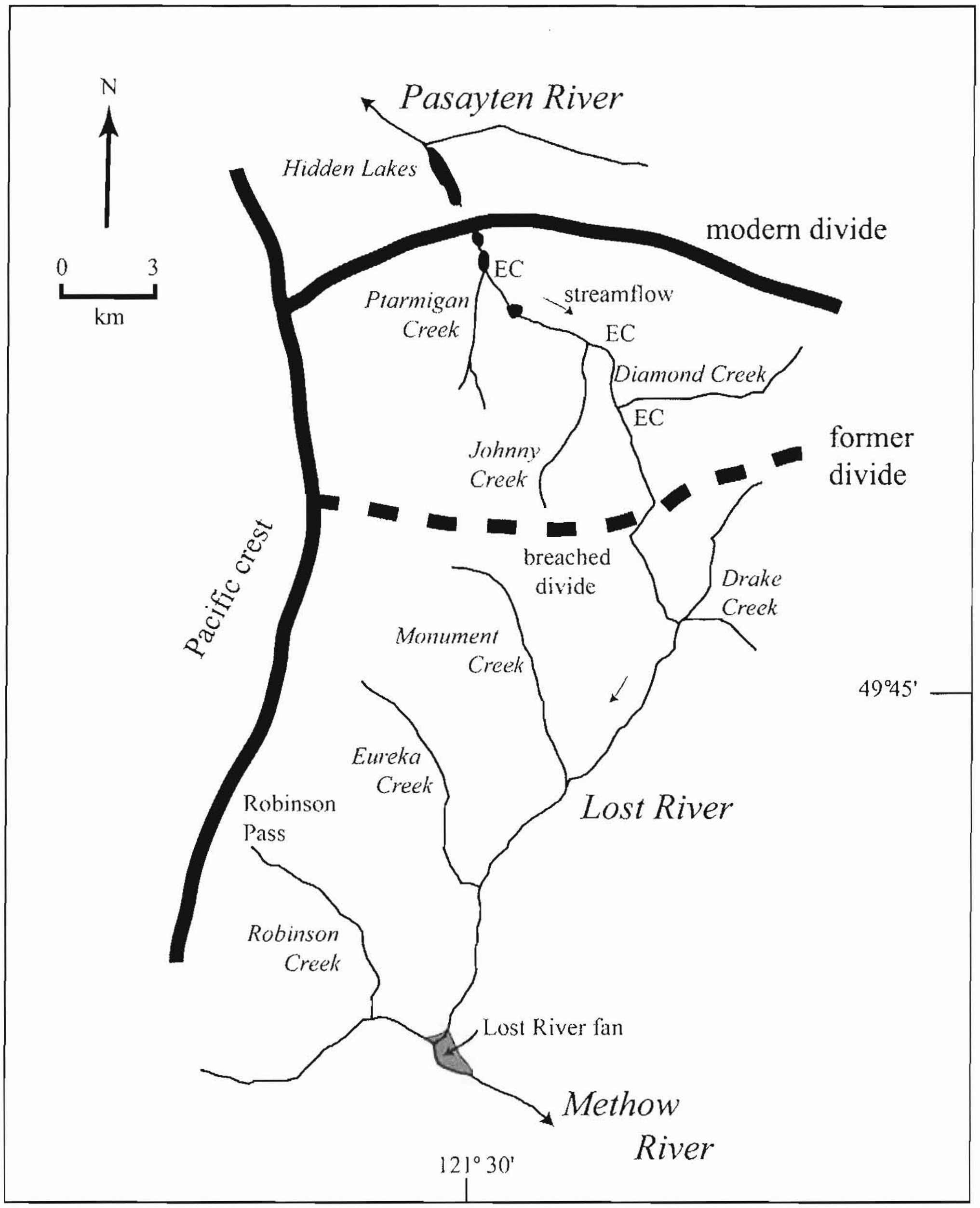

Figure 2-10. **Drainage pattern and divide changes in the upper Lost River area. Note elbow of capture (EC) and barbed tributaries of Ptarmigan, Johnny, and Diamond creeks, which once were part of north-draining Pasayten River.**

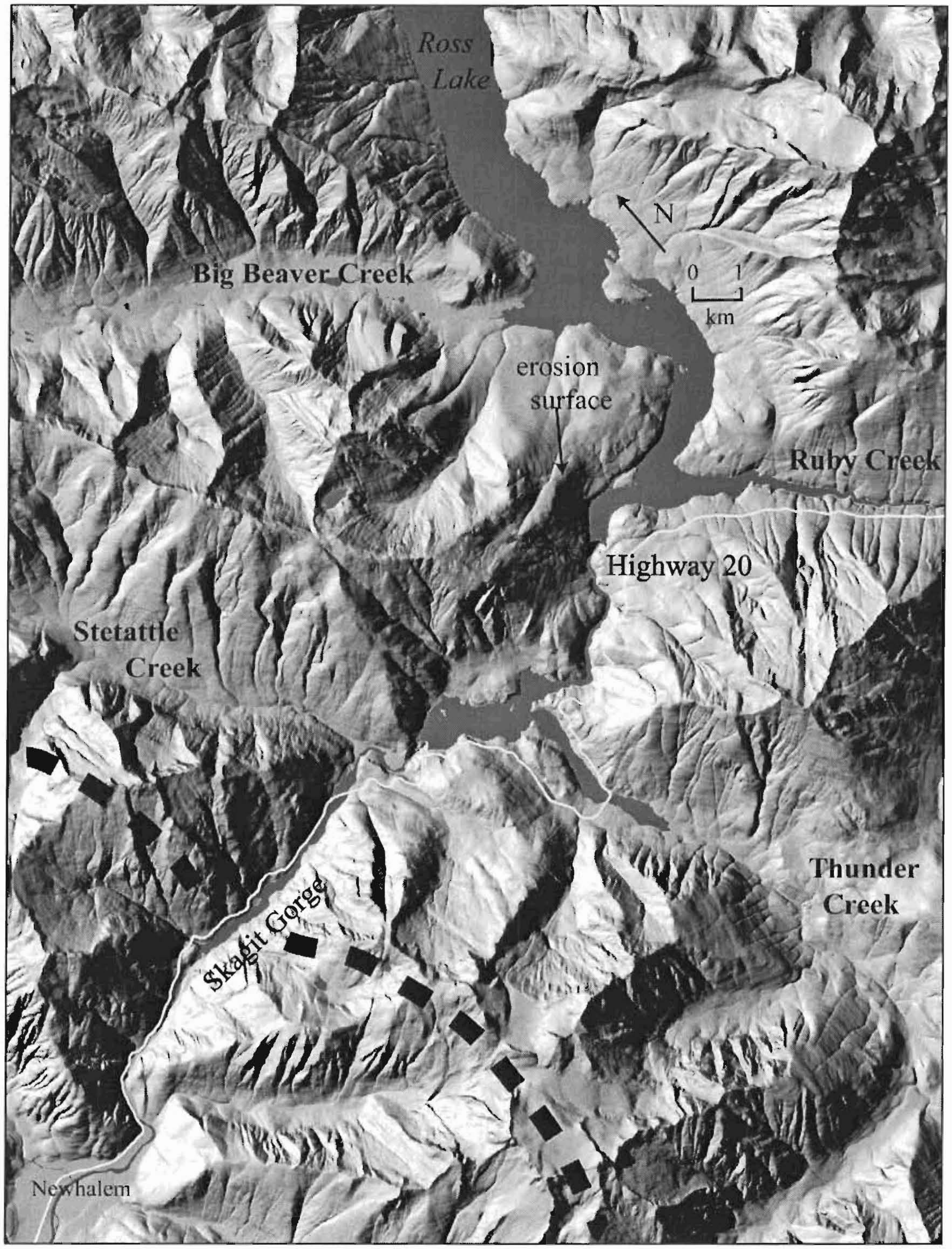

Figure 2-11. Shaded relief image of Skagit Gorge (northwest sun angle). The approximate location of the breached divide is shown as a dashed line.

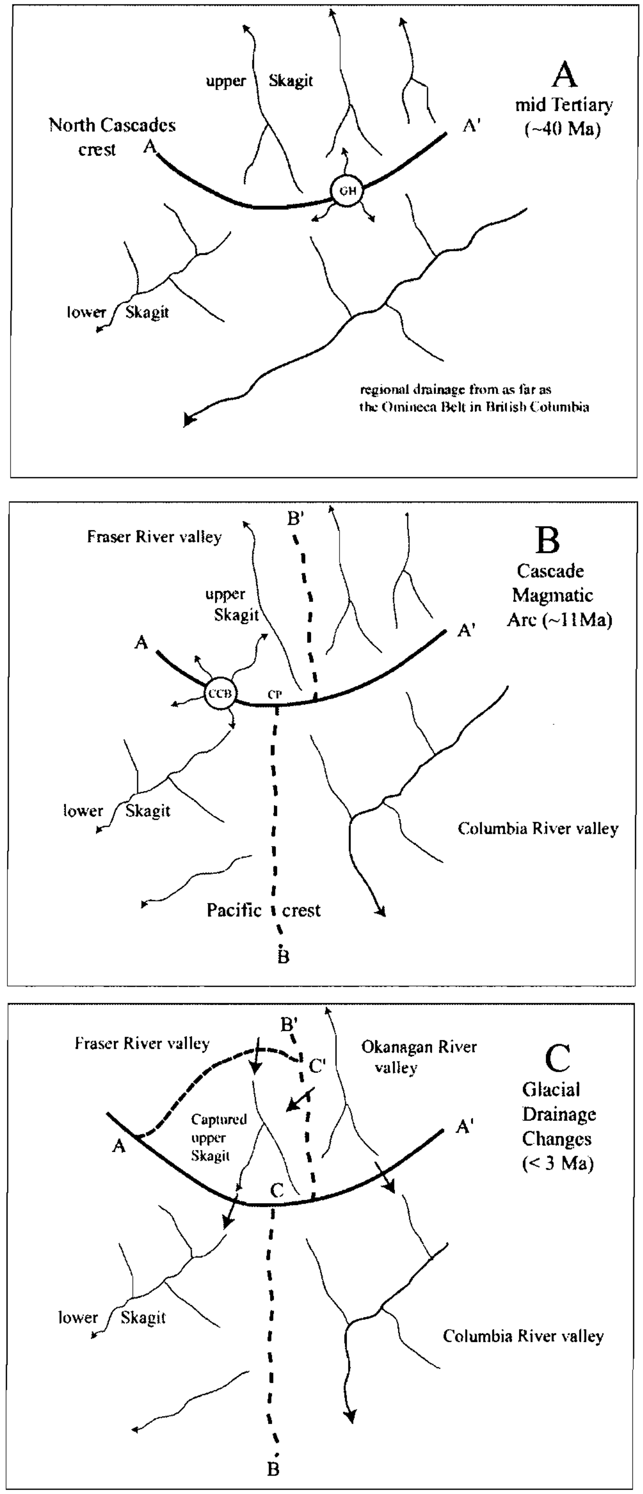

Figure 2-12. **Schematic diagram of drainage pattern and divide changes in the Skagit River watershed from (A) mid-Tertiary, through (B) late Tertiary, to (C) the Pleistocene. Note radial drainage associated with the Golden Horn Batholith (GH) and Chilliwack Composite Batholith (CCB).**

Tables

Table 2-1. Alpha values for selected drainage basins [1]

Area glaciated by ice sheet	Alpha value
Western Scotland (Broom and Assynt)	6.6
Greenland (Sondre Stromfjord)	6.6
North Cascades (Skagit)	5.7
Eastern Scotland (Skye and Mull)	2.1
Western British Columbia (Squamish)	2.1
Western British Columbia (Stein)	1.2

[1] Data for all areas except the North Cascades from Haynes (1977).

Table 2-2. Geomorphic changes along routes of Cordilleran Ice Sheet drainage [1]

Breached divide	Regional divide [2]	Meltwater canyon stream	Water destination	Max. lake elevation (m)	Divide migration distance (km)	Modern divide elevation (m)	Divide elevation change (m)
Chilliwack Pass	NCC	Pass Cr.	Skagit	310	0.8	1269	161
Hicks Pass	Local	Post Cr.	Fraser	1015	5.9	990	620
Skagit Gorge	NCC	Skagit	Skagit	1015	50	680	660
Snass Pass	PC	Snass Cr.	Skagit	unknown	4.4	1470	320
Skaist Pass	PC	Skaist Cr.	Skagit	unknown	7.6	1517	220
Hozomeen Pass	PC	Lightning Cr.	Skagit	1311	5	1219	320
Holman Pass	PC	Canyon Cr.	Skagit	unknown	7	1551	357
Lost River Pass	NCC	Lost R.	Columbia	1311	12	1316	556
Ashnola Pass	NCC	Lake Cr.	Columbia	unknown	1	1890	262

[1] Data sources in addition to this study: Mathews (1968); Waitt (1971); Clague and Luternauer (1982); and Goff (1993).
[2] NCC, North Cascades crest; PC, Pacific crest.

Reference List

Armstrong, J.E., and Tipper, H.W., 1948. Glaciation in north central British Columbia. American Journal of Science 246: 283-310.

Armstrong, J.E., Crandell, D.R., Easterbrook, D.J., and Noble, J.B., 1965. Late Pleistocene stratigraphy and chronology in southwestern British Columbia and northwestern Washington. Geological Society of America Bulletin 76: 321-330.

Barksdale, J.D., 1941. Glaciation of the Methow valley, Washington. Journal of Geology 49: 721-737.

Bishop, P., 1995. Drainage rearrangement by river capture, beheading and diversion. Progress in Physical Geography 19: 449-473.

Booth, D.K., 1987. Timing and processes of deglaciation along the southern margin of the Cordilleran Ice Sheet. In: Ruddiman, W.F., and Wright, Jr., H.E. (eds.), North America and Adjacent Oceans during the Last Deglaciation. Geological Society of America, The Geology of North America K-3: 71-90.

Booth, D.K., and Hallet, B., 1993. Channel networks carved by subglacial water: Observations and reconstruction in eastern Puget Lowland of Washington. Geological Society of America Bulletin 105: 671-683.

Booth, D.B., Troost, K.G., Clague, J.J., and Waitt, R.B., 2004. The Cordilleran Ice Sheet. In: Gillespie, A.R., Porter, S.C., and Atwater, B.F. (eds.), The Quaternary Period in the U.S. Elsevier Development in Quaternary Science 1: 17-43.

Bretz, J.H., 1913. Glaciation of Puget Sound Region. Washington Geological Survey Bulletin 8.

Clague, J.J., 1981. Late Quaternary Geology and Geochronology of British Columbia. Part I: Radiocarbon Dates. Geological Survey of Canada Paper 80-13.

Clague, J.J., 1989a. Cordilleran ice sheet. In: Fulton, R.J. (ed.), Quaternary Geology of Canada and Greenland. Geological Survey of Canada, Geology of North America K-1: 40-42.

Clague, J.J., and Luternauer, J.L., 1982. Excursion 30A: Late Quaternary Sedimentary Environments, Southwestern British Columbia. International Association of Sedimentologists, 11th International Congress on Sedimentology, Hamilton, ON, Field Excursion Guidebook.

Drost, B.W., and Lombard, R.E., 1978. Water in the Skagit River Basin, Washington. Washington Department of Ecology Water Supply Bulletin 47.

Dury, G.H., 1953. A glacial breach in the north western highlands. Scottish Geographic Magazine 69: 106-117.

Easterbrook, D.J., Rowland, D.L., Carson, R.J., and Naeser, N.D., 1988. Application of fission-track dating, and tephra correlation to lower Pleistocene sediments in Puget Lowland. In: Geological Society of America Special Paper 227: 139-165.

Eyles, N., and Clague, J.J., 1991. Glaciolacustrine sedimentation during advance and retreat of the Cordilleran Ice Sheet in central British Columbia. Géographie physique et Quaternaire 45: 317-331.

Flint, R.F., 1971. Glacial and Quaternary Geology. John Wiley and Sons, New York, NY.

Fulton, R.J., 1969. Glacial Lake History, Southern Interior Plateau, British Columbia. Geological Survey of Canada Paper 69-37.

Goff, J., 1993. Late Pleistocene and Holocene Sedimentation in Silverhope Valley, British Columbia. Ph.D. thesis, University of Western Ontario, London, ON.

Haugerud, R.A., 1985. Geology of the Hozameen Group and the Ross Lake Shear Zone, Maselpanik Area, North Cascades, Southwestern British Columbia. Ph.D. thesis, University of Washington, Seattle, WA.

Haugerud, R.A., Brown, E.H., Tabor, R.W., Kriens, B.J., and McGroder, M.F., 1994. Late Cretaceous and early Tertiary orogeny in the North Cascades. In: Swanson, D.A., and Haugerud, R.A. (eds.), Geologic Field Trips in the Pacific Northwest. University of Washington Department of Geological Sciences, Seattle, WA, 2: 2E1-2E51.

Haynes, V.M., 1977. The modification of valley patterns by ice sheet activity. Geografiska Annaler 59A: 195-207.

Holmes, A., 1965. Principles of Physical Geology. Thomas Nelson Ltd., London.

Johnson, S.Y., 1984. Stratigraphy, age and paleogeography of the Eocene Chuckanut Formation, northwest Washington. Canadian Journal of Earth Sciences 21: 92-106.

Kansky, J., 1963. Structure of Transportation Networks: Relationships Between Network Geometry and Regional Characteristics. University of Chicago, Department of Geography Research Paper 84.

Kerr, F.A., 1936. Quaternary glaciation in the Coast Range, northern British Columbia and Alaska. Journal of Geology 44: 681-700.

Linton, D.L., 1967. Divide elimination by glacial erosion. In: Wright, Jr., H.E., and Osburn, W.H. (eds.), Arctic and Alpine Environments (Proceedings 7th INQUA Congress). Indiana University Press, Indianapolis, IN, pp. 241-248.

Mackin, J.H., 1941. Glacial geology of the Snoqualmie-Cedar area, Washington. Journal of Geology 49: 449-481.

Mathews, W.H., 1944. Glacial lakes and ice retreat in south-central British Columbia. Royal Society of Canada Transactions, Series 3, 38: 39-57.

Mathews, W.H., 1964. Potassium-argon age determinations of Cenozoic volcanic rocks from British Columbia. Geological Society of America Bulletin 75: 465-468.

Mathews, W.H., 1968. Geomorphology of Lightning Creek valley, Manning Park, southwest B.C. Syesis 1: 65-78.

Mathews, W.H., 1991. Development of Cordilleran landscapes during the Quaternary. In: Fulton, R.J. (ed.), Quaternary Geology of Canada and Greenland. Geological Survey of Canada, Geology of North America K-1: 32-44.

Penck, A., 1905. Glacial features in the surface of the Alps. Journal of Geology 13: 1-19.

Porter, S.C., and Swanson, T., 1998. Radiocarbon age constraints on rates of advance and retreat of the Puget lobe of the Cordilleran Ice Sheet during the last glaciation. Quaternary Research 50: 205-213.

Reiners, P.W., Ehlers, T.A., Garner, J.I., Mitchell, S.G., Montgomery, D.R., Vance, J.A., and Nicolescu, S., 2002. Late Miocene erosion and uplift of Washington Cascade Range. Geological Society of America Bulletin 31: 767-770.

Reiners, P.W., Ehlers, T.A., Mitchell, S.G., and Montgomery, D.R., 2003. (U-Th)/He thermochronology and orogeny of the Washington Cascades. Geological Society of America, Abstracts with Program 126-9: 307.

Riedel, J.L., and Haugerud, R.H., 1994. Glacial rearrangement of drainage in the northern North Cascade Range, Washington. Geological Society of America Abstracts with Program 26: 7.

Riedel, J.L., Haugerud, R.A., and Clague, J.J., 2007. Geomorphology of a Cordilleran Ice Sheet drainage network through breached divides in the North Cascades Mountains of Washington and British Columbia. Geomorphology, in press.

Ruddiman, W.F., and Wright, Jr., H.E., 1987. Introduction. In: Ruddiman, W.F., and Wright, Jr., H.E. (eds.), North America and Adjacent Oceans during the Last Deglaciation. Geological Society of America, Geology of North America K3: 1-12.

Ryder, J.M., 1989. Glacial history of the southern Okanagan Range, British Columbia. Canadian Quaternary Association Program with Abstracts 34: A116.

Saunders, I.R., Clague, J.J., and Roberts, M.C., 1987. Deglaciation of Chilliwack River valley, British Columbia. Canadian Journal of Earth Sciences 24: 915-923.

Suess, E., 1888. The Face of the Earth 2. Clarendon Press, Oxford, pp. 326-345 [translated by Sollas, H.B.C., 1906].

Tabor, R.W., and Haugerud, R.A., 1999. Geology of the North Cascades: A Mountain Mosaic. The Mountaineers, Seattle, WA.

Tabor, R.W., Haugerud, R.A., Miller, R.B., Brown, E.H., and Babcock, R.S., 1989. Accreted terranes of the North Cascades, Washington. 28th International Geological Congress, Washington, D.C., Field Trip Guidebook T307.

Thorson, R.M., 1980. Ice-Sheet glaciation of the Puget Lowland, Washington, during the Vashon stade. Quaternary Research 13: 303-321.

Tipper, H.W., 1971. Glacial Geomorphology and Pleistocene History of Central British Columbia. Geological Survey of Canada Bulletin 196.

Tribe, S., 2002. Geomorphic evidence for Tertiary drainage networks in southern Coast Mountains, British Columbia. Geological Survey of Canada Current Research 2002-A13: 1-8.

Tucker, D.S., 2004. Geology and Eruptive History of the Hannegan Caldera, North Cascades, Washington. M.S. thesis, Western Washington University, Bellingham, WA.

Waitt, Jr., R.B., 1971. Geomorphology and Glacial Geology of the Methow Drainage Basin, Eastern North Cascade Range, Washington. Ph.D. thesis, University of Washington, Seattle, WA.

Waitt, Jr., R.B., 1975. Late Pleistocene alpine glaciers and the Cordilleran Ice Sheet at Washington Pass, North Cascade Range, Washington. Arctic and Alpine Research 7: 25-32.

Waitt, Jr., R.B., 1977. Evolution of glaciated topography of upper Skagit drainage basin, Washington. Arctic and Alpine Research 9: 183-192.

Waitt, Jr., R.B., 1979. Rockslide-avalanche across a distributary lobe of the Cordilleran Ice Sheet in the Pasayten Valley, Northern Washington. Arctic and Alpine Research 11: 33-40.

Waitt, Jr., R.B., and Thorson, R.M., 1983. The Cordilleran Ice Sheet in Washington, Idaho, and Montana. In: Porter, S.C. (ed.), Late-Quaternary Environments of the United States, Vol. 1, The Late Pleistocene. University of Minnesota Press, Minneapolis, MN, pp. 54-70.

Ward, B.C., and Thomson, B., 2004. Late Pleistocene stratigraphy and chronology of lower Chehalis River Valley, southwestern BC: Evidence for a restricted Coquitlam Stade. Canadian Journal of Earth Sciences 41: 881-895.

Waters, A., 1939. Resurrected erosion surface in central Washington. Geological Society of America Bulletin 50: 638-659.

Willis, B., 1888. Changes in River Courses in Washington Territory Due to Glaciation. U.S. Geological Survey Bulletin 40: 474-87.

Zernitz, E.R., 1932. Drainage patterns and their significance. Journal of Geology 40: 498-521.

Chapter 3: Chronology and extent of Evans Creek stade alpine glaciation in Skagit valley, Washington

Abstract

A study of sediments in Skagit valley in the North Cascades, Washington, has provided important new information on the chronology and extent of alpine glaciation during the Evans Creek stade of the Fraser Glaciation. Radiocarbon-dated sediments at the Cedar Grove section record two advances of the Baker Glacier between 25,040 and 16,400 ^{14}C yr BP, separated by a period of glacier retreat and forest growth on outwash from the earlier advance. Three radiocarbon ages from lacustrine sediments record damming of the upper Skagit River by Big Beaver Glacier about 24,000 ^{14}C yr BP. The 25,040 ^{14}C yr BP date is the first radiocarbon age constraint on the beginning of the Evans Creek stade in the Cascade Range.

Alpine glaciers from Baker and Big Beaver valleys blocked Skagit River creating glacial Lakes Skymo and Concrete, which covered a combined area of nearly 100 km^2. Horizontally laminated silt and bedded sand and gravel up to 50 m thick record deposition in glacial Lake Skymo over a period of 8000 years. The persistence of the lake indicates that alpine glaciers in upper Skagit valley remained in advanced positions throughout most of the Evans Creek stade. The lake sediments are unconformably overlain by till and outwash deposited after 16,400 ^{14}C yr BP, consistent with regional evidence for diachronous growth of the Cordilleran Ice Sheet and the beginning of the Vashon stade.

Keywords: Alpine glaciation; geochronology; North Cascades; Skagit valley; Washington; Evans Creek stade

Introduction

Our understanding of glaciation in British Columbia and Washington State during the Fraser Glaciation (Late Wisconsinan, marine oxygen isotope 2) is based primarily on data from Puget and Fraser lowlands (Figure 3-1; Armstrong et al., 1965; Clague, 1989). Most of the mountains surrounding these lowlands remain unstudied, leaving unanswered important questions about climate change and glacier growth and decay during the late Pleistocene. This chapter reports the results of a study of exposures of fluvial, glacial, and glaciolacustrine sediments in Skagit River valley in the Cascade Range of northern Washington. The sediments contain abundant plant macrofossils that have provided 24 new radiocarbon ages and an environmental record extending from about 32,000 to 16,000 ^{14}C yr BP, making it one of the longest and most detailed for the Fraser Glaciation in the Pacific Northwest (Figure 3-2). The stratigraphic, sedimentologic, and geochronologic information obtained during this study addresses several important questions about the earliest part of the Fraser Glaciation, which in the Cascade Range is named the Evans Creek stade: When did it begin? How long did it last? Were alpine glaciers in Skagit valley in phase with glaciers elsewhere in the Pacific Northwest?

Late Pleistocene setting

Three main stades are recognized within the Fraser Glaciation, which spans the period from about 30,000 to 10,000 ^{14}C yr BP: the Evans Creek, Vashon, and Sumas (Figure 3-2; Armstrong et al., 1965). The Evans Creek stade marks the beginning of the Fraser Glaciation and the end of the Olympia nonglacial interval (60,000 to 30,000 yr BP; Clague, 1981a and 1981b; Gascoyne et al., 1981). Stratigraphic evidence for the Evans Creek stade in the Cascade Range has been reported at several localities in the Pacific Northwest (Figures 3-1 and 3-2), but the event is poorly dated. At the Evans Creek type section near Mt. Rainier, Carbon Glacier is inferred to have advanced shortly after 25,800 ^{14}C yr BP (Figure 3-1; Crandell and Miller, 1974), yet no radiometric age control is available for the Cascades more than three decades after this seminal study (Kaufman et al., 2004). Alpine glaciers constructed moraines and deposited outwash in Hoh and Queets valleys on Olympic Peninsula during the Hoh Oxbow 3 advance ca. 22,000-19,300 ^{14}C yr BP and during the Twin Creek 1 advance ca. 19,300-18,300 ^{14}C yr BP (Figure 3-1; Thackray, 1999). A piedmont glacier advanced into Fraser Lowland during the Coquitlam stade between 21,300 and 18,700 ^{14}C yr BP (Armstrong and Hicock, 1975; Hicock and Armstrong, 1981; Hicock and Lian, 1995; Lian et al., 2001). Recent work in the eastern Fraser

Lowland indicates that the extent of Coquitlam stade glaciation was more limited there. The Coquitlam stade ended with glacier retreat and deposition of the nonglacial Sisters Creek Formation during the Port Moody interstade between 18,700 and 17,700 ^{14}C yr BP (Armstrong and Hicock, 1975; Hicock and Lian, 1995). Many authors have argued that the Evans Creek and Coquitlam stades are equivalent (Porter, 1976; Alley and Chatwin, 1979; Clague et al., 1980; Hicock and Armstrong, 1981; Porter et al., 1983; Kaufman et al., 2004).

The Vashon stade is defined by expansion of the Cordilleran Ice Sheet south into Fraser and Puget lowlands and the North Cascades Range along the upper Skagit, Pasayten, and Methow valleys (Figure 3-1; Waitt and Thorson, 1983). The Puget lobe of the Cordilleran Ice Sheet reached the mouth of the Skagit valley approximately 15,500 ^{14}C yr BP (Porter and Swanson, 1998), and the Okanagan lobe flowed into upper Skagit valley from the northeast, although the timing of this event is unknown (Waitt, 1977).

Methods

Early Fraser deposits were examined at six localities along Ross Lake and Skagit River between Concrete and Lyman. The most complete sections, near Skymo Creek and Rainbow Point on Ross Lake and at Cedar Grove and Big Boy near Concrete, are described in this paper (Figures 3-1, 3-3, and 3-4). The Ross Lake sections were logged when the reservoir was low during spring drawdown between 2002 and 2006.

Elevations at the Ross Lake sections were determined using a survey level and reservoir level as a datum. All surveys were closed and elevations were not accepted if the error exceeded 1 cm. Elevations at the Skagit River sections were determined with a tape and hand level, using temporary datums established above the river and located on large-scale topographic maps with 12 m contour intervals. Appendix 3-1 lists site coordinates.

Lithostratigraphic units were defined on the basis of color, texture, sorting, sedimentary structures, macrofossils, and contacts (Appendix 3-2). Stratigraphic terms and nomenclature follow Eyles et al. (1983). Age control is provided by radiocarbon ages on plant macrofossils and by a tephra in the lower part of the Big Boy section. Standard radiometric and AMS radiocarbon dating was done by Beta Analytic Inc. (Miami), the University of California-Irvine, Isotrace Laboratory (Toronto), and Lawrence Livermore Laboratory (Berkeley) (Table 3-1). Microprobe analysis of glass shards separated from tephra at the Big Boy section was performed at Washington State University (Pullman).

The Cordilleran Ice Sheet removed landforms deposited by alpine glaciers during the Evans Creek stade, consequently alpine glaciers of interest in this study were reconstructed using three approaches. First, the locations of termini of the glaciers flowing down Big Beaver and Baker valleys during the Evans Creek stade were inferred from the distribution of buried lacustrine sediments and alpine glacier till in Skagit valley (Figures 3-3 and 3-4). Second, prominent erosion features, including the floors of hanging valleys, truncated valley spurs, and the upper limits of over-steepened valley walls, were identified on a 10-m digital elevation model, providing a first-order estimate of glacier surface slope and elevation. Third, ice thickness (**h**) was checked using a variant of the basic glacier flow law (Paterson, 1981):

$$\mathbf{h = \tau_0 / F\ (\rho g \sin \alpha)}$$

where ρ is ice density, **g** is gravitational acceleration, τ_0 is basal shear stress, $\sin \alpha$ is ice surface slope estimated from trimlines or valley slope, and **F** is a shape factor. I assume perfect ice plasticity, τ_0 = 50-150 KPa, and **F** = 0.65-0.74. **F** was determined by measuring valley width and ice depth at the centerline of the former glacier at one or more locations per glacier (Paterson, 1981).

Uncertainties in glacier reconstructions stems from several factors, including modification of the Evans Creek landscape by the Cordilleran Ice Sheet and volcanism at Mt. Baker. Holocene volcanic deposits in Baker valley are more than 200 m thick, and the area above 2230 m asl formed in postglacial time (Hildreth et al., 2003). The reconstructed Evans Creek glaciers are the smallest that could dam Skagit River and impound lakes, and they may have extended farther downvalley. However, well logs and a single radiocarbon age and Stratigraphy at the Heller (1980) Prevedell Road section at Lyman indicate that the Evans Creek stade Baker Glacier did not extend much farther downvalley than Birsdview. The distribution of silt and clay sediments in two sections and deep well logs constrain the upvalley extent of the glacier to the Cedar Grove Section.

Stratigraphy

Early Fraser Glaciation fluvial, glaciolacustrine, and glacial sediments are exposed at two main sites near Ross Lake at 465-490 m elevation (Figure 3-1). They are preserved down-valley of prominent bedrock spurs, which protected them from erosion by the south-flowing Cordilleran Ice Sheet. Each of the exposures has a unique stratigraphy, but sedimentology and radiocarbon ages facilitated correlation. Early Fraser Glaciation deposits are also exposed at the Big Boy and

Cedar Grove sites along Skagit River near Concrete, Washington, about 75 km southwest of Ross Lake (Figure 3-1).

Rainbow Point

Rainbow Point is a bedrock spur extending west into Ross Lake (Figure 3-3). Five sections were measured over a horizontal distance of 80 m along the shoreline directly south of Rainbow Point. Plant macrofossils are rare at this site, but three radiocarbon ages define a depositional record spanning 14,000 years, from about 32,000 to 18,000 ^{14}C yr BP (Table 3-1, Figure 3-5).

The lower third of the section contains several gravel units with thin silt and sand beds containing charcoal (Figure 3-5). Unit 1 is poorly sorted cobble gravel with subrounded clasts of a variety of lithologies in a cemented sand matrix. An AMS radiocarbon age of 31,760 ^{14}C yr BP on a piece of charcoal in a thin silt bed (unit 2) is the oldest age obtained in this study (Table 3-1). Units 3 and 5 are poorly sorted, sandy pebble gravels, with subround to subangular clasts of phyllite, chert, granite, and greenstone. Unit 4 includes thin beds of tan, laminated silt and brown sand. Unit 6 is a massive cobble gravel bed that is distinct from most of the gravels at this site because of its coarse texture and mixed clast lithology, which indicate deposition by a larger stream in a fluvial setting.

Overlying the gravel-dominated fluvial sequence at the base of the section is a thick sequence of stratified sand and silt. Unit 7 is sand with a single thin bed of brown to red silt. An AMS age of 23,620 ^{14}C yr BP on a piece of charcoal from this silt bed marks the approximate time of the change from a fluvial environment to a glaciolacustrine one (Table 3-1). Rhythmically stratified silt and clay beds become thicker and more numerous up-section; units 8 and 10 are each about 1.2 m thick, whereas silt units lower in the section are less than 30 cm thick. Silt-clay couplets in unit 8 number in the hundreds and range in thickness from 1 mm to 5 cm. The silt units are separated by massive, poorly sorted, sandy pebble gravels (units 9, 11, and 13). A 16-cm-thick gray silt bed within unit 11 at 489 m asl contains plant macrofossils that yielded a radiocarbon age of 18,020 ^{14}C yr BP (Table 3-1). A conspicuous, cross-stratified sand bed, abruptly bounded above and below by silt, can be traced laterally for 80 m (Figure 3-6).

Rhythmically laminated silt of unit 11 is overlain by massive and cross-bedded sand and pebble gravel (unit 13). The uppermost unit at the Rainbow Point section is diamict (unit 14), which unconformably overlies the stratified sequence. Unit 14 is interpreted to be Vashon till based on stratigraphic position, clast texture, lithology, and matrix support of clasts. Sediments beneath the till are cut by south-dipping clastic dikes and faults, which are interpreted as glaciotectonic structures.

Skymo Creek

Early Fraser Glaciation deposits are exposed in a section on the west side of Ross Lake, 3 km south of the mouth of Skymo Creek (Figures 3-1 and 3-3). The deposits crop out in a small gully over a vertical distance of 25 m (Figure 3-5).

The lowest exposed sediments are weathered, poorly sorted, clast-supported sandy pebble gravel with sand lenses cemented with iron and manganese oxides (unit 1, Figure 3-5). Clasts are subrounded and of mixed lithology. A piece of wood from a 4-cm-thick silt layer (unit 3) at the top of the gravel yielded a radiocarbon age of 23,970 ^{14}C yr BP (Table 3-1). The gravel is overlain by alternating units of silt and diamict (units 2-8; Figure 3-7). Units 2, 5, and 7 diamicts contain abundant local, angular phyllite clasts supported by a silty sand matrix. Long axes of clasts dip toward the valley center. The diamict layers are debris flow deposits that interrupted fine-grained glaciolacustrine deposition and likely originated on the adjacent valley wall.

Units 4, 6, and 8 are massive to stratified silt and sand (Figures 3-5 and 3-7). Sand beds in units 4 and 6 are 10-20 cm thick; some of them contain south-dipping cross-beds. Sand decreases, and silt increases, up-section, and individual silt layers thin from 50 mm in unit 4 to 3-5 mm in unit 8. Rhythmically laminated silts of units 6 and 8 are similar to the stratified silt in the upper part of the Rainbow Point section and, like them, were deposited in a low-energy glaciolacustrine environment. Several radiocarbon ages from units 2, 6, and 8 constrain the time of glaciolacustrine deposition to the period 23,970 to 20,310 ^{14}C yr BP (Table 3-1, Figure 3-5).

Unit 9 is a matrix-supported, weakly stratified diamict with abundant, subrounded, striated clasts in a dense silt matrix. Cobbles and boulders within the diamict are mainly granitic and sedimentary lithologies of northern provenance. The section is capped by a thick, dense, matrix-supported diamict, which forms a bluff above the full-pool water level of Ross Lake (unit 10). Based on stratigraphic position, sediment texture, density, the presence of striated clasts, and clast fabric and lithology, this diamict is interpreted to be till deposited by the Cordilleran Ice Sheet. A 30-cm-wide clastic dike dipping 50 degrees to the south penetrates units 6, 7, and 8 (Figure 3-5). Considering the 18,020 ^{14}C yr BP age obtained from the laminated silt at Rainbow

Point, ice sheet glaciation may have removed more than 2000 years of glaciolacustrine sediment at the Skymo section.

Roland Point

A dense, weathered diamict is exposed just south of Roland Point on the east side of Ross Lake. More than 60 percent of 147 clasts examined are either Skagit Gneiss or granodiorite, the two main rock types in Big Beaver valley (Table 3-2; Tabor et al., 2003). In contrast, less than 28% of the clasts in till attributed to the Cordilleran Ice Sheet 1 km east of Roland Point are gneiss and granodiorite (Table 3-2). Although there are no radiocarbon ages on the weathered diamict at Roland Point, the local provenance and matrix support of the subround clasts, and its location indicate that it is till deposited by the Big Beaver Glacier during the Evans Creek stade.

Cedar Grove

Evans Creek stade sediments are exposed along the south bank of Skagit River near the community of Cedar Grove (Figures 3-1 and 3-4). Dense, deformed, stratified, fine sand and silt beds (unit 2) at the base of the section are successively overlain by sand and gravel, a boulder diamict, and more sand and gravel (Figure 3-8).

Unit 1 at the base of the section is a 20-cm-thick silt bed with abundant plant detritus, including flattened sticks and pieces of wood. A large stick from this bed returned an AMS radiocarbon age of 25,040 ^{14}C yr BP (Table 3-1, Figure 3-8). Overlying the organic bed is a 4-m-thick sequence of stratified sand and silt (unit 2). Unit 3 ranges in thickness across the section from 4 to 5 m and comprises cross-bedded sand and gravel filling channels. Gravel clasts are well rounded and are mainly andesite from Mt. Baker and granodiorite from the Chilliwack batholith in upper Baker valley (Tabor et al., 2003). Together, units 2 and 3 comprise a fining-upward outwash sequence.

Unit 3 is overlain by a 30-cm-thick bed composed almost entirely of organic material (unit 4). A flattened stick from this bed yielded an AMS radiocarbon age of 20,730 ^{14}C yr BP. (Table 3-1). Unit 5 is a boulder diamict that unconformably overlies units 3 and 4 (Figure 3-9). The diamict contains boulders up to 3 m in diameter. Clasts are mainly granodiorite and greenschist derived from the Baker River watershed (Table 3-3). Clast lithology and size indicate that the diamict is till deposited by Baker Glacier. The top of the section is poorly exposed, but appears to consist mainly of stratified sand and gravel.

Big Boy

The Big Boy section is a 29-m-high, near-vertical cliff on the south side of Skagit River, 5 km upstream of the Cedar Grove section (Figures 3-4, 3-8, and 3-10). The deposits underlie an extensive terrace and consist of glacial, glaciolacustrine, and glaciofluvial sediments dating to the latter half of the Evans Creek stade.

The base of the section, which is below the low-water level of Skagit River, is organic-rich silt (unit 1). A small piece of wood from these sediments yielded an AMS radiocarbon age of 19,940 ^{14}C yr BP (Table 3-1). Unit 2 at the upstream end of the section consists of sand and pebble gravel that extends only 10 m horizontally down river. Unit 3 is a 10-cm-thick peat bed containing abundant small pieces of wood.

Silt beds 1, 7, 9, 11, and 13 are brown or blue gray in color, extremely dense, have wavy or irregular contacts, and show evidence of soft-sediment deformation (Figure 3-8). Isolated, subrounded dropstones disturb underlying silt beds. Silt and fine sand beds in unit 5 range from 4 to 16 mm thick, whereas rhythmic layers in unit 7 are markedly thinner and finer-grained. In contrast, rhythmites in units 9, 11, and 13 are 7-15 cm thick. An Engelmann spruce cone in unit 13 yielded an age of 16,400 ^{14}C yr BP (Table 3-1, Figure 3-8).

Silt and sand units in the lower half of the Big Boy section are interbedded with sandy pebble gravel. Gravel units near the base of the eastern part of the section are 5-15 cm thick and are separated by very dense silt beds of similar thickness (Figure 3-11). Higher in section, gravel fills channels incised several metres into underlying silt beds. Clasts are angular, 2-5 mm in diameter, and are derived primarily from the Chilliwack Group in this part of Skagit valley (Tabor et al., 2003). Together, these features indicate deposition in a shallow lacustrine or deltaic setting (Ashley et al., 1985), probably by paleo-Jackman Creek (Figure 3-4). Five radiocarbon ages from silt beds in the lower half of the Big Boy section (units 1-13) indicate that it was deposited in a 3500 year period between about 19,940 and 16,400 ^{14}C yr BP (Table 3-1, Figure 3-8).

A 2-3-mm-thick, dacitic ash layer is present in unit 7 (Figures 3-8 and 3-10). Its glass composition is similar to that of tephra produced by several eruptive phases at Mt. St. Helens, including sets J, S, and M (Table 3-4; Busacca et al., 1992). Considering the age of the enclosing sediments and chemical similarities with the St. Helens M and Mc tephra, it appears to be a product of the Cougar eruptive period (Mullineaux, 1986; Pringle, 1993). The same tephra has been found in the southern Washington Cascades and eastern Washington. It has been previously dated to between 20,350 and 18,530 ^{14}C yr BP (Busacca et al., 1992; Pringle, 1993). The new radiocarbon ages from the Big Boy section more tightly constrain the eruption to after 18,810 (Table 3-1, Figure 3-8).

The upper middle part of the Big Boy section consists mainly of planar and cross-bedded sand and gravel that unconformably overlie the glaciolacustrine sediments (Figures 3-8 and 3-9). Most clasts in unit 14 gravel are granitic and metamorphic lithologies derived from upper Skagit valley east of Marblemount (Figure 3-1). Silt beds within unit 14 have no organic material and are massive, in contrast to fine-grained sediments in the lower half of the section.

The Big Boy section is capped by a matrix-supported diamict with boulders up to 2 m in diameter (unit 15). Large silt rip-up clasts occur near the base of the unit (Figure 3-8). The upper part of the diamict contains lenses of sand and gravel. Its age, stratigraphic position, clast lithology, and matrix support indicate that this unit is Vashon till.

Glacier reconstructions

The distributions of glacial lake sediments and alpine drift delineate the approximate minimum extent of Evans Creek stade glaciers on the floor of Skagit valley. The reconstructed Baker Glacier is 60 km long and extended across the floor of Skagit valley (Figure 3-4). Basal shear stresses of 120 KPa or more are required to build a glacier to thicknesses matching trimlines and other ice-marginal landforms in the valley. Ice was approximately 400 m thick on the floor of Baker valley and thicker where tributary glaciers coalesced (Figure 3-4). Big Beaver Glacier was 24 km long and terminated at about 200 m asl (Figure 3-3). It was several hundred metres thick from lower Luna and McMillan creeks down to the mouth of the valley.

Discussion

Glacial lakes Concrete and Skymo

Stratified silt, sand, and clay at the Big Boy, Skymo, and Rainbow Point sites are interpreted to be glacial lake deposits. Striated, subrounded dropstones in these sediments were probably deposited from icebergs (Ovenshire, 1970). Rhythmically stratified silts may be varves deposited in relatively deep water from overflow, underflow, and interflow plumes (Ashley et al., 1985).

Alpine glaciers and their deposits blocked Skagit valley during the Evans Creek stade, impounding lakes that persisted for thousands of years. Till and outwash were left by Evans Creek glaciers at Roland Point and at the Cedar Grove section downstream of the glaciolacustrine deposits. Thick silt, sand and clay deposits are found only above these tributary valleys, and previous workers have argued that Evans Creek tributary glaciers advanced into Skagit valley (Waitt, 1977; Heller, 1980). The alternative explanation, that large landslides dammed the Skagit at two locations at the same time for extended periods, is unlikely. There is no evidence for large landslides downstream of the stratified, fine-grained sediments. Furthermore, landslide dams are unlikely to survive along a major river for many thousands of years, as would be required for lakes Skymo and Concrete (Costa and Schuster, 1988). No large eruptive events on Mt. Baker have been reported for Evans Creek time (Hildreth et al., 2003; Scott et al., 2003), and it is very unlikely that an unrecognized lahar dammed Skagit River for thousands of years.

When Baker Glacier advanced across Skagit valley after 20,730 ^{14}C yr BP, it reached the divide between Skagit and Finney creeks and blocked Skagit River, creating glacial Lake Concrete (Figure 3-4). Sediments in the lower half of the Big Boy section record nearly 4000 years of continuous glaciolacustrine sedimentation. Well logs indicate that 'blue clay' up to 40 m thick underlies the valley between Concrete and Marblemount (Figure 3-12), thus Lake Concrete extended at least 10 km up Skagit valley from the glacier dam. The lower of two possible outlets is Sauk River at Darrington at 150 m asl (Figures 3-1 and 3-4). However, an alpine glacier flowing down the Sauk valley may have blocked this route during the Evans Creek stade. The higher outlet is the Finney–Skagit divide, which continues as an ice-marginal channel along Finney Creek and around the mouth of Baker valley (Figure 3-4). The present low point on this divide is 177 m asl, but thick Vashon-age drift obscures the Lake Concrete outlet. With either outlet, the depth of Lake Concrete was never more than 80 m, not enough to float the ice dam and periodically drain the lake.

The Big Beaver Glacier dammed Skagit River at Roland Point, 5 km south of Rainbow Point, approximately 24,000 ^{14}C yr BP (Figure 3-3), creating glacial Lake Skymo (Figure 3-3). Lake Skymo deposits are present over an area of 40 km^2, approximately half the area of modern Ross Lake. The distribution and age range of the deposits indicate that Lake Skymo inundated the entire valley and was not a short-lived, ice-marginal feature restricted to one side of the valley. Lake Skymo overflowed across the low area east of Roland Point at 510 m asl (Figure 3-3). When this outlet was active, Lake Skymo was no more than 40 m deep (outlet elevation minus elevation of lowest glaciolacustrine sediment). If this outlet was blocked, the lake would have overflowed to the north via Klesilkwa Pass at 560 m asl, and lake depth could have been as much as 90 m. Glacial lakes Concrete and Skymo had stable bedrock outlets, which allowed fine-grained sediment to accumulate without being eroded due to sudden lake-level changes or drainage through unstable ice dams (Thorarinsson, 1939; Atwater, 1986).

Average sedimentation rates in glacial Lake Skymo can be estimated using the radiocarbon ages and assuming no significant breaks in sedimentation (Table 3-1; Figure 3-5). About 2.5 m of silt (unit 8) at the Skymo section accumulated in about 600 years, giving an average sedimentation rate of 4.3 mm/yr. At Rainbow Point, 10.8 metres of sediment accumulated in 6905 years, an average rate of 1.6 mm/year. Poor exposure and the presence of multiple pebble gravel beds suggest there are unidentified disconformities in the Rainbow Point section. Twenty metres of fine-grained sediment accumulated in glacial Lake Concrete in 4100 years, an average rate of 4.9 mm/yr (Table 3-1; Figure 3-8).

Sedimentation rates of 4-5 mm/yr are low in comparison to rates of 10-100 mm/year reported from contemporary montane lakes in British Columbia (Gilbert, 1975; Gilbert and Desloges, 1992). However, no compensation was made for compaction of the glaciolacustrine sediments by the Cordilleran Ice Sheet in these estimates, thus sedimentation rates may have been higher. Also, meltwater and sediment from the Big Beaver and Baker glaciers may have bypassed the lakes (Figures 3-3 and 3-4), causing them to function more as distal glacial lakes than ice-marginal ones (Ashley et al., 1985).

Deposition of silt and clay at Rainbow Point was interrupted by high-energy flows that left beds of massive and cross-bedded sand (Figure 3-6). The sand beds were deposited by either large subaqueous grain flows or outburst floods. Atwater (1986) interpreted similar sediments in the Sanpoil valley in eastern Washington as flood beds that entered glacial Lake Columbia during recurrent outbursts from glacial Lake Missoula. Mathews (1968) and Riedel et al. (2007) have suggested that water impounded by the Cordilleran Ice Sheet in the Similkameen and Fraser valleys in British Columbia drained south into upper Skagit valley early in the Vashon stade (Chapter 2). Outburst floods from lakes in these valleys may also have flowed into Skagit valley.

Extent of Evans Creek alpine glaciers

Reconstructed alpine glaciers are 40-50 m thick on steep slopes along the flanks of Mt. Baker and at valley heads where sliding velocities were presumably high (Figure 3-3; Chapter 5). These estimates are in agreement with present-day ice thicknesses at Mt. Rainier (Hodge, 1974) and Mt. Baker (Harper, 1992). The relation between ice thickness and surface slope suggested for the Evans Creek glaciers on Mt. Baker is also consistent with that for similar size late Wisconsinan glaciers in northern Yellowstone National Park (Pierce, 1979). On valley floors and in areas of convergent flow, paleo-ice thicknesses were several hundred metres.

The distribution of glaciolacustrine sediments indicates that large parts of Skagit valley were ice-free during the Evans Creek stade. Heller (1980) suggested that ice flowed out of Baker valley and up Skagit valley to Rockport (Figure 3-4). Stratified, fine-grained deposits at the Big Boy section and outwash at the Cedar Grove section show that the glacier could not have extended that far any time after 25,030 ^{14}C yr BP (Figure 3-4). However, ice must have extended far enough into Skagit valley to reach Cedar Grove and the Skagit-Finney divide (Figure 3-4).

Heller (1980) placed the down-valley terminus of the Evans Creek Baker Glacier at the site of a possible alpine till near Lyman (Figure 3-1). A radiocarbon age of 23,500 ^{14}C yr BP was obtained on a silt bed above this diamict (Table 3-1, Figure 3-12). The origin of the diamict at the base of the section remains uncertain, but fine-grained fluvial sediments and Cordilleran Ice Sheet advance outwash and till overlie the dated horizon. Therefore, it is unlikely that an alpine glacier advanced this far down Skagit valley any time after 23,500 ^{14}C yr BP.

Waitt (1977) reconstructed the distribution of Evans Creek glaciers in the upper Skagit River watershed on the basis of valley geomorphology. His Skagit valley glacier system, which included the Big Beaver Glacier, filled the Ross Lake basin as far downstream as Ross Dam. Glaciolacustrine beds of Evans Creek age between Silver Creek and Rainbow Point, however, indicate that alpine glaciers were less extensive than suggested by Waitt (1977) between 23,970 and 18,020 ^{14}C yr BP (Figure 3-3).

Evans Creek stade chronology

Sediments at the Skymo, Rainbow Point, Big Boy, and Cedar Grove sections span the last part of oxygen isotope stage 3 and much of stage 2. Radiocarbon ages place them within the late Olympia nonglacial interval, the Evans Creek (Coquitlam) stade, the Port Moody interstade, and the Vashon stade (Figure 3-13). The 15,000-year record is one of the longest detailed Quaternary records in the Pacific Northwest.

Sand and gravel at the Skymo and Rainbow sections at Ross Lake date between 31,760 and 23,620 ^{14}C yr BP. Clast weathering and iron and manganese oxide cements are characteristic of gravels of this age, including those in the upper Cowichan Head Formation (Armstrong and Clague, 1977) and Bessette Sediments (Fulton, 1965, 1975; Fulton and Smith, 1978). Unit 1 at the Skymo section and units 1-6 at Rainbow Point are interpreted to be paleo-Skagit River channel deposits based on clast size and roundness and northern provenance. These sediments are distinct from finer-grained, more angular gravels deposited by local small tributary streams and debris flow deposits derived from adjacent mountain slopes.

Sand and gravel were deposited on top of stratified silt and sand and an organic bed at Cedar Grove after 25,040 ^{14}C yr BP. This deposit is considered Baker valley outwash because it is dominated by clasts derived from Baker valley. Radiocarbon ages of 24,080, 23,970, and 23,620 ^{14}C yr BP from sites 20 km apart along Ross Lake date initial damming of upper Skagit valley when Big Beaver Glacier reached Roland Point (Figure 3-3). Taken together, the four radiocarbon ages provide the first radiometric age control on the initiation of the Evans Creek stade in the Cascade Range (Figure 3-13; Kaufman et al., 2004). However, alpine glaciers had to have been advancing for some time before they reached positions sufficiently far advanced to block Skagit River, and the beginning of the Evans Creek stade was likely close to Crandell's (1963) inferred date for the beginning of the Evans Creek stade at 25,800 ^{14}C yr BP.

Vegetation became established on early Evans Creek stade drift at Cedar Grove about 20,730 ^{14}C yr BP, following retreat of Baker Glacier. Unit 6, which overlies this dated organic bed, is interpreted to be till deposited by Baker Glacier based on the presence of clasts up to 3 m in diameter, poor sorting, striations on some clasts, and the dominance of Baker valley lithologies (Figure 3-9). It records a readvance of Baker Glacier during the last half of the Evans Creek stade (Figure 3-13). Lacustrine deposition continued until 16,400 ^{14}C yr BP at the upstream Big Boy section, indicating that Baker Glacier and/or its drift dammed Skagit River late in the Evans Creek stade for 4000 years.

Evidence for two Evans Creek stade alpine glacier advances in the study area is consistent with observations elsewhere in the region and globally (Figure 3-13). Hoh Oxbow 3 drift on Olympic Peninsula was deposited between 22,000 and 19,000 ^{14}C yr BP, although the maximum age is based on a rough estimate of the duration of a previous advance (Thackray, 2001, p. 267). Twin Creek 1 drift in Hoh valley was deposited between 19,000 and 18,300 ^{14}C yr BP. Leavenworth I and II moraines were constructed between 20,000 and 16,000 ^{36}Cl yr BP (Kaufman et al., 2004). Coquitlam drift was deposited in the western Fraser Lowland and adjacent valleys in the southern Coast Mountains between 21,300 and 18,700 ^{14}C yr BP, roughly in-phase with the later Evans Creek advance in Skagit valley (Hicock and Armstrong, 1981; Hicock and Lian, 1995). Pierce et al. (1976) used obsidian hydration dating to show that Pinedale glaciers in the Rocky Mountains remained near their maximum limits between 20,000 and 15,000 yr BP. Sturchio et al. (1994) used uranium-series ages to date two late Wisconsinan advances of northern Yellowstone glaciers to between 30,000 and 22,500 yr BP and between 19,000 and 15,500 yr BP. Licciardi et al. (2001) reported cosmogenic ages for the late Pinedale terminal moraines of the northern Yellowstone outlet glacier as young as 16,200 ^{10}Be yr BP. Lobes of the Laurentide Ice Sheet attained advanced positions between 25,000 and 18,000 ^{14}C yr BP (Mickelson and Colgan, 2004). Porter (2001) observed closely nested alpine moraines constructed between 27,000 and 16,000 ^{14}C yr BP in the tropics.

The 16,400 ^{14}C yr BP age from upper glacial Lake Concrete sediments is a minimum age for the end of the Evans Creek stade, although evidence presented in Chapter 4 indicates it may have ended earlier. The Vashon stade began after 17,700 ^{14}C yr BP in the lower Fraser valley of British Columbia (Armstrong et al., 1965; Clague, 1981; Ward and Thomson, 2004). Vashon drift was deposited in upper Skagit valley after 17,400 ^{14}C yr BP and in lower Skagit valley after 16,333 ± 60 ^{14}C yr BP, consistent with diachronous growth of the Cordilleran Ice Sheet (Table 3-1, Figure 3-13). Clague et al. (1988) presented evidence that lower Chilliwack valley near the British Columbia-Washington border (Figure 3-13) was ice-free until about 16,600 ^{14}C yr BP. Porter and Swanson (1998) constructed a detailed chronology of the advance and retreat of the Puget lobe of the Cordilleran Ice Sheet. Using their advance rate of 135 m/yr, the ice sheet did not reach the mouth of the Skagit valley until approximately 15,500 ^{14}C yr BP and the mouth of the Baker valley until several hundred years later. These dates are consistent with the youngest radiocarbon ages and stratigraphy at the Big Boy section.

Deposition of mixed lithology gravels after 16,400 ^{14}C yr BP at the Big Boy section indicates that lower Skagit valley was free of alpine glaciers before the Cordilleran Ice Sheet reached the mouth of the valley approximately 1000 years later (Porter and Swanson, 1998). Mackin (1941), Crandell (1963), Armstrong et al. (1965), and Clague (1981a, b) suggested that alpine glaciers on the west slope of the Cascades and southern Coast Mountains receded before the Vashon stade. Retreat may correlate with the Port Moody interstade in Fraser Lowland. My results support the conclusion that alpine glaciers in the Olympic Mountains (Thackray, 2001) and elsewhere around the world (Gillespie and Molnar, 1994) were out-of-phase with the Cordilleran Ice Sheet during marine oxygen isotope stage 2.

Conclusions

Several important questions about the timing of the Evans Creek stade are answered by this research:

When did the Evans Creek stade begin?

The Evans Creek stade began approximately 25,040 ^{14}C yr BP in Skagit valley. By 24,000 ^{14}C yr BP, Big Beaver Glacier reached Roland Point and impounded glacial Lake Skymo. Radiocarbon ages from the Big Boy section constrain the maximum age of the regionally important Mt St Helens M tephra to after 18,810 ^{14}C yr BP.

How long did the Evans Creek stade last?

The Evans Creek stade lasted about 8600 years in Skagit valley. Evidence of continued alpine glacier activity through this period includes the Cedar Grove drift sheets deposited after 25,040 ^{14}C yr BP and after 20,730 ^{14}C yr BP, and the persistence of glacial Lake Concrete until 16,400 ^{14}C yr BP. The Puget lobe of the Cordilleran Ice Sheet advanced into lower Skagit valley after 16,300 ^{14}C yr BP, and the Okanagan lobe reached the south end of Ross Lake sometime after 17,400 ^{14}C yr BP.

Were alpine glaciers in Skagit valley in phase with other Evans Creek stade glaciers in the region?

Considering the entire Skagit record, glaciers in the western Olympic Mountains, southern Coast Mountains, and Cascade Range were broadly in phase with Skagit alpine glaciers between 25,040 and 16,400 ^{14}C yr BP (Figure 3-13). Available evidence indicates that the Evans Creek and Coquitlam stades are equivalent. However, better age control on the beginning of the Fraser Glaciation is needed, and the Coquitlam and Skagit deposits represent different styles of glaciation. A growing body of evidence indicates that alpine glaciers fluctuated in response to millennial-scale climate events within the Fraser Glaciation.

Acknowledgements

The research was supported by an NSERC Discovery Grant to John Clague, the Shrum Research Endowment at Simon Fraser University, a grant from the Skagit Environmental Endowment

Commission, and the U.S. National Park Service. GIS support for the glacier reconstructions was provided by Michael Larrabee.

Figures

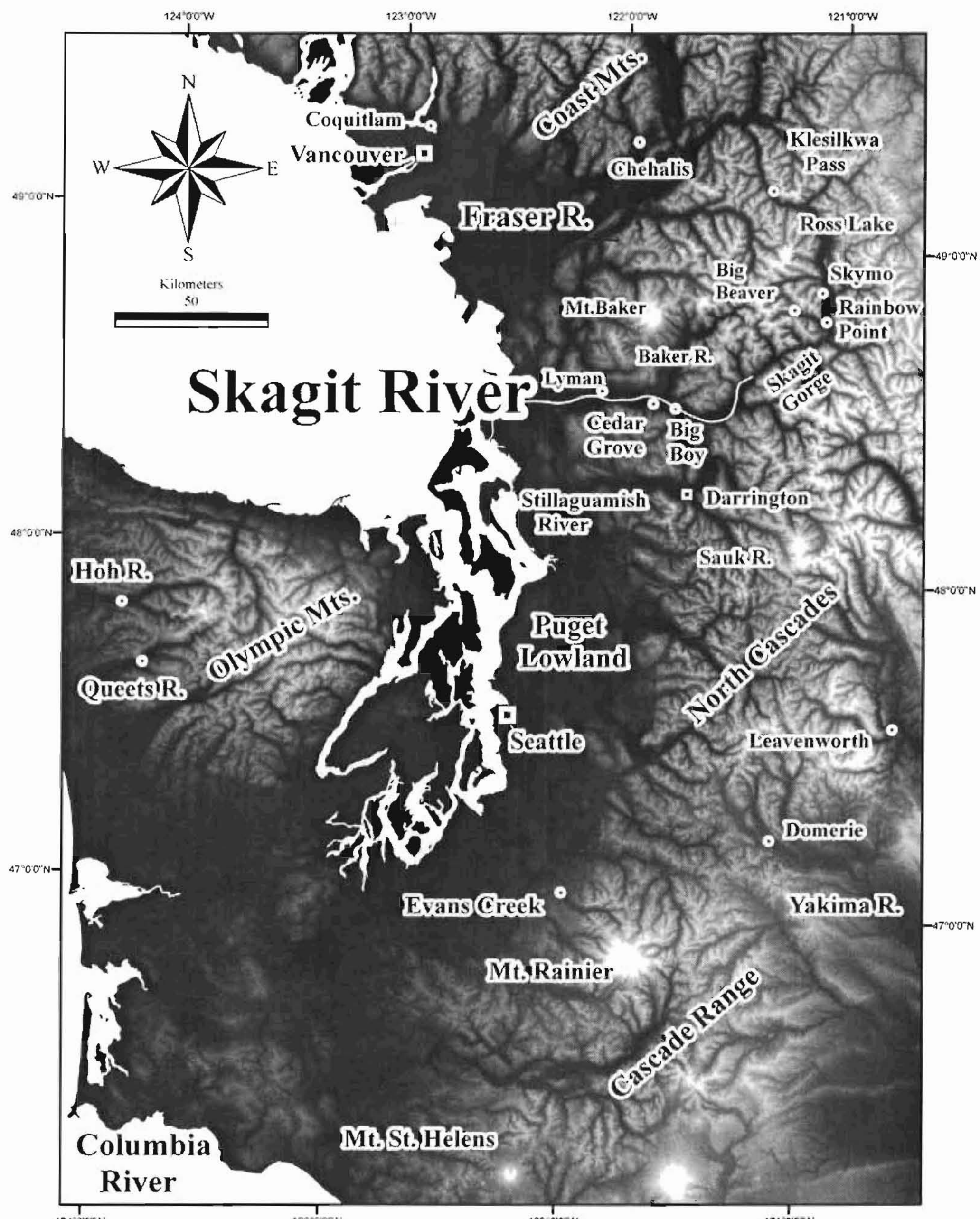

Figure 3-1. Digital elevation model of the Pacific Northwest showing locations of early Fraser Glaciation stratigraphic sites. New stratigraphic sections in the Skagit valley reported in this paper include Cedar Grove, Big Boy, Skymo, and Rainbow Point.

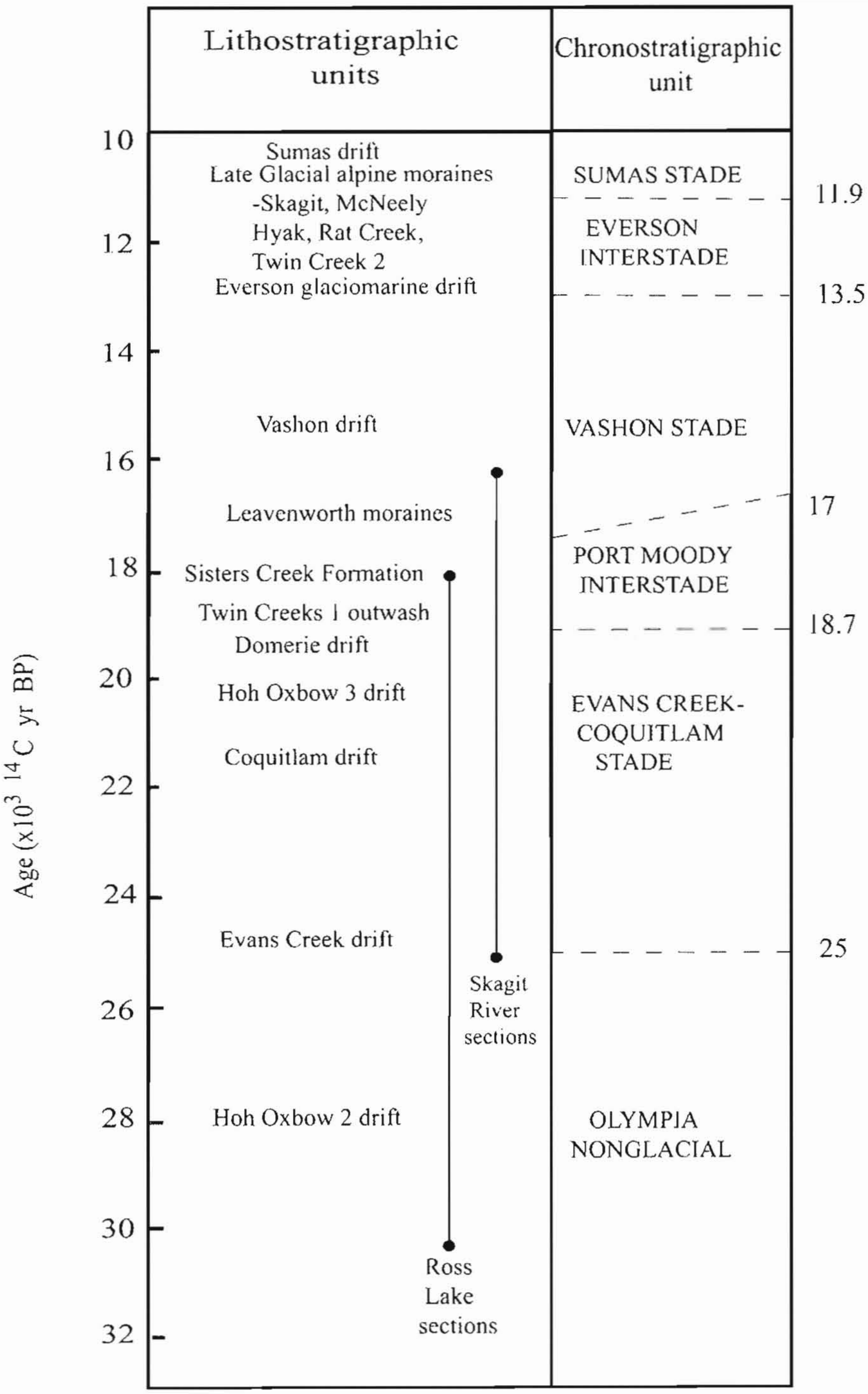

Figure 3-2. Early Fraser Glaciation lithostratigraphic and chronostratigraphic units in the Pacific Northwest (from Crandell, 1963; Armstrong et al., 1965; Porter, 1976; Hicock and Armstrong, 1981; Dethier et al., 1995; Hicock and Lian, 1995; Swanson and Porter, 1997; Porter and Swanson, 1998; Thackray, 2001; Hicock et al., 1999; and Kovanen and Easterbrook, 2001).

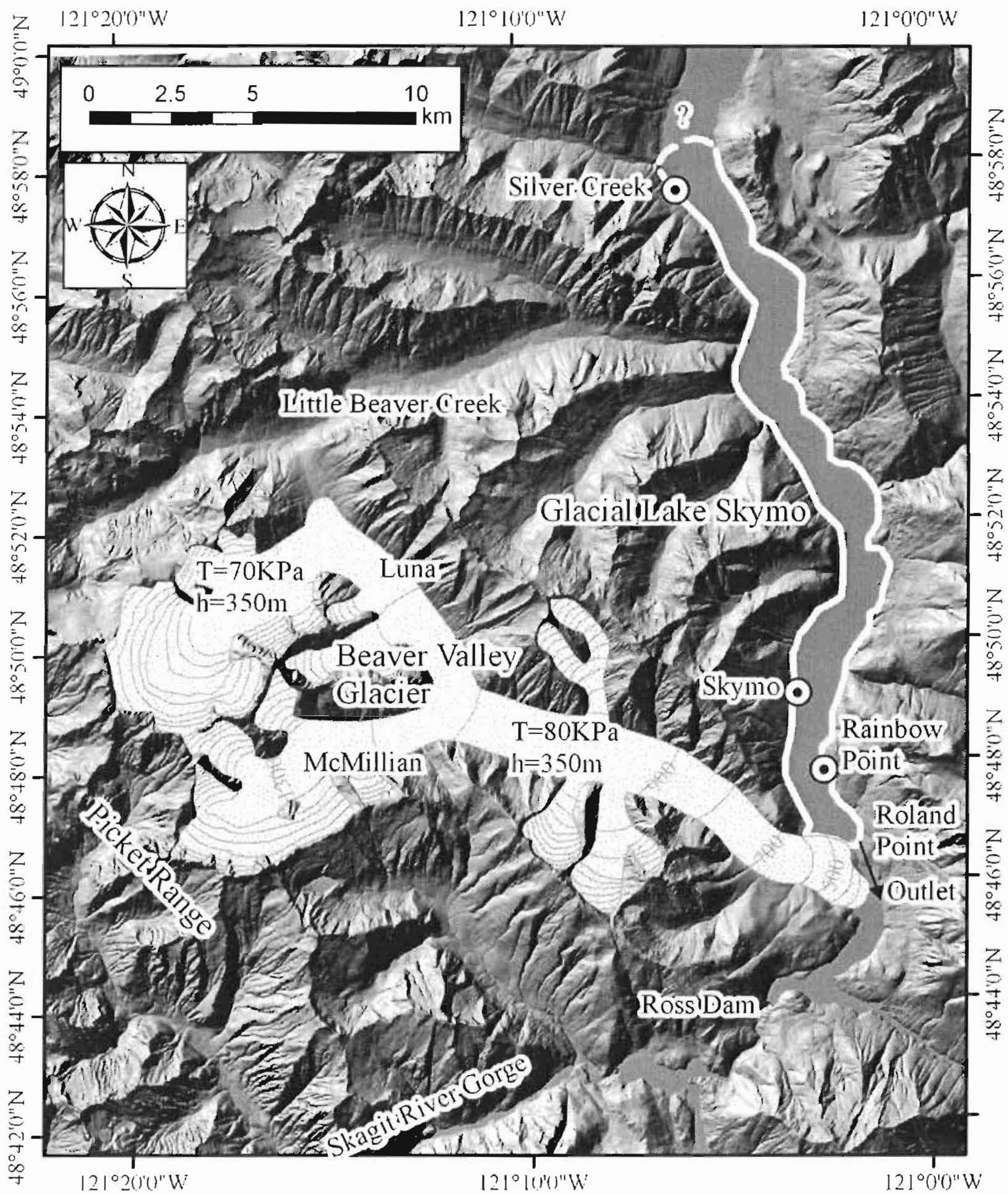

Figure 3-3. Reconstruction of Big Beaver Glacier during the Evans Creek stade. Also shown are key stratigraphic locations and the approximate extent of Glacial Lake Skymo. Ice surface contour interval 100 m. Valley glaciers in adjacent valleys are not shown and were likely extensive, but did not enter Skagit valley.

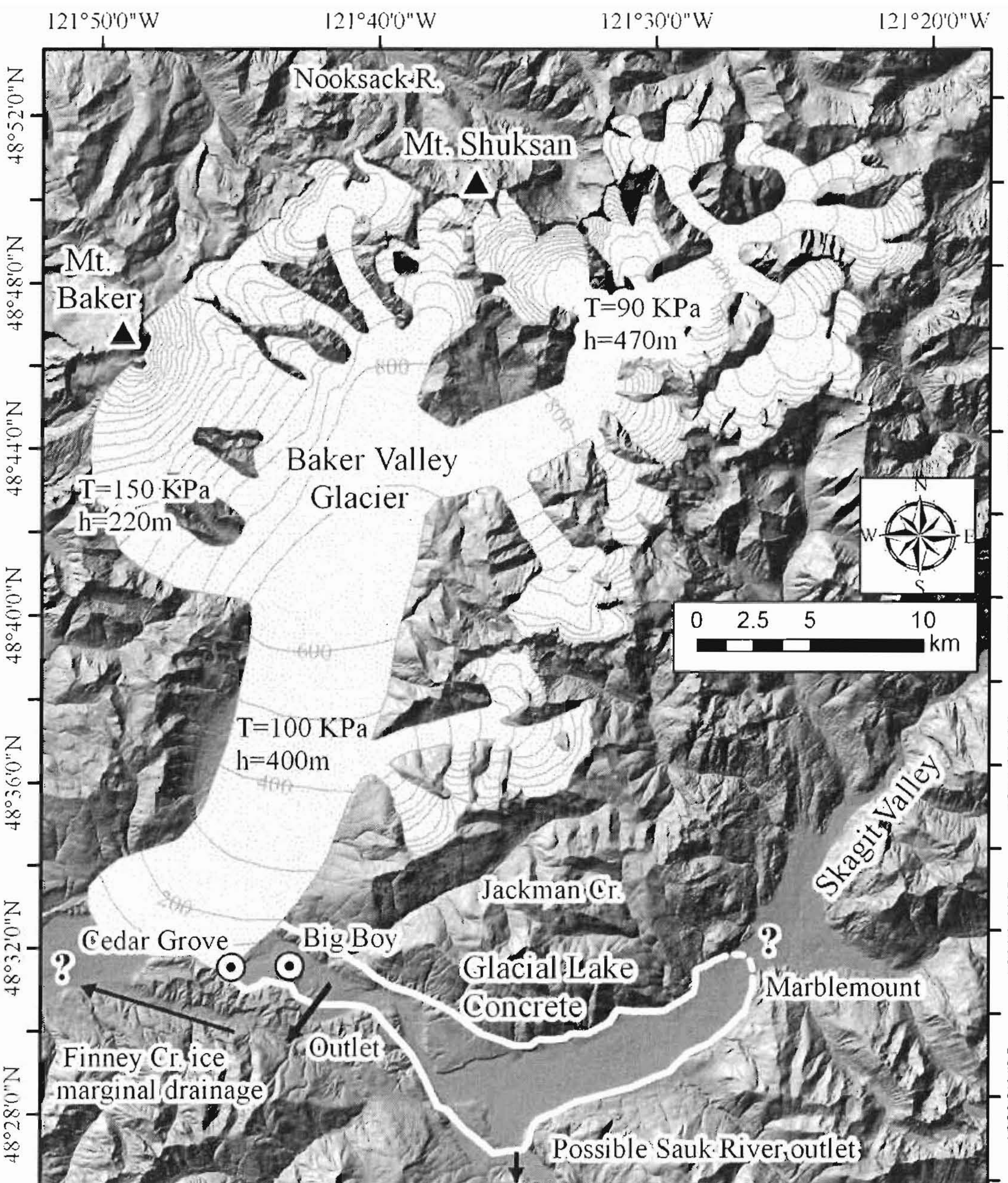

Figure 3-4. Reconstruction of Baker Glacier during the Evans Creek stade. Also shown are key stratigraphic locations and the approximate extent of Glacial Lake Concrete. Ice surface contour interval 100 m.

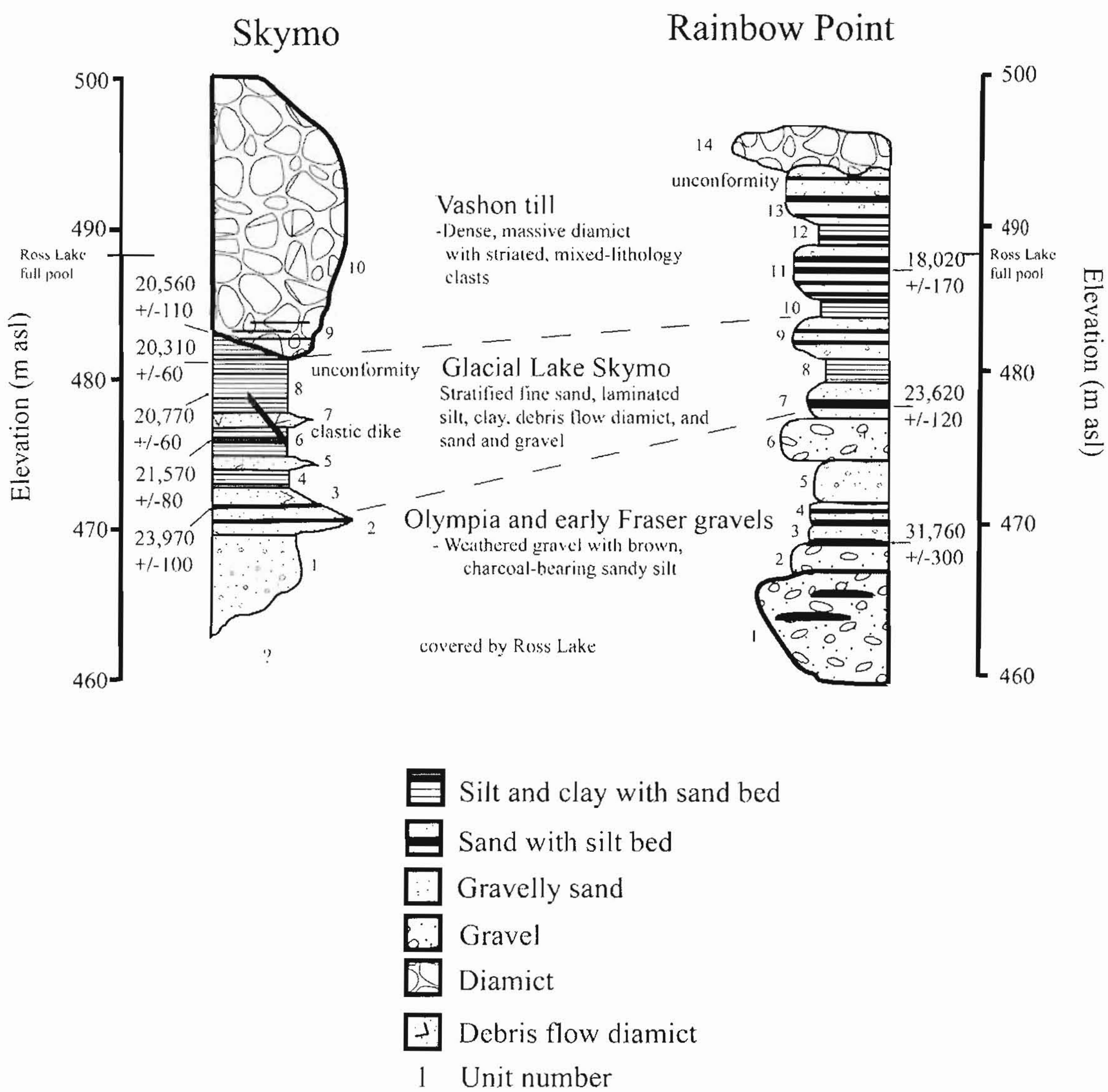

Figure 3-5. Stratigraphy of the Skymo and Rainbow Point sections.

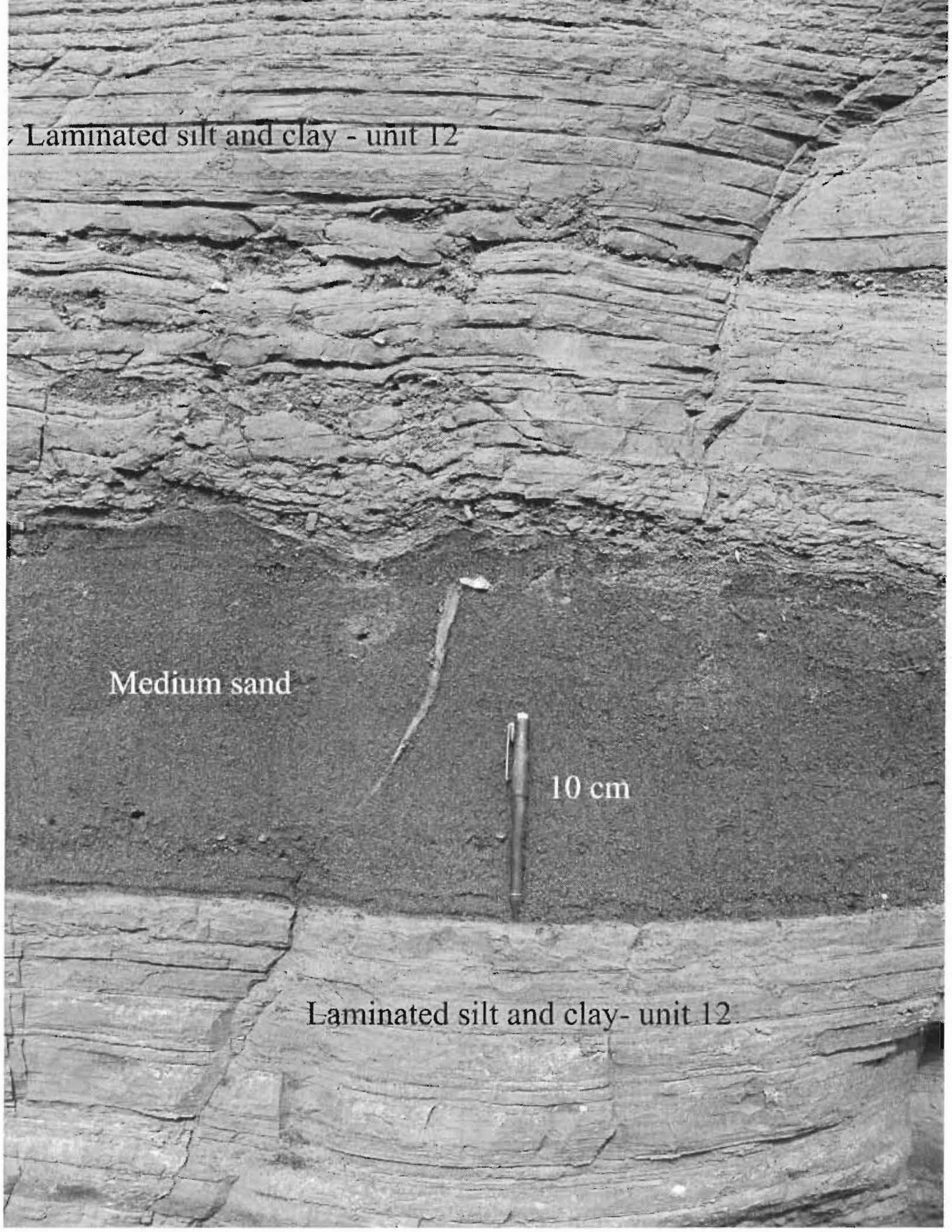

Figure 3-6. Glacial Lake Skymo laminated silt and clay (units 12 a and c), separated by sand (unit 12b) near the top of the Rainbow Point section.

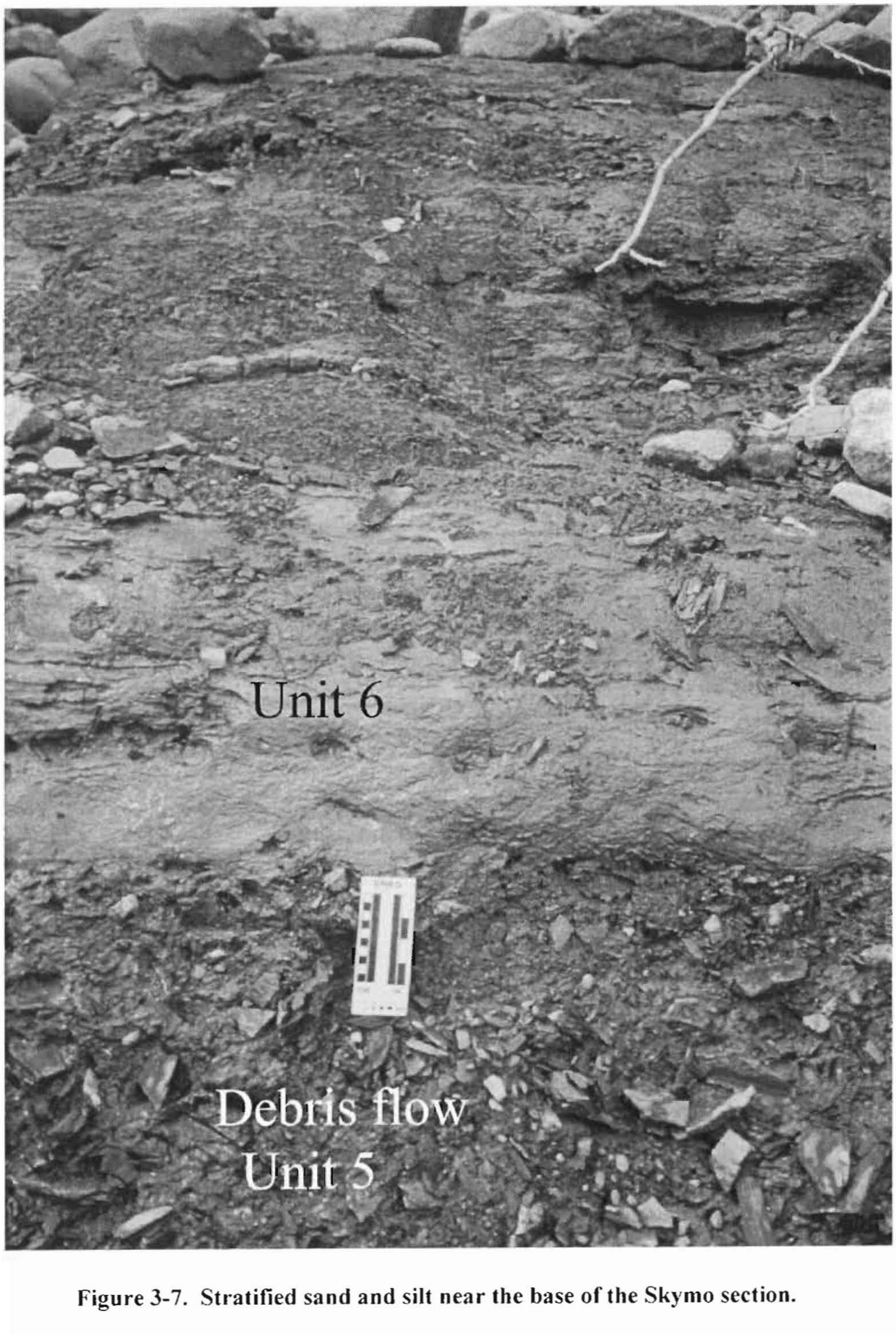

Figure 3-7. Stratified sand and silt near the base of the Skymo section.

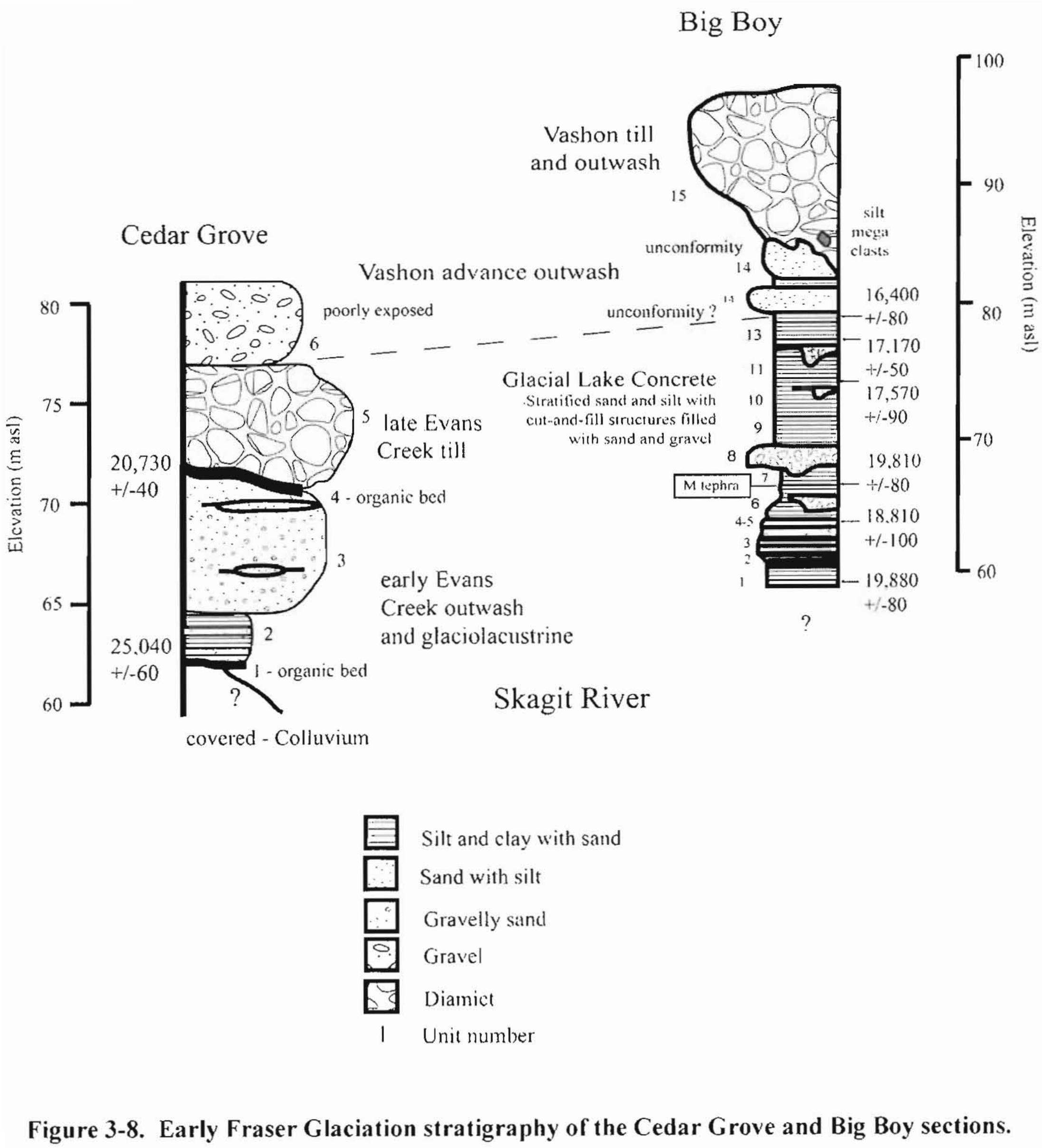

Figure 3-8. Early Fraser Glaciation stratigraphy of the Cedar Grove and Big Boy sections.

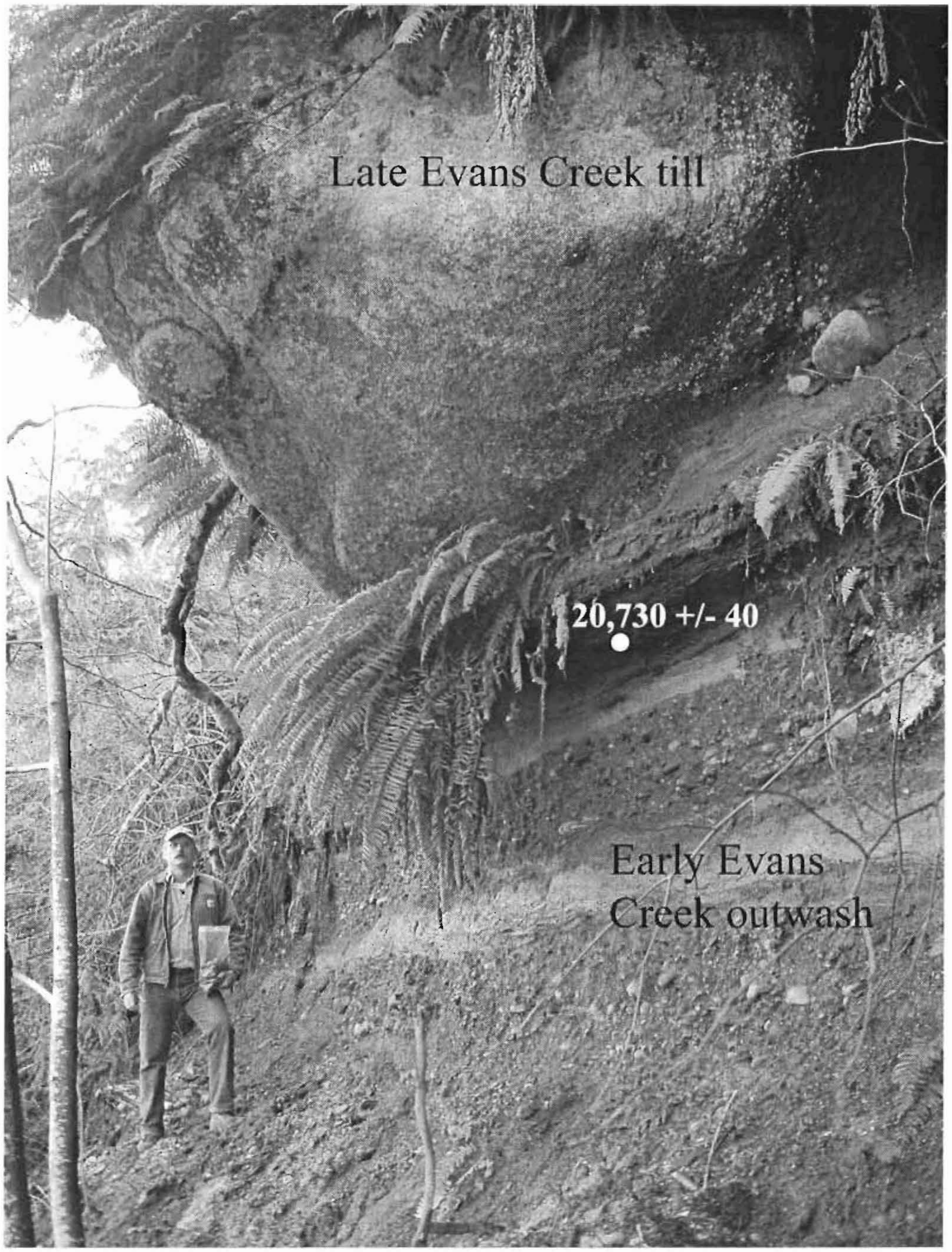

Figure 3-9. Upper portion of the Cedar Grove section.

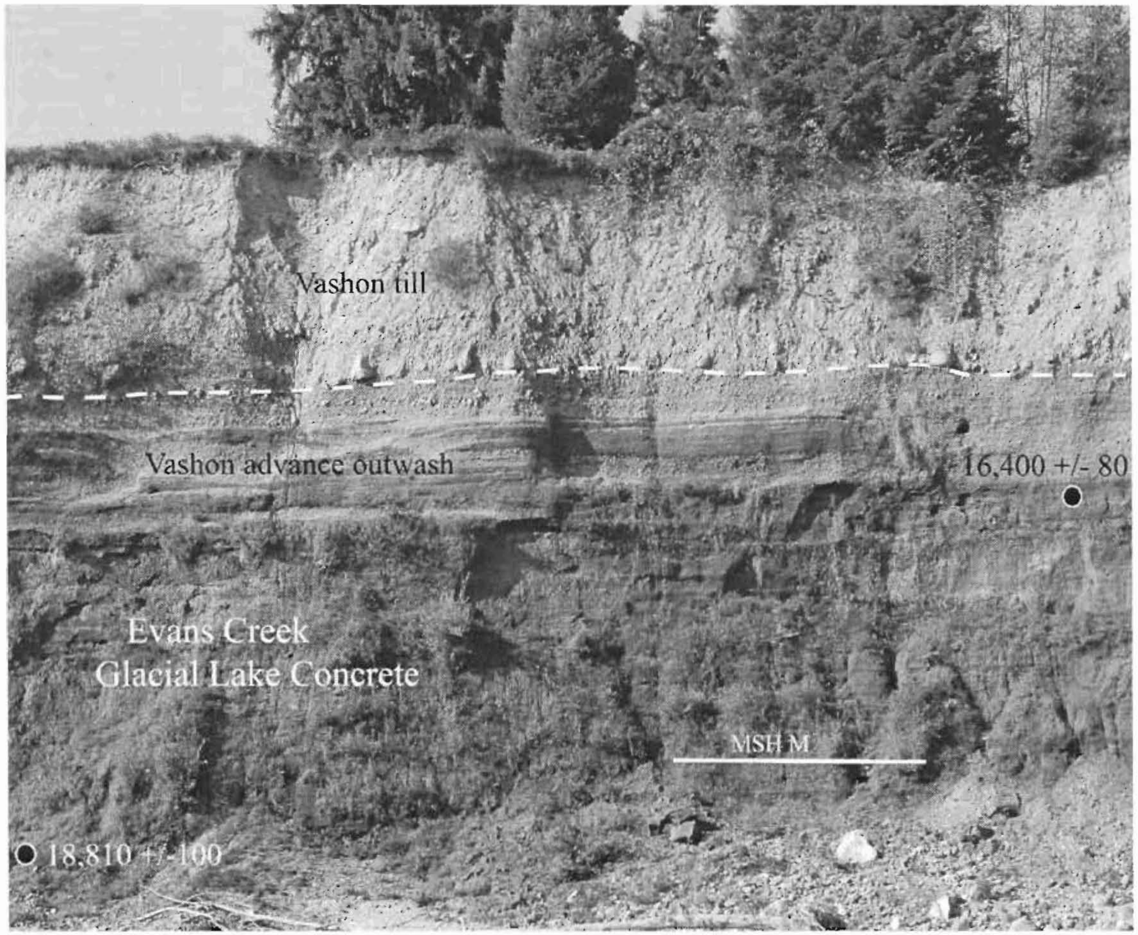

Figure 3-10. The Big Boy section from the north side of Skagit River.

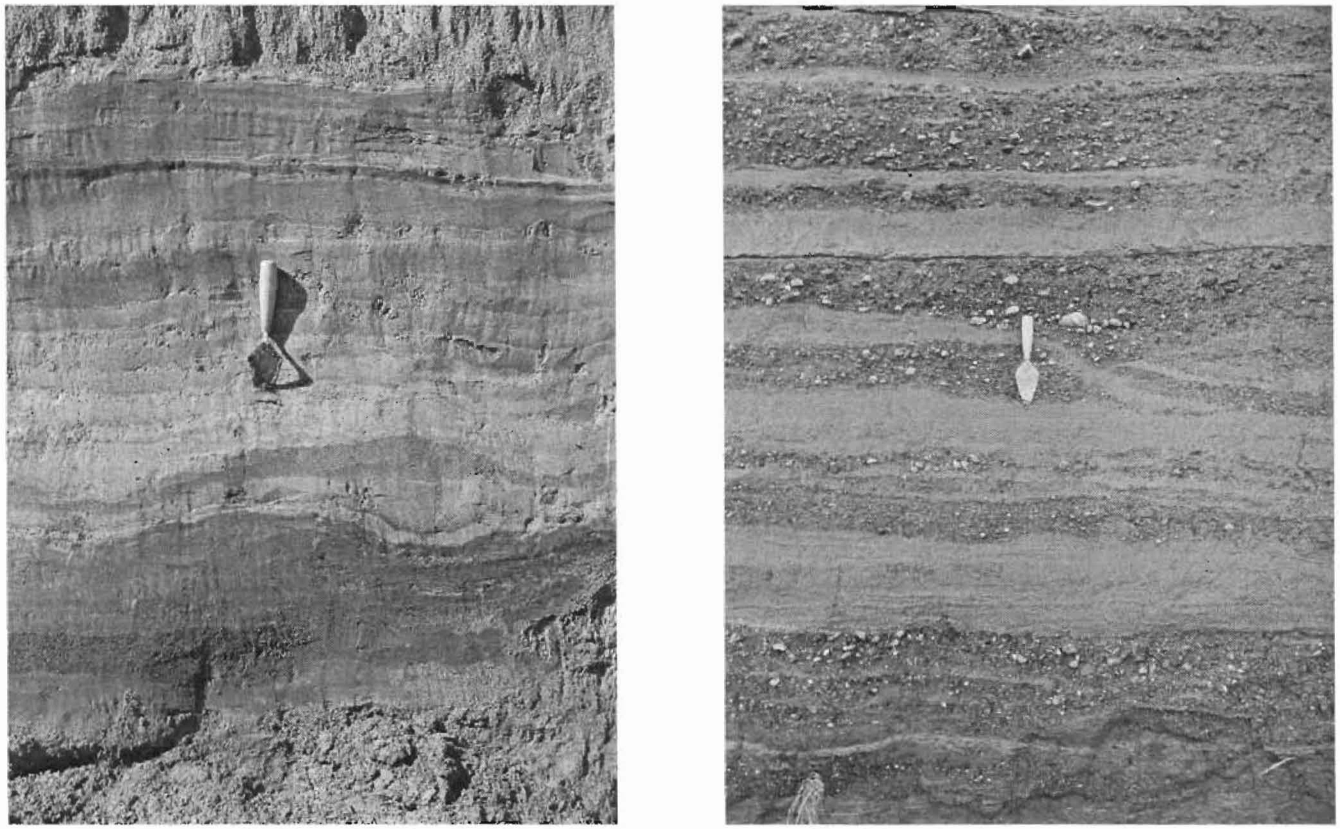

Figure 3-11. Glacial Lake Concrete rhythmically bedded, fine-grained sediments in unit 9 (left) and alternating sand and gravel (right) at the base of the Big Boy section.

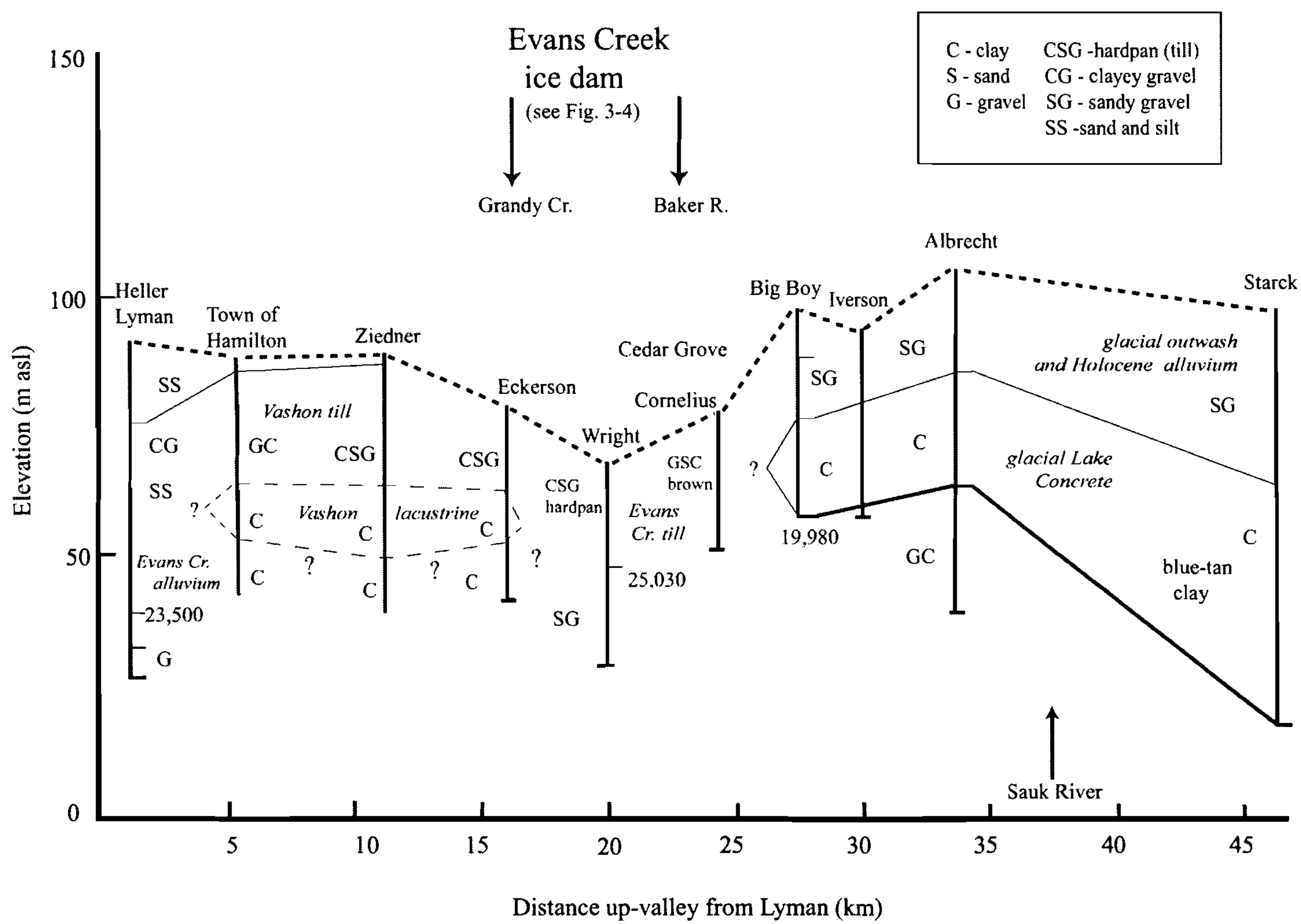

Figure 3-12. Subsurface geology of lower Skagit valley inferred from deep well logs.

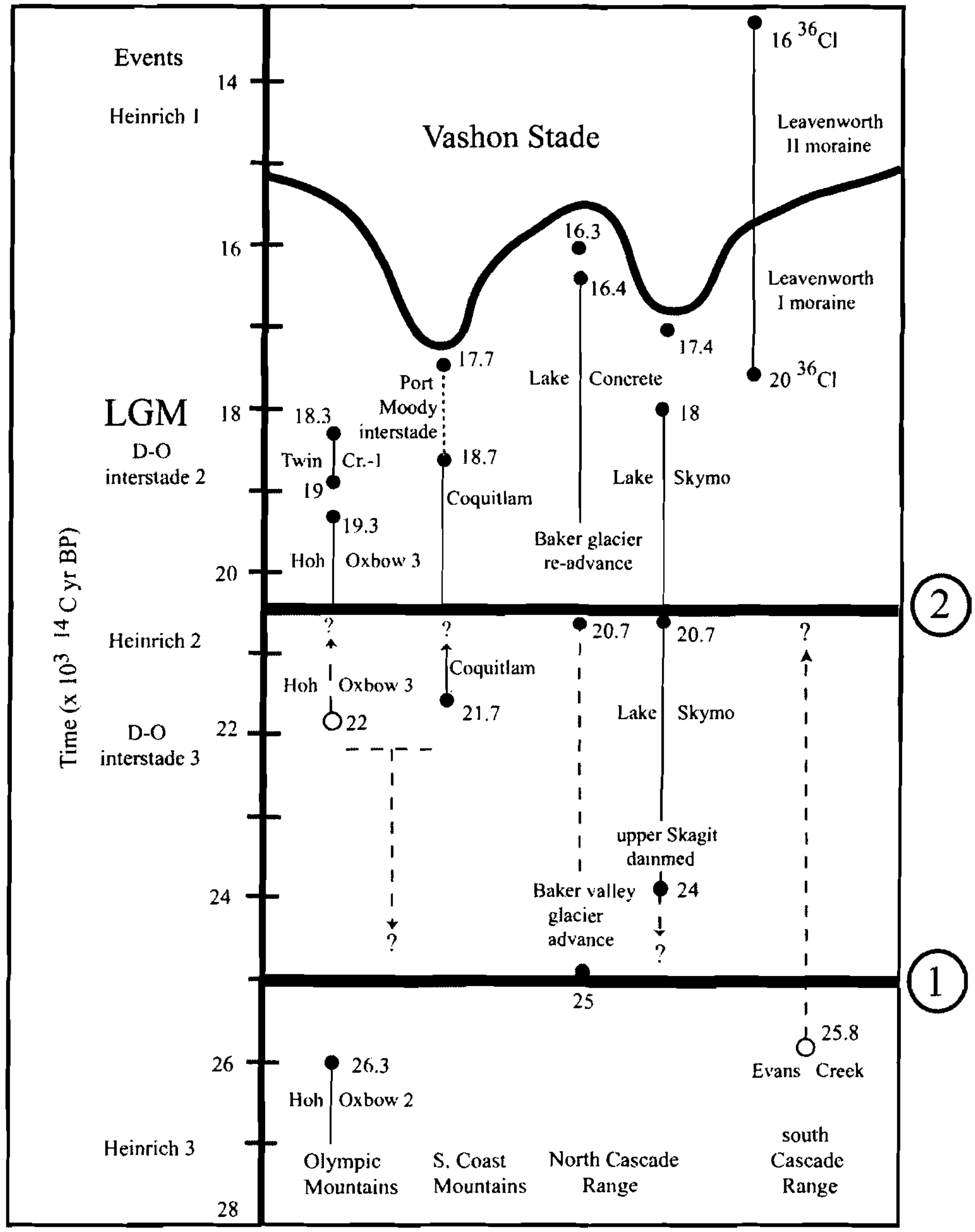

Figure 3-13. Revised chronology of the early Fraser Glaciation based on Skagit valley deposits. Circles represent inferred dates; dots are radiocarbon dates, except for ^{36}Cl. Important events highlighted at the right include (1) first radiometric age constraint on beginning of the Evans Creek stade 25,000 ^{14}C yr BP, (2) a second advance of the Baker Glacier after 20,730 ^{14}C yr BP, and persistence of glacial lakes Skymo and Concrete.

Tables

Table 3-1. Radiocarbon ages from upper Skagit valley.

Site/sample	m asl	Lab no.[1] / method	Material	$^{13}C/^{12}C$	^{14}C age +/- 1σ yr BP	cal. age +/- 1σ yr BP [2]
Skymo NOCA 1989	488.6	Beta - 33923 radiometric	wood	n/a	20,560 +/- 110	24,448 +/- 157
Skymo NOCA 4	482.6	GSC - 6736 radiometric	wood (*Picea)*	-24.2	20,900 +/- 220	24,979 +/- 325
Skymo NOCA 5	478.7	GSC - 6738 radiometric	wood	-24.43	21,400 +/- 240	25,681 +/- 352
Skymo NOCA 6	477.6	Beta - 178536 radiometric	wood	-24.6	21,570 +/- 80	25,947 +/- 133
Ruby Cr. NOCA 13	467.7	GSC - 6742 radiometric	wood	-27.28	17,400 +/- 350	20,610 +/- 414
Skymo NOCA 19	472.1	Beta - 178537 radiometric	wood	-23.3	23,970 +/- 100	28,700 +/- 175
Skymo NOCA 37	480.0	Beta - 216087 AMS	wood	-24.3	20,770 +/- 80	24,794 +/- 164
Skymo NOCA 40B	482.5	UC-1 - 34410 AMS	wood (*Picea engelmannii*)	-25.6	20,310 +/- 60	24,216 +/- 87
Rainbow Pt. NOCA 23	488.9	Beta - 178538 radiometric	wood	-24.9	18,020 +/- 170	21,402 +/- 270
Rainbow Pt. NOCA 28	478.2	LLNL - 114612 AMS	charcoal	-25.0	23,620 +/- 120	28,307 +/- 192
Silver Creek NOCA 84	486.0	Beta - 220960 AMS	charred wood	-23.2	24,080 +/- 170	28,823 +/- 230
Rainbow Pt. NOCA 80	469.0	LLNL - 114613 radiometric	charcoal	-25.0	31,760 +/- 300	37,141 +/- 339

(continued on next page)

Table 3-1 (continued). Radiocarbon ages from upper Skagit valley.

Site/sample	m asl	Lab no.[1] / method	Material	$^{13}C/^{12}C$	^{14}C age +/- 1σ yr BP	cal. age +/- 1σ yr BP [2]
Big Boy NOCA 85	74.0	Beta - 195976 radiometric	wood	-25.9	17,570 +/- 90	20,778 +/- 140
Big Boy NOCA 88	61.0	Beta - 195973 AMS	wood	-24.7	18,810 +/- 100	22,396 +/- 107
Big Boy NOCA 89	79.0	Beta - 195974 AMS	cone (*Picea engelmannii*)	-22.7	16,400 +/- 80	19,515 +/- 97
Big Boy NOCA 104	76.0	Beta - 215977 AMS	wood	-24.6	17, 170 +/- 50	20,345 +/- 70
Big Boy NOCA 107	59.0	Beta - 211363 AMS	wood	-28.6	19,880 +/- 80	23,754 +/- 126
Big Boy NOCA 109	66.0	Beta - 216088 AMS	wood	-25.4	19,810 +/- 80	23,670 +/- 126
Lyman NOCA 117	40.0	Beta - 21364 AMS	wood	-28.3	23,500 +/- 130	28,172 +/- 203
Mastodon NOCA 125a	??	Beta - 220961 AMS	wood	-26.6	16,333 +/- 60	19,451 +/- 83
Cedar Grove NOCA 125b	62.0	UC-I - 31865 AMS	wood	-27.5	25,040 +/- 60	30,112 +/- 54
Cedar Grove NOCA 126	71.0 AMS	UC-I - 31866	wood	-26.6	20,730 +/- 40	24,725 +/- 116

[1] Beta – Beta Analytic; GSC – Geological Survey of Canada; LLNL – Lawrence Livermore National Laboratory; UC-I – University of California, Irvine

[2] From Fairbanks et al. (2005).

Table 3-2. Roland Point alpine and ice sheet till clast lithologies (unit 4, Figure 3-6).

Lithology	Alpine till clasts # (%)	Ice sheet till clasts # (%)
Phyllite	3 (2)	11 (9)
Granodiorite	47 (34)	17 (15)
Greenstone	15 (11)	30 (26)
Gneiss	65 (46)	15 (13)
Porphyritic volcanic		12 (10)
Hozomeen chert	5 (4)	14 (12)
Sandstone		3 (3)
Pebble conglomerate		1 (1)
Other	5 (4)	13 (11)
Total number of clasts	140	116

Table 3-3. Cedar Grove till clast lithology (unit 4, Figure 3-6).

Lithology	Clasts # (%)
Granodiorite	59 (54)
Greenschist	21 (19)
Chilliwack Group	14 (13)
Gneiss	6 (5)
Andesite	5 (4)
Chert	2 (2)
Meta-quartz diorite	2 (2)
Pebble conglomerate	1 (1)
Total number of clasts	110

Table 3-4. Microprobe glass chemistry of tephra from the Big Boy section and Mt. St. Helens tephras M, Mc, and Mm from other sites in southern and eastern Washington.

	Big Boy[1]	MSH M[2]	MSH Mc[3]	MSH Mm[3]
SiO_2	76.28 (0.89)	76.20	76.16	76.45
Al_2O_3	13.49 (0.34)	13.28	13.92	13.81
Fe_2O_3	1.39 (0.31)	1.52	1.40	1.39
TiO_2	0.14 (0.03)	0.24	0.30	0.16
NaO^2	3.92 (0.46)	3.99	3.88	3.96
K_2O	2.77 (0.27)	2.65	2.37	2.36
MgO	0.30 (0.10)	0.33	0.36	0.32
CaO	1.57 (0.17)	1.60	1.57	1.48
Cl	0.13 (0.06)	0.18	0.16	0.13
Correlation coefficient		0.950	0.948	0.952

[1] Percent and 1σ standard deviation based on analysis of 30 shards.
[2] Lamb - Central Washington University (unpublished).
[3] Busacca et al. (1992).

Reference List

Alley, N.F., and Chatwin, S.C., 1979. Late Pleistocene history and geomorphology, southwestern Vancouver Island, British Columbia. Canadian Journal of Earth Sciences 11: 1220-1235.

Armstrong, J.E., Crandell, D.R., Easterbrook, D.J., and Noble, J.B., 1965. Late Pleistocene stratigraphy and chronology in southwestern British Columbia and northwestern Washington. Geological Society of America Bulletin 76: 321-330.

Armstrong, J.E., and Clague, J.J., 1977. Two major Wisconsin lithostratigraphic units in southwest British Columbia. Canadian Journal of Earth Sciences 14: 1471-1480.

Armstrong, J.E., and Hicock, S.R., 1975. Quaternary landscapes: Present and past – at Mary Hill, Coquitlam, British Columbia (92G/2F). Geological Survey of Canada Paper 75-1B: 99-103.

Ashley, G.M., Shaw, J., and Smith, N.D., 1985. Glacial Sedimentary Environments. Society of Economic Paleontologists and Mineralogists Short Course No. 16.

Atwater, B.F., 1986. Pleistocene Glacial-lake Deposits of the Sanpoil River Valley, Northeastern Washington. U.S. Geological Survey Bulletin 1661.

Busacca, A.J., Nelstead, K.T., McDonald, E.V., and Purser, M.D., 1992. Correlation of distal tephra layers in loess in the Channeled Scabland and Palouse of Washington State. Quaternary Research 37: 281-303.

Clague, J.J., 1981. Late Quaternary Geology and Geochronology of British Columbia. Part I: Radiocarbon Dates. Geological Survey of Canada Paper 80-13.

Clague, J.J., 1981. Late Quaternary Geology and Geochronology of British Columbia, Part II: Summary and Discussion of Radiocarbon-dated Quaternary History. Geological Survey of Canada Paper 80-35.

Clague, J.J., 1989c. Quaternary geology of the Canadian Cordillera. In: Fulton, R.J. (ed.), Quaternary Geology of Canada and Greenland. Geological Survey of Canada, Geology of Canada 1: 17-83.

Clague, J.J., Armstrong, J.E., and Mathews, W.H., 1980. Advance of the late Wisconsin Cordilleran Ice Sheet in southern British Columbia since 22,000 yr B.P. Quaternary Research 13: 322-326.

Clague, J.J., Saunders, I.R., and Roberts, M.C., 1988. Ice-free conditions in southwestern British Columbia at 16,000 years BP. Canadian Journal of Earth Sciences 25: 938-941.

Costa, J.E., and Schuster, R.L., 1988. The formation and failure of natural dams. Geological Society of America Bulletin 100: 1054-1068.

Crandell, D.R., 1963. Surficial Geology and Geomorphology of the Lake Tapps Quadrangle, Washington. U.S. Geological Survey Professional Paper 388-A.

Crandell, D.R., and Miller, R.D., 1974. Quaternary Stratigraphy and Extent of Glaciation in the Mount Rainier Region, Washington. U.S. Geological Survey Professional Paper 847.

Dethier, D.L., Pessl, F., Keuler, R.F., Balzarini, M.A., and Pevear, D.R., 1995. Late Wisconsinan glaciomarine deposition and isostatic rebound, northern Puget Lowland, Washington. Geological Society of America Bulletin 107: 1288-1303.

Eyles, N.E., Eyles, C.H., and Miall, A.D., 1983. Lithofacies types and vertical profile models: an alternative approach to the description and environmental interpretation of glacial diamict and diamictite sequences. Sedimentology 30: 393-410.

Fairbanks, R.G., Mortlock, R.A., Tzu-Chien, C., Li, C., Kaplan, A., Guilderson, T.P., Fairbanks, T.W., and Bloom, A.L., 2005. Marine radiocarbon calibration curve spanning 0-50,000 years B.P. based on paired $^{230}Th/^{234}U/^{238}U$ and ^{14}C dates on pristine corals. Quaternary Science Reviews 24: 1781-1796.

Fulton, R.J., 1965. Silt deposition in late-glacial lakes of southern British Columbia. American Journal of Science 263: 553-570.

Fulton, R.J., 1975. Quaternary Geology and Geomorphology, Nicola-Vernon Area, British Columbia (82L W ½ and 92I E ½). Geological Survey of Canada Memoir 380.

Fulton, R.J., and Smith, G.W., 1978. Late Pleistocene stratigraphy of south-central British Columbia. Canadian Journal of Earth Sciences 15: 971-980.

Gascoyne, M., Ford, D.C., and Schwarcz, H.P., 1981. Late Pleistocene chronology and paleoclimate of Vancouver Island determined from cave deposits. Canadian Journal of Earth Sciences 18: 1643-1652.

Gilbert, R., 1975. Sedimentation in Lillooet Lake, British Columbia, Canada. Canadian Journal of Earth Sciences 12: 1697-1711.

Gilbert, R., and Desloges, J.R., 1992. The late Quaternary sedimentary record of Stave Lake, southwestern British Columbia. Canadian Journal of Earth Sciences 29: 1997-2006.

Gillespie, A., and Molnar, P., 1994. Asynchronous maximum advances of mountain and continental glaciers. Reviews of Geophysics 33: 311-364.

Grigg, L.D., and Whitlock, C., 2002. Patterns and causes of millennial-scale climate change in the Pacific Northwest during Marine Isotope Stages 2 and 3. Quaternary Science Reviews 21: 2067-2083.

Harper, J.T., 1992. The Dynamic Response of Glacier Termini to Climatic Variation during the Period 1940-1990 on Mount Baker Washington. M.S. thesis, Western Washington University, Bellingham, WA.

Heller, P.L., 1980. Multiple ice flow directions during the Fraser Glaciation in the lower Skagit River drainage, North Cascade Range, Washington. Arctic and Alpine Research 12: 299-308.

Hicock, S.R., and Armstrong, J.E., 1981. Coquitlam Drift: A pre-Vashon Fraser glacial formation in the Fraser Lowland, British Columbia. Canadian Journal of Earth Sciences 18: 1443-1451.

Hicock, S.R., and Lian, O.B., 1995. The Sisters Creek Formation: Pleistocene sediments representing a nonglacial interval in southwestern British Columbia at about 18 ka. Canadian Journal of Earth Sciences 32: 758-767.

Hicock, S.R., Lian, O.B., and Mathewes, R.W., 1999. 'Bond cycles' recorded in terrestrial Pleistocene sediments of southwestern British Columbia, Canada. Journal of Quaternary Science 14: 443-449.

Hildreth, W., Fierstein, J., and Lanphere, M., 2003. Eruptive history and geochronology of the Mount Baker volcanic field, Washington. Geological Society of America Bulletin 115: 729-764.

Hodge, S.M., 1974. Variations in sliding of a temperate glacier. Journal of Glaciology 13: 349-369.

Kaufman, D.S., Porter, S.C., and Gillespie, A.R., 2004. Quaternary alpine glaciation in Alaska, the Pacific Northwest, Sierra Nevada and Hawaii. In: Gillespie, A.R., Porter, S.C., and Atwater, B.F. (eds.), The Quaternary Period in the United States. Elsevier Developments in Quaternary Science 1: 77-103.

Kovanen, D.J., and Easterbrook, D.J., 2001. Late Pleistocene, post-Vashon, alpine glaciation of the Nooksack drainage, North Cascades, Washington. Geological Society of America Bulletin 113: 247-288.

Lian, O.B., Mathewes, R.W., and Hicock, S.R., 2001. Paleo-environmental reconstruction of the Port Moody interstade, a nonglacial interval in southwestern British Columbia at about 18,000 ^{14}C yr B.P. Canadian Journal of Earth Sciences 38: 943-952.

Licciardi, J.M., Clark, P.U., Brook, E.J., Pierce, K.L., Kurz, M.D., Elmore, D., and Sharma, P., 2001. Cosmogenic ^{3}He and ^{10}Be chronologies of the late Pinedale Northern Yellowstone ice cap, Montana. Geology 29: 1095-1098.

Mackin, J.H., 1941. Glacial geology of the Snoqualmie-Cedar area, Washington. Journal of Geology 49: 449-481.

Mathews, W.H., 1968. Geomorphology of Lightning Creek valley, Manning Park, southwest B.C. Syesis 1: 65-78.

Mickelson, D.M., and Colgan, P.M., 2004. The southern limit of the Laurentide Ice Sheet. In: Gillespie, A.R., Porter, S.C., and Atwater, B.F. (eds.), The Quaternary Period in the United States. Elsevier Developments in Quaternary Science 1: 1-16.

Mullineaux, D.R., 1986. Summary of pre-1980 tephra-fall deposits from Mount St. Helens, Washington State, USA. Bulletin of Volcanology 48: 17-26.

Ovenshire, A.T., 1970. Observations on iceberg rafting in Glacier Bay, Alaska, and identification of ice-rafted deposits. Geological Society of America Bulletin 81: 891-894.

Paterson, W.S.B., 1981. The Physics of Glaciers. Pergamon Press, Oxford.

Pierce, K.L., 1979. History and Dynamics of Glaciation in the Northern Yellowstone National Park Area. U.S. Geological Survey Professional Paper 729-F.

Pierce, K.L., Obradovich, J.D., and Friedman, I., 1976. Obsidian hydration dating and correlation of Bull Lake and Pinedale glaciations near West Yellowstone, Montana. Geological Society of America Bulletin 37: 703-710.

Porter, S.C., 1976. Pleistocene glaciation in the southern part of the North Cascade Range, Washington. Geological Society of America Bulletin 87: 61-75.

Porter, S.C., 2001. Snowline depression in the tropics during the last glaciation. Quaternary Science Reviews 20: 1067-1091.

Porter, S.C., and Swanson, T., 1998. Radiocarbon age constraints on rates of advance and retreat of the Puget lobe of the Cordilleran Ice Sheet during the last glaciation. Quaternary Research 50: 205-213.

Porter, S.C., Pierce, K.L., and Hamilton, T.D., 1983. Late Wisconsin mountain glaciation in the Western United States. In: Porter, S.C. (ed.), Late-Quaternary Environments, Vol. 1, The Late Pleistocene. University of Minnesota Press, Minneapolis, MN, pp. 71-111.

Pringle, P.T., 1993. Roadside Geology of Mount St. Helens National Volcanic Monument and Vicinity. Washington Department of Natural Resources, Olympia, WA.

Riedel, J.L., Haugerud, R.A., and Clague, J.J., 2007. Geomorphology of a Cordilleran Ice Sheet drainage network through breached divides in the North Cascades Mountains of Washington and British Columbia. Geomorphology, in press.

Scott, K.M., Tucker, D., and McGeehin, J., 2003. Island of fire in a sea of ice – The growth of Mount Baker volcano and the Fraser Glaciation in the North Cascades. 16th INQUA Congress, Reno, NV, Programs with Abstracts: 51-9.

Sturchio, N.C., Pierce, K.L., Morrell, M.T., and Sorey, M.L., 1994. Uranium-series ages of travertines and timing of the last glaciation in the northern Yellowstone area, Wyoming-Montana. Quaternary Research 41: 265-277.

Swanson, T.W., and Porter, S.C., 1997. Cosmogenic isotope ages of moraines in the southeastern North Cascade Range. Pacific Northwest Friends of the Pleistocene Field Excursion Guidebook, 18 p.

Tabor, R.W., Haugerud, R.A., Hildreth, W., and Brown, E.H., 2003. Geologic Map of the Mount Baker 30-by-60-Minute Quadrangle, Washington. U.S. Geological Survey Geologic Investigations Series I-2660.

Thackray, G.D., 1999. Pacific moisture delivery and the variability of mountain glacier chronologies in western North America. Geological Society of America Abstracts with Programs 31(4): A58.

Thackray, G.D., 2001. Extensive early and middle Wisconsin glaciation on the western Olympic Peninsula, Washington, and the variability of Pacific moisture delivery to the northwestern United States. Quaternary Research 55: 257-70.

Thorarinsson, S., 1939. The ice dammed lakes of Iceland with a particular reference to their values as indicators of glacial oscillations. Geografiska Annaler 21: 216-242.

Waitt, Jr., R.B., 1977. Evolution of glaciated topography of upper Skagit drainage basin, Washington. Arctic and Alpine Research 9: 183-192.

Waitt, Jr., R.B., and Thorson, R.M., 1983. The Cordilleran Ice Sheet in Washington, Idaho, and Montana. In: Porter, S.C. (ed.), Late-Quaternary Environments of the United States, Vol. 1, The Late Pleistocene. University of Minnesota Press, Minneapolis, MN, pp. 54-70.

Ward, B.C., and Thomson, B., 2004. Late Pleistocene stratigraphy and chronology of lower Chehalis River Valley, southwestern BC: Evidence for a restricted Coquitlam Stade. Canadian Journal of Earth Sciences 41: 881-895.

Appendices

Appendix 3-1. Site coordinates of the Ross Lake and Skagit River sections.

Site name	Longitude	Latitude
Skymo	121° 03.220'	48° 49.397'
Rainbow Point	121° 02.293'	48° 47.736'
Silver	121° 06.000'	48° 57.548'
Big Boy	121° 43.220'	48° 31.273'
Mastodon	121° 43.044'	48° 30.175'
Cedar Grove	121° 45.536'	48° 31.579'
Lyman	122° 03.633	48° 31.829'

Appendix 3-2. Detailed description of sedimentary facies.

Facies 1 – Lacustrine silt and clay (Fl, Flm, Fs, Fm, FSm, and FSl). Moderately well sorted, tan to gray silt with fine sand interbeds; massive, laminated, or bedded, with laminae ranging from 2-6 mm thick and beds as thick as 10 cm. Laminae comprise couplets of light (coarse) and dark (fine) sediment and resemble varves. Laminae are commonly interlayered with thin beds of well sorted, massive or cross-bedded sand. This facies was deposited in a relatively deep lake by suspension settling of silt, clay, and fine sand. Examples: Devil's Creek, units 2, 3, and 5.

Facies 2 – Lacustrine sand (Sm, Sms). Well sorted, horizontally? and cross-bedded fine to medium grained sand; typically has abrupt contacts with facies 1. This facies is lacustrine sediment deposited by turbidity currents, possibly triggered by glacial outburst floods. Examples: Rainbow section unit 32; Rainbow C, unit AC.

Facies 3 – Fluvial gravel (SGm, GSm). Moderately to poorly sorted, pebble-cobble gravel and minor sand. Facies is dominated by angular to subangular clasts of local lithologies, but includes some better sorted beds with round, mixed-lithology clasts. Depositional environment is fluvial. Poorly sorted sediment was deposited by small streams tributary to Skagit River; better sorted, texturally more mature sediment may have been deposited by Skagit River itself. Examples: Rainbow C, unit 14; Rainbow D-F, unit I; Devil's B, units 2, 4, and 6.

Facies 4 – Glacial outwash (SGms). Massive to crudely stratified sand and cobble gravel. Gravel clasts are well rounded and of local and exotic lithologies. Facies is interpreted to be advance outwash based on its stratigraphic position – it conformably overlies lacustrine sediments and is unconformably overlain by Vashon till. Examples: Ruby Creek, units 12, 13, and 14.

Facies 5 – Debris flow deposits (DSG, DFm). Massive clast- to matrix-supported diamict. Clasts range from 5 to 50 cm in diameter, are angular, and are of local valley-wall lithologies. The facies contains thin (<5 cm), lenticular beds of silt and sand that pinch out over distances of a few tens of metres. Diamict clast fabric indicates that the sediment was transported down the valley wall toward the center of the valley. This facies was deposited by local debris flows. Examples: Devil's Creek D, units 3A and 4.

Facies 6 –Till (Dm). Dense, massive, matrix-supported diamict. Matrix is a mixture of silt and sand. Clasts are primarily subrounded to subangular and up to 1 m in diameter. They are dominantly exotic granitic and metamorphic lithologies. Some clasts are striated and most are faceted. The diamict is interpreted to be Vashon till on the basis of its stratigraphic position, northern-provenance clasts, and strong clast fabric. Examples: Ruby, unit 15; Devil's D, unit 7; Rainbow C, unit 38; and Rainbow DF, unit 26.

Facies 7 – Waterlaid till (Dml). Massive to weakly stratified, matrix-supported diamict. Matrix consists of silt and sand. Clasts are dominantly exotic lithologies (95%), including gabbro, greenstone, and granodiorite up to many tens of centimetres in diameter. Smaller (<10 cm), local phyllite clasts are rare. This facies was deposited in a lake close to or beneath a floating glacier margin. Example: Thursday Creek, unit 6.

Chapter 4: Paleoecology of Skagit valley, Washington, during the Evans Creek stade

Abstract

Macrofossils in Skagit valley, Washington, provide information on climate and environmental change in the North Cascades during the Evans Creek stade of the Fraser Glaciation. Between 24,000 and at least 18,020 ^{14}C yr BP the floor of upper Skagit valley was dominated by subalpine species, including whitebark pine (*Pinus albicaulis*), Engelmann spruce (*Picea engelmannii*), and subalpine fir (*Abies lasiocarpa*). Other taxa indicative of a subalpine forest include bark beetles (Scotylidae) and bog birch (*Betula nana*). Treeline during the Evans Creek stade was about 500 m asl, or 1200 ± 150 m below its present elevation, which corresponds to an approximately 7 ±1 °C decrease in mean July temperature. Northern spikemoss (*Selaginella selaginoides)* and willow (*Salix*) macrofossils are particularly abundant in fossil plant assemblages in lake sediments deposited in lower Skagit valley between 19,980 and 17,570 ^{14}C yr BP. Coleopteran macrofossils include ground beetles (Staphylinidae) and leaf beetles (Chrysomelidae); no bark beetles indicative of substantial forest cover were found.

The floral and faunal assemblages also reveal second-order climate changes within the Evans Creek stade. Increases in Sitka spruce (*Picea sitchensis*), mountain hemlock (*Tsuga mertensiana*), and Pacific silver fir (*Abies amabilis*) macrofossils in glacial Lake Skymo sediments after 20,770 ^{14}C yr BP indicate an increase in precipitation of about 200 mm from amounts of the previous cold dry period. An increase in the abundance and diversity of conifer macrofossils, and the absence of northern spikemoss fossils by 17,170 ^{14}C yr BP mark a shift to more mesic conditions near the end of the Evans Creek stade in Skagit valley.

Keywords: Macrofossils; climate change; Fraser Glaciation; Skagit valley; Washington; North Cascades

Introduction

Recent discovery of rich plant and animal macrofossil assemblages in Skagit River valley extends knowledge of the paleoecology of the last glaciation into the Cascade Range of Washington State (Figure 4-1). The assemblages were recovered from glacial lake sediments dating to the Evans Creek stade of the Fraser Glaciation (marine oxygen isotope stage 2). Most of what was known about the plant and animal communities of this period comes from a few sites in coastal and lowland environments in south-coastal British Columbia and adjacent Washington. Pollen studies at these sites have identified the basic pattern of environmental change during the Evans Creek stade, but little is known of the contemporary ecology of mountain areas in the Pacific Northwest (Barnosky et al., 1987). Further, paleoenvironmental research at new sites is needed to confirm hypothesized millennial-scale climate changes during the Evans Creek stade (Grigg and Whitlock, 2002).

Evans Creek glacial lake sediments in Skagit valley span 8000 years and contain sufficient macrofossils to assess changes in conifer abundance and diversity through time at the species level. Combined with stratigraphic information, the macrofossils provide the first long, detailed ice age record in the North Cascades (Figure 4-2). The objective of this paper is to use the macrofossil assemblages to reconstruct the vegetation and climate of Skagit valley during the Evans Creek stade. Specific research questions include: What was the vegetation in Skagit valley during the Evans Creek stade? What was the elevation of treeline in Skagit valley during the Evans Creek stade? Do changes in macrofossil abundance and diversity through time support independent evidence of a mid-Evans Creek stade warm period? Did the Port Moody interstade, a late Evans Creek mesic interval in the Fraser Lowland of British Columbia (Figure 4-1), extend south to Skagit valley? What are the magnitude and range of climate changes during the Evans Creek stade?

Modern climate and forest ecology

Skagit River is the largest river flowing into Puget Sound (Figure 4-1). Its watershed has an area of 8000 km^2 and spans a range of physical and ecologic environments. Fluvial and glacial erosion have deeply cut the valley into metamorphic and granitic bedrock. The floor of the valley at Ross Lake, more than 150 km from Puget Sound, is only 400 m above sea level. Winter storms are funnelled east up Skagit River into the heart of the North Cascades Range. Annual precipitation on the valley floor ranges from 170 cm at Concrete to 188 cm at Diablo Dam and 100 cm at Hozomeen. Mean annual temperature on the valley floor is moderated by a maritime influence in the western part of the watershed, but there is a marked temperature range in the east due to the stronger continental influence there. Mean January and July temperatures are 2.8°C and 18.1°C, respectively, at Concrete, and 0.7°C and 18.6°C at Ross Dam (Figure 4-1).

There are also strong temperature and precipitation gradients with elevation in Skagit valley (Figure 4-3). Precipitation increases significantly above 1300 m asl, with annual values reaching 300 cm in upper Baker valley and 270 cm in upper Skagit valley. Summer temperature lapse rate ranges from 0.44^{0}C/100 m in Baker valley to 0.6^{0}C/100 m in the more continental upper Skagit basin (U.S. Government, unpublished).

Vegetation on the floor of lower Skagit valley is dominated by lowland forest species, including red cedar (*Thuja plicata)*, Douglas-fir (*Pseudotsuga menziesii)*, and western hemlock (*Tsuga heterophylla)*. Lowland forest species also dominate the valley floor near Ross Lake, but more xeric, low elevation species such as Ponderosa pine (*Pinus ponderosa*) are also present in drier microclimates.

Strong temperature and precipitation gradients with altitude and distance from the Pacific moisture source control the distribution of tree species at treeline. Treeline in the western part of the watershed is lowered by heavy winter snowfall, reaching 1400 m asl in upper Baker valley (Figure 4-3; Franklin and Dyrness, 1973). Treeline rises to 1700 m asl on the east side of Ross Lake near Hozomeen (Arno and Hammerly, 1984). Subalpine fir (*Abies lasiocarpa*) and mountain hemlock (*Tsuga mertensiana*) dominate the heavy snow and cool summer environments at treeline in the western Skagit watershed, whereas Englemann spruce (*Picea engelmannii*) and whitebark pine (*Pinus albicaulis*) are the treeline species near Hozomeen (Figure 4-1, Table 4-1).

Little information is available about beetle (Coleoptera) communities in the diverse climate, vegetation, and aquatic environments of Skagit valley. A survey of Big Beaver valley near Ross Lake yielded 360 species of terrestrial and aquatic beetles in 49 families (LaBonte, 1998).

Methods

Macrofossils are the focus of this study because they are abundant in accessible, subaerially exposed beds, and coniferous macrofossils can be identified to species level, unlike most coniferous pollen. Furthermore, macrofossils are not likely to have been transported as far as pollen in river-fed lakes (Dunwiddie, 1987).

Bulk samples were collected from nine glaciolacustrine silt beds at three locations to span as much of the Evans Creek stade as possible (Figures 4-1, 4-4). The Big Boy section macrofossils range in age from 19,940 to 16,400 ^{14}C yr BP, and the Skymo-Rainbow Point sections extend from 23,970 to 18,020 ^{14}C yr BP (Table 4-2).

Macrofossils were recovered from 1 litre sediment samples by soaking, swirling, and then sieving with warm tap water. The sample processing technique proved to be critical for recovery of relatively intact, identifiable macrofossils. Week-long soaking and gentle agitation produced a significant increase in identifiable macrofossils. Samples were weighed, and the volume of organic material estimated, by water displacement. The organic concentrate was passed through a set of nested screens (4, 0.85, 0.425, and 0.25 mm). All material greater than 0.425 mm was analyzed under a binocular microscope; only part of the smaller fraction was examined. An attempt was made to use an oil flotation techniques to isolate fossil insects, but it proved unsuccessful due to the compactness of the samples and adherence of fine silt to the fossils. Samples are archived at the National Park Service curation facility in Marblemount, Washington.

Plant macrofossils and fossil insects were isolated, identified, enumerated, and photographed by Alice Telka of Paleotec Services, Ottawa. Conifer macrofossils included needles, cone scales, seeds, seed wings, and seed wing fragments. Conifer needles from two beds were separated to the genus level by A. Telka. Species identification of a subset of the conifer needles was performed by Alecia Spooner under the direction of Dr. Linda Brubaker and Dr. Estella Leopold. Needles were identified to species on the basis of needle length, tip and base morphology, and the density and number and location of rows of stomata (Hitchcock and Cronquist, 1973; Dunwiddie, 1985). Identifications were confirmed by comparison with modern reference collections at Paleotec, Simon Fraser University, and the University of Washington.

Problems in using conifer macrofossils to identify climate changes include variable needle production, taphonomic processes, inability to identify fossils to species level, hybridization, and sample size (Birks and Birks, 1981). Conifer species produce different amounts of needles and retain them for different lengths of time. Based on relatively slow sedimentation rates in glacial lakes Skymo and Concrete (Chapter 3), each sample should span more than 50 years, thereby reducing the effect of variability in needle production between species and the influence of short-term disturbance events in needle production. Taphonomic processes, including needle preservation and redistribution of needles by water in low-energy environments, are primarily an issue when comparing assemblages of the same age from different sites. The focus of this study is on changes through time at specific sites. I assume that taphonomic factors, such as wind and water depth, which might cause differential sorting of needles, were constant through time for a number of samples at a given site. However, inverted radiocarbon ages at both the Big Boy and Skymo sections indicate that some older fossils were mixed into younger beds. Excellent fossil preservation, the absence of gravel cut-and-fill structures, the presence of new species, and a series of stratigraphically correct dates provide confidence that the most important beds are not contaminated with older fossils.

Sitka spruce needles, which are abundant in some samples, are differentiated from Engelmann spruce needles by their straight, relatively blunt tips, flattened cross-section, prominent abaxial midrib, and presence of stomata on only one side (Dunwiddie, 1985). White spruce (*Picea glauca*), Englemann spruce, and Sitka spruce hybridize with one another, and white spruce presently grows at low elevations as far south as eastern Washington (Daubenmire, 1973; Farrar, 1995). Although possible, it is unlikely that white spruce needles were misidentified as Sitka spruce and/or Engelmann spruce. Halliday and Brown (1943) suggest that white spruce was extirpated from western North America during the last ice age, and Krajina (1970) notes that it is not well adapted to subalpine conditions.

Conifer needles were particularly abundant in three of the beds analyzed, with more than 10,000 needles identified to genus. The statistical validity of the assumption that samples from the three beds are random was checked by identifying all *Picea* sp. and *Abies* sp. needles in one of the three beds, then proportionally counting the best-preserved needles in each genus to species. Ratios of genera, and of species within a given genus, were compared between the random counts and proportional total counts.

I used two approaches to estimate changes in bioclimatic variables from needle counts at the Skymo and Big Boy sections. The first approach was to use elevation limits of indicator species and lapse rates to estimate temperature changes recorded by fossil assemblages (Heusser, 1977). The second approach involved shifts in bioclimatic indicators along species range boundaries (Figure 4-5; Thompson et al., 1999).

Depression of mean July temperature for the Evans Creek stade assemblages was derived by first estimating changes in treeline (Figure 4-3; Heusser, 1977). Treeline depression was referenced to the mid 20^{th} century elevation of 1700 m near the Skymo section (Arno and Hammerly, 1984). Although treeline is controlled by both precipitation and temperature, Heusser (1983) suggests that it is near the 10°C average July temperature isotherm (Figure 4-3). Errors in this approach include the fact that treeline typically spans a vertical range of ± 150 m due to aspect, which corresponds to 1 °C based on a 0.6°C/100 m lapse rate (Franklin and Dyrness, 1973).

Indicator species have been used in previous paleoecological studies to estimate past climate change (Birks and Birks, 1981; Barnosky, 1984; Isarin and Bohncke, 1999). Barnosky (1984) used mountain hemlock and Engelmann spruce as primary indicators of climate in the fossil record because they are currently distributed at opposite ends of a maritime-to-continental climate transect at treeline (Franklin and Dyrness, 1973; Mathewes, 1993). I used bioclimatic variables affecting the distribution of these species to estimate the magnitude of climate change in cases where the relative abundance of the species changed between beds. Bioclimatic indicators include mean temperature of the coldest month, moisture index, and mean annual temperature (Thompson et al., 1999, 2004).

Inferred changes in climate based on conifer macrofossils were checked by comparison with other elements of the floral and faunal assemblages. Fossils of species that are not presently found in the watershed and that are cold adapted confirmed conifer evidence of treeline during the Evans Creek stade. Examples include bog birch *(Betula nana),* northern spikemoss *(Selaginella selaginoides)*, and alpine pondweed (*Potamogeton alpinus).* Presence of non-arboreal fossils provide evidence of open forest conditions.

Glacial Lake Skymo assemblages

Macrofossils were recovered from glacial Lake Skymo sediments at two locations along the shoreline of Ross Lake (Figure 4-1). Most of the plant macrofossils and all of the faunal remains came from the Skymo section on the west shore of the reservoir; only conifer needles have been recovered to date at the Rainbow Point section (Figure 4-4). Results presented below begin with the oldest beds and focus on select species; Tables 4-3, 4-4, and Appendix 4-1 provide complete macrofossil results.

NOCA-73 (23,970 ± 100 ^{14}C yr BP)

Few macrofossils were recovered from the lowest exposed bed at the Skymo section (472 m asl). This sample contains less than 1% organic material and only a single charred spruce needle was identified. Charcoal extracted from the sample gave an AMS radiocarbon age of 23,970 ± 100 ^{14}C yr BP. No insect fossils were found in this sample.

NOCA-56 (23,620 ± 120 14C yr BP)

Only four needles from unit 7 at the Rainbow Point section were identified to species. They include two Sitka spruce needles, one mountain hemlock needle, and one Douglas fir/western hemlock needle.

NOCA 33-34-77 (21,570 ± 80 14C yr BP)

This sample, collected from a bed at 476.5 m asl, contains 16% organic matter. Macrofossils are abundant, diverse, and well preserved, although many are flattened and impregnated with silt. The fossils include seven species of conifers, one deciduous shrub, and one evergreen shrub, sedge, and moss (Table 4-4).

Subalpine species dominate the coniferous macrofossil assemblage (Table 4-3). Englemann spruce accounts for 78% of the 104 needles identified, and most of the remainder are mountain hemlock and subalpine fir needles. Whitebark pine fascicles, some containing needle bases, and needles are also abundant (Figure 4-6).

Sedge macrofossils include achenes and peryginial fragments, representing lenticular and trigonus types (Table 4-4). Four nutlets of heath (black crowberry) and three nutlets of birch were recovered; two of the nutlets appear to be bog birch based on size (1 mm) and a narrow seed wing (Figure 4-7). Several hundred whole and half seeds of aquatic buttercup (*Ranunculus aquatilus* L.) were counted (Table 4-4).

Body parts of 49 beetles include both terrestrial (rove, bark, and moss beetles) and aquatic (water scavenger and predaceous diving beetles) groups (Figure 4-7; Appendix 4.1).

Other aquatic macrofossils include ephippia of water fleas (*Daphnia* sp.), caddis fly larva head capsules (Trichoptera), and several hundred lentic midge (Chironomidae) head capsules.

NOCA 36 (>20,770 ± 80 14C yr BP)

Sample NOCA 36, collected from a bed at 479.4 m asl, was analyzed only for conifer macrofossils (Table 4-3). Of the 419 needle fragments recovered, only 141 tips and bases could be identified to species. One hundred of the needle tips and bases are Engelmann spruce; the remainder could not be identified beyond genus due to poor preservation. However, based on results from overlying and underlying samples, several of the *Picea* needle fragments could be Sitka spruce (*Picea sitchensis*).

NOCA 37 (20,770 ± 80 14C yr BP)

This sample was collected 0.5 m above sample NOCA 36 to better document changes in species diversity between samples NOCA 36 and NOCA 40 (Table 4-4). Organic content is 25%, with about 15% wood and twigs as long as 7 cm. Preservation of macrofossils is fair to good, but most specimens are flattened and have adhering fine silt.

More than 9,000 conifer macrofossils were recovered from the sample, including whole needles, twig terminals, seed wing fragments, and one cone scale fragment (Table 4-4). Approximately half of the needles identified to the species level are Engelmann spruce, with equal numbers of subalpine fir and Sitka spruce needles and a few grand fir/silver fir (Table 4-3). Ninety-four five-needle-type fascicles and nearly 500 needle tips and bases were identified as whitebark pine on the basis of needle stature and stomata on both surfaces (Table 4-4).

Other macrofossils include one bog birch nutlet with a partial wing, one crowberry nutlet, achenes of pond weed (*Potamogeton* sp.), and lenticular and trigonus-type sedges. Four of the pondweed achenes were identified as alpine pondweed (*Potamogeton alpinus*), a cold-adapted species of shallow lakes and ponds (Figure 4-6). A few of the sedge achenes retain whole or partial perigynia. The sample also yielded whole and half achenes of whitewater buttercup (*Ranunculus aquatilus*).

Thirty-two beetle body parts were identified, including four articulated specimens. The assemblage includes the same terrestrial and aquatic groups found in underlying NOCA 33 (Appendix 4.1).

NOCA 40 and 40B (20,310 ± 60 14C yr BP)

Two samples from the same bed were analyzed to assess the accuracy of random needle counts. Seventeen percent of sample NOCA 40 is organic matter, mainly conifer macrofossils. Other organic material includes flattened wood and twigs and a single, unidentified species of moss. With a few exceptions, fossil preservation in this sample is fair to poor; aquatic fossils are slightly better preserved than terrestrial ones.

Seven conifer species are present among the more than 8000 macrofossils recovered from sample NOCA 40 (Table 4-4). The remains include several dozen seeds, seed-wing fragments, and cone-scale fragments of Pinaceae. About half of the conifer macrofossils are *Abies* sp., including 36 whole needles and 49 flattened twig terminals. Most of the remaining macrofossils are *Picea* sp., including more than 100 whole needles and twig terminals. Five-needle- type fascicles and several hundred needle tips and bases are whitebark pine. Relative to underlying samples, NOCA 40 records a large increase in the abundance of mountain hemlock and a modest increase in Douglas-fir/western hemlock and grand fir/silver fir (Table 4-3).

Proportional counts of needles to species level based on all needles pre-sorted by genus reveal a similar pattern to random needle counts. In the genus-sorted sample of all needles, *Picea* sp. accounts for 45% of the specimens, compared to 66% in the random count. The ratio of Engelmann spruce to Sitka spruce in the genus count is 2.5, compared to 2.0 in the random count.

No heath or birch fossils were found in NOCA 40, in contrast to samples lower in the sequence. One bud of willow (*Salix* sp.) was recovered from the sample. The presence of white water buttercup achenes record continuation of this species from lower in the section. Sedge, sheathed pond weed (*Potamogeton vaginatus* Turcz.), which is a cold-adapted circumboreal species (Brayshaw, 1985), and aquatic buttercup are present in this sample in proportions similar to those in NOCA 37 (Figure 4-7).

The fossil beetle assemblage in NOCA 40 is similar to that of overlying beds and includes the same forest and riparian beetle groups. Beetle body parts include heads, pronota femurs, and elytra (Appendix 4.1). Three of the specimens are articulated (Figure 4-7).

NOCA-61/98 (18,020 ± 170 14C yr BP)

Due to low fossil content, two samples were collected at Rainbow Point at 489 m asl near the full pool level of Ross Lake, approximately 7km east of and 6 m above sample NOCA 40.

The two samples, although large, yielded only 21 coniferous macrofossils that could be identified to species level. The macrofossils are mainly Engelmann spruce, but include mountain hemlock, subalpine fir, and four needles of either western hemlock or Douglas-fir (Tables 4-3 and 4-4).

Glacial Lake Concrete assemblages

The 29-m-high Big Boy section is 75 km downstream from Ross Lake, on the south bank of Skagit River near the town of Concrete (Figures 4-1 and 4-4). It generally has less abundant and diverse macrofossil assemblages than the Ross Lake sites. Only one sample, NOCA 104, at the top of the glaciolacustrine sequence contained abundant plant macrofossils (Tables 4-3 and 4-4).

NOCA 107 (19,880 ± 80 ^{14}C yr BP)

NOCA 107 was collected at 58 m asl from the base of the section, below the high-water level of Skagit River. It contains only a few identifiable conifer macrofossils, including subalpine fir and grand fir/silver fir needles, but no spruce (Table 4-3).

NOCA 100 (<19,880 ± 80 14C yr BP)

This sample was collected 1 m above NOCA 107. It contains 43% organic material, but yielded small numbers of identifiable conifer macrofossils (Figure 4-4). About 75 percent of the organic material is roots, horsetail (*Equisetum* sp.), twigs, and wood fragments. The macrofossil assemblage includes many spores of the soil-borne fungus *Cenococcum geophilum*, which forms a mycorrhizal relationship with tree roots (Table 4-4). Also abundant are macrofossils include sedge achenes, woodrush (*Luzula* sp.) seeds, and more than 40 megaspores of northern spikemoss (*Selaginella selaginoides*), which were identified on the basis of large spore size (0.48-0.53 mm) and yellow-green color (Figure 4-6; Tyron, 1949). Northern spikemoss macrofossils have not been previously reported from Pleistocene sediments in the Cascade Range (Heusser and Igarashi, 1994). Less abundant macrofossils include Engelmann spruce needle tips and bases, conifer twigs, and two seed capsules and three persistent buds of willow (Tables 4-3 and 4-4).

Thirty-two beetle body parts span six families. Most of the specimens are rove beetles (Staphylinidae; Appendix 4.1) and include *Olophrum boreale* (Payk.), and *Tachnius* sp. Ground beetles (Carabidae, *Elaphrus clairvillei*), weevils (Curculionidae, *Isochnus rufipes* ?), pill beetles (Byrrhidae), and leaf beetles (Chrysomelidae) are also present (Figure 4-8).

NOCA 101 (18,810 ± 100 14C yr BP)

This sample, collected 2 m above the base of the section at 61 m asl, consists almost entirely of organic material. Fossil preservation is fair to poor, and most fossils are likely underrepresented in the inventory due to problems encountered in disaggregating the sample. Half of the organic material is fine plant detritus, including moss, horsetail stem fragments, and bark. The only conifer macrofossils recovered are a spruce seed, needle tip, and needle base. The most common macrofossils are northern spikemoss megaspores and sedge achenes. Willow is represented by persistent buds, four twigs with persistent buds, and a half seed capsule (Table 4-4).

Preservation of insect macrofossils is better than in the underlying sample. Ninety-two beetle body parts include heads, elytra, sternites, coxa, and pronota of terrestrial and riparian beetles (*Bembidion* sp., *Aleocharinae* sp., and *Olophrum consimilie* Gyll.). The sample includes two groups not found in NOCA 100: feather-wing beetles (Ptiliidae) and click beetles (Elateridae; Appendix 4.1).

NOCA 105 (>17,570 ± 90 14C yr BP)

Sample NOCA 105, collected from a dark gray silt bed at 63 m asl, contains 40 percent organic material, three-quarters of which is moss and most of the remainder flattened twigs and bark, horsetail fragments, and deciduous bud scales. Fossil preservation is good, but most macrofossils were coated with fine silt, making identification difficult.

An AMS age from this sample of 19,760 ± 60 ^{14}C yr BP is anomalous, based on a younger age from lower in section (18,810 ^{14}C yr BP; Table 4-1 and Figure 4-4). It is one of two samples from unit 7 that returned ages older than underlying beds. The few macrofossils found in this bed, therefore, probably include reworked older specimens.

Identified coniferous macrofossils are limited to two subalpine fir needles (Table 4-3). The assemblage is dominated by sedge achenes, nearly 70% of which retain partial seed coats. The second most common group of macrofossils is willow seed capsules, twigs, and persistent buds (Table 4-4). The sample also contains plant macrofossils of a number of taxa not observed lower in the section, including buckwheat (*Polygonum ?* sp.) and silverweed cinquefoil (*Argentina anserina* L. Rybd.).

The beetle assemblage comprises heads, elytra, pronota, coxa, and sternites, with several articulated specimens of long-horned leaf beetles (*Plateumaris* sp.) and rove beetle (*Stenus* sp.; Figure 4-8). Nine genera of rove beetles were identified, compared to six in sample NOCA 101 (Appendix 4.1). Pill beetles, leafhoppers, and click beetles constitute the remainder of the faunal assemblage.

NOCA 104 (17,170 +/-50 ^{14}C yr BP)

This sample was collected at 76 m asl, near the top of the glaciolacustrine part of the section. It yielded more abundant and diverse macrofossils than any other Big Boy sample. It contains 39% organic matter, about 70% of which are branches as long as 18 cm and twigs, some of which were worn.

Conifer macrofossils include two cone scales, a seed, seed wings, two seed wing fragments, and 878 whole and partial conifer needles. Species-level identification was completed on 127 specimens, with Englemann spruce accounting for 33% of the needles, followed by subalpine fir at 15%, Sitka spruce at 10%, and Douglas-fir/western hemlock at 7% (Table 4-3). The floral assemblage contains much greater species diversity than assemblages lower in section (Table 4-4). Taxa observed only in this bed, although in low numbers, include birch (Betulaceae), goosefoot (Chenopodiaceae), pink (Caryophyllaceae), and mustard (Brassicaceae). Willow, sedge, and cinquefoil are also present. Spikemoss megaspores, which are so abundant in samples lower in the section, are notably absent.

Only 23 beetle body parts were recovered from this sample, and most of them are poorly preserved. Identified specimens are either hygrophilous or terrestrial, and all taxa are present in lower Big Boy samples (Appendix 4-1).

NOCA 89 (16,400 ± 80 ^{14}C yr BP)

A complete Engelmann spruce cone provided the AMS age for this sample and a date for the end of the glacial Lake Concrete fossil record (Figure 4-4). Twigs were also recovered, but no needles or other macrofossils were found in the sample.

Discussion

Evans Creek stade plant and insect communities

Long-lived glacial lakes in Skagit valley were bordered by diverse plant and insect communities between 24,000 and 16,400 ^{14}C yr BP. The plant and animal communities were located on the floor of the valley between large tributary alpine glaciers (Figure 4-1).

There are several reasons why parts of Skagit valley remained unglaciated during the Evans Creek stade. The North Cascades are much wider and higher than the Cascade Range farther south, resulting in more variable climate and topography. Upper Skagit valley lies between two hydrologic divides and is relatively arid for a west-draining valley in the Cascades. Aridity was probably enhanced by growth of the Laurentide and Cordilleran ice sheets, which may have steered storms south of Skagit valley (Barnosky et al., 1987; Lian et al., 2001; Grigg and Whitlock, 2002). The valley also shares several low divides with adjacent areas (Riedel et al., 2007). The absence of a high-elevation geographic barrier allowed plants and animals to migrate into and out of Skagit valley as higher elevation mountain valleys were occupied by alpine glaciers.

Plant communities surrounding glacial lakes Skymo and Concrete were diverse. Macrofossils of Douglas-fir/mountain hemlock, Sitka spruce, Engelmann spruce, whitebark pine, and subalpine fir demonstrate that the forest community was a changing mix of coastal, inland, lowland, and subalpine species. These species today occur at different elevations and distances from the Pacific moisture source. Other full-glacial plant communities in the Pacific Northwest typically do not have modern analogues (Heusser, 1974, 1977; Barnosky, 1981; Whitlock 1992; Lian et al., 2001). Ecological diversity in the Skagit refugia is also reflected in the 10 species of vascular plants in the glacial Lake Skymo assemblages, and 14 species in the glacial Lake Concrete assemblages (Table 4-4).

Three species of bark beetles found in glacial Lake Skymo sediments are indicative of a mature forest. Several species of predaceous diving beetles and water scavenger beetles lived in the waters of glacial Lake Skymo, together with other aquatic species such as caddisflies, water fleas, and midges (Chironomidae). The Skymo assemblage also includes the rove beetle *Olophrum borealis*, which is not found in modern samples from Big Beaver valley (LaBonte, 1998).

Insect fossils recovered from glacial Lake Concrete sediments point to a wetland environment, with willow and small numbers of Engelmann spruce. Abundant northern spikemoss megaspores indicate cold, perhaps boreal alpine conditions (Heusser and Peteet, 1988). Most of the insects in sample NOCA 105, including beetles, are aquatic and semi-aquatic (Appendix 4-1). The absence of bark beetles, fewer species of rove beetles, and a scarcity of tree macrofossils indicate that extensive forest was not present until after 17,570 ^{14}C yr BP.

The presence of Sitka spruce fossils several hundred kilometres inland from the Pacific coast is interesting. Sitka spruce is not tolerant of shade, has a moderate tolerance to frost, and prefers a hyper-maritime climate and nitrogen-rich soils (Franklin and Dyrness, 1973; Peterson et al., 1997). Sitka spruce is not found today in Skagit valley. Its presence during the Evans Creek stade, however, may not be unusual, because of the valley's low elevation and modern populations in adjacent Fraser and Chilliwack valleys (Figure 4-1; Krajina et al., 1982). Sitka spruce occurs up to 1500 m asl in southwest British Columbia, and its range expands inland 200 km to the north along major river corridors (Sudworth, 1967; Peterson et al., 1997). In more continental climates, it occupies sites with high available soil moisture, such as floodplains and shorelines (Peterson et al., 1997). It is commonly associated with western hemlock, western red cedar, mountain hemlock, silver fir, and black cottonwood. Considering these habitat requirements, Sitka spruce may have been restricted to the shores of glacial Lake Skymo.

Early Evans Creek stade environmental variability

Changes in the abundance and diversity of macrofossils in the glacial Lake Skymo sequence reveal climate and environmental changes within the early Evans Creek stade. Sparse conifer macrofossils in the oldest Lake Skymo sediments suggest that a subalpine forest grew at the lake shore from at least 23,620 until as late as 20,770 ^{14}C yr BP. Approximately 80% of the needles identified in this bed are Engelmann spruce and subalpine fir, which tolerate frozen ground for more than a few months a year (Krajina, 1970). Engelmann spruce today favours dry and cold sites near treeline east of Ross Lake (Figure 4-1). The presence of bog birch, whitebark pine, and cold-adapted alpine pondweed, and the Skagit-blocking advance of Big Beaver Glacier (Chapter 3), support the interpretation of cold, dry conditions prior to 20,770 ^{14}C yr BP (Brayshaw, 1985).

Vegetation in Puget Lowland and Fraser Lowland during the early part of the Evans Creek stade was subalpine parkland growing under a cold, dry climate (Hicock et al., 1982;

Barnosky, 1984; Barnosky et al., 1987). The Skagit macrofossil data suggest that this environment was widespread, extending from the south end of Puget Lowland to the lower Fraser valley and into unglaciated parts of valleys in the North Cascades.

A shift from cold and dry to wetter and warmer conditions sometime after 20,770 ^{14}C yr BP is recorded by large increases in conifer macrofossil abundance and diversity (Tables 4-2 and 4-3). By 20,310 ^{14}C yr BP, the Skymo assemblage includes abundant mountain hemlock and silver fir/grand fir (Table 4-3). Decreases in sedge achene abundance and an absence of bog birch and black crowberry (heath) seeds support evidence of environmental change at this time (Table 4-4).

Several researchers have associated increases in mountain hemlock pollen and macrofossils to a shift to more mesic conditions during the Evans Creek stade (Barnosky, 1984; Lian et al., 2001). Mountain hemlock is sensitive to drought (Minore, 1979) and requires an insulating snow cover that persists for at least three months to keep roots from freezing (Krajina, 1970; Franklin and Dyrness, 1973; Wardle, 1974). It also requires an average of at least 505 mm precipitation per year, in contrast to a minimum of 235 mm for Engelmann spruce. Therefore, the increase in abundance of mountain hemlock macrofossils at the expense of Engelmann spruce by 20,310 ^{14}C yr BP indicates a rise in mean annual precipitation of about 200 mm (Figure 4-5). Increased precipitation could explain most of the shift in relative macrofossil diversity and abundance, with little change in temperature. Determining the magnitude of temperature change based on the increased abundance of mountain hemlock and other mesophytic conifers is problematic because the temperature ranges of conifers represented in the Skagit assemblages overlap (Figure 4-5).

Previous research has also identified a change in pollen and macrofossil abundance and diversity about 21,000 ^{14}C yr BP (Figure 4-9). Heusser (1977) reported a significant increase in Douglas-fir and mountain hemlock pollen and a decrease in non-arboreal pollen 21,000 ± 750 ^{14}C yr BP at Bogachiel Bog on western Olympic Peninsula. Barnosky (1981) noted a drop in arboreal pollen and a peak in spruce pollen about 20,500 ± 500 ^{14}C yr BP at Davis Lake. Grigg and Whitlock (2002) documented an increase in arboreal pollen at Little, Fargher, and Carp lakes in southern Puget Lowland 20,500 ^{14}C yr BP and attributed it to increased precipitation . AMS radiocarbon ages from Skagit valley date this event to sometime after 20,770 ± 80 ^{14}C yr BP (Figure 4-9).

Late Evans Creek stade environmental variability

The development of forest vegetation on early Evans Creek stade drift at Cedar Grove was interrupted by resurgence of Baker Glacier after 20,730 ^{14}C yr BP (Chapter 3). The glacier advanced over forest and impounded glacial Lake Concrete. This advance occurred at about the same time as the Hoh Oxbow 3 and Twin Creeks 1 advances in western Olympic Peninsula (Figure 4.9; Thackray, 2001).

Macrofossils deposited in glacial Lake Concrete soon after it formed include Englemann spruce needles and cones and northern spikemoss megaspores, indicating that the nearby environment was cold and relatively dry conditions from about 19,800 to at least 17, 570 ^{14}C yr BP (Table 4-4; Heusser and Peteet, 1988). Engelmann spruce grows today above 1500 m asl in the relatively arid eastern parts of Skagit valley. The presence of its fossils in glacial Lake Concrete sediments indicates a westward shift of continental climate (i.e. lower precipitation). The importance of this species in identifying a cold, dry Evans Creek stade climate in Puget Lowland was emphasized by Whitlock (1992). Northern spikemoss is currently not found in Washington, although it is present at wet sites at high elevations in the Rocky Mountains in Idaho, Wyoming, and Montana (Scoggan, 1978). It is also present in Port Moody interstade pollen assemblage in Fraser Lowland (Figure 4-1; Lian at al., 2001). High numbers of macrofossils of this species in glacial Lake Concrete sediments support the inference of a cold climate similar to that found in wet sites at high elevations and high latitudes today. Due to inverted radiocarbon ages in unit 7 at the Big Boy section and poor fossil preservation, it is difficult to draw more detailed conclusions can not be drawn about the environment around glacial Lake Concrete during this period.

Similar conditions have been inferred elsewhere in Puget Lowland for the period 20,000-17,000 ^{14}C yr BP based on the presence of xeric taxa such as sagebrush (*Artemesia* sp.) and the absence of mesophytic taxa (Barnosky, 1984). Barnosky et al. (1987) and Thackray (1999) argued this interval was the coldest and driest of the Fraser Glaciation.

A large increase in abundance and diversity of conifer needles in the upper sediments of glacial Lake Concrete indicates that warmer and wetter conditions prevailed after about 17,570 ^{14}C yr BP (Tables 4-3 and 4-4). This interpretation is supported by the absence of northern spikemoss macrofossils after 17,570 ^{14}C yr BP. Almost all Evans Creek stade fossil sites in the Pacific Northwest record an increase in percentages of tree pollen and an associated drop in non-arboreal pollen at this time (Figure 4-9). The event is marked by pollen zone boundaries at

Fargher Lake at 17,100 ± 650 ^{14}C yr BP (Heusser and Heusser, 1980) and at Bogachiel Bog about 16,850 ± 630 ^{14}C yr BP (Heusser, 1978). Western hemlock pollen increased after about 18,000 ^{14}C yr BP at Kalaloch (Heusser, 1977). Barnosky (1985) identified an interstadial warm period between 17,000 and15,000 ^{14}C yr BP at Battleground Lake in the southern Puget Lowland, based on increased abundance of Douglas fir, Sitka spruce, and red alder macrofossils.

The Sisters Creek Formation was deposited in Fraser Lowland during the Port Moody interstade from about 18,700 to 17,700 ^{14}C yr BP (Hicock et al., 1982, 1999; Hicock and Lian, 1995). Vegetation in Fraser Lowland at that time has been described as open forest parkland, similar to modern subalpine vegetation in the British Columbia interior, an environment characterized by long, cold, wet winters and wet, frost-free summers (Hicock et al., 1982; Lian et al., 2001).

The Sisters Creek Formation contains moss and leaf litter beetles, ground beetles, weevils, and bark beetles. Miller et al. (1985) interpreted the assemblage as indicative of an open forest floor community near treeline. A beetle assemblage in central Puget Lowland, dated at 16,400 ^{14}C yr BP, suggests temperate, dry conditions (Nelson and Coope, 1982).

The Port Moody interstade ended about 17,700 ^{14}C yr BP (Hicock et al., 1982; Hicock and Lian, 1995). Persistence of ice-dammed, glacial Lake Skymo until after 18,020 ^{14}C yr BP and glacial Lake Concrete until 16,400 ^{14}C yr BP, and the presence of Engelmann spruce macrofossils in the uppermost lake Concrete beds are evidence that subalpine forest was widespread in the region through the Evans Creek stade and Port Moody interstade up to the beginning of the Vashon stade. The presence of non-arboreal Poaceae, cinquefoil, Caryophyllaceae, and Brassicaceae macrofossils suggest that forest cover was patchy.

In summary, Skagit valley macrofossils and stratigraphy record millennial- or sub-millennial-scale fluctuations of climate during the early part of the Fraser Glaciation (Figure 4-9). The Evans Creek stade included two cold phases that ended with wetter and warmer periods centered around 20,310 and 17,170 ^{14}C yr BP. Based on pollen and macrofossil data, Grigg and Whitlock (2002) suggested that climate during the early Fraser Glaciation oscillated between cold-dry and cold-wet. Thackray (1999) suggested that millennial-scale climate oscillations controlled the advance and retreat of glaciers on western Olympic Peninsula. Fluctuations in the extent of glaciers in southwestern British Columbia during the Fraser Glaciation have been related to Bond cycles (Hicock et al., 1999). Pollen and radiolaria from Pacific Ocean cores also reveal millennial-scale climate variability (Pisias et al., 2001).

Treeline change

Macrofossil data suggest that treeline was near 500 m asl ca. 24,000 ^{14}C yr BP, when Big Beaver Glacier first impounded glacial Lake Skymo. Although a few lowland species are present in the macrofossil assemblages, abundant Engelmann spruce, whitebark pine, and subalpine fir macrofossils are compelling evidence that treeline was within a few hundred metres of the lake. Other macrofossil indicators of cold climate include bog birch, sheathed pond weed, and the insects *Olophrum borealis* and *Eucnecosum tenue* (Brayshaw, 1985).

A decrease in treeline from its modern elevation of 1700 m asl to as low as 500 m asl in upper Skagit valley corresponds to a maximum ~7 ± 1°C drop in mean July temperature, assuming a measured local lapse rate of 0.6°C/100 m (Figure 4-3). Another method for assessing paleo-temperature change from treeline changes assumes that modern treeline has a mean July temperature of 10°C. Modern mean July temperature at Ross Lake is 18°C, an 8°C temperature depression would be required to depress treeline to 500 m asl.

Evans Creek treeline depression and temperature reduction in Skagit valley are comparable to other regional estimates. A 1200-1500 m lowering of treeline and 8°C temperature reduction have been reported for the Sisters Creek Formation at 18,300 ^{14}C yr BP (Hicock et al., 1982; Telka et al., 2003). Whitlock (1992) suggested that mean annual temperature was 5-7°C lower than at present at Battleground Lake in southern Washington between 20,000 and 16,000 ^{14}C yr BP. The Davis Lake record in southern Puget Lowland was used to infer a reduction in mean annual temperature of 7 °C over the same period. Treeline depression in the western U.S. at the last glacial maximum has been estimated to be 700-1000 m (Antevs, 1954; Baker 1970).

Conclusions

Returning to the questions posed at the beginning of this chapter:

What was the vegetation in Skagit valley during the Evans Creek stade?

Skagit valley contained at least two important plant and insect communities during the early Fraser Glaciation. In upper Skagit valley, glacial Lake Skymo was surrounded by subalpine parkland with some lowland species. An extensive willow wetland surrounded shallow glacial Lake Concrete in lower Skagit valley. Forest expanded around the lake after 17,570 ^{14}C yr BP.

What was the elevation of treeline in Skagit valley during the Evans Creek stade?

Macrofossils of several species indicate that treeline in upper Skagit valley during the Evans Creek stade was about 500 m asl. The strongest evidence for a subalpine environment at low elevations is abundant subalpine tree macrofossils in the fossil record of glacial lakes Skymo and Concrete. Other plant indicators of cold conditions include bog birch, northern spikemoss, and sheathed pond weed.

Do changes in macrofossil abundance and diversity through time support independent evidence of a mid-Evans Creek stade warm period?

A significant change in abundance and diversity of conifer macrofossils in the glacial Lake Skymo record after 20,770 ^{14}C yr BP signals a shift toward warmer and more mesic conditions. These data are consistent with geologic evidence at the Cedar Grove site for glacier retreat before 20,730 ^{14}C yr BP, and for a second Evans Creek glacier advance after this date.

Did the Port Moody interstade extend south to Skagit valley?

The Port Moody interstade extended from Fraser Lowland at least as far south as Skagit valley. Increased abundance and diversity of macrofossils in glacial Lake Concrete sediments after 17,570 ^{14}C yr BP signal this change. Evidence collected in this study, however, does not confirm that the Port Moody interstade began as early as 18,700 ^{14}C yr BP, as suggested by others.

What are the magnitude and range of climate changes during the Evans Creek stade?

A maximum 1200 m depression of treeline implies a 7 ± 1 °C drop in mean annual temperature compared to present during the Evans Creek stade. Precipitation increased at least 200 mm between 20,770 and 20,310 ^{14}C yr BP.

Acknowledgements

This research would not have been possible without the contribution of Alice Telka, who painstakingly processed, identified, and helped place in context hundreds of macrofossils. Alecia Spooner processed and identified conifer needles in separate samples, and Dr. Rolf Mathewes and Dr. Linda Brubaker confirmed identification of some species. Financial support was provided by a grant from the Skagit Environmental Endowment Commission, by the U.S. National Park Service, and by an NSERC Discovery Grant to John Clague.

Figures

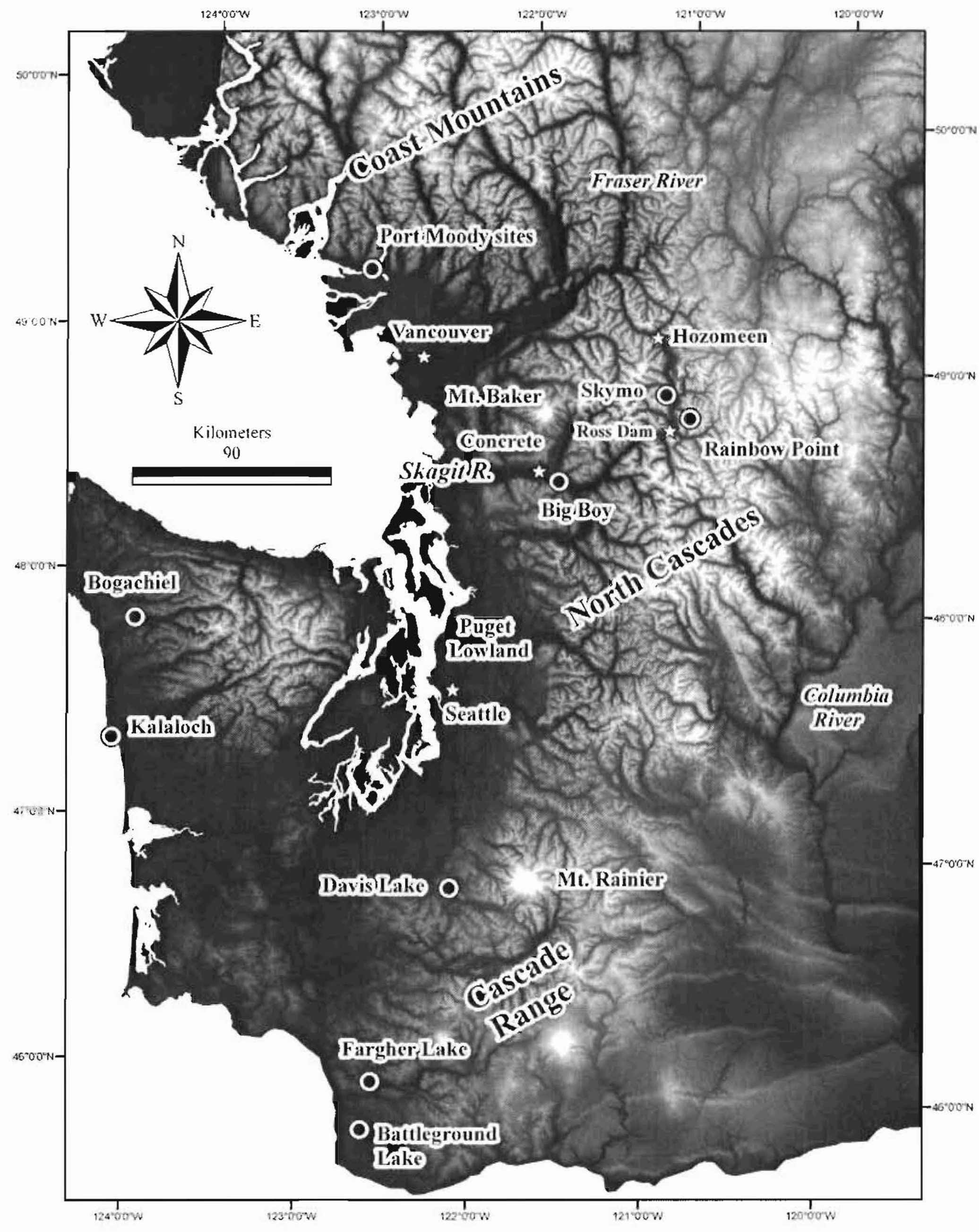

Figure 4-1. Locations of the Skagit valley study area and Evans Creek stade paleoecological sites in the Pacific Northwest. See Chapter 3 for more detailed Skagit site locations.

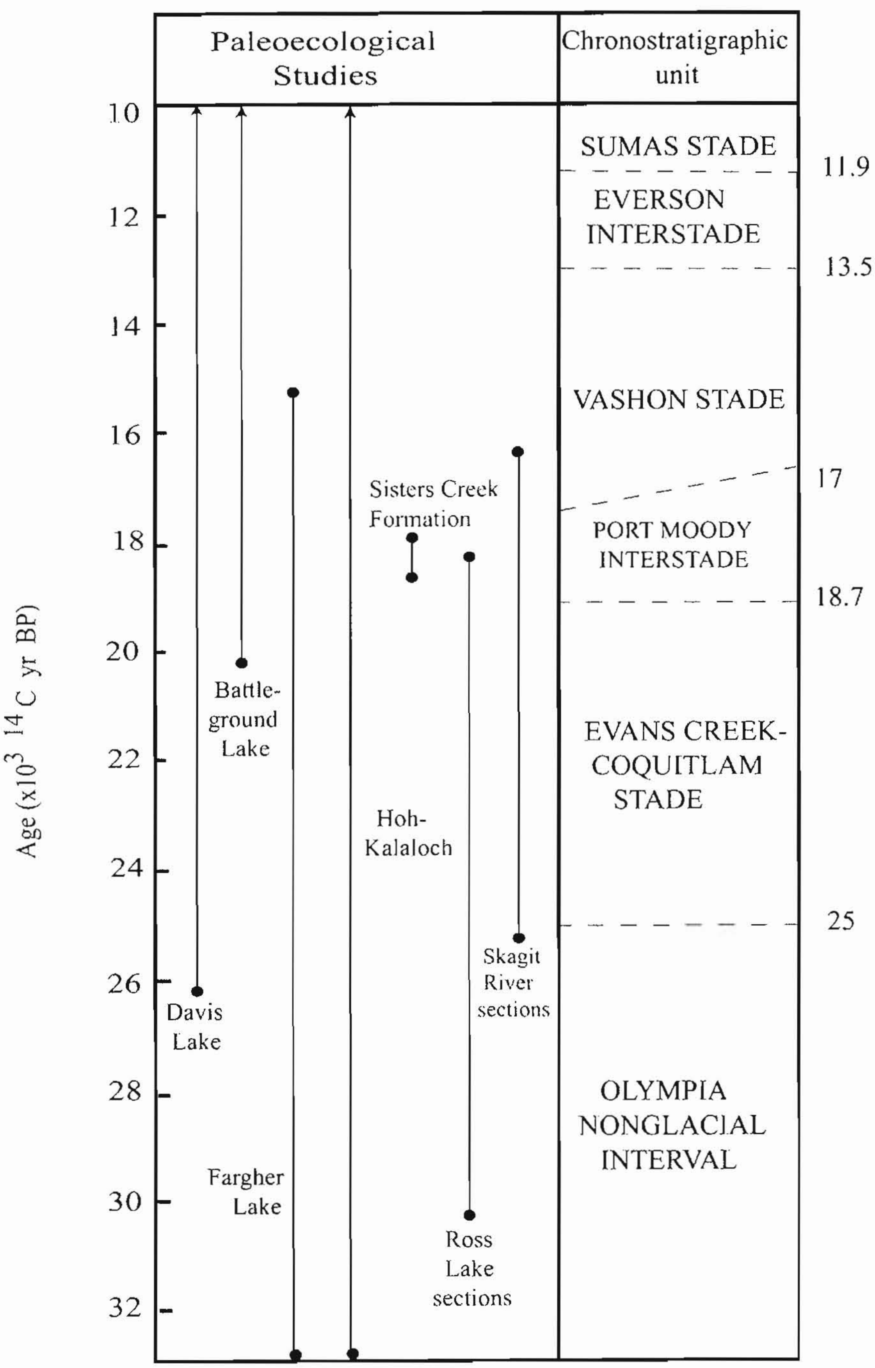

Figure 4-2. Paleoenvironmental records of the Fraser Glaciation for Washington and British Columbia (modified from Armstrong et al., 1965).

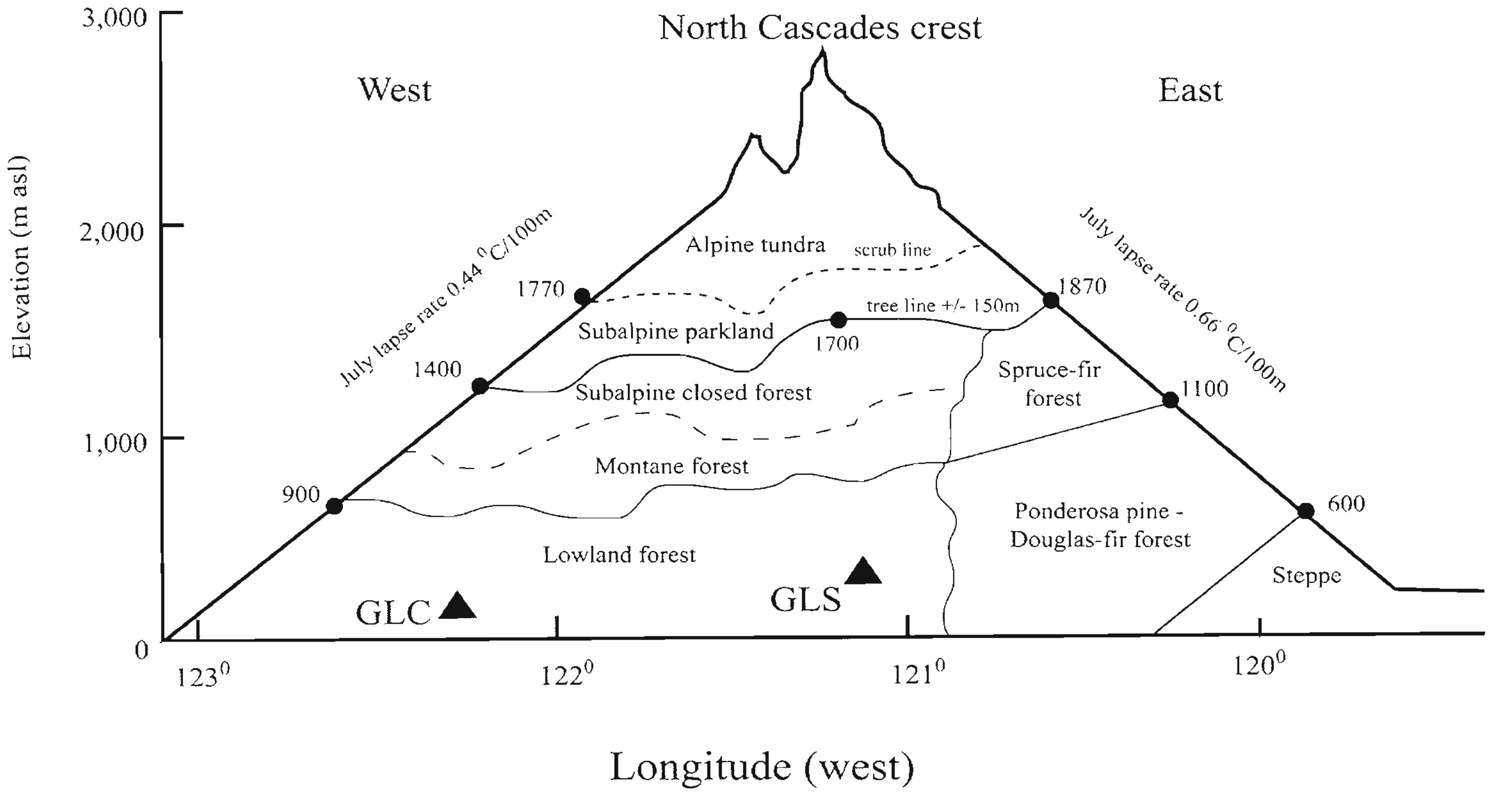

Figure 4-3. Modern vegetation zonation in the North Cascade Range (modified from Heusser, 1983). GLC – glacial Lake Concrete; GLS – glacial Lake Skymo.

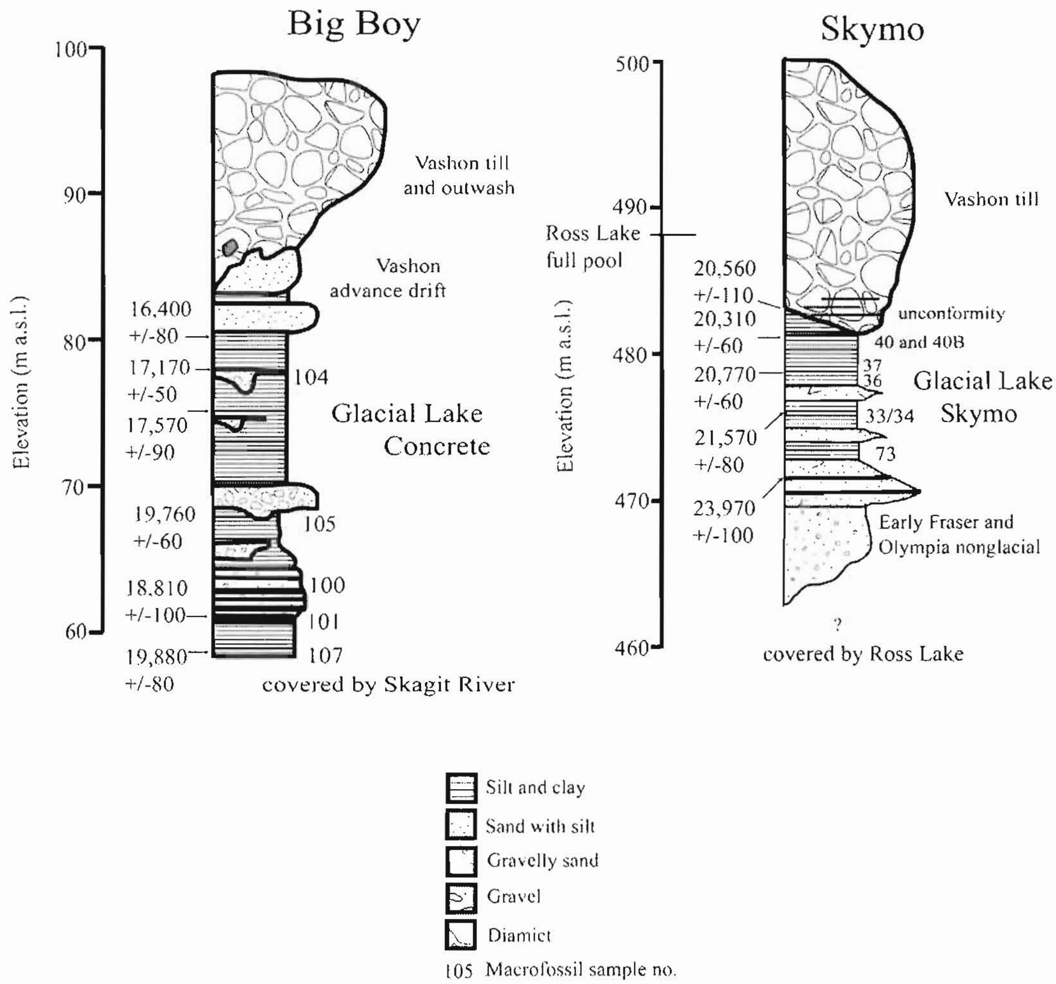

Figure 4-4. Stratigraphy of the Skymo and Big Boy sections showing macrofossil sample locations.

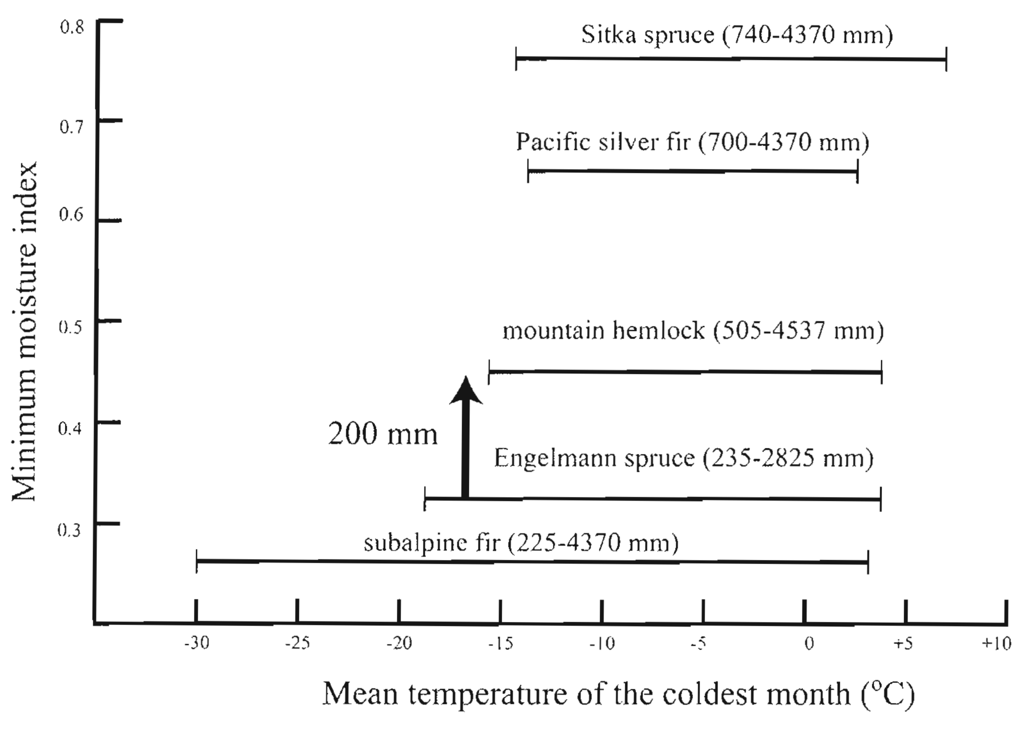

Figure 4-5. Range of conifer species based on bioclimatic variables, with mean annual precipitation in millimetres.

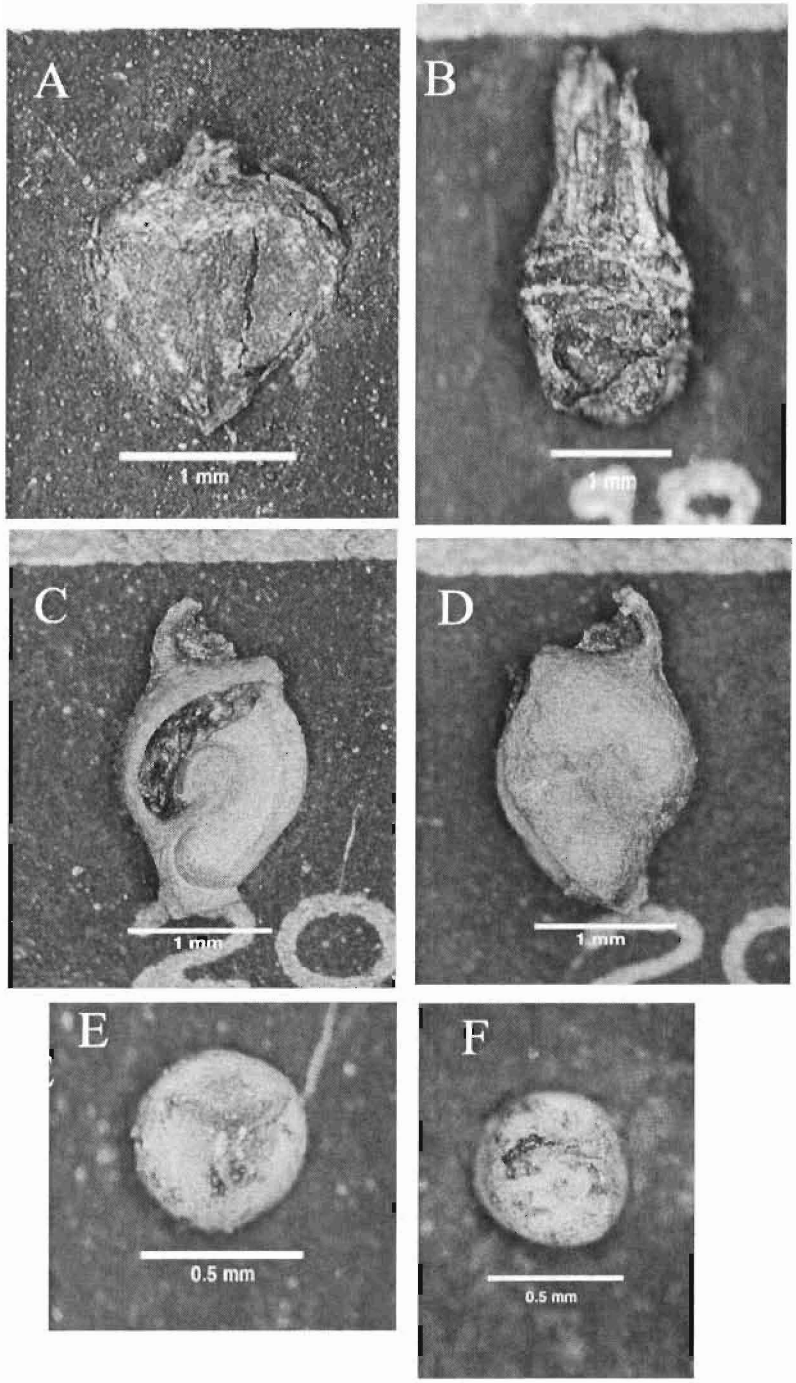

Figure 4-6. Selected cold-adapted plant macrofossils from glacial lakes Skymo and Concrete sediments. A) Bog birch (*Betula glandulosa/nana* type) nutlets, B) Whitebark pine (*Pinus albicaulis*) fascicles, C-D) alpine pondweed (*Potamogeton alpinus*) seeds, E-F) Northern spikemoss (*Selaginella selaginoides*) megaspores. Photos by Alice Telka.

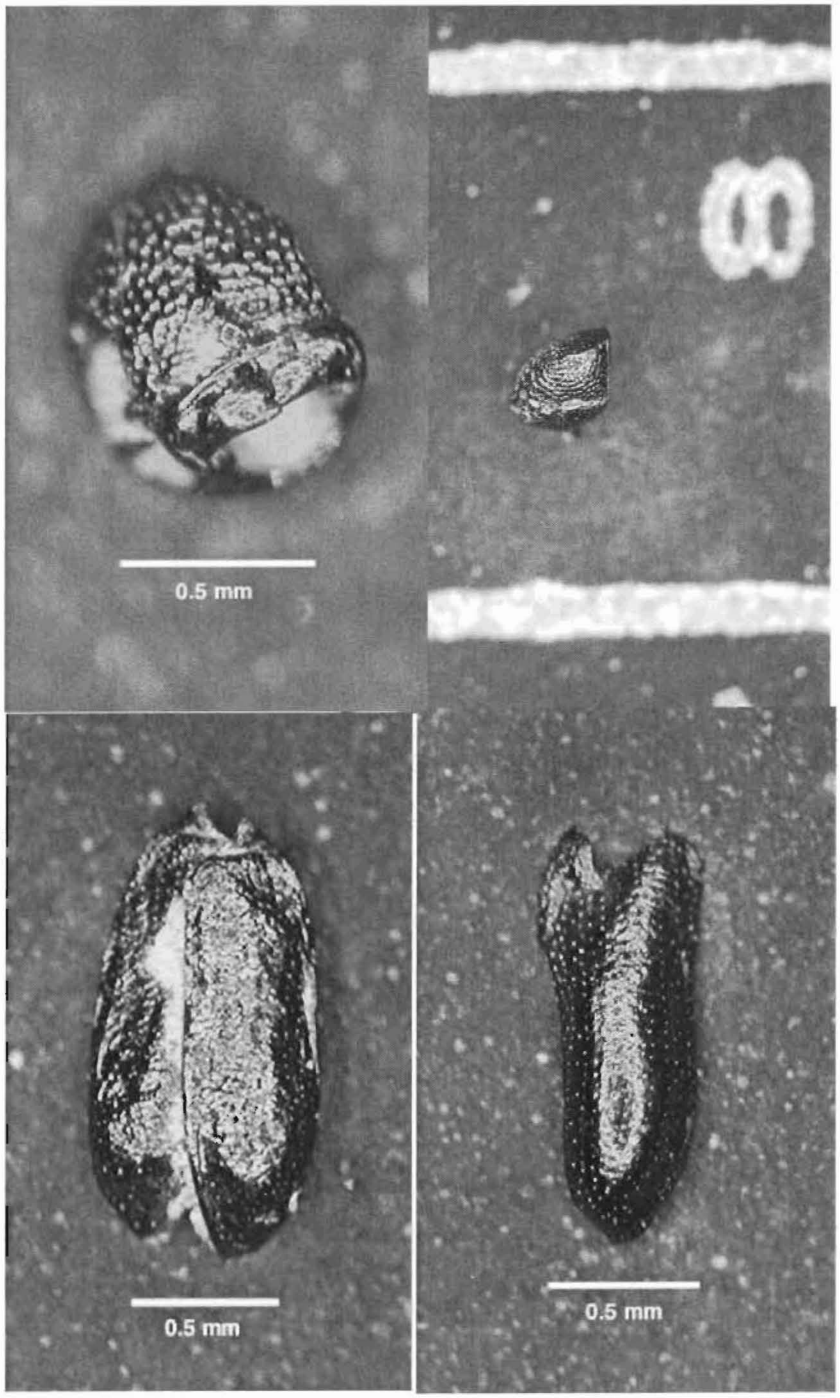

Figure 4-7. Selected bark beetle (*Pityophthorus* sp.) fossils from glacial Lake Skymo sediments. Clockwise from upper left, head, prothorax, elytron, and articulated elytra. Photos by Alice Telka.

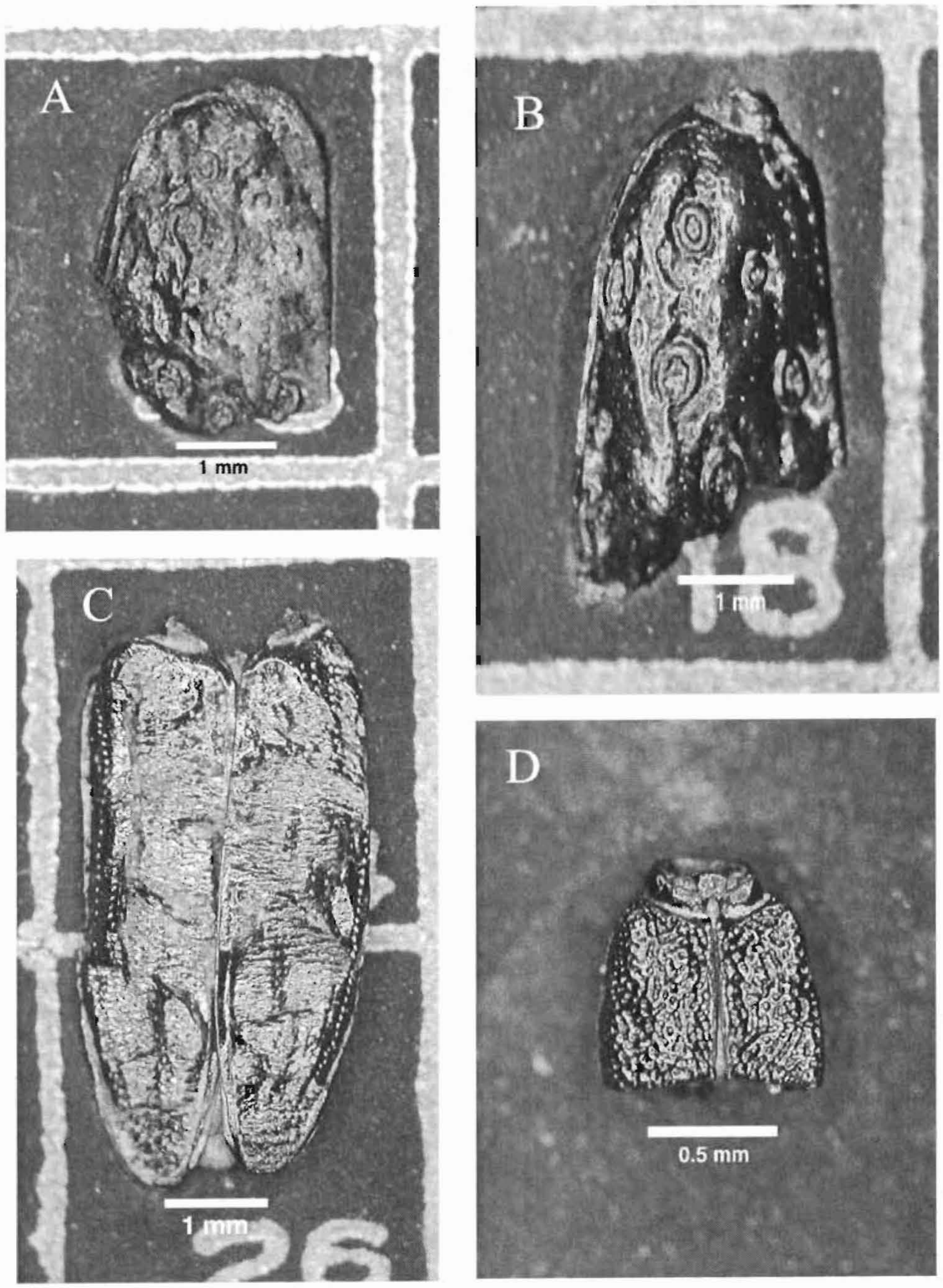

Figure 4-8. **Selected beetle fossils from glacial Lake Concrete sediments. A-B) ground beetle (*Elaphrus clairvillei*) half elytra, C) leaf beetle (*Plateumaris* sp.) articulated elytra and prothorax, and D) rove beetle (*Stenus* sp.) articulated elytra. Photos by Alice Telka.**

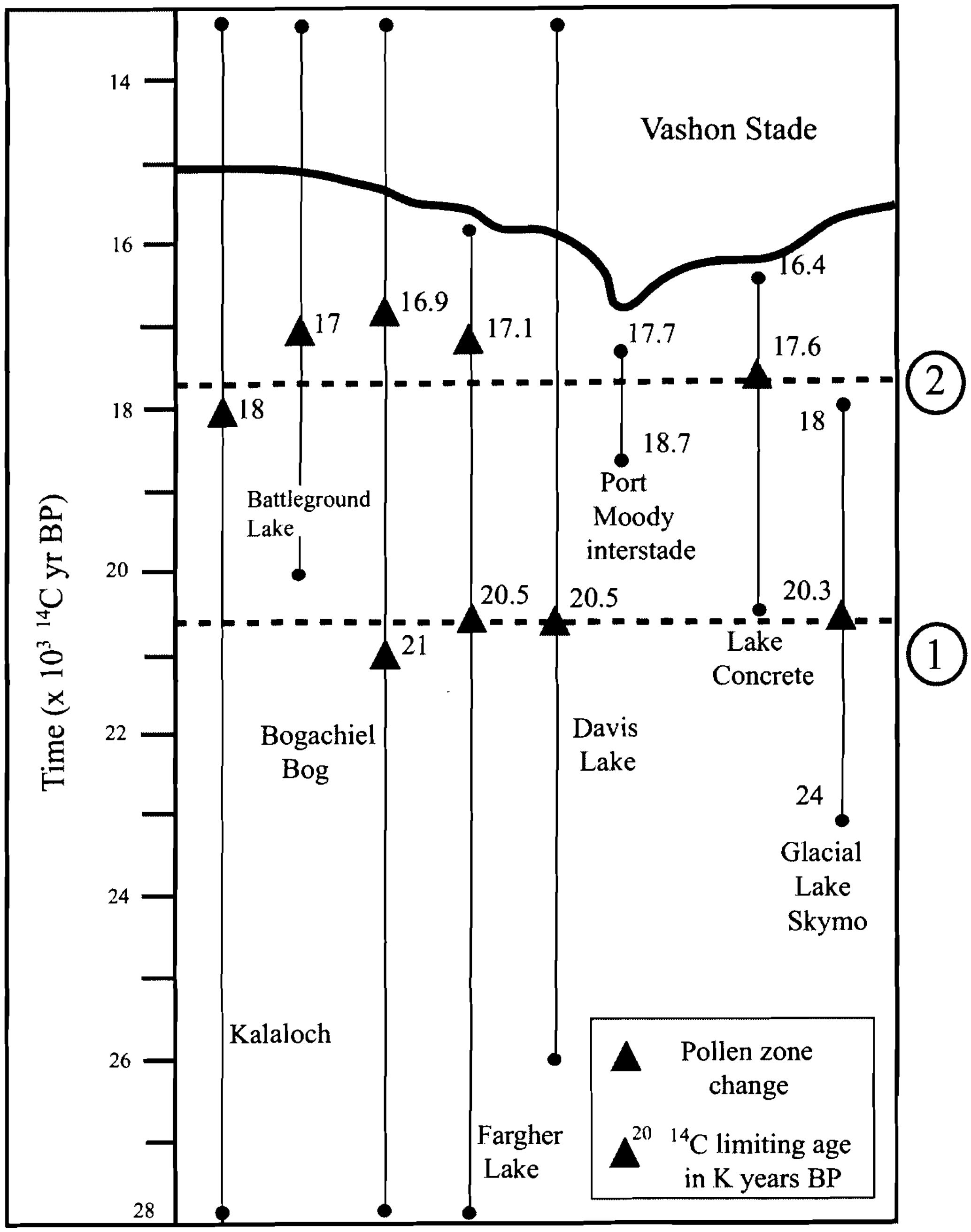

Figure 4-9. Important events identified by Skagit macrofossil assemblages during the early part of the Fraser Glaciation including: (1) warmer and wetter conditions about 20,740 ^{14}C yr BP; and (2) a return to milder conditions during the Port Moody interstade, after 17,570 ^{14}C yr BP. See text for references to other paleoecological studies noted.

Tables

Table 4-1. Radiocarbon ages from upper Skagit valley.

Site/sample	m asl	Lab no.[1] / method	Material	$^{13}C/^{12}C$	^{14}C age +/- 1σ yr BP	mean cal. age +/- 1σ yr BP [2]
Skymo NOCA 1989	488.6	Beta - 33923 radiometric	wood	n/a	20,560 +/- 110	24,448 +/- 157
Skymo NOCA 4	482.6	GSC - 6736 radiometric	wood (*Picea*)	-24.2	20,900 +/- 220	24,979 +/- 325
Skymo NOCA 5	478.7	GSC - 6738 radiometric	wood	-24.43	21,400 +/- 240	25,681 +/- 352
Skymo NOCA 6	477.6	Beta - 178536 radiometric	wood	-24.6	21,570 +/- 80	25,947 +/- 133
Ruby Cr. NOCA 13	467.7	GSC - 6742 radiometric	wood	-27.28	17,400 +/- 350	20,610 +/- 414
Skymo NOCA 19	472.1	Beta - 178537 radiometric	wood	-23.3	23,970 +/- 100	28,700 +/- 175
Skymo NOCA 37	480.0	Beta - 216087 AMS	wood	-24.3	20,770 +/- 80	24,794 +/- 164
Rainbow Pt. NOCA 23	488.9	Beta - 178538 radiometric	wood	-24.9	18,020 +/- 170	21,402 +/- 270
Rainbow Pt. NOCA 28	478.2	LLNL - 114612 AMS	charcoal	-25.0	23,620 +/- 120	28,307 +/- 192

(continued on next page)

Table 4-1 (continued). Radiocarbon ages from upper Skagit valley.

Site/sample	m asl	Lab no.[1] / method	Material	$^{13}C/^{12}C$	^{14}C age +/- 1σ yr BP	mean cal. age +/- 1σ yr BP [2]
Skymo NOCA 40	482.5	UC-I – 34410 AMS	wood	-25.6	20,310 +/- 60	24,216 +/- 87
Silver Creek NOCA 84	486.0	Beta - 220960 AMS	charred wood	-23.2	24,080 +/- 170	28,823 +/- 230
Rainbow Pt. NOCA 80	469.0	LLNL - 114613 radiometric	charcoal	-25.0	31,760 +/- 300	37,141 +/- 339
Big Boy NOCA 85	74.0	Beta - 195976 radiometric	wood	-25.9	17,570 +/- 90	20,778 +/- 140
Big Boy NOCA 88	61.0	Beta - 195973 AMS	wood	-24.7	18,810 +/- 100	22,396 +/- 107
Big Boy NOCA 89	79.0	Beta - 195974 AMS	cone (*Picea engelmannii*)	-22.7	16,400 +/- 80	19,515 +/- 97
Big Boy NOCA 104	76.0	Beta - 215977 AMS	wood	-24.6	17, 170 +/- 50	20,345 +/- 70
Big Boy NOCA 105	68.0	UC-I – 34411 AMS	wood	-27.5	19,760 +/- 60	23,611 +/- 108
Big Boy NOCA 107	59.0	Beta - 211363 AMS	wood	-28.6	19,880 +/- 80	23,754 +/- 126
Big Boy NOCA 109	66.0	Beta - 216088 AMS	wood	-25.4	19,810 +/- 80	23,670 +/- 126

(continued on next page)

Table 4-1 (continued). Radiocarbon ages from upper Skagit valley.

Site/sample	m asl	Lab no.[1] / method	Material	$^{13}C/^{12}C$	^{14}C age +/- 1σ yr BP	mean cal. age +/- 1σ yr BP[2]
Lyman NOCA 117	40.0	Beta - 21364 AMS	wood	-28.3	23,500 +/- 130	28,172 +/- 203
Mastodon NOCA 125a	??	Beta - 220961 AMS	wood	-26.6	16,333 +/- 60	19,451 +/- 83
Cedar Grove NOCA 125b	62.0	UC-I - 31865 AMS	wood	-27.5	25,040 +/- 60	30,112 +/- 54
Cedar Grove NOCA 126	71.0 AMS	UC-I - 31866	wood	-26.6	20,730 +/- 40	24,725 +/- 116

[1] Beta – Beta Analytic; GSC – Geological Survey of Canada; LLNL – Lawrence Livermore National Laboratory; UC-I – University of California, Irvine

[2] From Fairbanks et al. (2005).

Table 4-2. Extreme modern climate ranges for select tree species (Thompson et al., 1999.)

	January precipitation (mm)	Mean annual precipitation (mm)	Mean July temperature (˚C)	Mean temperature coldest month (˚C)	Moisture index*
Mountain hemlock *Tsuga mertensiana*	35-616	505-4730	7.8-20.9	-15.6 - +4.1	0.44
Subalpine fir *Abies lasiocarpa*	9-616	225-4370	7.1-22.7	-30 - +3.5	0.24
Engelmann spruce *Picea engelmannii*	11-451	235-2825	7.1-22.4	-18.7 - +4.2	0.32
Whitebark pine *Pinus albicaulis*	12-612	285-4370	7.1-22.4	-18.7 - +2.2	0.34
Sitka spruce *Picea sitchensis*	63-616	740-4370	7.8-19	-14.7 - + 7.6	0.77
Bog birch *Betula nana*	4-332	1115-4130	4.5-16.4	-34.8 - -0.5	0.28

* Moisture index = actual evaporation divided by potential evaporation

Table 4-3. Abundance and diversity of Evans Creek stade conifer macrofossils recovered from sediments of glacial lakes Skymo and Concrete.

Radiocarbon age (sample no.)	Western hemlock / Douglas-fir	Sitka spruce	Mountain hemlock	Amabilis fir / Grand fir	Subalpine fir	Engelmann spruce	Total number/litre
<u>Glacial Lake Concrete</u>							
17,140 (104)	13	18	-	2	33	61	127
>17,570 (105)	-	-	-	1	2	-	3
18,810 (100)	-	4	-	-	1	15	20
<u>Glacial Lake Skymo</u>							
18,020 (61, 98) *	3	-	1	5	2	10	21
20,310 (40)	10	14	53	18	59	116	270
20,770 (37)	-	47	-	8	47	101	203
21,560 (33, 34, 77)	3	4	6	-	4	63	80
23,620 (56)	1	-	1	-	-	2	4

Note: Count includes cones, fascicles, and needle tips and bases.
* Sample from Rainbow Point; all others from Skymo section.

Table 4-4A. Glacial Lake Skymo deciduous plant and insect macrofossils per litre sediment.

Taxon	Skymo* NOCA 40 + 40B <20,770 ^{14}C yr BP	Skymo NOCA 37 <20,770 ^{14}C yr BP	Skymo NOCA 33 21,560 ^{14}C yr BP
Bryophytes	46 fragments	458 fragments	74 fragments
Pinaceae	17 seeds, 15 seed wings, 29 cone scales	29 seed wings, 29 seeds, 1 cone scale	5 seed wing fragments, 2 half seeds, 11 twig terminals
Abies spp.	36 whole needles, 4,163 needle tips and bases, 1 seed, 62 twig terminals	136 whole needles, 1,395 tips and bases, 15 twig terminals	11 twig terminals, uncounted needle fragments
Picea spp.	50 whole needles, 3,380 tips and bases, 53 twig terminals	804 whole needles, 6,165 tips and bases, 110 twig terminals	uncounted needles, 69 twig terminals
Pinus albicaulis	1 whole needle, 44 needle fascicles, 451 needle tips and bases	496 needle tips and bases, 94 needle fascicles	83 needle fascicles, uncounted needles
Salix	1 persistent bud	--	--
Betula	--	1 *Betula nana* type nutlet	1 *Betula nana* type nutlet, 2 *Betula* sp. nutlets
Potamogeton spp.	*P. vaginatus*: 37 achenes	*P. alpinus*: 6 achenes	--
Ranunculus aquatilis	107 achenes	20 achenes, 26 half achenes	90 achenes, 158 half achenes
Carex sp. lent. type	57 achenes	226 achenes	47 achenes
Carex sp. trigonus type	54 seeds, perigynium fragments	23 achenes	22 achenes
Empetrum nigrum	--	1 nutlet	4 nutlets
Coleoptera	5 species, 29 body parts, 1 articulated	7 species, 32 body parts, 4 articulated	5 species, 16 body parts, 9 articulated
Diptera-Chironomidae	176 larvae head capsules	17 larvae head capsules	199 larvae head capsules
Crustacea–*Daphnia* sp.	383 ephippia	122 ephippia	463 ephippia
Hymenoptera	4 heads, 2 thorax fragments	--	4 thoracic fragments
Arachnida	5 mites, 1 spider thorax	1 mite	2 mites
Other animal	14 small mammal fecal pellets	1 Lepidoptera mandible	

* Double volume.

Table 4-4B. Glacial Lake Concrete plant and insect macrofossils per litre sediment.

Macrofossil	Big Boy, NOCA 104 17,170 ^{14}C yr BP	Big Boy, NOCA 105 >17,570 ^{14}C yr BP	Big Boy, NOCA 100 18,810 ^{14}C yr BP	Big Boy, NOCA 101 18,810 – 19,880 ^{14}C yr BP
Unidentified	--	--	2 seeds	8 seeds
Fungal sclerotia	52	3	157	2
Bryophytes	Many fragments of a few types	Many fragments of a few types	*Sphagnum* sp.: fragment	Leaves and stem fragments, stem fragments
Carex lent. type	33 achenes with partial perigynia, 22 achenes	Type 1: 264 achenes with partial perigynia, 120 achenes without perigynia Type 2: 4 achenes with partial perigynia	32 achenes, 8 achenes with perigynia	7 achenes with partial perigynia Type 1: 135 achenes
Carex trigonous type	1 achene	3 achenes *Eriophorum* sp.: 2 achenes	--	1 achene
Selaginella sp.	--	1 megaspore	*Selaginoides* (L.) Link: 43 megaspores	*Selaginoides* (L.) Link: 462 megaspores
Pinaceae	431 medial needle fragments, 2 cone scales, 1 seed, 1 seed wing, 2 seed wing fragments	3 medial needle fragments	--	1 seed
Abies sp.	Needles: 4 whole, 196 tips and bases, 7 terminal fragments	Needles: 2 tips, 1 base	1 needle tip, 1 fragment, 1 twig terminal fragment	--
Picea sp.	Needles: 6 whole, 237 tips and bases, 11 twig terminal fragments	--	Needles: 1 tip, 3 bases, 1 half, 6 fragments	Needles: 1 tip, 1 base, 1 fragment
Tsuga/Pseudotsuga sp.	Needles: 2 whole, 2 bases, 1 medial fragment	--	--	--

(continued on next page)

Macrofossil	Big Boy, NOCA 104 17,170 ^{14}C yr BP	Big Boy, NOCA 105 >17,570 ^{14}C yr BP	Big Boy, NOCA 100 18,810 ^{14}C yr BP	Big Boy, NOCA 101 18,810 – 19,880 ^{14}C yr BP
Equisetum sp.	~11 stem fragments	~67 stem fragments	~10 stem fragments	~18 stem fragments
Juncaceae	*Juncus bufonius?*: ~3 seeds	*Juncus bufonius?*: ~10 seeds	*Luzula* sp.: 26 seeds	~20 seeds
Salix sp.	2 seed capsules, 6 half capsules, ~68 buds, ~21 twigs with buds	4 seed capsules, 11 half capsules, ~52 buds, ~5 twigs with buds	2 seed capsules, 3 buds	1 half seed capsule, 92 buds, 4 twigs with buds
Polygonum? sp.	--	1 achene	--	--
Rosaceae	*Rubus idaeus* L.: 1 half stone	Argentina anserine (L.) Rydb.: 3 half achenes; *Potentilla* sp., 8 achenes	--	--
Betulaceae	*Alnus?* sp.: 1 seed	--	--	--
Chenopodium sp.	4 seed fragments	--	--	--
Caryophyllaceae	1 seed fragment	--	--	--
Brassicaceae	2 seeds	--	--	--
Others	Twig/wood fragments, ~30 deciduous leaf fragments, ~50 leaf blades, 4 bud scales, bark fragments	~20 bud scales, bark fragments, twig fragments, root fragments, 1 deciduous leaf fragment	Root fragments, wood/twig fragments, 3 charcoal fragments, 2 deciduous leaf fragments	Wood, twig, and bark fragments
Coleoptera (see Appendix 4-1)	27 body parts	104 body parts	17 body parts	88 body parts
Diptera and Tipulidae	2 half pupae, 2 larval head capsules, 2 half head capsules	7 larval head capsules, 12 half head capsules	--	4 half pupae, 26 fragments, 1 half larval head capsule
Crustacea	--	--	--	1 ephippium
Hymenoptera	1 head, 2 thoracic fragments	4 heads, 2 thorax fragments	--	3 thoracic fragments

(continued on next page)

Macrofossil	Big Boy, NOCA 104 17,170 ^{14}C yr BP	Big Boy, NOCA 105 >17,570 ^{14}C yr BP	Big Boy, NOCA 100 18,810 ^{14}C yr BP	Big Boy, NOCA 101 18,810 – 19,880 ^{14}C yr BP
Arachnida	1 mite, 2 half mites, 1 chelicer spider	3.5 mites, 1 spider palp, 2 male cephalothoraces	1 mite	18 mites
Other	~34 small mammal fecal pellets; pupa: 2 whole, 2 half, 1 fragment	~50 half pupa and fragments, 3 larval head capsules, 3 immature mandibles	2 pupa fragments, 1 larval head capsule	5 small mammal fecal pellets (star-shaped in cross-section), 1 pupa and 2 fragments, 5 half larval head capsules

Reference List

Antevs, E., 1954. Climate of New Mexico during the last glacio-pluvial. Journal of Geology 62: 182-191.

Armstrong, J.E., Crandell, D.R., Easterbrook, D.J., and Noble, J.B., 1965. Late Pleistocene stratigraphy and chronology in southwestern British Columbia and northwestern Washington. Geological Society of America Bulletin 76: 321-330.

Arno, S.F., and Hammerly, R.P., 1984. Timberline: Mountain and Arctic Forest Frontiers. The Mountaineers, Seattle, WA.

Baker, R.G., 1970. Pollen sequence from late Quaternary sediments in Yellowstone Park. Science 168: 1449.

Barnosky, C.W., 1981. A record of Quaternary vegetation from Davis Lake, southern Puget Lowland, Washington. Quaternary Research 16: 221-239.

Barnosky, C.W., 1984. Late Pleistocene and early Holocene environmental history of southwestern Washington state, U.S.A. Canadian Journal of Earth Sciences 31: 619-629.

Barnosky, C.W., 1985. Late Quaternary vegetation near Battle Ground Lake, southern Puget Trough, Washington. Geological Society of America Bulletin 96: 263-271.

Barnosky, C.W., Anderson, P.M., and Bartlein, P.J., 1987. The northwestern U.S. during deglaciation: Vegetational history and paleoclimatic implications. In: Ruddiman, W.F., and Wright, Jr., H.E. (eds.), North America and Adjacent Oceans during the Last Deglaciation. Geological Society of America, The Geology of North America K-3: 289-321.

Birks, H.J.B., and Birks, H.H., 1981. Quaternary Paleoecology. E. Arnold Press, London.

Brayshaw, T.C., 1985. Pondweeds and Bur-reeds, and Their Relatives: Aquatic Families of Monocotyledons in British Columbia. British Columbia Provincial Museum Occasional Paper 26.

Daubenmire, R., 1973. Taxonomic and ecologic relationships between *Picea glauca* and *Picea engelmannii*. Canadian Journal of Botany 52: 1545-1560.

Dunwiddie, P.W., 1985. Dichotomous key to conifer foliage in the Pacific Northwest. Northwest Science 59: 185-191.

Dunwiddie, P.W., 1987. Macrofossil and pollen representation of coniferous trees in modern sediments from Washington. Ecology 68: 1-11.

Fairbanks, R.G., Mortlock, R.A., Tzu-Chien, C., Li, C., Kaplan, A., Guilderson, T.P., Fairbanks, T.W., and Bloom, A.L., 2005. Marine radiocarbon calibration curve spanning 0-50,000 years B.P. based on paired $^{230}Th/^{234}U/^{238}U$ and ^{14}C dates on pristine corals. Quaternary Science Reviews 24: 1781-1796.

Farrar, J.L., 1995. Trees in Canada. Fitzhenry and Whiteside Ltd. and Canadian Forest Service, Ottawa, ON.

Franklin, J.F., and Dyrness, C.T., 1973. Natural Vegetation of Oregon and Washington. U.S. Forest Service Technical Report PNW-8.

Halliday, W.E.D., and Brown, A.W.A., 1943. The distribution of some important forest trees in Canada. Ecology 33: 31-41.

Heusser, C.J., 1974. Quaternary vegetation, climate, and glaciation of the Hoh River Valley, Washington. Geological Society of America Bulletin 85: 1547-1560.

Heusser, C.J., 1977. Quaternary palynology of the Pacific Slope of Washington. Quaternary Research 8: 282-306.

Heusser, C.J., 1978. Palynology of Quaternary deposits of the lower Bogachiel River area, Olympic Peninsula, Washington. Canadian Journal of Earth Sciences 15: 1568-1578.

Heusser, C.J., 1983. Vegetational history of the northwestern United States including Alaska. In: Porter, S.C. (ed.), Late-Quaternary Environments, Vol. 1, The Late Pleistocene. University of Minnesota Press, Minneapolis, MN, pp. 239-258.

Heusser, C.J., and Heusser, L.E., 1980. Sequence of pumiceous tephra layers and the late Quaternary environmental record near Mount St. Helens. Science 210: 1007-1009.

Heusser, C.J., and Igarashi, Y., 1994. Quaternary migration pattern of *Selaginella selaginoides* in the North Pacific. Arctic and Alpine Research 26: 187-192.

Heusser, C.J., and Peteet, D.M., 1988. Spores of *Lycopodium* and *Selaginella* of North Pacific America. Canadian Journal of Botany 66: 508-525.

Hicock, S.R., and Lian, O.B., 1995. The Sisters Creek Formation: Pleistocene sediments representing a nonglacial interval in southwestern British Columbia at about 18 ka. Canadian Journal of Earth Sciences 32: 758-767.

Hicock, S.R., Hebda, R.J., and Armstrong, J.E., 1982. Lag of the Fraser glacial maximum in the Pacific Northwest: Pollen and macrofossil evidence from western Fraser Lowland, B.C. Canadian Journal of Earth Sciences 19: 2288-2296.

Hicock, S.R., Lian, O.B., and Mathewes, R.W., 1999. 'Bond cycles' recorded in terrestrial Pleistocene sediments of southwestern British Columbia, Canada. Journal of Quaternary Science 14: 443-449.

Hitchcock, C.L., and Cronquist, A., 1973. Flora of the Pacific Northwest. University of Washington Press, Seattle, WA.

Isarin, R.F.B., and Bohncke, S.J.P., 1999. Mean July temperatures during the Younger Dryas in Northwestern and Central Europe as inferred from climate indicator plant species. Quaternary Research 51: 158-173.

Krajina, V.J., 1970. Ecology of Forest Trees in British Columbia. University of British Columbia, Department of Botany, Ecology of Western North America 2.

Krajina, V.J., Klinka, K., and Worrall, J., 1982. Distribution and Ecological Characteristics of Trees and Shrubs in British Columbia. University of British Columbia, Faculty of Forestry, Vancouver, BC.

LaBonte, J., 1998. Terrestrial Riparian Arthropod Investigations in the Big Beaver Creek Research Natural Area, North Cascades National Park Service Complex, 1995-1996: Part II, Coleoptera. U.S. Department of Interior, National Park Service, Technical Report NPS/NRNOCA/NRTR/98-02.

Lian, O.B., Mathewes, R.W., and Hicock, S.R., 2001. Paleo-environmental reconstruction of the Port Moody interstade, a nonglacial interval in southwestern British Columbia at about 18,000 ^{14}C yr B.P. Canadian Journal of Earth Sciences 38: 943-952.

Mathewes, R.W., 1993. Evidence for Younger Dryas-age cooling on the North Pacific Coast of America. Quaternary Science Reviews 12: 321-331.

Miller, R.F., Morgan, A.V., and Hicock, S.R., 1985. Pre-Vashon fossil Coleoptera of Fraser age from the Fraser Lowland, British Columbia. Canadian Journal of Earth Sciences 22: 498-505.

Minore, D., 1979. Comparative Autecological Characteristics of Northwestern Tree Species – A Literature Review. U.S. Forest Service, Pacific Northwest Forest and Range Experiment Station, General Technical Report PNW-87.

Nelson, R.E., and Coope, G.R., 1982. A late Pleistocene insect fauna from Seattle, Washington. American Quaternary Association Abstracts with Program, p. 146.

Peterson, E.B., Peterson, N.M., Weetman, G.F., and Martin, P.J., 1997. Ecology and Management of Sitka Spruce, Emphasizing Its Natural Range in British Columbia. University of British Columbia Press, Vancouver, BC.

Pisias, N.G., Mix, A.C., and Heusser, L., 2001. Millennial scale climate variability of the northeast Pacific Ocean and northwest North America based on radiolarian and pollen. Quaternary Science Reviews 20: 1561-1576.

Scoggan, H.J., 1978. The Flora of Canada, Part 3. Canada National Museum of Natural Sciences Publication in Botany 7.

Sudworth, G.B., 1967. Forest Trees of the Pacific Slope. Dover Publications, Toronto, ON.

Telka, A., Ward, B.C., and Mathewes, R.W., 2003. Plant and insect macrofossil evidence of Port Moody interstade in eastern Fraser Lowland, Chehalis watershed, southwestern British Columbia. CANQUA-CGRG Conference Program and Abstracts 139.

Thackray, G.D., 2001. Extensive early and middle Wisconsin glaciation on the western Olympic Peninsula, Washington, and the variability of Pacific moisture delivery to the northwestern United States. Quaternary Research 55: 257-70.

Thompson, R.S., Anderson, K.H., and Bartlein, P.J., 1999. Atlas of Relations between Climatic Parameters and Distributions of Important Trees and Shrubs in North America – Introduction and Conifers. U.S. Geological Survey Professional Paper 1650-A.

Thompson, R.S., Shafer, S.L., Strickland, L.E., Van de Water, P.K., and Anderson, K.H., 2004. Quaternary vegetation and climate change in the western United States: Developments, perspectives, and prospects. In: Gillespie, A.R., Porter, S.C., and Atwater, B.F. (eds.), The Quaternary Period in the United States. Elsevier, Amsterdam, pp. 403-427.

Tyron, A.F., 1949. Spores of the genus *Selaginella* in North America north of Mexico. Annals of the Missouri Botanical Garden 36: 413-431.

Wardle, P., 1974. Alpine treelines. In: Ives, J.D., and Barry, R.G. (eds.), Arctic and Alpine Environments. Mehuen & Co., London, pp. 371-402.

Whitlock, C., 1992. Vegetational climatic history of the Pacific Northwest during the last 20,000 years: Implications for understanding present-day diversity. The Northwest Environmental Journal 8: 5-28.

Appendix

Appendix 4-1. List of Coleopteran remains recovered from glacial Lake Skymo and Lake Concrete sediments.

Taxa	Skeletal parts	Number of individuals
NOCA 40 - <20,770 ^{14}C yr BP		
Carabidae (ground beetles)	Metasternum	1
Nebria (?)	Half elytron	1
Dytiscidae (predaceous diving beetles)	Head, half elytron	1
Staphylinidae (rove beetles)		
Omaliinae	Elytron	1
Eucnecosum tenue (Lec.)	Pronotum, elytron	1
Olophrum sp.	Elytron	1
Olophrum boreale (Payk.)	Pronotum	1
Curculionidae (weevils)	Prothorax	1
Scolytidae (bark beetles)	Prothorax, head, half elytron	3
Pityophthorus sp.	Elytron	1
NOCA 37 20,770 ^{14}C yr BP		
Dytiscidae (predaceous diving beetles)		
Hydroporus sp.	Elytron, metacoxal plate	1
Genus?	Articulated adult	1
Hydrophilidae	Elytron	1
Staphylinidae (rove beetles)		
Bledius sp.	Pronotum	1
Omaliinae	Head, elytra	2
Olophrum sp.	Elytron	1
Tachinus sp.	Elytron	1
Aleocharinae	Elytron	1
Curculionidae (weevils)	Pronotal, articulated pro-and mesosternum, articulated sternites	3

Taxa	Skeletal parts	Number of individuals
Genus?	Elytra	1
Scolytidae (bark beetles)		
Pityophthorus sp.	Pronotum	1
Genus?	Head fragments (mandibles)	2
Unidentified to family	Elytron, articulated pro and mesosterna, sternites femurs, articulated legs	4
NOCA 33 21,570 ^{14}C yr BP		
Dytiscidae (predaceous diving beetles)	Femur	1
Hydroporus sp.	Head, pronotum, elytra, plates	3
Hydrophilidae		
Helophorus sp.	Elytron	1
Staphylinidae (rove beetles)		
Omaliinae	Elytron	2
Aleocharinae	Pronotum	1
Byrrhidae	Pronotum	1
Curimopsis sp.	Head	1
Curculionidae (weevils)	¾ elytron	1
Scolytidae (bark beetles)	Articulated pro and mesosterna	2
Pityophthorus sp.	Articulated head and prothorax, elytron and articulated sternum, elytra	6
Polygraphus rufipennis? (Kirby)	Elytron	1
NOCA 104 17,170 ^{14}C yr BP		
Carabidae (ground beetles)		
Bembidion sp.	Pronotum, elytra fragments	2
Staphylinidae (rove beetles)	Half head, articulated sternites, articulated pro and mesosternum	3

Taxa	Skeletal parts	Number of individuals
Stenus sp.	Elytron	1
Aleocharinae	Articulated pro and mesothorax and elytra, pronotum; elytron	2
Ptiliidae	Articulated head, prothorax, and elytra; elytra	2
Scarabaeidae		
Aegialia sp.	Half pronotum, pronotum fragment, elytra	2
Elateridae	Half elytra (two types)	1
Chrysomelidae	Elytron	1
Curculionidae (weevils)	Half elytra, prothoracic fragments	1
NOCA 105		
Carabidae (ground beetles)	Mesosternum	1
Bembidion sp.	Elytra	1
Agonum sp.	Head, pronotum, elytra	2
Dytiscidae (predaceous diving beetles)		
Genus?	Head, pronotum, elytron, metacoxal plate	1
Hydrophilidae	Head	1
Helophorus eclectus? d'Orchymont	Pronotum	1
Staphylinidae (rove beetles)	Elytra, heads, articulated meso and metasterna, mesosterna	7
Bledius sp.	Pronotum	1
Omaliinae	Heads, elytra, half elytron	7
Olophrum sp.	Elytra	2
Olophrum consimile Gyll.	Pronotum	1
Stenus sp.	Articulated elytra	1
Quedius sp.	Head, pronotum, elytra	2
Genus 1	Pronota	2
Genus 2	Pronota	3
Genus 3	Pronota	2

Taxa	Skeletal parts	Number of individuals
Aleocharinae	Pronotum, elytron	1
Helodidae	Heads, pronotum, half pronotum, half elytra, elytral fragments	3
Byrrhidae		
Byrrhus sp.	Articulated abdomen including elytron, sternites and leg fragments, left elytron	1
Elateridae	Elytra, articulated sternites	2
Chrysomelidae		
Plateumaris sp.	Articulated abdomen (including two elytra, meso and metasternum and sternites), head fragments, prothoraces, half prothoraces, elytra, apical halves, basal half, elytral fragments, prosternum, mesosternum, miscellaneous fragments (legs, trochanters, sternites)	4
Curculionidae (weevils)		
Isochnus sp.	Elytron	1
	Pronotum	1
NOCA 101		
Carabidae (ground beetles)	Head, half head, prothoraces, half elytra, prosternum, metasterna, coxa	
Elaphrus clairvillei Kby.	Half elytron	1
Bembidion sp.	Head, pronotum elytron	2
Staphylinidae (rove beetles)	Head, articulated elytra, half elytra, prosternum, mesosterna	2
Omaliinae	Head, elytron, half head	3
Olophrum sp.	Head, elytron	1
Olophrum consimile Gyll.	Half pronota	2
Genus 1	Half pronotum	1
Genus 2	Pronota	2
Aleocharinae	Pronotum	1
Ptiliidae	Articulated mesosternum and elytron	1

Taxa	Skeletal parts	Number of individuals
Scarabaeidae		
Aphodius sp.	¾ elytron	1
Byrrhidae	Half head, half pronotum pronotal fragments	2
Byrrhus sp.	Head, half elytra, elytral fragments	3
Elateridae	Half elytron	1
Chrysomelidae	Pronotum, elytron	1
Curculionidae (weevils)	Prothoracic fragments	3
Isochnus sp.	Elytra, articulated elytra, head, articulated abdomen with two elytra	3
NOCA 100		
Carabidae (ground beetles)	Half elytron	1
Elaphrus clairvillei Kby.	Half elytron, elytral (lateral) fragment	1
Genus?	¾ pronotum	10
Staphylinidae (rove beetles)	Elytron	1
Omaliinae	Head, half head	2
Olophrum sp.	Elytron	1
Olophrum boreale (Payk.)	Half pronotum	1
Tachinus sp.	Half pronotum	1
Genus?	Half pronotum	1
Byrrhidae		
Byrrhus sp.	Head, pronotum, half pronotum, ¾ elytron	1
Chrysomelidae?	Articulated elytra	1
Curculionidae (weevils)		
Isochnus rufipes? (LeConte)	Elytron	1
Genus?	Half elytron	1

Chapter 5: Equilibrium line altitudes of alpine glaciers during the Fraser Glaciation in Skagit valley, Washington

Abstract

Moraines, non-glacial deposits, and glacier physics were used to reconstruct the extent of alpine glaciers at seven sites in the Cascade Range, Washington, during the Evans Creek and Sumas stades of the Fraser Glaciation (marine oxygen isotope stage 2). Tributary alpine glaciers advanced into Skagit valley at two locations early during the Fraser Glaciation (Evans Creek stade). ELA depression from the modern glaciation threshold for this advance is 970 ± 70 m for the maritime Baker valley and 730 ± 50 m for the more arid Big Beaver valley.

Skagit valley alpine glaciers advanced several times to positions 5-10 km below valley heads between 12, 200 and 9,975 ^{14}C yr BP (Sumas stade). Equilibrium line altitudes for these glaciers were estimated using a spreadsheet developed by Osmaston (2005), a balance ratio of 2, and an accumulation area ratio of 0.65. ELA depression for the Sumas stade ranges from 340 ± 100 m to 590 ± 75 m, with generally lower values in western Skagit valley. The pattern of less ELA depression to the east reflects lower balance gradient and a higher temperature lapse rate. Estimated variability of ELA between successive Sumas stade advances of Deming Glacier is 100 m.

Skagit ELA depression values are about 200 m less than those reported for the southern North Cascades during the Sumas stade. The effect of the Cordilleran Ice Sheet on precipitation at this time likely caused ELAs to be higher in the Skagit valley than in the southern North Cascades.

Keywords: Glaciers, equilibrium line altitude, climate change, Evans Creek stade, Sumas stade, North Cascades, Skagit valley, Washington.

Introduction

Moraines in the Cascade Range of Washington State are sensitive indicators of climate change because the glaciers that built them were relatively small, had short lag times and steep balance gradients, and were distributed along strong climatic gradients (Porter, 1977; Clark and Bartlein, 1995; Clague et al., 1997; Hodge et al., 1997). However, a limitation of using moraines to reconstruct climate in the Cascades is that the record is commonly incomplete in any single valley. Therefore, many valleys must be investigated before a meaningful reconstruction of former climate changes based on glacial deposits can be made.

Moraines, glaciolacustrine and glaciofluvial deposits, and non-glacial sediments in and near Skagit valley add important details to a regional understanding of glaciation and climate change in the Pacific Northwest during the Late Wisconsin Fraser Glaciation, ca. 30,000-10,000 ^{14}C yr BP (Figure 5-1). Their distribution is used here to reconstruct glacier extent and equilibrium line altitude (ELA) at two sites during the early Fraser Glaciation (Evans Creek stade) and at five sites during readvances near the end of the Fraser Glaciation (Sumas stade) (Figure 5-2). ELA is the elevation at which ablation balances accumulation for a given year and is a sensitive measure of the relationship between climate and glacier mass balance (Benn and Lehmkuhl, 2000). In this chapter, I use ELA estimates for the Fraser Glaciation to address several research questions: How do results using different ELA estimation procedures compare? What is the error in ELA estimated by the balance ratio approach? What are the magnitudes of ELA change for the Evans Creek and Sumas stades? How variable were ELAs during different advances of the Sumas stade? Were late-glacial ELAs affected by the Cordilleran Ice Sheet?

Methods

I chose seven sites in the Skagit River watershed with evidence that allowed me to reconstruct the geometry of Evans Creek and Sumas glaciers (Figure 5-1). The sites are spread along a strong climatic gradient from maritime (west) to continental (east), allowing me to evaluate regional trends in glacier size and ELA depression. Age control for the moraines was provided by radiocarbon ages on inset deposits and on tephra and cosmogenic surface exposure ages on the moraines. Beryllium 10 exposures dates are based on production rates of 5 atoms/yr; measurements were made at the University of Washington and Lawrence Livermore Laboratories.

Reconstruction of alpine glaciers during the Evans Creek and Sumas stades differ. Evans Creek lateral and end moraines and related ice-marginal landforms were removed by subsequent ice sheet erosion during the Vashon stade of the Fraser Glaciation. The extent of glaciers flowing down Big Beaver and Baker valleys during the Evans Creek stade was thus inferred from the distribution of alpine till and of glaciolacustrine deposits of glacial lakes Concrete and Skymo in Skagit valley (Chapter 3) (Figure 5-3). I did not include terrain above 2230 m asl on Mount Baker as part of the accumulation area of Baker Glacier because that part of the volcano formed after the Evans Creek stade (Hildreth et al., 2003). The Sumas stade occurred after the Carmello Eruptive phase on Mount Baker, thus I included the upper part of the volcano in the accumulation zone of paleo Deming Glacier. Abundant ice-marginal landforms guided reconstruction of five Sumas stade glaciers (Figure 5-3). Alpine glaciers left Sumas terminal moraines at all five sites, and long lateral moraines at the Deming, Silver, and Arriva sites .

Accurate estimates of paleo-ice thickness are necessary to determine ELAs in the steep terrain of Skagit valley. Two approaches were used to check ice surface elevations and to calculate glacier hypsometry. Prominent erosion features, including the floors of hanging valleys, truncated valley spurs, and upper limits of over-steepened valley walls, were identified on a 10-m digital elevation model, providing a first-order estimate of ice surface gradient. Ice surface elevations were checked by estimating ice thickness (**h**) using a modification of the basic glacier flow law (Paterson, 1981):

$$h = \tau_o / F\ (\rho g \sin \alpha)$$

where $\boldsymbol{\rho}$ is ice density, **g** is gravitational acceleration, $\boldsymbol{\tau_o}$ is basal shear stress, **sin** $\boldsymbol{\alpha}$ is ice surface slope estimated from trimlines or valley slope, and **F** is the shape factor. I assumed perfect ice plasticity, τ_o = 50-150 KPa, and F = 0.65-0.74. The shape factor was determined by measuring valley width and ice depth at the centerline 100 m above the terminus (Paterson, 1981).

Three-dimensional models of the former glaciers were constructed on a 10-m digital elevation base in ArcInfo (Figure 5-3A-F). This approach allowed me to test a range of equilibrium line altitudes (ELA) for each glacier, to rapidly and accurately estimate hypsometry in 100-m elevation bands, and to compare ELA location with ice-marginal landforms.

ELAs were estimated using the area-balance-ratio (ABR) and accumulation-area-ratio (AAR) methods (Porter, 1975, 1977; Furbish and Andrews, 1984; Benn and Gemmel, 1997; Osmaston, 2005). These methods depend on accurate reconstructions of former glaciers; they further assume that the glaciers were not debris-covered and that they did not surge to build the moraines. None of the moraines used to reconstruct the Sumas stade glaciers is a looping moraine belt resembling of deposits of surging glaciers (Benn and Evans, 1998).

Use of the AAR method allowed me to compare my data directly with previous regional ELA estimates (Porter et al., 1983; Hurley, 1996). I used an accumulation-to-ablation area ratio of 0.65, derived from the study of local glaciers (Meier and Post, 1962; Porter, 1975). The AAR approach has several shortcomings, particularly in areas where the range of glacier area-altitude distributions is large. The ABR approach addresses several of these limitations, including the important influence of hypsometry and balance gradient on ELA (Furbish and Andrews, 1984; Benn and Gemmel, 1997; Osmaston, 2005).

A spreadsheet developed by Osmaston (2005) was used to estimate ELA by the ABR method. It requires estimates of balance ratio and glacier area in 100 or 200 m bands (Appendix 5.2). The program iteratively examines a range of mass balance and area combinations to arrive at the pair of altitudes where the balance changes sign. Final ELA is chosen by estimating the proportions of the two net balances. Advantages of this program are that it comes with sample trial data sets and correct outputs and it rapidly and accurately calculates ELA for a range of balance ratios (Table 5-1; Osmaston, 2005).

ELA determined by the ABR method is affected by choice of the balance ratio value, glacier hypsometry, and uncertainty in the terminal locations determined for the Evans Creek glaciers. The Osmaston program is sensitive to balance ratio, as shown in Table 5-1. Benn and Evans (1998) suggest that a balance ratio of 2 is generally representative of modern mid-latitude glaciers. However, Furbish and Andrews (1984) found that balance ratios near Mount McKinley in Alaska range from 1 to 3.

Two major sources of error are quantified in this study. Ice surface elevation in the accumulation zone is typically difficult to determine because of the absence of lateral moraines. However, a majority of the accumulation zones of concern here are on steep slopes, where uncertainties in ice thicknesses are small because they restrict ice thickness to less than 50 m. Potential error from incorrect ice surface elevation in these settings is conservatively estimated at $\pm$ 25 m, or half of the maximum ice thickness on steep slopes. The second source of quantifiable error is the balance ratio. I report the standard deviation of a range of ELA values determined using balance ratios from 1 to 3. The total error is the square root of the sum of the squares of the elevation and balance ratio errors (Table 5-1).

ELA values have not been corrected for lower sea level or for isostatic depression associated with the waning Cordilleran Ice Sheet. Although sea level was up to 120 m lower than today during the Fraser Glaciation, Osmaston (2006) suggests that, for consistency, all values be indexed to modern sea level. Booth (1987) estimates full Vashon isostatic depression for the western North Cascades Range of ~160 m, and Clague (1989c) estimates a value of 250 m for southwest British Columbia. These values are larger than, although of the same order of magnitude as, contemporaneous eustatic sea-level lowering. Most isostatic recovery in the Cascade Range and adjacent Puget Lowland was complete by 12,000 ^{14}C yr BP (Ruddiman and Wright, 1987); at that time, residual isostatic depression and eustatic sea-level lowering approximately compensated each other.

The modern glaciation threshold (Porter, 1977) was used as the benchmark for estimating ELA depression because regional variability in ELAs of modern monitored glaciers is 200 m (Figure 5-4). Glaciation threshold is averaged over a wider area than ELA and is more representative of regional climate. Furthermore, in the North Cascades Range, glacier aspect at the head of a valley can be different from that along the axis of the valley below. As glaciers expand beyond cirques, regional climate becomes increasingly significant in ELA depression. Because glaciation threshold is typically lower than modern ELA, this approach decreases estimates of ELA depression by 100-200 m compared to studies using modern ELA as a benchmark.

Results

ELA estimates for the Evans Creek and Sumas stade advances produced by the AAR method are typically 100-200 m lower than those generated by the ABR method (Table 5-2). The exception is Bacon Creek Glacier during the Sumas stade, where the AAR value is 120 m higher than the ABR value.

A change in balance ratio from 1 to 3 has a large effect on ELA, particularly for larger, more complex glaciers such as Bacon and Silver (Table 5-1; Figure 5-3). Smaller glaciers with less complex hypsometry tend to be less sensitive to changes in balance ratio (e.g. Arriva and Fisher).

Thicknesses of all of the reconstructed glaciers generally are no more than 40-50 m on steep slopes on the flanks of Mount Baker and at valley heads where sliding velocities were high (Hodge, 1974). On valley floors and at points of convergent flow, ice thicknesses were several hundred metres. Calculations for selected sites are presented in Appendix 5.1.

Evans Creek stade

Evans Creek stade alpine glaciers were much larger, and extended to lower elevations, than their Sumas stade counterparts (Figures 5-3 and 5-5). The Evans Creek glacier in Baker valley had an area of more than 530 km^2. In contrast, nearby Deming and Bacon Creek glaciers had areas of 20 km^2 or less during the Sumas stade. The Evans Creek Big Beaver Glacier in upper Skagit valley near Ross Lake had an area of about 100 km^2, dwarfing the Sumas Silver Creek Glacier (16 km^2).

Assuming a balance ratio of 2, ELAs for Baker and Big Beaver glaciers are, respectively, 980 ± 70 m asl and 1300 ± 60 m asl (Table 5-2, Figure 5-3). ELA depression from the modern glaciation threshold during the Evans Creek stade was 970 ± 70 m for Baker Glacier and 730 ± 50 m for Big Beaver Glacier.

Sumas stade

Sumas stade ELAs, assuming a balance ratio of 2, range from 1280 ± 90 m asl (Bacon Creek) to 1920 ± 40 m asl (Fisher Creek) (Table 5-2). ELA depression from the modern glaciation threshold ranges from 340 to 590 m. Assuming a balance ratio of 2, the Deming Glacier ELA is 1740 ± 100 m, which is high considering the glacier is west of the Silver and Bacon sites, and its paleo-accumulation zone reached to 3000 m asl. Paleo-ELA depression at Deming Glacier is 340 ± 100 m below the modern glaciation threshold, a value comparable to those in eastern Skagit valley.

Lateral moraines at the Deming site were used to reconstruct the glacier at two times during the Sumas stade (Figure 5-3). The glacier that built the outermost moraine (M1) had an area of about 9 km^2; a younger, smaller glacier (8 km^2) built the innermost moraine (M3). The balance ratio ELA for the later, less extensive advance is 1840 m asl, or about 90 m higher than the ELA for the earlier advance (Table 5-2).

Discussion

Estimates of ice thickness for the reconstructed glaciers are in agreement with present-day ice thicknesses at Mount Rainier (Hodge, 1974) and Mount Baker (Harper, 1992). The relation between ice thickness and surface slope indicated by my reconstructions is also consistent with results for late Wisconsinan glaciers in northern Yellowstone National Park (Pierce, 1979).

The ABR method and the Osmaston (2005) program provide robust estimates of paleo-ELA (Stansell et al., 2007). However, uncertainties in balance ratios of glaciers along a strong climatic gradient during periods of extreme climate change are problematic. Furthermore, other factors affect the accuracy of the ABR method, including debris cover and errors in glacier reconstruction. In steep terrain, avalanching of snow and debris cover may limit the utility of the ABR approach (Benn and Lehmkuhl, 2000). However, relief in Skagit valley is relatively small compared to the Himalayan examples cited by Benn and Lehmkuhl (2000). Large lateral moraines at the Deming, Bacon, and Arriva sites may reflect significant debris cover on these glaciers (Benn and Lehmkuhl, 2000).

Balance ratios for Skagit alpine glaciers during the Fraser Glaciation were probably between 1.8 and 2.2, which are averages for Alaskan glaciers and South Cascade Glacier, Washington, respectively. ELA is relatively insensitive to balance ratios between 1.8 and 2.2, with an average difference in ELA of 28 m among the seven reconstructed glaciers.

ELA determined by the AAR method is typically 100-200 m lower than ELA determined by the ABR method for both stades (Table 5-2). This difference is comparable in magnitude to the error associated with the choice of balance ratio and ice surface elevation. It probably reflects the improved accuracy of the ABR method due to the influence of the area-altitude distribution and balance ratio on glacier ELA. Sumas stade Bacon Glacier has a slightly lower ABR ELA than AAR ELA, which is likely due to the insensitivity of the reconstructed glacier to ELA change below 1400 m elevation (Figure 5-3). Silver, Deming, and Bacon glaciers have large, high accumulation zones that feed into narrow canyons. A change in ELA within the narrow canyons has little effect on glacier extent. For example, Deming Glacier enters a steep, narrow canyon below 1900 m asl, and lowering of ELA by 100 m adds only 3% to accumulation zone area.

The difference between ABR ELA and AAR ELA increases significantly to the west, where glaciers are larger and hypsometry is more complex (Table 5-2). Because the error associated with the selection of balance ratio is low for smaller, east-side glaciers with simple hypsometry during both stades, the ELA estimates for the Big Beaver, Arriva and Fisher sites may be the most accurate (Table 5-2).

Evans Creek stade ELA change

ELA during the alpine glacier advances early in the Fraser Glaciation was as high as 3000 m asl in the Rocky Mountains (Meyer et al., 2003), and decreased to below 1000 m asl in the western North Cascades. The ELA of Baker Glacier during the Evans Creek stade was 330 m lower than that of Big Beaver Glacier because of the strong climatic gradient in the North Cascades.

ELA depression was at least 600 m greater during the Evans Creek stade than during the Sumas stade (Figures 5-3 and 5-4) and about 1000 m greater than during Neoglaciation (Figure 5-6; Porter, 1986; Riedel, 1987).

AAR ELA depression during the Evans Creek stade ranges from 700 to 1000 m, consistent with the few previously reported values for the region. ELA depression for the Fraser Glaciation Domerie advance in the Yakima valley, based on the AAR method, is 950 m (Figure 5-1; Porter, 1976; Porter et al., 1983). Heller (1980) used an AAR value of 0.65 to estimate an ELA of 900 m asl for Baker Glacier during the Evans Creek stade. Heller's estimate is higher than mine, which is unexpected given that his glacier extended much farther up and down Skagit valley. He did not, however, factor into his estimate ice surface elevation or a reduction in the accumulation area near the top of Mount Baker due to postglacial growth of the stratovolcano.

Waitt (1977) used differences between the median elevations of modern glaciers and those of inferred Evans Creek glaciers to estimate ELA changes. Based on a geomorphic reconstruction of an Evans Creek glacier that filled Ross Lake valley, Waitt estimated an ELA lowering of 700 m. Despite the very different approaches and different assumptions about the extent of glaciers in Skagit valley, this value is close to my glaciation threshold-ABR estimate of 730 ± 60 m for the same area. Waitt's estimate of ELA change is, however, 200 m less than my AAR ELA estimate. The similarities between these results suggest that large-scale topographic features are useful first-order indicators of the extent of former valley glaciers in the absence of dated landforms and sediments.

Sumas stade ELA change

Preliminary age estimates for four moraines in Skagit valley indicate they were deposited during the Sumas stade at the end of the Fraser Glaciation, at about the same time as the Deming, Rat Creek, and Hyak moraines were constructed (Porter et al., 1983; Kovanen and Slaymaker, 2005; Figure 5-2; Appendices 5-3 and 5-4). The Skagit results are tentative pending better age control on the moraines, but volcanic tephra and minimum limiting radiocarbon ages are consistent with a Sumas age. The ^{10}Be cosmogenic results are problematic due to limited sample size, sample quality, and large errors. Nonetheless, 1σ age estimates for four of the six samples fall within the Sumas Stade.

The available chronology provides regional evidence of a series of valley glacier advances at the end of the Fraser Glaciation between about 12,000 and 10,000 ^{14}C yr BP. Late-glacial moraines at each site are close to one another, thus ELA differences are small and have generally been ignored. However, the detailed moraine record at Deming Glacier provides an opportunity to evaluate ELA variations between Sumas advances. Glacier reconstructions were completed for two terminal configurations; one for the outer M1 moraine and another for the less extensive glacier associated with the inner M3 moraine (Figure 5-3C). Changes in glacier hypsometry between the two configurations result in a 90 m difference in balance ratio ELA for the two advances (Table 5-2).

The upper limits of well preserved lateral moraines at the Silver, Deming, and Arriva sites generally coincide with reconstructed ABR ELAs (Figure 5-3). This observation provides independent support for my ELA estimates (Andrews, 1975).

Sumas ELA depressions of 250-600 m are within the range of values reported for glaciers on Mount Baker (Kovanen and Slaymaker, 2005), a Baker valley tributary (Burrows, 2001), and Mount Rainier (Heine, 1998; Table 5-2). ELAs of 1920 and 1740 m asl reported, respectively, for the McNeely 1 advance at Mount Rainier and paleo-Deming Glacier are high compared to most of the regional data, but may result from local mass balance factors including rain shadows, unfavourable aspect, and wind erosion of snow. The McNeely moraines examined by Heine (1998) are located on the dry northeast flank of the volcano, and Deming Glacier is northeast of the Twin Sisters Range. ELA depressions during the McNeely 1 advance and the Deming M3 advance are closer to the values obtained for east-side Fisher and Arriva glaciers, indicating that local patterns of accumulation and ablation, superimposed on the regional west-east precipitation gradient, have a strong influence on ELA.

Kovanen and Slaymaker (2005) used a different glacier geometry and spreadsheet, and a balance ratio of 2.2 to estimate a late-glacial ELA at Deming Glacier of 1565 m asl and ELA depression at 355 m (Table 5-2). Using the same balance ratio, the Osmaston (2005) spreadsheet, an ice surface elevation constrained by glacier physics, and more extensive ice at the terminus, I estimate late-glacial ELA to be 1740 m asl for a glacier terminating at the outermost moraine. The substantial geometric differences between my reconstructed glacier and that of Kovanen and Slaymaker (2005) should have resulted in a lower ELA for my paleo-Deming Glacier, consequently the differences are probably due to the different methods used to calculate ELA. Despite the 200 m difference in ELA estimates, Kovanen and Slaymaker's (2005) latest Sumas ELA depression (355 m) is close to my ABR estimate of 340 ± 100 m. The convergence of the two estimates of ELA change, despite the different paleo-ELA estimates, is due to Kovanen and Slaymaker selecting a modern ELA for Deming Glacier of 1920 m asl, which is well below the glaciation threshold and the modern ELA on adjacent Easton Glacier (2160 m asl). I conclude, therefore, that the Sumas stade ELA of Deming Glacier was closer to 1740 m asl than 1565 m asl.

Bacon Glacier was larger than Deming Glacier during the Sumas stade and its terminus extended several hundred metres lower. Its Sumas-age ELA was 460 m lower than that of Deming Glacier. These differences are due to three factors. First, Bacon Glacier had two large accumulation zones above 1400 m asl (Figure 5-3D). Second, the paleo-valley glacier faced southeast and thus had a well shaded ablation zone, in contrast to paleo-Deming Glacier, which faced southwest. Third, upper Deming Glacier lost snow to wind erosion, whereas Bacon Glacier headed in large cirques that accumulated additional snow by wind drifting and avalanching off steep slopes. Modern ELA measurements illustrate these differences: modern ELA on the south side of Mount Baker is 200 m higher than at Noisy Glacier near Bacon Peak (Figure 5-3, 5-4; Pelto and Riedel, 2001; Riedel and Burrows, 2003). Due to these factors, Deming Glacier advanced only about 3 km beyond its present terminus during the Sumas stade, while many other glaciers in the area advanced more than 10 km (Porter et al., 1983; Hurley, 1996).

Regional Sumas stade ELA trends

Two regional trends are evident in the Sumas stade ELA data (Table 5-2, Figure 5-7). The rapid increase in ELA eastward across the Skagit watershed is similar to the regional pattern from the Pacific Ocean eastward across the western North American Cordillera. ELA values for the late-glacial period in the northern Rocky Mountains in Idaho and Montana and the Wallowa and Blue Mountains in Oregon are greater than 2000 m due to the relatively arid climate of these areas (Meyer et al., 2003). Increased accumulation nearer the Pacific Ocean in the North Cascades brought late-glacial ELAs down to 1380 m asl in the Bacon Creek watershed.

The gradient of the late-glacial ELA in the North Cascades rises, on average, 7m/km to the east, consistent with the rise in the median elevation of modern glaciers at this latitude (Post et al., 1971). Modern ELA gradients are generally lower in the northern North Cascades because the range there is much wider than farther south where Porter et al. (1983) estimated modern and late-glacial ELA gradients to be 10m/km (Figure 5-7).

The change in ELA from west to east in Skagit valley is 350 m for the Evans Creek stade and 180 m for the Sumas stade, ignoring the anomalously low Bacon ELA (Table 5-2). Ohmura et al. (1992) noted that larger temperature lapse rates in drier climates make glaciers in these areas less sensitive to climate change. The modern lapse rate in the maritime Baker valley is 0.44°C/100 m, whereas it is 0.66 °C/100 m in the more arid eastern Skagit valley. Lower lapse rates combined with other mass balance factors produce conditions more favourable for rapid glacier expansion in western Skagit valley (Tangborn, 1980).

Rapid changes in glacier size and ELA along strong climatic gradients have been observed at other sites in western North America. ELA depression associated with the late-glacial Crowfoot moraines in the Canadian Rockies is only slightly greater than that for Little Ice Age moraines (Reasoner et al., 1994). Higher lapse rates account for similar late-glacial and Little Ice Age ELAs in arid parts of the North Cascades Range and Canadian Rockies. These conclusions support the inference of Meyer et al. (2003) that the magnitude of ELA depression during late Pleistocene glaciation in western North America is strongly influenced by precipitation. Further, since summer solar radiation values in the middle latitudes of the Northern Hemisphere during late-glacial time were 20-30% higher than at present (Berger, 1978), relatively high summer ablation was not offset by winter accumulation, to the detriment of glaciers in arid regions and in local rain shadows.

Recent work in the Icicle Creek drainage near Leavenworth, Washington, suggests that late-glacial ELA depression was as little as 100 m, only slightly more than the Little Ice Age ELA lowering (Table 5-2; Bilderback and Clark, 2003). The aridity of the site, located 30 km east of the Pacific crest, may be responsible for the low ELA depression.

The second regional trend is a north-south one. The average magnitude of late Fraser Glaciation ELA depression estimated by the AAR method in Skagit valley is approximately 200 m less than values reported for the same interval 150 km to the south (Figure 5-7; Table 5-2). Poor age control raises the possibility that some of the 200-m difference in ELA between the two areas is due to differences in the ages of the advances that built the moraines. However, I observed only a 100-m difference in ELA between the two Deming advances, thus at least half of the 200-m difference between the Skagit and Yakima valleys must be due to climate.

The trend toward greater lowering of late-glacial ELA?? in the southern North Cascades is opposite the modern regional trend (Flint, 1971; Post et al., 1971; Sugden and John, 1976). On the east side of the Pacific crest, the southerly increase in late-glacial ELA of 2.2 m/km is much higher than the northerly decrease in modern ELA of 0.4 m/km.

The anomalous trend of greater ELA depression to the south provides an important clue to the late-glacial climate in the North Cascades. The reversed and steepened, late-glacial latitudinal gradient suggests that the north was drier than the south during the Sumas stade. A possible reason for lower ELA to the south is the influence of the Cordilleran Ice Sheet on climate and ELA late during the Fraser Glaciation. Because isostatic effects on Sumas stade ELAs in Skagit valley were probably minimal, it is likely the ice sheet, lingering just north of the International Boundary, had an important effect on precipitation.

Southern displacement of the polar front in late-glacial time and strong winds off the ice sheet may have steered storms south from Skagit valley to the latitude of Snoqualmie and Yakima valleys (Mann and Hamilton, 1995). The sensitivity of the region's modern and late Pleistocene climate and glaciers to the position of the jet stream has been noted by Hodge et al. (1997), Bitz and Battisti (1998), and Thackray (1999).The ice sheet may have reduced precipitation in Skagit valley during late-glacial time, making decreased temperature the primary cause of late-glacial advances of alpine glaciers. This conclusion is supported by the greater response of glaciers in maritime western Skagit valley, and lower Sumas stade ELAs in the southern North Cascades. Locke (1990) came to a similar conclusion in western Montana by noting that cirque floors in the north are more than 100 m above a regional trend surface. He attributed this anomaly to the presence of the ice sheet and its effects on the jet stream, storm tracks, and thus moisture availability, as well as isostatic depression.

Conclusions

How do results using different ELA estimation procedures compare?

Equilibrium line altitudes determined by the accumulation area method are generally 100-200 m lower than ELAs determined by the balance ratio method using the Osmaston (2005) program. A balance ratio of three with an accumulation area ratio AAR of 0.65, or a balance ratio of two and with and AAR of 0.4 are required to bring the estimates into agreement.

What is the error in ELA estimated by the balance ratio approach?

Error in the balance ratio approach is due to assumptions about debris cover and snow avalanching, choice of an appropriate balance ratio, and the accuracy of glacier reconstructions. I estimate this error for glaciers in the Skagit watershed to range from 40 to 100 m.

What are the magnitudes of ELA change for the Evans Creek and Sumas stades?

Evans Creek stade ELAs were depressed 700-1000 m below modern glaciation threshold. Sumas stade ELAs were depressed 300-600 m. The values are greater in western Skagit valley because its more maritime climate results in higher balance gradients and lower temperature lapse rates.

How variable were ELAs during different advances of the Sumas stade?

ELA differed by about 100 m between the advances that constructed the inner and outer moraines at the Deming site. Radiocarbon ages constrain the time of the younger advance to after 10,600 ^{14}C yr BP.

Were late-glacial ELAs affected by the Cordilleran Ice Sheet?

Sumas stade ELA was depressed 200 m more in Yakima and Snoqualmie valleys than in Skagit valley. This observation supports the theory that strong airflow off the Cordilleran Ice Sheet displaced the jet stream south of Skagit valley in late-glacial time. Late-glacial advances of alpine glaciers in Skagit valley may have been caused primarily by colder temperatures, while colder temperatures and higher precipitation fed glaciers with lower ELAs in Snoqualmie and Yakima valleys to the south.

Acknowledgements

Financial support for this work was provided by a grant from the Skagit Environmental Endowment Commission, by indirect support from the National Park Service, and from an NSERC Discovery Grant to John Clague. GIS support for the glacier reconstructions was provided by Michael Larrabee and Jeanna Wenger.

Figures

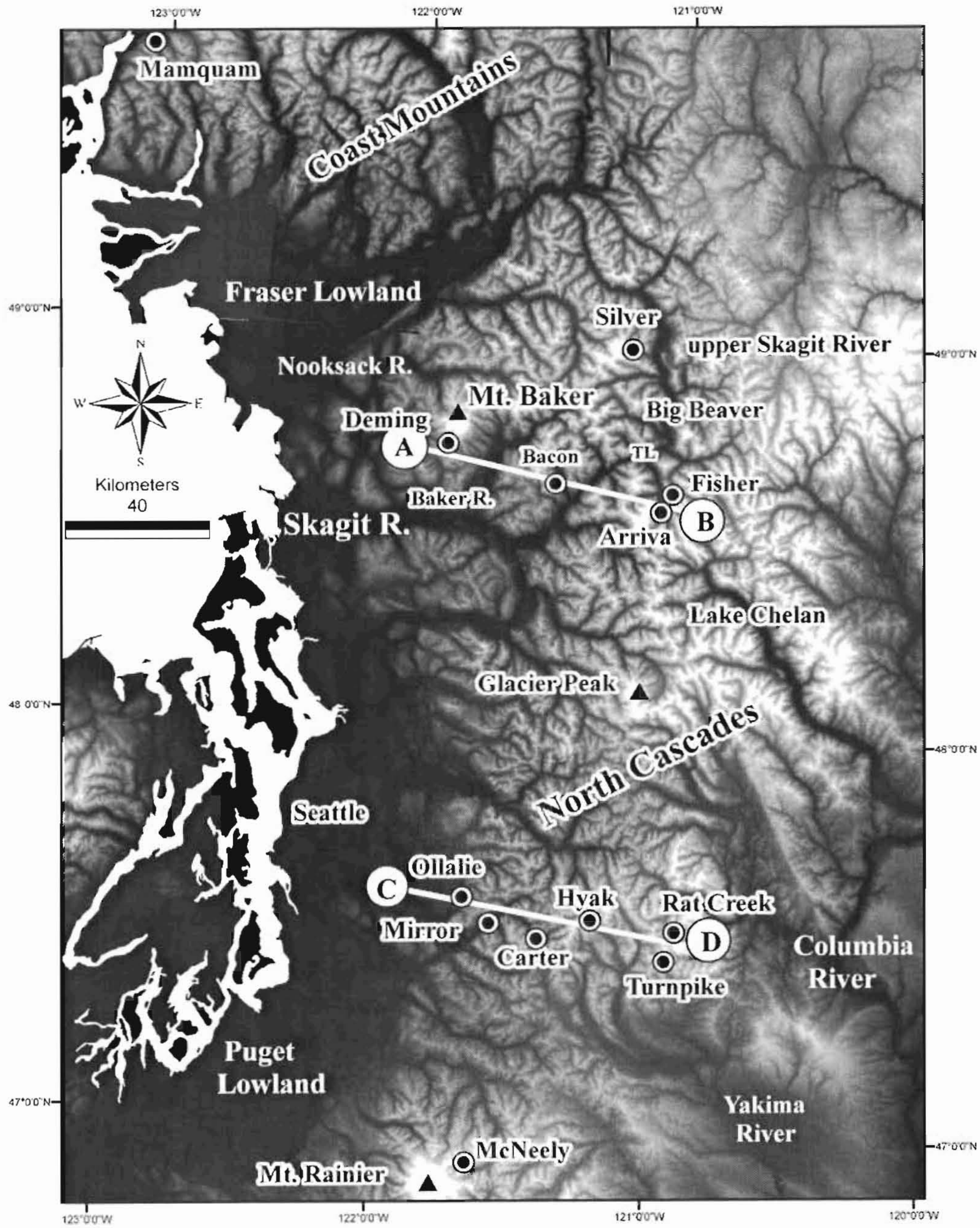

Figure 5-1. Map of northern Washington, showing the locations of Skagit valley and other areas where late Pleistocene equilibrium line altitude (ELA) reconstructions have been made. A-B and C-D are ELA transsections shown in Figure 5-7.

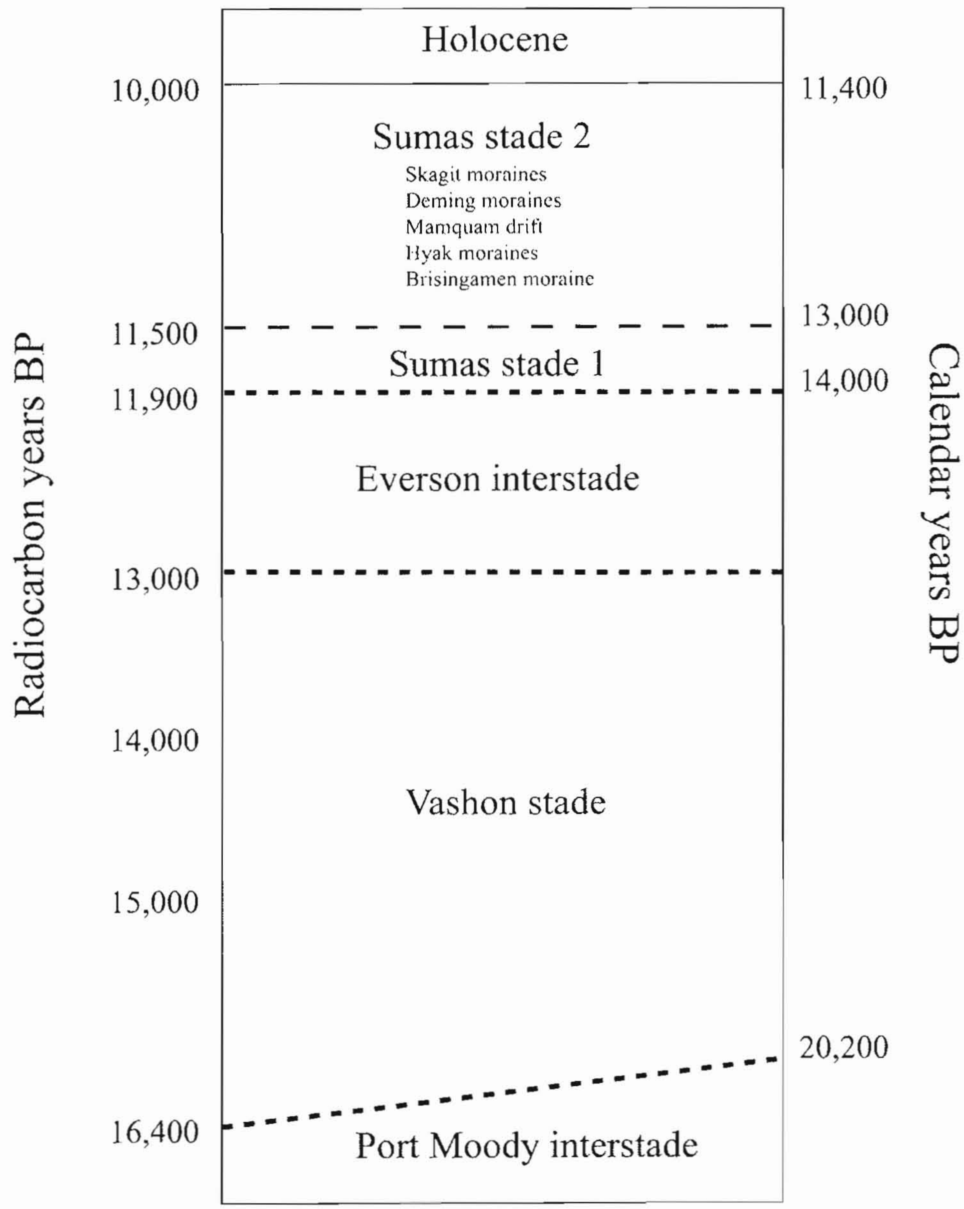

Figure 5-2. Fraser Glaciation timescale for Washington and British Columbia (modified from Armstrong et al., 1965 and Clague et al., 1997).

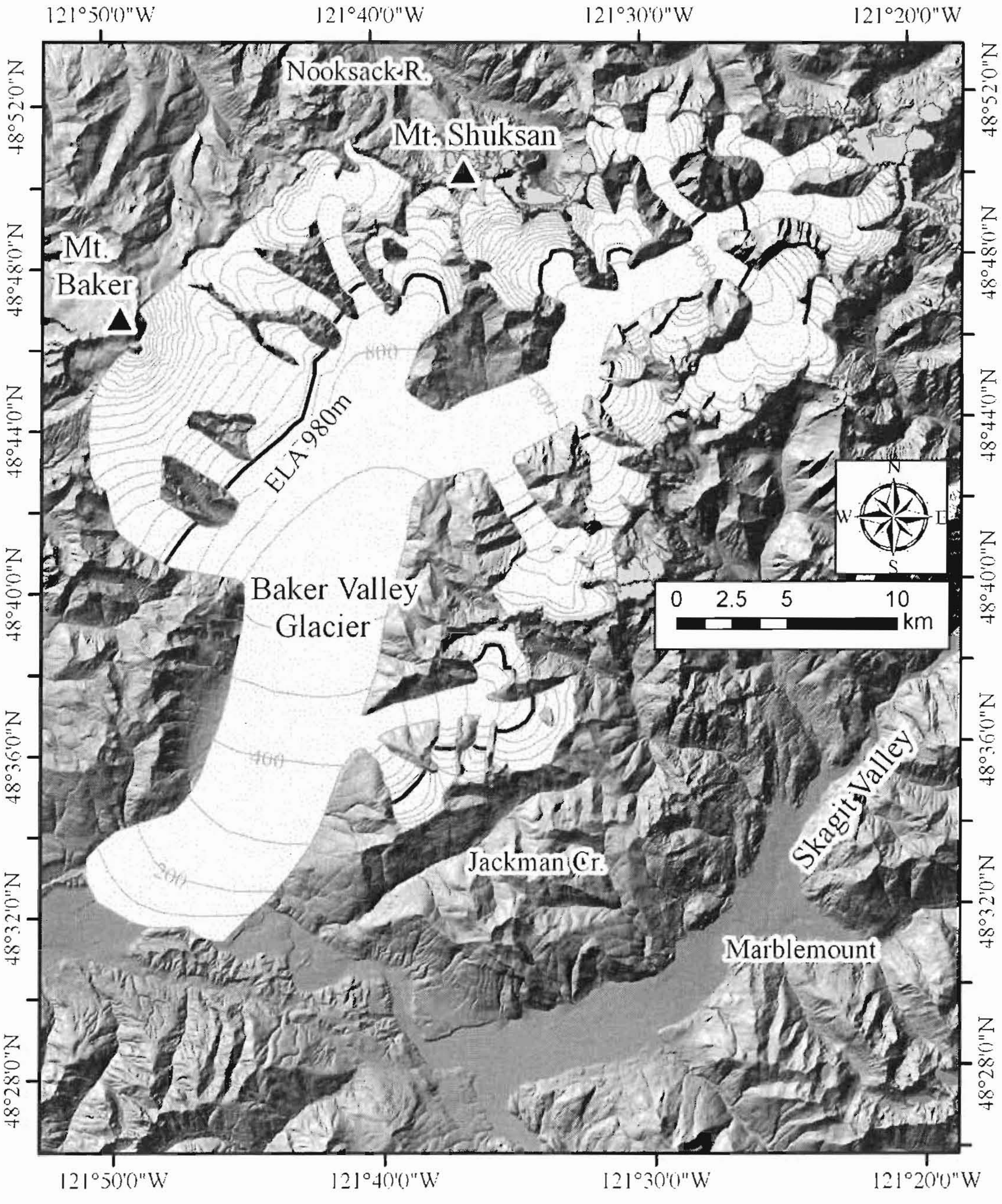

Figure 5-3A. Baker River Glacier during the Evans Creek stade. The Evans Creek ELA is marked by the heavy contour. The ice surface elevation contour interval is 100 m.

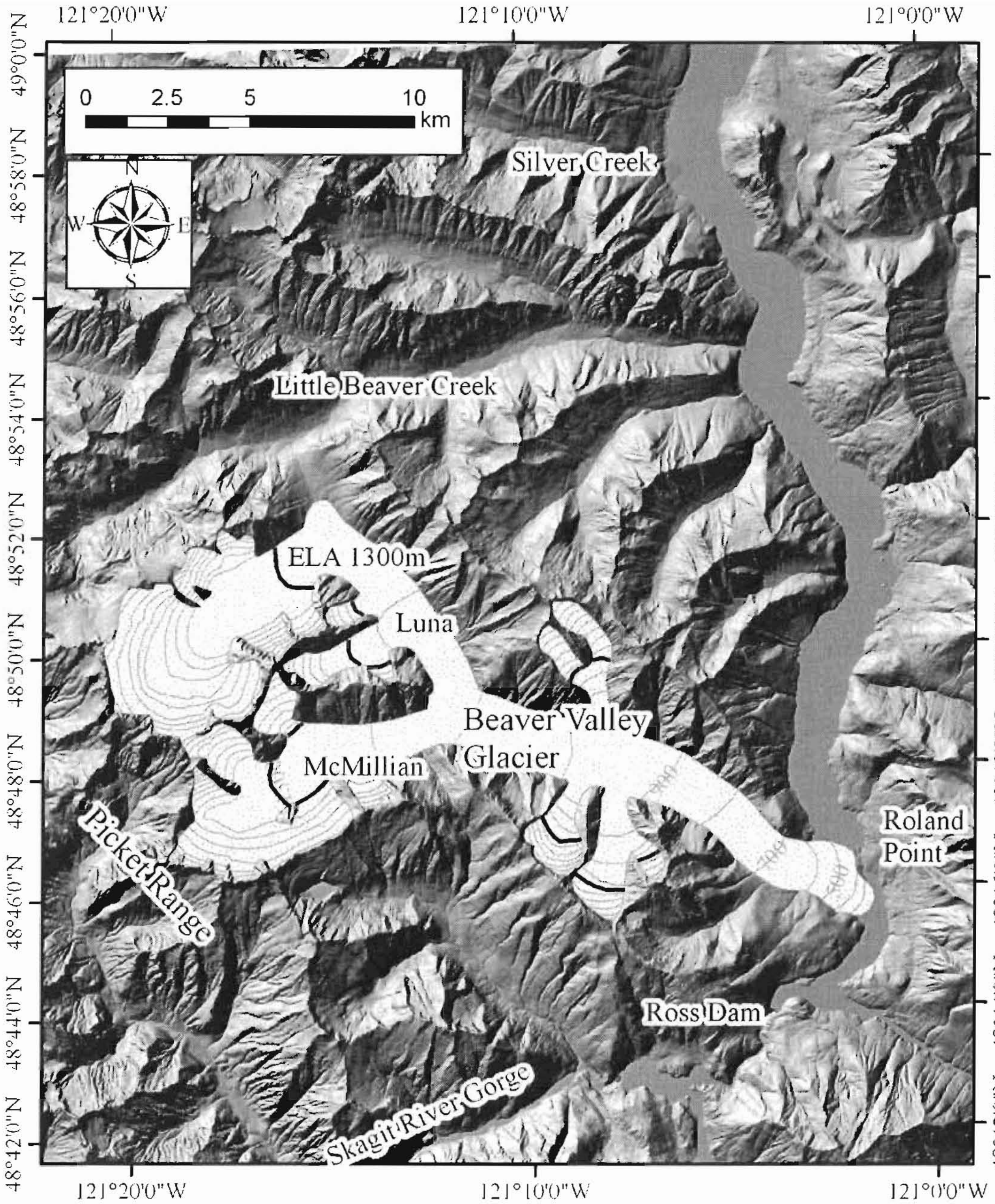

Figure 5-3B. Big Beaver Glacier during the Evans Creek stade. Evans Creek ELA marked by the heavy contour. The ice surface elevation contour interval is 100 m.

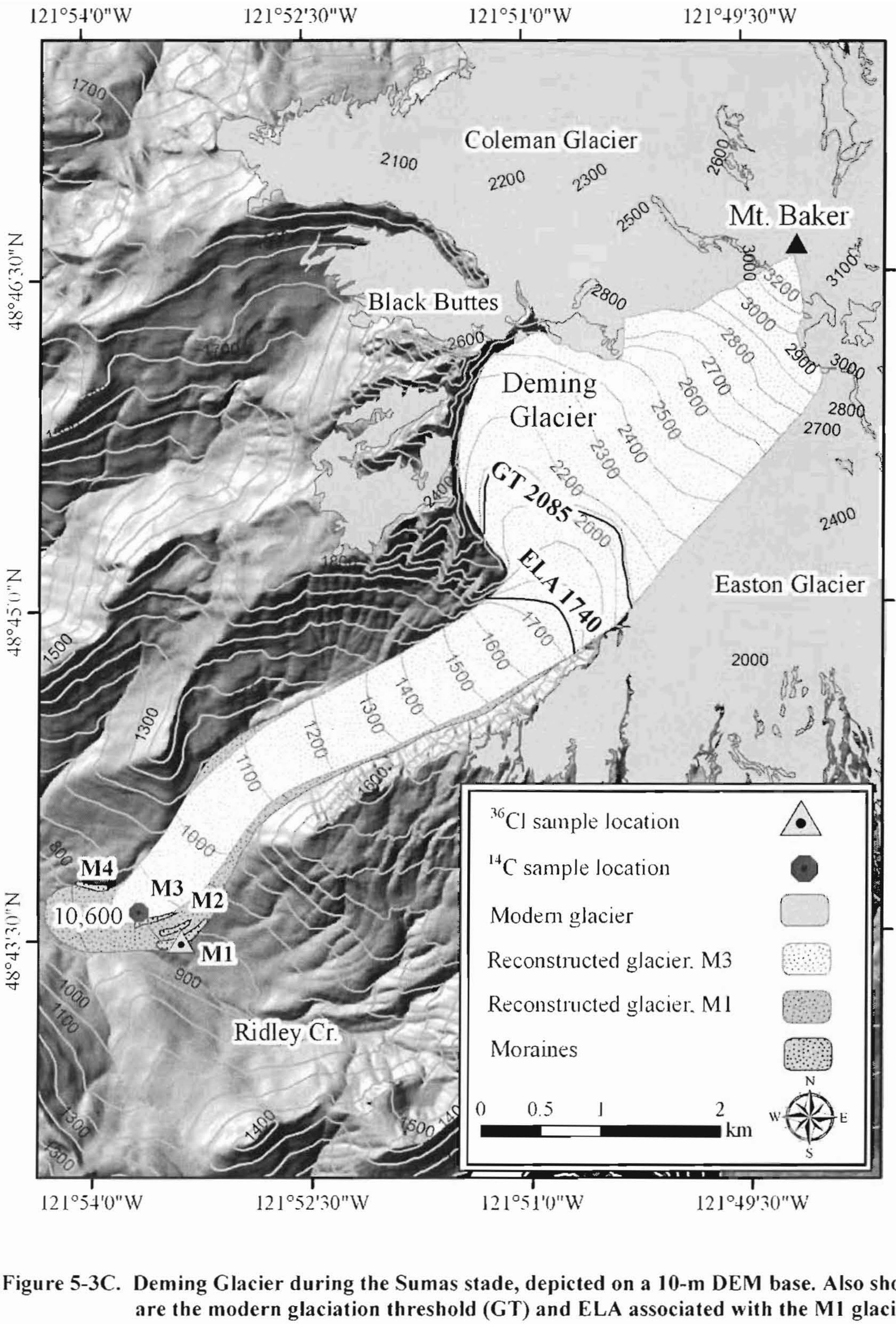

Figure 5-3C. Deming Glacier during the Sumas stade, depicted on a 10-m DEM base. Also shown are the modern glaciation threshold (GT) and ELA associated with the M1 glacier.

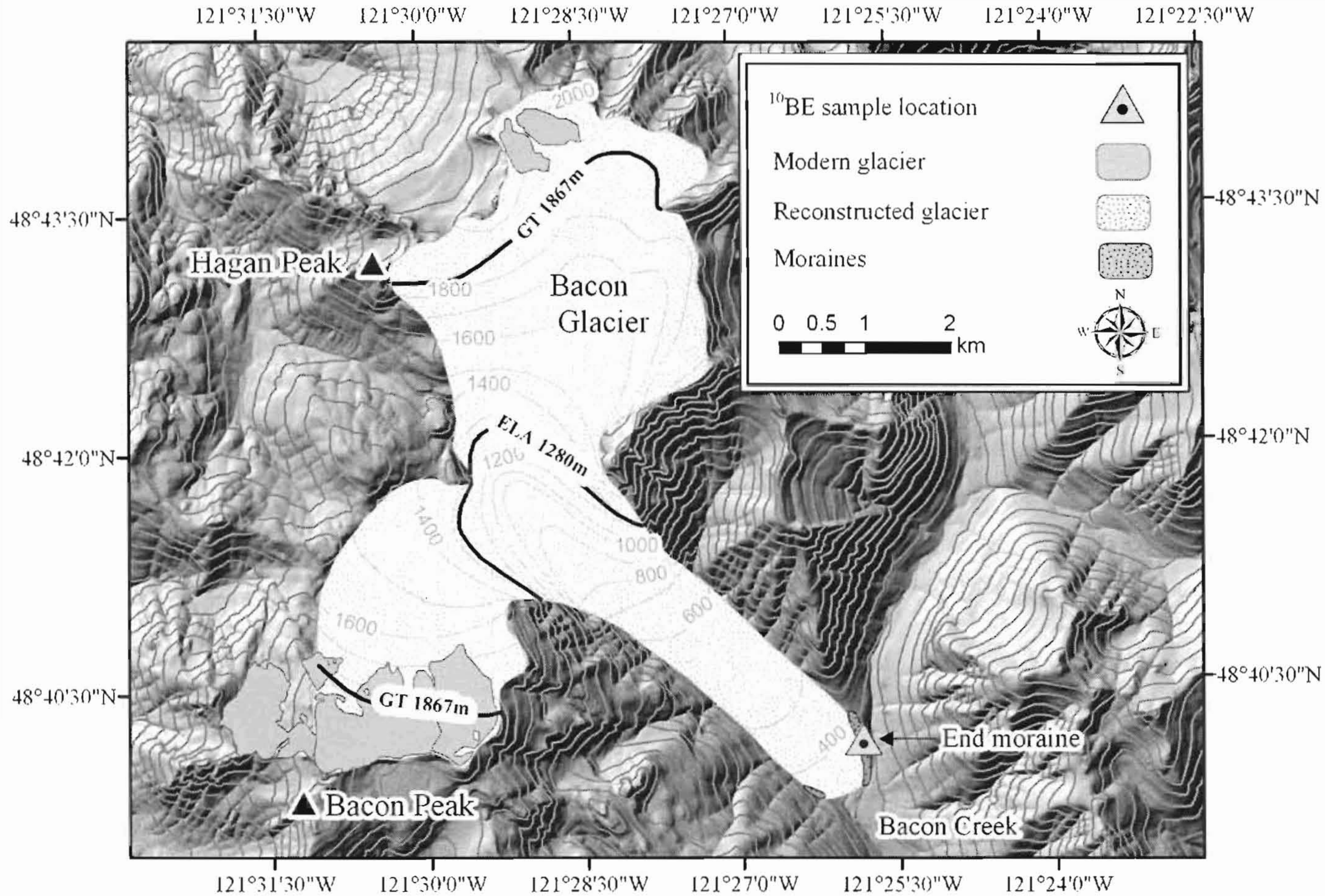

Figure 5-3D. Bacon Glacier during the Sumas stade, depicted on a 10-m DEM base. Also shown are the Sumas-age ELA and the modern glaciation threshold (GT).

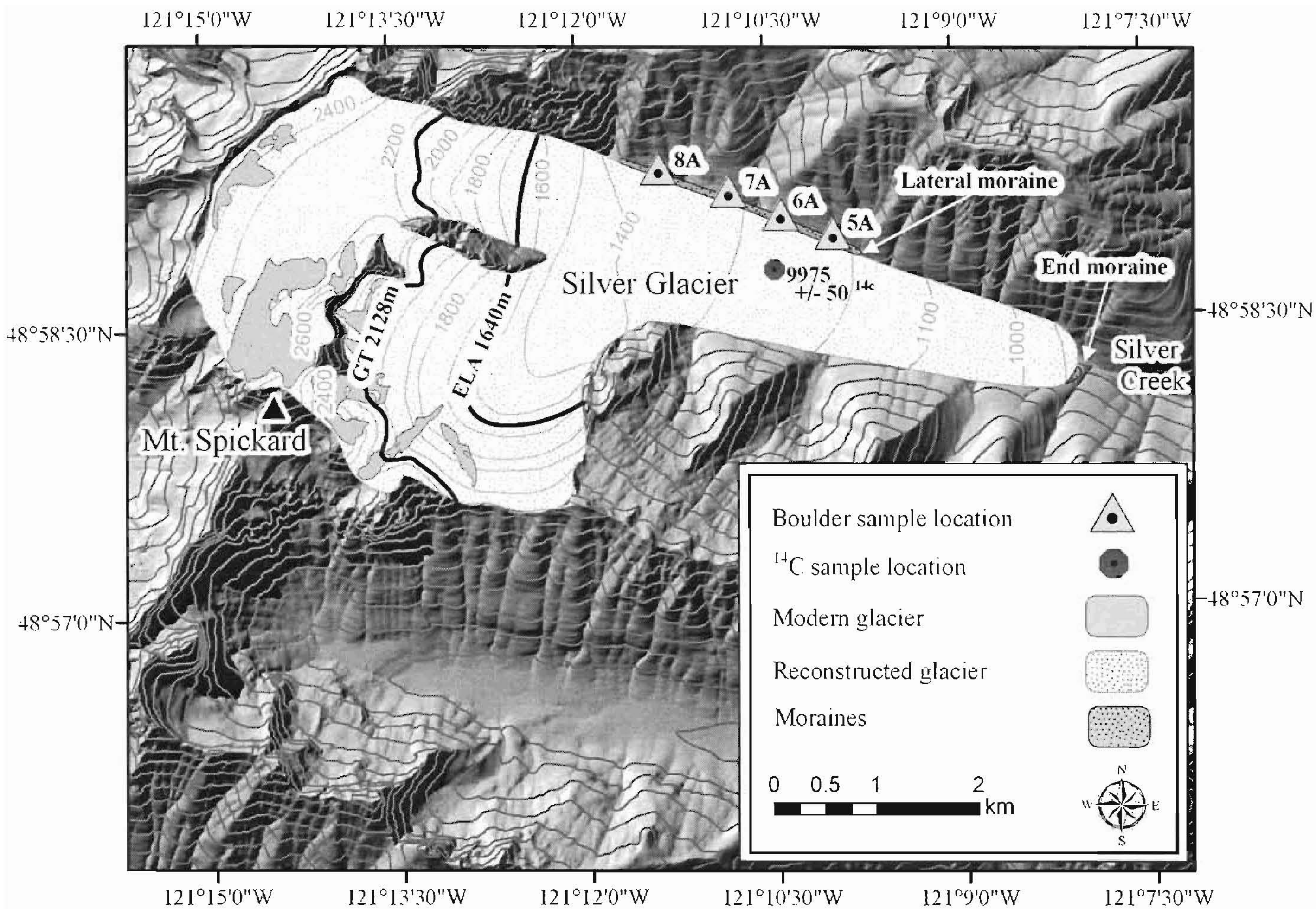

Figure 5-3E. Silver Glacier during the Sumas stade, depicted on a 10-m DEM base. Also shown are the Sumas-age ELA and modern glaciation threshold (GT).

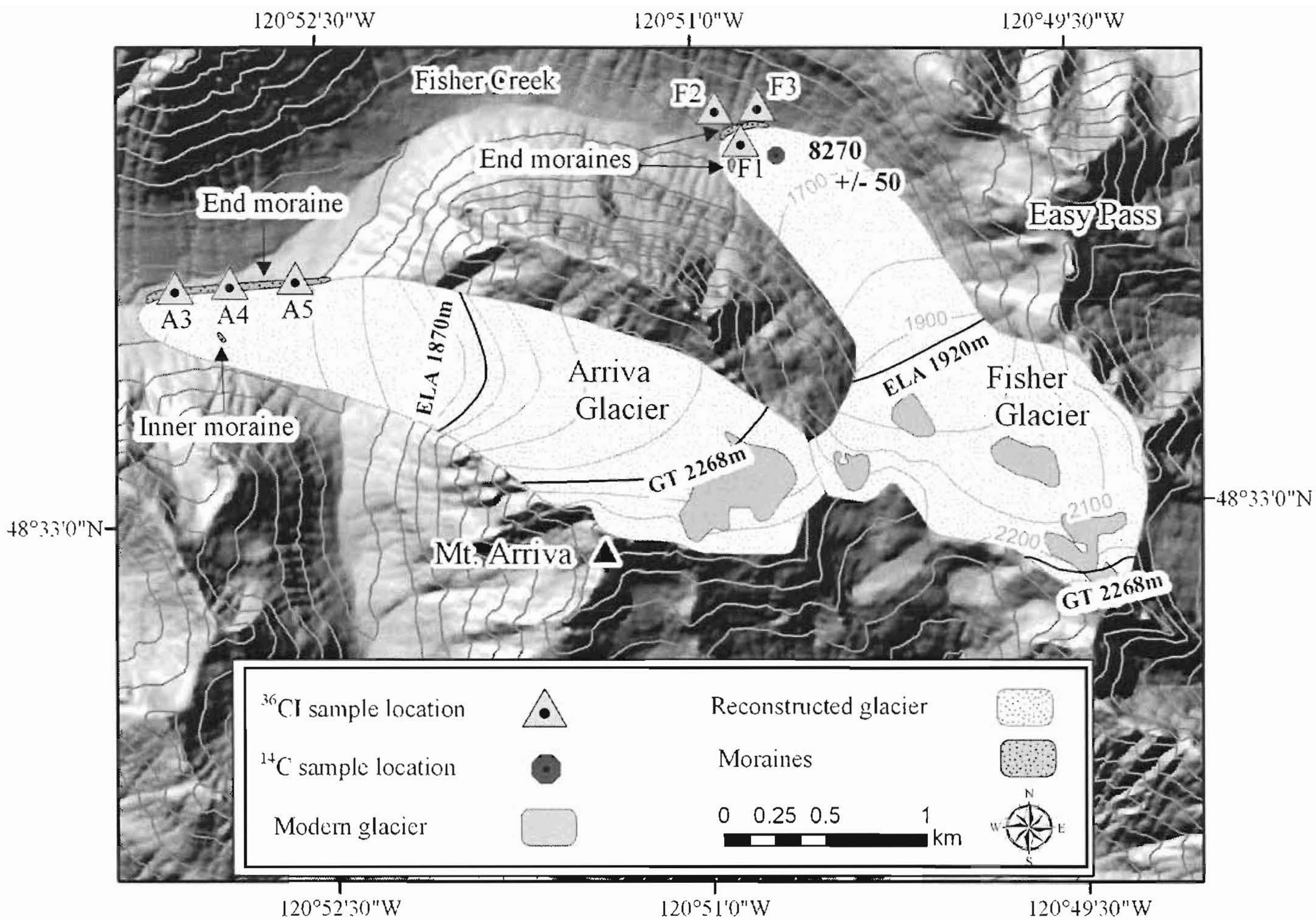

Figure 5-3F. Arriva and Fisher glaciers during the Sumas stade, depicted on a 10 m DEM base. Also shown are Sumas-age ELA and modern glaciation threshold (GT).

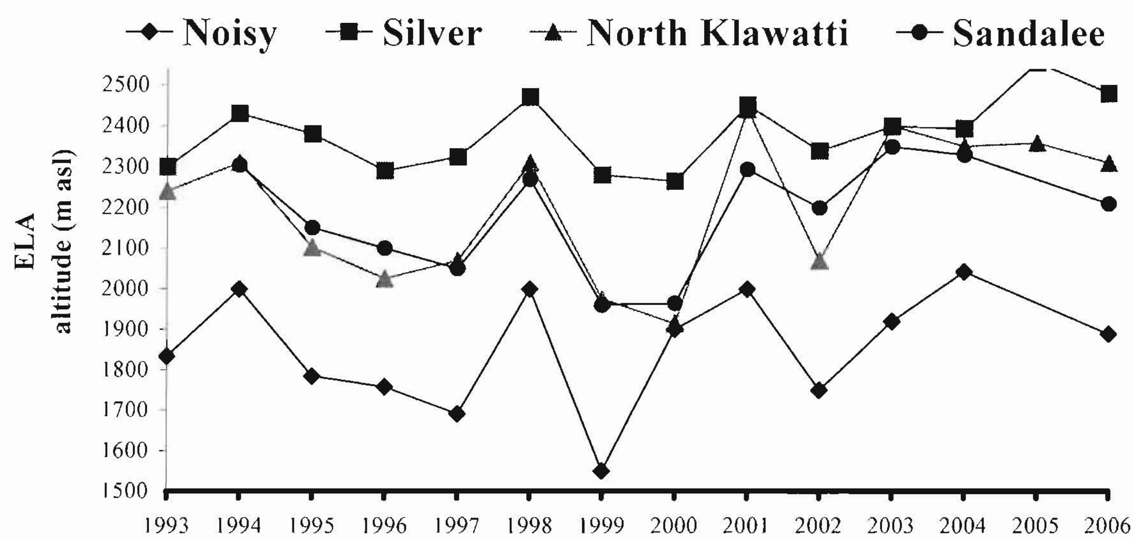

Figure 5-4. ELAs of modern glaciers in the North Cascades based on mass balance measurements of the North Cascades National Park Glacier Monitoring Program (nps.gov/noca/massbalance).

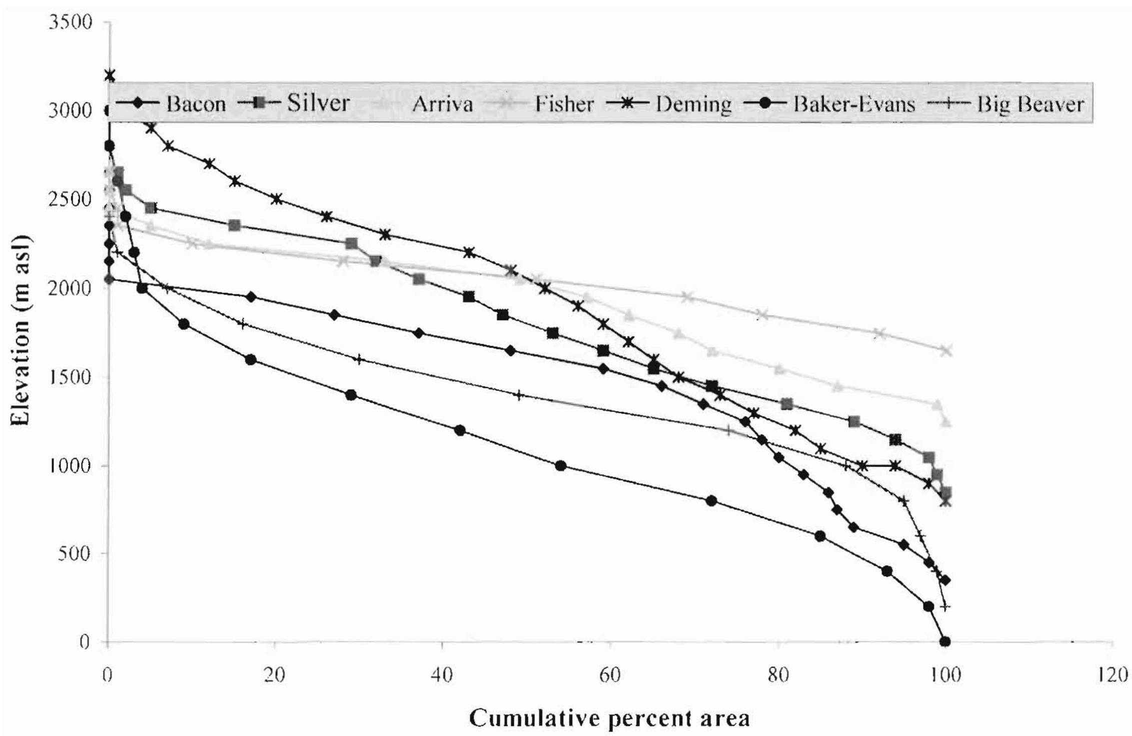

Figure 5-5. Hypsometric curves for Evans Creek and Sumas alpine glaciers in Skagit valley.

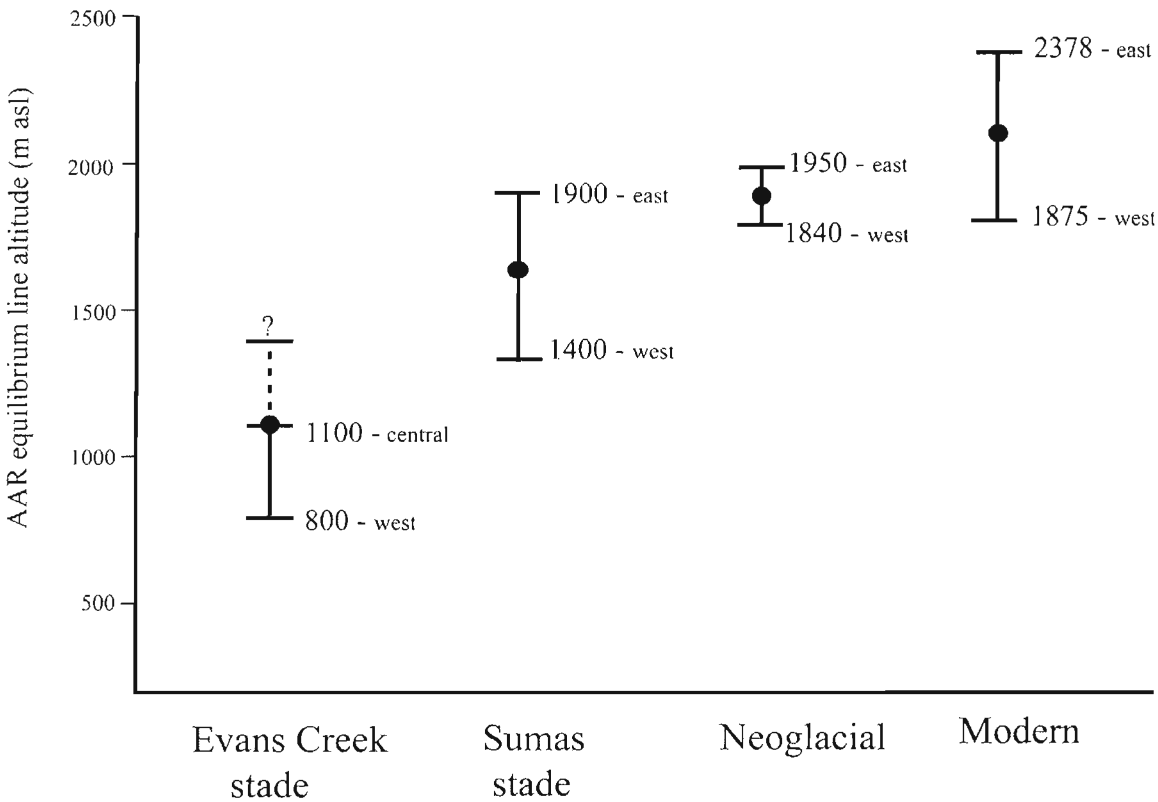

Figure 5-6. Comparison of ELAs for Skagit valley glaciers during the past 25,000 years.

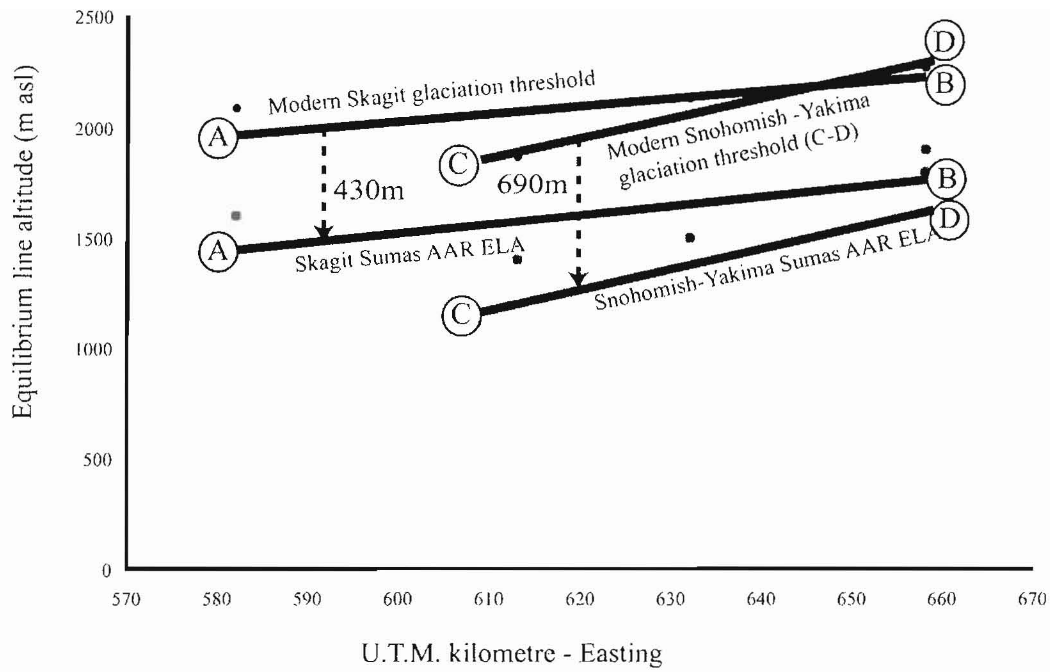

Figure 5-7. Trends of modern and Sumas stade equilibrium line altitudes determined by the AAR method from west to east along transects A-B and C-D (Figure 5-1). Transect C-D is based on data from Porter (1977), Porter et al. (1983), and Hurley (1996).

Tables

Table 5-1. Evans Creek and Sumas ELAs calculated using the ABR method for a range of balance ratios.

Balance Ratio	Baker (Evans Ck.)	Beaver (Evans Ck.)	Deming (Sumas)	Bacon (Sumas)	Silver (Sumas)	Arriva (Sumas)	Fisher (Sumas)
1	1116	1413	1938	1441	1771	1970	1977
1.2	1079	1386	1887	1394	1734	1944	1962
1.4	1047	1362	1844	1361	1703	1921	1949
1.6	1020	1342	1806	1331	1671	1901	1939
1.8	**997**	**1324**	**1733**	**1305**	**1653**	**1883**	**1929**
2	**977**	**1308**	**1743**	**1280**	**1633**	**1867**	**1921**
2.2	**959**	**1293**	**1717**	**1257**	**1615**	**1852**	**1914**
2.4	943	1280	1693	1236	1598	1839	1906
2.6	929	1268	1671	1217	1583	1827	1900
2.8	916	1258	1650	1199	1569	1816	1893
3	905	1248	1631	1181	1557	1806	1887
+/- 1σ	69	54	100	83	70	54	29
error (m)	73	59	103	87	73	59	38

Note: Bold numbers indicate values calculated using what are considered to be reasonable balance ratio values for glaciers in this region (Furbish and Andrews, 1984; Benn and Evans, 1998).

Table 5-2. Comparison of modern glaciation threshold (Gt) and equilibrium line altitudes (ELA) of Evans Creek and Sumas stade glaciers in the North Cascades.

Location	Modern Gt (m asl)[1]	Fraser Glaciation ELA (m asl) Bal. Ratio 2	ΔELA	AAR 0.65	ΔELA
Skagit Evans Creek stade					
Baker	1945	977	968	800	1145
Big Beaver	2034	1308	726	1100	934
Skagit Sumas stade transect A-B					
Deming –M1	2085	1743	342	1600	485
Deming – M3	2085	1835	250	1900	385
Bacon	1867	1280	587	1400	467
Silver	2128	1633	495	1500	628
Arriva	2268	1867	401	1800	468
Fisher	2268	1921	347	1900	368
Snoqualmie-Yakima Sumas stade transect C-D					
Ollalie[2]	1900			1205	698
Mirror[2]	1975			1285	695
Carter[2]	1800			1110	690
Turnpike[2]	2290			1620	690
Hyak[3]	2000			1275	725
Rat Creek[4]	2460			1800	660
Other Cascade Sumas stade					
Deming	1920	1565	355		
Brisingamen[5]	2460	2365	95		
Swift Creek[6]	1890			1400	490
McNeely[7]	2350-2150			1920-1710	500-550

Note: Locations of Transects A-B and C-D are shown in Figure 5-1.
[1] Glaciation threshold from Porter (1977).
[2] Hurley (1996).
[3] Porter (1976) and Porter et al. (1983).
[4] Waitt et al. (1982).
[5] Bilderback and Clark (2003).
[6] Burrows (2001).
[7] Heine (1998).

Reference List

Andrews, J.T., 1975. Glacial Systems: An Approach to Glaciers and Their Environments. Duxbury Press, North Scituate, MA.

Armstrong, J.E., Crandell, D.R., Easterbrook, D.J., and Noble, J.B., 1965. Late Pleistocene stratigraphy and chronology in southwestern British Columbia and northwestern Washington. Geological Society of America Bulletin 76: 321-330.

Benn, D.I., and Evans, D.J.A., 1988. Glaciers and Glaciation. E. Arnold Press, London.

Benn, D.I., and Gemmel, A.M.D., 1997. Calculating equilibrium line altitudes of former glaciers by the balance ratio method: A new computer spreadsheet. Glacial Geology and Geomorphology. http://ggg.ac.uk/ggg/papers/full/1997/tn011997/tn01.html

Benn, D.I., and Lehmkuhl, F., 2000. Mass balance and equilibrium-line altitudes of glaciers in high-mountain environments. Quaternary International 65/66: 15-19.

Berger, A.L., 1978. Long-term variations of caloric insolation resulting from the Earth's orbital elements. Quaternary Research 9: 139-167.

Bilderback, E.L., and Clark, D.H., 2003. Timing and paleoclimatic significance of latest Pleistocene and Holocene cirque glaciation in the Enchantment Lakes basin, North Cascades, Washington, U.S.A. XVI INQUA Congress Programs with Abstracts, p. 163.

Bitz, C.M., and Battisti, D.S., 1998. Interannual to interdecadal variability in climate and the glacier mass balance in northern Washington, western Canada, and Alaska. Journal of Climate 12: 3181-3196.

Burrows, R.A., 2001. Glacial Chronology and Paleoclimatic Significance of Cirque Moraines near Mts. Baker and Shuksan, North Cascade Range, Washington. M.S. thesis, Western Washington University, Bellingham, WA.

Clague, J.J., 1989b. Development of Cordilleran landscapes during the Quaternary. In: Fulton, R.J. (ed.), Quaternary Geology of Canada and Greenland. Geological Survey of Canada, Geology of North America K-1: 17-96.

Clague, J.J., Mathewes, R.W., Guilbault, J.-P., Hutchinson, I., and Ricketts, B.D., 1997. Pre-Younger Dryas resurgence of the southwestern margin of the Cordilleran ice sheet, British Columbia, Canada. Boreas 26: 261-277.

Clark, P.U., and Bartlein, P.J., 1995. Correlation of late Pleistocene glaciation in the western United States with North Atlantic Heinrich events. Geology 23: 483-486.

Flint, R.F., 1971. Glacial and Quaternary Geology. John Wiley and Sons, New York, NY.

Furbish, D.J., and Andrews, J.T., 1984. The use of hypsometry to indicate long-term stability and response of valley glaciers to changes in mass transfer. Journal of Glaciology 31: 205-213.

Grigg, L.D., and Whitlock, C., 2002. Patterns and causes of millennial-scale climate change in the Pacific Northwest during Marine Isotope Stages 2 and 3. Quaternary Science Reviews 21: 2067-2083.

Harper, J.T., 1992. The Dynamic Response of Glacier Termini to Climatic Variation during the Period 1940-1990 on Mount Baker Washington. M.S. thesis, Western Washington University, Bellingham, WA.

Heine, J.T., 1998. Extent, timing and climatic implications of glacier advances, Mount Rainier, Washington, U.S.A. at the Pleistocene Holocene transition. Quaternary Science Reviews 17: 1139-1148.

Heller, P.L., 1980. Multiple ice flow directions during the Fraser Glaciation in the lower Skagit River drainage, North Cascade Range, Washington. Arctic and Alpine Research 12: 299-308.

Hildreth, W., Fierstein, J., and Lanphere, M., 2003. Eruptive history and geochronology of the Mount Baker volcanic field, Washington. Geological Society of America Bulletin 115: 729-764.

Hodge, S.M., 1974. Variations in sliding of a temperate glacier. Journal of Glaciology 13: 349-369.

Hodge, S.M., Trabant, D.C., Krimmel, R.M., Heinrichs, T.A., March, R.S., and Josberger, E.G., 1997. Climate variations and changes in mass of three glaciers in western North America. Journal of Climate 11: 2161-2179.

Hurley, T.M., 1996. Late-glacial Equilibrium-line Altitudes of Glaciers in the Southern North Cascade Range, Washington. M.Sc. thesis, University of Washington, Seattle, WA.

Kovanen, D.J., and Slaymaker, O., 2005. Fluctuations of the Deming Glacier and theoretical equilibrium line altitudes during the Late Pleistocene and early Holocene on Mount Baker, Washington, USA. Boreas 34: 157-175.

Locke, W.W., 1990. Late Pleistocene glaciers and the climate of western Montana, U.S.A. Arctic and Alpine Research 22: 1-13.

Mann, D.H., and Hamilton, T.D., 1995. Late Pleistocene and Holocene paleoenvironments of the North Pacific coast. Quaternary Science Reviews 14: 449-471.

Meier, M.F., and Post, A.F., 1962. Recent variations in mass net budgets of glaciers in western North America. International Association of Scientific Hydrology Publication 58: 63-77.

Meyer, G.A., Fawcett, P.J., and Locke, W.W., 2003. Late Pleistocene equilibrium line altitudes, atmospheric circulation, and timing of mountain glacier advances in the interior northwestern United States. 16th INQUA Congress, Program with Abstracts, p. 73.

Ohmura, A., Kasser, P., and Funk, M., 1992. Climate at the equilibrium line of glaciers. Journal of Glaciology 38: 397-411.

Osmaston, H., 2005. Estimates of glacier equilibrium line altitudes by the Area x Altitude, the Area x Altitude Balance Ratio and the Area x Altitude Balance Index methods and their validation. Quaternary International 138-139: 22-31.

Osmaston, H., 2006. Should Quaternary sea-level changes be used to correct glacier ELAs, vegetation belt altitudes and sea level temperatures for inferring climate changes? Quaternary Research 65: 244-251.

Paterson, W.S.B., 1981. The Physics of Glaciers. Pergamon Press, Oxford.

Pelto, M.S., and Riedel, J.L., 2001. Spatial and temporal variations in annual balance of North Cascades glaciers, Washington. Hydrological Processes 15: 3461-3472.

Pierce, K.L., 1979. History and Dynamics of Glaciation in the Northern Yellowstone National Park Area. U.S. Geological Survey Professional Paper 729-F.

Porter, S.C., 1975. Equilibrium line altitudes of late Quaternary glaciers in the Southern Alps, New Zealand. Quaternary Research 5: 27-47.

Porter, S.C., 1976. Pleistocene glaciation in the southern part of the North Cascade Range, Washington. Geological Society of America Bulletin 87: 61-75.

Porter, S.C., 1977. Present and past glaciation threshold in the Cascade Range, Washington, U.S.A.: Topographic and climatic controls, and paleoclimatic implications. Journal of Glaciology 18: 101-116.

Porter, S.C., 1986. Pattern and forcing of northern hemisphere glacier variations during the last millennium. Quaternary Research 26: 27-48.

Porter, S.C., Pierce, K.L., and Hamilton, T.D., 1983. Late Wisconsin mountain glaciation in the Western United States. In: Porter, S.C. (ed.), Late-Quaternary Environments, Vol. 1, The Late Pleistocene. University of Minnesota Press, Minneapolis, MN, pp. 71-111.

Post, A., Richardson, D., Tangborn, W., and Rosselot, F.L., 1971. Inventory of Glaciers in the North Cascades, Washington. U.S. Geological Survey Professional Paper 705-A.

Reasoner, M.A., Osborn, G., and Rutter, N.W., 1994. Age of the Crowfoot advance in the Canadian Rocky Mountains: A glacial event coeval with the Younger Dryas oscillation. Geology 22: 439-442.

Riedel, J.L., 1987. Chronology of Late Neoglacial Glacier Recession in the Cascade Range and the Deposition of a Recent Esker in the North Cascade Mountains, Washington. M.S. thesis, University of Wisconsin, Madison, WI.

Riedel, J.L., and Burrows, R., 2003. Glacier mass balance monitoring at North Cascades and Mount Rainier National Parks, Washington. Geological Society of America, Abstracts with Programs 34: 132.

Ruddiman, W.F., and Wright, Jr., H.E., 1987. Introduction. In: Ruddiman, W.F., and Wright, Jr., H.E. (eds.), North America and Adjacent Oceans during the Last Deglaciation. Geological Society of America, Geology of North America K3: 1-12.

Stansell, N.D., Polissar, P.J., and Abbott, M.B., 2007. Last glacial maximum equilibrium line altitude and paleo-temperature reconstructions for Cordillera de Mérida, Venezuelan Andes. Quaternary Research, in press.

Stuiver, M., and Reimer, P.J., 1993. Extended ^{14}C data base and revised CALIB 3.0 ^{14}C age calibration program. Radiocarbon 35: 215-230.

Stuiver, M., Grootes, P.M., and Braziunas, T.F., 1995. The GISP2 $\delta^{18}O$ climate record of the past 16,500 years and the role of the sun, ocean, and volcanoes. Quaternary Research 44: 341-354.

Sugden, D.E., and John, B.S., 1976. Glaciers and Landscape. E. Arnold Press, London.

Swanson, T.W., and Porter, S.C., 1997. Cosmogenic isotope ages of moraines in the southeastern North Cascade Range. Pacific Northwest Friends of the Pleistocene Field Excursion Guidebook, 18 p.

Tangborn, W.F., 1980. Two models for estimating the climate-glacier relationships in the North Cascades, Washington. Journal of Glaciology 25: 3-21.

Thackray, G.D., 2001. Extensive early and middle Wisconsin glaciation on the western Olympic Peninsula, Washington, and the variability of Pacific moisture delivery to the northwestern United States. Quaternary Research 55: 257-70.

Waitt, Jr., R.B., 1977. Evolution of glaciated topography of upper Skagit drainage basin, Washington. Arctic and Alpine Research 9: 183-192.

Waitt, Jr., R.B., Yount, J.C., and Davis, P.T., 1982. Regional significance of an early Holocene moraine in Enchantment Lakes basin, North Cascade Range, Washington. Quaternary Research 17: 191-210.

Appendices

Appendix 5-1. Calculations constraining reconstructed glacier thickness.

Glacier thickness (h) using the ice flow law (Paterson, 1981):

$$h = \tau_o / F\ (\rho g \sin \alpha)$$

Where ρ is ice density, **g** is gravitational acceleration, τ_0 is basal shear stress, $\sin \alpha$ is ice surface slope estimated from trimlines or valley slope, and **F** is a shape factor.

1) Deming Glacier lower canyon:	h = 96/ 0.7 (0.9 x 9.81 x 0.156) = 100 m
2) Deming Glacier upper canyon:	h = 104/ 0.7 (0.9 x 9.81 x 0.21) = 80 m
3) Modern upper Deming Glacier: (shape factor = 1)	h = 130/ (0.9 x 9.81 x 0.37) = 45 m
4) Bacon Glacier near terminus:	h = 63/ 0.68 (0.9 x 9.81 x 0.035) = 300 m
5) Bacon Glacier: at head of lower valley (first rise)	h = 117/ 0.68 (0.9 x 9.81 x 0.078) = 250 m
6) Bacon Glacier: ice fall below cirques (strong convergent flow)	h = 126/ 0.68 (0.9 x 9.81 x 0.14) = 150 m
7) Lower Silver Glacier: near lateral moraines	h = 120/ 0.7 (0.9 x 9.81 x 0.104) = 187 m
8) Silver Glacier ice fall:	h = 142/ 0.7 (0.9 x 9.81 x 0.5) = 47 m
9) Lower Fisher Glacier:	h = 57/ 0.65 (0.9 x 9.81 x 0.05) = 199 m
10) Upper Fisher Glacier:	h = 119/ 0.65 (0.9 x 9.81 x 0.26) = 80 m
11) Arriva Glacier: ice fall below cirque basin	h = 140/ 0.74 (0.9 x 9.81 x 0.48) = 45 m
12) Arriva Glacier: upper cirque basin	h = 117/ 0.74 (0.9 x 9.81 x 0.10) = 180 m

Appendix 5-2. Equilibrium line altitude (ELA) spreadsheets.

Silver Glacier, Sumas stade, 200 m contour interval.

Contour (m)	Mean zone altitude (m)	Contour zone area (km^2)	Mean altitude x area (m asl)	Balance ratio	ELA trial reference contour [1]
600	700	0	0	**2.0**	1411 m asl
800	900	0.23	207		
1000	1100	1.5	1650		
1200	1300	2.74	3562		
1400	1500	2.23	3345		
1600	1700	2	3400		
1800	1900	1.61	3059		
2000	2100	1.36	2856		
2200	2300	3.64	8372		
2400	2500	0.97	2425		
2600	2700	0.18	486		
2800	2900	0	0		
3000	3100	0	0		
3200	3300	0	0		
3400	3500	0	0		
3600	3700	0	0		
3800	3900	0	0		
4000	4100	0	0		
4200	4300	0	0		
4400	4500	0	0		
TOTALS		16	29362		

RESULTS

AA ELA (median altitude x area, shortcut method) =	1784	**CHECK [1] =**	**TRUE**
AABR ELA for BR=1 (interpolated between contours) =			
AABR ELA for other BRs (interpolated between contours) =			

Balance ratio	**1**	**ELA estimate**	**1784**
Balance ratio	**2.00**	**ELA estimate**	**1644**
Difference			**140**

[1] Program checks to see if initial ELA estimate is within range of median altitude.

Deming Glacier M1, early Sumas stade, 200 m contour interval.

Contour (m)	Mean zone altitude (m)	Contour zone area (km^2)	Mean altitude x area (m asl)	Balance ratio	ELA trial reference contour [1]
500	600	0	0	**2.0**	1500 m asl
700	800	0.4	320		
900	1000	0.78	780		
1100	1200	0.77	924		
1300	1400	0.8	1120		
1500	1600	0.61	976		
1700	1800	0.53	954		
1900	2000	0.78	1560		
2100	2200	1.32	2904		
2300	2400	1.2	2880		
2500	2600	0.75	1950		
2700	2800	0.62	1736		
2900	3000	0.33	990		
3100	3200	0	352		
3300	3400	0	0		
3500	3600	0	0		
3700	3800	0	0		
3900	4000	0	0		
4100	4200	0	0		
4300	4400	0	0		
TOTALS		9	17446		

RESULTS					
AA ELA (median altitude x area, shortcut method) =			1938	**CHECK [1] =**	**TRUE**
AABR ELA for BR=1 (interpolated between contours) =					
AABR ELA for other BRs (interpolated between contours) =					
Balance Ratio	**1**	**ELA estimate**	**1938**		
Balance Ratio	**2.00**	**ELA estimate**	**1743**		
Difference			**195**		

[1] Program checks to see if initial ELA estimate is within range of median altitude.

Deming Glacier M3, late Sumas stade, 200 m contour interval.

Contour (m)	Mean zone altitude (m)	Contour zone area (km^2)	Mean altitude x area (m asl)	Balance ratio	ELA trial reference contour [1]
600	700	0	0	**2.0**	1516 m asl
800	900	0.43	387		
1000	1100	0.76	836		
1200	1300	0.57	741		
1400	1500	0.58	870		
1600	1700	0.53	901		
1800	1900	0.64	1216		
2000	2100	0.88	1848		
2200	2300	1.45	3335		
2400	2500	1.03	2575		
2600	2700	0.71	1917		
2800	2900	0.45	1305		
3000	3100	0.16	496		
3200	3300	0	330		
3400	3500		0		
3600	3700		0		
3800	3900		0		
4000	4100		0		
4200	4300		0		
4400	4500		0		
TOTALS		8	16757		

RESULTS					
AA ELA (median alt x area, shortcut method) =			2021	**CHECK [1] =**	**TRUE**
AABR ELA for BR=1 (interpolated between contours) =					
AABR ELA for other BRs (interpolated between contours) =					
Balance Ratio	**1**	**ELA estimate**	**2021**		
Balance Ratio	**2.00**	**ELA estimate**	**1835**		
Difference			**186**		

[1] Program checks to see if initial ELA estimate is within range of median altitude.

Bacon Glacier, Sumas stade, 200 m contour interval.

Contour (m)	Mean zone altitude (m)	Contour zone area (km^2)	Mean altitude x area (m asl)	Balance ratio	ELA trial reference contour [1]
200	250	0	100	**2.0**	1000 m asl
300	350	0.4	140		
400	450	0.7	315		
500	550	1.5	825		
600	650	0.5	325		
700	750	0.3	225		
800	850	0.6	510		
900	950	0.7	665		
1000	1050	0.4	420		
1100	1150	0.5	575		
1200	1250	1.2	1500		
1300	1350	1.1	1485		
1400	1450	1.7	2465		
1500	1550	3	4030		
1600	1650	3	4125		
1700	1750	2	4200		
1800	1850	2	4440		
1900	1950	3	6045		
2000	2050	1	1845		
2100	2150	0	0		
TOTALS		24	34235		

RESULTS

AA ELA (median alt x area, shortcut method) = 1432 **CHECK [1] = TRUE**

AABR ELA for BR=1 (interpolated between contours) =

AABR ELA for other BRs (interpolated between contours) =

Balance Ratio	**1**	**ELA estimate**	**1432**
Balance Ratio	**2.00**	**ELA estimate**	**1280**
Difference			**152**

[1] Program checks to see if initial ELA estimate is within range of median altitude.

Fisher Glacier, Sumas stade, 200 m contour interval.

Contour (m)	Mean zone altitude (m)	Contour zone area (km^2)	Mean altitude x area (m asl)	Balance ratio	ELA trial reference contour [1]
1500	1550	0	0	**1.8**	1820 m asl
1600	1650	0.2	330		
1700	1750	0.3	525		
1800	1850	0.2	370		
1900	1950	0.4	780		
2000	2050	0.5	1025		
2100	2150	0.4	860		
2200	2250	0.2	450		
2300	2350	0.02	47		
2400	2450	0.002	5		
2500	2550	0	0		
2600	2650	0	0		
2700	2750	0	0		
2800	2850		0		
2900	2950		0		
3000	3050		0		
3100	3150		0		
3200	3250		0		
3300	3350		0		
3400	3450		0		
TOTALS		2	4392		

RESULTS			
AA ELA (median alt x area, shortcut method) =	1977	**CHECK [1] =**	**TRUE**
AABR ELA for BR=1 (interpolated between contours) =			
AABR ELA for other BRs (interpolated between contours) =			

Balance Ratio	**1**	**ELA estimate**	**1977**
Balance Ratio	**1.80**	**ELA estimate**	**1930**
Difference			**47**

[1] Program checks to see if initial ELA estimate is within range of median altitude.

Arriva Glacier, Sumas stade, 200 m contour interval.

Contour (m)	Mean zone altitude (m)	Contour zone area (km^2)	Mean altitude x area (m asl)	Balance ratio	ELA trial reference contour [1]
1200	1250	0	0	**1.8**	1700 m asl
1300	1350	0.04	54		
1400	1450	0.27	392		
1500	1550	0.15	233		
1600	1650	0.17	281		
1700	1750	0.09	158		
1800	1850	0.13	241		
1900	1950	0.12	234		
2000	2050	0.17	349		
2100	2150	0.37	796		
2200	2250	0.47	1058		
2300	2350	0.14	329		
2400	2450	0.12	294		
2500	2550	0	0		
2600	2650	0	0		
2700	2750	0	0		
2800	2850	0	0		
2900	2950	0	0		
3000	3050	0	0		
3100	3150	0	0		
TOTALS		2	4415		

RESULTS			
AA ELA (median alt x area, shortcut method) =	1971	**CHECK [1] =**	**TRUE**
AABR ELA for BR=1 (interpolated between contours) =			
AABR ELA for other BRs (interpolated between contours) =			

Balance Ratio	**1**	**ELA estimate**	**1971**
Balance Ratio	**1.80**	**ELA estimate**	**1883**
Difference			**88**

[1] Program checks to see if initial ELA estimate is within range of median altitude.

Beaver Glacier, Evans Creek stade, 200 m contour interval.

Contour (m)	Mean zone altitude (m)	Contour zone area (km^2)	Mean altitude x area (m asl)	Balance ratio	ELA trial reference contour [1]
0	100		0	**2.0**	1400 m asl
200	300	0.32	96		
400	500	1.515	758		
600	700	3.164	2215		
800	900	6.276	5648		
1000	1100	14.42	15862		
1200	1300	24.721	32137		
1400	1500	18.823	28235		
1600	1700	13.306	22620		
1800	1900	9.107	17303		
2000	2100	5.887	12363		
2200	2300	0.725	1668		
2400	2500		0		
2600	2700		0		
2800	2900		0		
3000	3100		0		
3200	3300		0		
3400	3500		0		
3600	3700		0		
3800	3900		0		
TOTALS		98	138904		

RESULTS			
AA ELA (median alt x area, shortcut method) =	1414	**CHECK [1] =**	**TRUE**
AABR ELA for BR=1 (interpolated between contours) =			
AABR ELA for other BRs (interpolated between contours) =			

Balance Ratio	**1**	**ELA estimate**	**1414**
Balance Ratio	**2.00**	**ELA estimate**	**1308**
Difference			**106**

[1] Program checks to see if initial ELA estimate is within range of median altitude.

Baker Glacier, Evans Creek stade, 200 m contour interval.

Contour (m)	Mean zone altitude (m)	Contour zone area (km^2)	Mean altitude x area (m asl)	Balance ratio	ELA trial reference contour [1]
0	100	7.4	740	**3.0**	500 m asl
200	300	31.4	9420		
400	500	44.1	22050		
600	700	64.7	45290		
800	900	100.3	90270		
1000	1100	65.4	71940		
1200	1300	68.8	89440		
1400	1500	64.4	96600		
1600	1700	45.3	77010		
1800	1900	23.7	45030		
2000	2100	9.2	19320		
2200	2300	5.5	12650		
2400	2500	4.5	11250		
2600	2700	2.3	6210		
2800	2900	1.2	3480		
3000	3100		0		
3200	3300		0		
3400	3500		0		
3600	3700		0		
3800	3900		0		
TOTALS		538	600700		

RESULTS			
AA ELA (median alt x area, shortcut method) =	1116	**CHECK [1] =**	**TRUE**
AABR ELA for BR=1 (interpolated between contours) =			
AABR ELA for other BRs (interpolated between contours) =			

Balance Ratio	**1**	**ELA estimate**	**1116**
Balance Ratio	**3.00**	**ELA estimate**	**905**
Difference			**211**

[1] Program checks to see if initial ELA estimate is within range of median altitude.

Appendix 5-3. Chronology of late Fraser alpine glacier and Cordilleran ice sheet advances in the North Cascades and vicinity.

Pacific Northwest geologic-climate units [1]	North Atlantic chronozones and minimum ages [2]	Glacier advance	Age and dating method
HOLOCENE	EARLY HOLOCENE (10,000 ^{14}C, 11,650 cal)	**Fisher** McNeely 2 Swift/Bagley **Silver Creek** **Fisher 3B**	**>8230 (minimum ^{14}C, lake)** 9800-8950 (^{14}C) >9650 (^{14}C, bog base) **>9975 (minimum ^{14}C, buried soil)** **10,830 +/- 4312 (Be^{10}, cal)**
	YOUNGER DRYAS (11,021 ^{14}C, 12,890 cal)	Deming M3 Mamquam **Bacon 2B** Hyak 2	~10,600 (^{14}C, log in till) 10,600 (^{14}C, log in till) **11,805+/- 1300 (Be^{10}, cal)** 12.2 +/- 0.8 (^{36}Cl, cal)
SUMAS STADE	ALLEROD (11,800 ^{14}C, 14,010 cal)	Sumas 2 Rat Creek 2 **Arriva** Hyak 1 McNeely 1	<11,300 (^{14}C) 13.4 +/-1.0 (^{36}Cl, cal) **12,327 +/- 1200 (Be^{10}, cal)** >11,050 (^{14}C, bog) 13.5 +/- 0.4 (^{36}Cl, cal) >11,300 (^{14}C, lake)
	OLDER DRYAS (12,000 ^{14}C, 14,090 cal)	Rat Creek 1 Sumas–1	>11,800 (^{14}C); 14.2. +/- 0.1 (^{36}Cl, cal) >11,900 (^{14}C)
EVERSON INTERSTADE	BOLLING (12,500 ^{14}C, 14,670 cal)		
VASHON STADE 17,600 ^{14}C	OLDEST DRYAS (14,500 ^{14}C)		
		Domerie Leavenworth III	16.0+/-3.5 to 15.1+/- 0.4 (^{36}Cl, cal) not dated

Note: Sites and ages in bold are from this study.

[1] Pacific Northwest geologic-climatic units from Armstrong et al. (1965).

[2] North Atlantic chronozones from Stuiver et al. (1995).

Other data sources: Porter (1976 and 1977), Waitt et al. (1982), Clague et al. (1997), Swanson and Porter (1997), Heine (1998), Burrows (2001), Kovanen and Easterbrook (2001), and Kovanen and Slaymaker (2005).

Appendix 5-4. Age control data for Skagit alpine moraines during the Sumas stade

Radiocarbon ages from upper Skagit valley

Site/sample	m asl	Lab no. / method	Material	$^{13}C/^{12}C$	^{14}C age +/- 1σ yr BP	cal. age[1]
Silver moraine NOCA 93 (48° 58.453' x 121° 09.294')	890	LLNL 11461	charcoal	-25	9975 +/- 35	11500
Fisher moraine NOCA 40A (48° 33.950' x 120° 50.884')	1594	Beta 184473	charcoal	-24.2	8230 +/- 50	9288

[1] CALIB 5.0.2 Stuiver and Reimer, 1993.

Beryllium-10 boulder surface exposure ages

Site/sample	m asl	Rock type	Exposure age	Internal error	External error	Total error
Bacon 1 336		granodiorite	6648	353	576	929
Bacon 2 342		granodiorite	11805	405	904	1309
Bacon 3 343		granodiorite	22088	604	1632	2236
Arriva 3A	1448	granodiorite	13606	326	987	1313
Arriva 4A	1456	granodiorite	11048	261	800	1061
Fisher 3B	1600	granodiorite	10830	2092	2220	4312

Notes: Radiocarbon dates are minimum estimates from sites inset within moraines, while cosmogenic dates were obtained on boulders from moraine surfaces. See Figure 5-3 for site locations.

Chapter 6: Synthesis

Skagit valley holds a wealth of information about landscape evolution and glacier and climate change during the Fraser Glaciation, ca. 30,000-10,000 ^{14}C yr BP. Alpine and continental glaciation have shaped the Skagit watershed. High elevation areas retain features of alpine glaciation, including cirques, hanging valleys, steep walls, and U-shaped valleys. Drainage patterns established in the Tertiary have been reorganized to accommodate southward drainage of glacial meltwater trapped in mountain valleys (Figure 6-1). Drainage of large proglacial lakes led to several hundred metres of erosion at divides. Many of these meltwater routes lead into upper Skagit valley, making the corridor a regional focal point for meltwater discharge from the Fraser and Okanagan watersheds in southern British Columbia to the Pacific Ocean. The key to establishment of this system was the breaching of a major regional divide at what is now Skagit Gorge, which resulted in the capture of upper Skagit valley by lower Skagit River. Patterns of drainage modification in the Skagit watershed caused by continental glaciation are similar to those in other mountain areas. The upper Skagit's interconnected valleys are similar to the great through-valleys of Scotland, trans-range valleys of British Columbia, and ice portals of Scandinavia. Identification of this drainage system should lead to refinement of meltwater discharge estimates from the Puget lobe (Booth and Hallet, 1993). I intend to apply this approach to examine the impact of continental glaciation on evolution of the Fraser, Okanagan, and Columbia rivers.

Tributary alpine glaciers heading in the high crystalline core of the North Cascades advanced to block Skagit River about 24,000 ^{14}C yr BP, early during the Fraser Glaciation. Ice dams created glacial lakes Skymo and Concrete, which slowly filled with fine-grained sediment. Silt and clay deposited in glacial Lake Concrete underlie the Skagit valley floor from the mouth of Baker River to near Marblemount.

The distribution of lake deposits and till allowed me to limit the extent of the two tributary alpine glaciers during the Evans Creek stade. Equilibrium line altitudes (ELAs) of these reconstructed glaciers are 730-970 m below the modern glaciation threshold, providing a regional measure of climate change at the last alpine glacial maximum. Along with recent work in the Rocky Mountains, these ELA estimates provide a framework for understanding patterns of glaciation and climate change in western North America (Meyer et al., 2003). Future work in other mountain valleys in the Cascades would refine our understanding of climate change during the last glaciation at local, regional, and global scales.

Sediments exposed at the Cedar Grove section provide evidence of two glacier advances during the Evans Creek stade (Figure 6-2). A forest established on early Evans Creek outwash at the mouth of Baker valley was overridden by Baker Glacier after 20,730 ^{14}C yr BP. The two advances of the Baker Glacier during the Evans Creek stade were in phase with other alpine glaciers in the region (Porter, et. al., 1983; Thackray, 2001).

Macrofossils preserved in sediments of glacial lakes Skymo and Concrete and dating to 24,000-16,400 ^{14}C yr BP provide important information on Fraser Glaciation environments and on the timing of substadial climate events in Skagit valley (Figure 6-2). The presence of subalpine parkland on the shores of glacial Lake Skymo indicates treeline depression of 1200 m, which corresponds to an approximate 7 ±1°C drop in mean July temperature. Increased abundance and diversity of macrofossils after 20,770 ^{14}C yr BP in glacial Lake Skymo sediments signal a moister and warmer period (Figure 6-2). Comparison of bioclimatic variables of indicator species allowed me to estimate an increase in mean annual precipitation of about 200 mm. A similar increase in macrofossil abundance and diversity occurs near the top of glacial Lake Concrete sequence at about 17,170 ^{14}C yr BP. This event is recognized in most of the pollen and macrofossil records in the region and is known as the Port Moody interstade in Fraser Lowland. Much more can be learned from the glacial lake sediments in Skagit valley. Future work could focus on diatoms, pollen, chironomids, and other fossils at these readily accessible sites. Samples from two organic beds at Cedar Grove are currently being examined, and I will continue working with Alice Telka on completion of macrofossil identification and interpretation.

Alpine glaciers in Skagit valley advanced two or more times during the Sumas stade after retreat of the Cordilleran Ice Sheet from the watershed. Beryllium-10 ages of boulders on three moraines fall within the Sumas stade (Appendix 5.3). A single radiocarbon age inside the Silver Creek moraine constrains the time of the advance that built the moraine to before 9975 ^{14}C yr BP, which is the oldest minimum limiting radiocarbon age for moraines in the Cascade Range reported to date. I plan to expand on this chronology with 17 chlorine-36 ages on boulders on four late-glacial moraines. Future work should focus on dating other moraines.

Equilibrium line altitudes during the Sumas stade were depressed 100-200 m more in maritime western Skagit valley than in more arid eastern tributaries, where they are within 100 m of Neoglacial values. This pattern is observed in mountain ranges throughout western North America. The Cordilleran Ice Sheet affected climate, glacier extent, and vegetation in Skagit valley during the Sumas stade. ELA depression in the Skagit watershed is 200 m lower than 100 km to the south, indicating that the ice sheet blocked storms and kept the Skagit watershed drier than valleys to the south. These results build on a database that can be used to calibrate regional and global climate change models. The method detailed in this thesis can be applied to estimate ELAs elsewhere in the region.

Figures

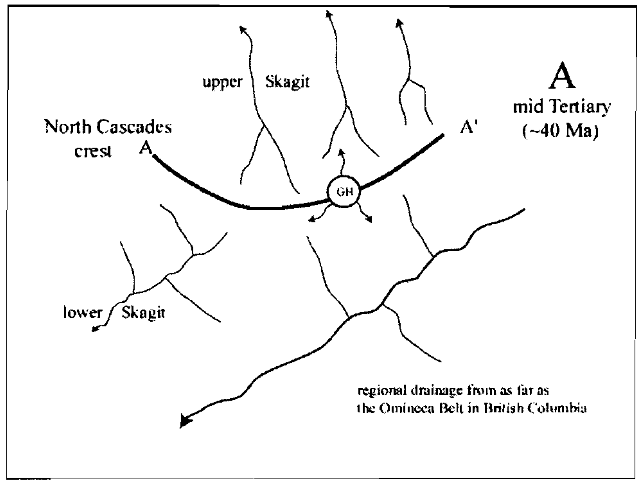

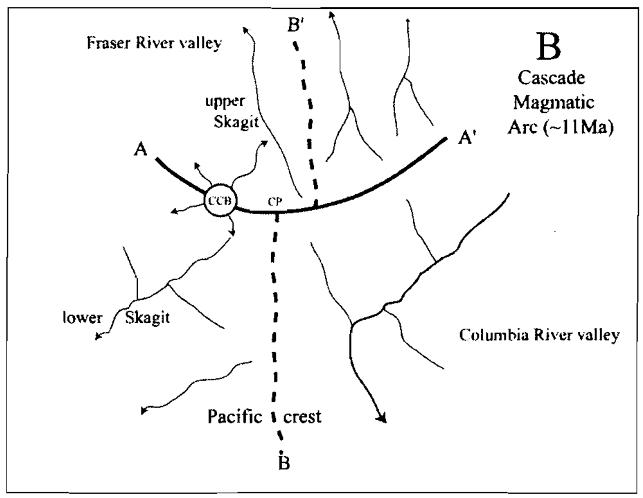

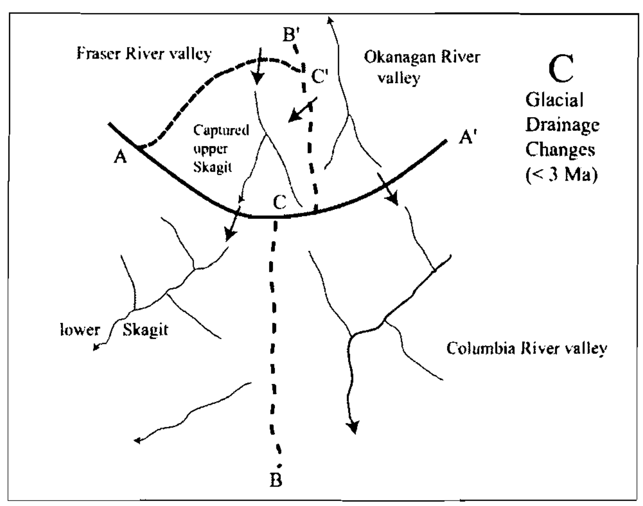

Figure 6-1. Schematic diagram of drainage pattern and divide changes in the Skagit River watershed from (A) mid-Tertiary, through (B) late Tertiary, to (C) the Pleistocene. Note radial drainage associated with the Golden Horn Batholith (GH) and Chilliwack Composite Batholith (CCB).

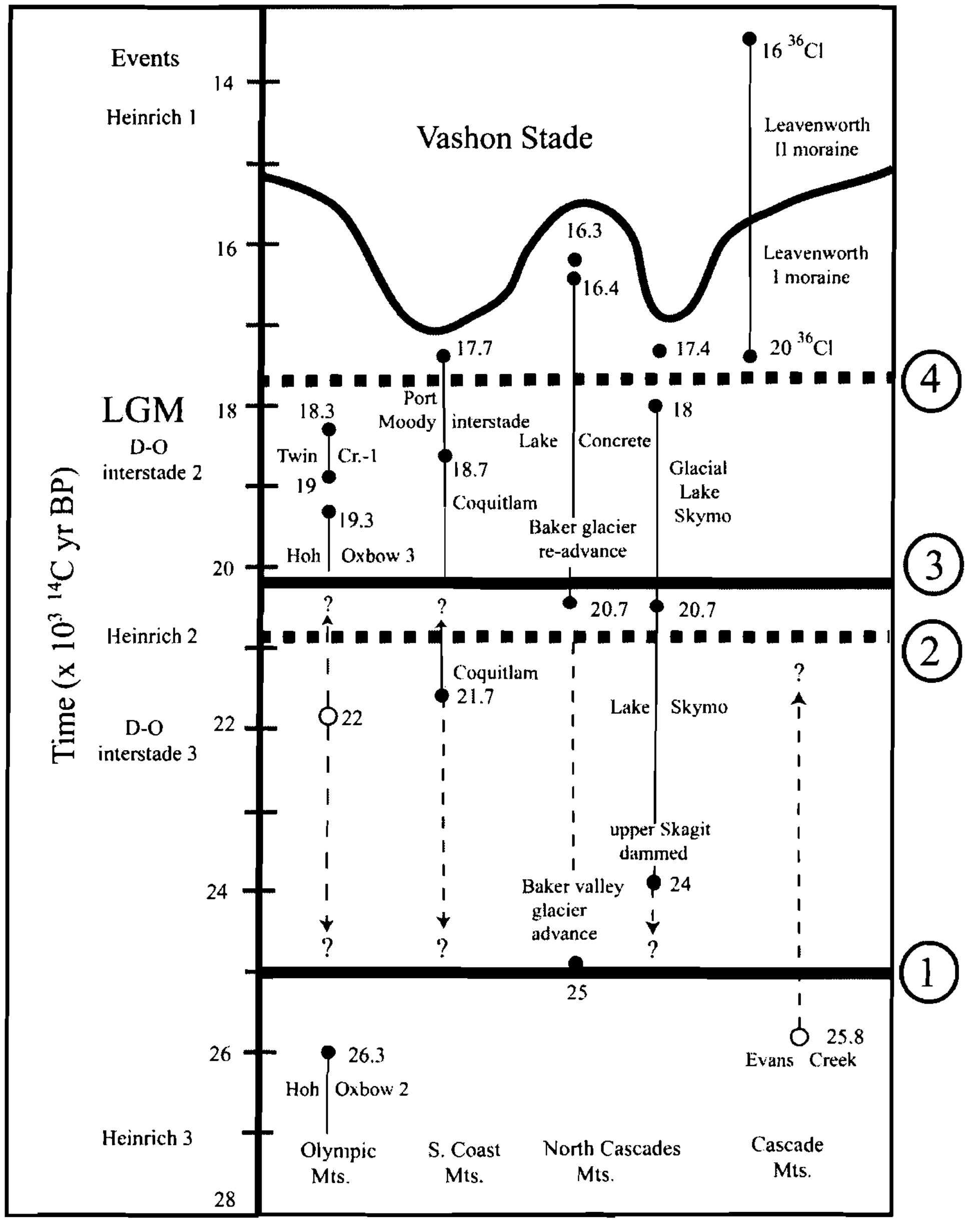

Figure 6-2. Revised chronology of the early part of the Fraser Glaciation based on Skagit valley sediments, radiocarbon ages, and macrofossils. Important events identified in this study include: (1) the beginning of the Evans Creek stade about 25,000 ^{14}C yr BP; (2) warmer and wetter conditions about 20,700 ^{14}C yr BP; (3) the advance of the Baker Glacier after 20,700 ^{14}C yr BP; and (4) a return to milder conditions during the Port Moody interstade, after 17,570 ^{14}C yr BP.

General Bibliography

Alley, N.F., and Chatwin, S.C., 1979. Late Pleistocene history and geomorphology, southwestern Vancouver Island, British Columbia. Canadian Journal of Earth Sciences 11: 1220-1235.

Andrews, J.T., 1975. Glacial Systems: An Approach to Glaciers and Their Environments. Duxbury Press, North Scituate, MA.

Antevs, E., 1954. Climate of New Mexico during the last glacio-pluvial. Journal of Geology 62: 182-191.

Armstrong, J.E., and Clague, J.J., 1977. Two major Wisconsin lithostratigraphic units in southwest British Columbia. Canadian Journal of Earth Sciences 14: 1471-1480.

Armstrong, J.E., and Hicock, S.R., 1975. Quaternary landscapes: Present and past – at Mary Hill, Coquitlam, British Columbia (92G/2F). Geological Survey of Canada Paper 75-1B: 99-103.

Armstrong, J.E., and Tipper, H.W., 1948. Glaciation in north central British Columbia. American Journal of Science 246: 283-310.

Armstrong, J.E., Crandell, D.R., Easterbrook, D.J., and Noble, J.B., 1965. Late Pleistocene stratigraphy and chronology in southwestern British Columbia and northwestern Washington. Geological Society of America Bulletin 76: 321-330.

Arno, S.F., and Hammerly, R.P., 1984. Timberline: Mountain and Arctic Forest Frontiers. The Mountaineers, Seattle, WA.

Ashley, G.M., Shaw, J., and Smith, N.D., 1985. Glacial Sedimentary Environments. Society of Economic Paleontologists and Mineralogists Short Course No. 16.

Atwater, B.F., 1986. Pleistocene Glacial-lake Deposits of the Sanpoil River Valley, Northeastern Washington. U.S. Geological Survey Bulletin 1661.

Baker, R.G., 1970. Pollen sequence from late Quaternary sediments in Yellowstone Park. Science 168: 1449.

Barksdale, J.D., 1941. Glaciation of the Methow valley, Washington. Journal of Geology 49: 721-737.

Barnosky, C.W., 1981. A record of Quaternary vegetation from Davis Lake, southern Puget Lowland, Washington. Quaternary Research 16: 221-239.

Barnosky, C.W., 1984. Late Pleistocene and early Holocene environmental history of southwestern Washington state, U.S.A. Canadian Journal of Earth Sciences 31: 619-629.

Barnosky, C.W., 1985. Late Quaternary vegetation near Battle Ground Lake, southern Puget Trough, Washington. Geological Society of America Bulletin 96: 263-271.

Barnosky, C.W., Anderson, P.M., and Bartlein, P.J., 1987. The northwestern U.S. during deglaciation: Vegetational history and paleoclimatic implications. In: Ruddiman, W.F., and Wright, Jr., H.E. (eds.), North America and Adjacent Oceans during the Last Deglaciation. Geological Society of America, The Geology of North America K-3: 289-321.

Benn, D.I., and Evans, D.J.A., 1988. Glaciers and Glaciation. E. Arnold Press, London.

Benn, D.I., and Gemmel, A.M.D., 1997. Calculating equilibrium line altitudes of former glaciers by the balance ratio method: A new computer spreadsheet. Glacial Geology and Geomorphology. http://ggg.ac.uk/ggg/papers/full/1997/tn011997/tn01.html

Benn, D.I., and Lehmkuhl, F., 2000. Mass balance and equilibrium-line altitudes of glaciers in high-mountain environments. Quaternary International 65/66: 15-19.

Berger, A.L., 1978. Long-term variations of caloric insolation resulting from the Earth's orbital elements. Quaternary Research 9: 139-167.

Bilderback, E.L., and Clark, D.H., 2003. Timing and paleoclimatic significance of latest Pleistocene and Holocene cirque glaciation in the Enchantment Lakes basin, North Cascades, Washington, U.S.A. XVI INQUA Congress Programs with Abstracts, p. 163.

Birks, H.J.B., and Birks, H.H., 1981. Quaternary Paleoecology. E. Arnold Press, London.

Bishop, P., 1995. Drainage rearrangement by river capture, beheading and diversion. Progress in Physical Geography 19: 449-473.

Bitz, C.M., and Battisti, D.S., 1998. Interannual to interdecadal variability in climate and the glacier mass balance in northern Washington, western Canada, and Alaska. Journal of Climate 12: 3181-3196.

Booth, D.K., 1987. Timing and processes of deglaciation along the southern margin of the Cordilleran Ice Sheet. In: Ruddiman, W.F., and Wright, Jr., H.E. (eds.), North America and Adjacent Oceans during the Last Deglaciation. Geological Society of America, The Geology of North America K-3: 71-90.

Booth, D.K., and Hallet, B., 1993. Channel networks carved by subglacial water: Observations and reconstruction in eastern Puget Lowland of Washington. Geological Society of America Bulletin 105: 671-683.

Booth, D.B., Troost, K.G., Clague, J.J., and Waitt, R.B., 2004. The Cordilleran Ice Sheet. In: Gillespie, A.R., Porter, S.C., and Atwater, B.F. (eds.), The Quaternary Period in the U.S. Elsevier Development in Quaternary Science 1: 17-43.

Brayshaw, T.C., 1985. Pondweeds and Bur-reeds, and Their Relatives: Aquatic Families of Monocotyledons in British Columbia. British Columbia Provincial Museum Occasional Paper 26.

Bretz, J.H., 1913. Glaciation of Puget Sound Region. Washington Geological Survey Bulletin 8.

Burrows, R.A., 2001. Glacial Chronology and Paleoclimatic Significance of Cirque Moraines near Mts. Baker and Shuksan, North Cascade Range, Washington. M.S. thesis, Western Washington University, Bellingham, WA.

Busacca, A.J., Nelstead, K.T., McDonald, E.V., and Purser, M.D., 1992. Correlation of distal tephra layers in loess in the Channeled Scabland and Palouse of Washington State. Quaternary Research 37: 281-303.

Clague, J.J., 1981. Late Quaternary Geology and Geochronology of British Columbia. Part I: Radiocarbon Dates. Geological Survey of Canada Paper 80-13.

Clague, J.J., 1981. Late Quaternary Geology and Geochronology of British Columbia, Part II: Summary and Discussion of Radiocarbon-dated Quaternary History. Geological Survey of Canada Paper 80-35.

Clague, J.J., 1989a. Cordilleran ice sheet. In: Fulton, R.J. (ed.), Quaternary Geology of Canada and Greenland. Geological Survey of Canada, Geology of North America K-1: 40-42.

Clague, J.J., 1989b. Development of Cordilleran landscapes during the Quaternary. In: Fulton, R.J. (ed.), Quaternary Geology of Canada and Greenland. Geological Survey of Canada, Geology of North America K-1: 17-96.

Clague, J.J., 1989c. Quaternary geology of the Canadian Cordillera. In: Fulton, R.J. (ed.), Quaternary Geology of Canada and Greenland. Geological Survey of Canada, Geology of Canada 1: 17-83.

Clague, J.J., and Luternauer, J.L., 1982. Excursion 30A: Late Quaternary Sedimentary Environments, Southwestern British Columbia. International Association of Sedimentologists, 11th International Congress on Sedimentology, Hamilton, ON, Field Excursion Guidebook.

Clague, J.J., Armstrong, J.E., and Mathews, W.H., 1980. Advance of the late Wisconsin Cordilleran Ice Sheet in southern British Columbia since 22,000 yr B.P. Quaternary Research 13: 322-326.

Clague, J.J., Saunders, I.R., and Roberts, M.C., 1988. Ice-free conditions in southwestern British Columbia at 16,000 years BP. Canadian Journal of Earth Sciences 25: 938-941.

Clague, J.J., Mathewes, R.W., Guilbault, J.-P., Hutchinson, I., and Ricketts, B.D., 1997. Pre-Younger Dryas resurgence of the southwestern margin of the Cordilleran ice sheet, British Columbia, Canada. Boreas 26: 261-277.

Clark, P.U., and Bartlein, P.J., 1995. Correlation of late Pleistocene glaciation in the western United States with North Atlantic Heinrich events. Geology 23: 483-486.

Costa, J.E., and Schuster, R.L., 1988. The formation and failure of natural dams. Geological Society of America Bulletin 100: 1054-1068.

Crandell, D.R., 1963. Surficial Geology and Geomorphology of the Lake Tapps Quadrangle, Washington. U.S. Geological Survey Professional Paper 388-A.

Crandell, D.R., and Miller, R.D., 1974. Quaternary Stratigraphy and Extent of Glaciation in the Mount Rainier Region, Washington. U.S. Geological Survey Professional Paper 847.

Daubenmire, R., 1973. Taxonomic and ecologic relationships between *Picea glauca* and *Picea engelmannii*. Canadian Journal of Botany 52: 1545-1560.

Dethier, D.L., Pessl, F., Keuler, R.F., Balzarini, M.A., and Pevear, D.R., 1995. Late Wisconsinan glaciomarine deposition and isostatic rebound, northern Puget Lowland, Washington. Geological Society of America Bulletin 107: 1288-1303.

Drost, B.W., and Lombard, R.E., 1978. Water in the Skagit River Basin, Washington. Washington Department of Ecology Water Supply Bulletin 47.

Dunwiddie, P.W., 1985. Dichotomous key to conifer foliage in the Pacific Northwest. Northwest Science 59: 185-191.

Dunwiddie, P.W., 1987. Macrofossil and pollen representation of coniferous trees in modern sediments from Washington. Ecology 68: 1-11.

Dury, G.H., 1953. A glacial breach in the north western highlands. Scottish Geographic Magazine 69: 106-117.

Easterbrook, D.J., Rowland, D.L., Carson, R.J., and Naeser, N.D., 1988. Application of fission-track dating, and tephra correlation to lower Pleistocene sediments in Puget Lowland. In: Geological Society of America Special Paper 227: 139-165.

Eyles, N., and Clague, J.J., 1991. Glaciolacustrine sedimentation during advance and retreat of the Cordilleran Ice Sheet in central British Columbia. Géographie physique et Quaternaire 45: 317-331.

Eyles, N.E., Eyles, C.H., and Miall, A.D., 1983. Lithofacies types and vertical profile models: an alternative approach to the description and environmental interpretation of glacial diamict and diamictite sequences. Sedimentology 30: 393-410.

Fairbanks, R.G., Mortlock, R.A., Tzu-Chien, C., Li, C., Kaplan, A., Guilderson, T.P., Fairbanks, T.W., and Bloom, A.L., 2005. Marine radiocarbon calibration curve spanning 0-50,000 years B.P. based on paired $^{230}Th/^{234}U/^{238}U$ and ^{14}C dates on pristine corals. Quaternary Science Reviews 24: 1781-1796.

Farrar, J.L., 1995. Trees in Canada. Fitzhenry and Whiteside Ltd. and Canadian Forest Service, Ottawa, ON.

Flint, R.F., 1971. Glacial and Quaternary Geology. John Wiley and Sons, New York, NY.

Franklin, J.F., and Dyrness, C.T., 1973. Natural Vegetation of Oregon and Washington. U.S. Forest Service Technical Report PNW-8.

Fulton, R.J., 1965. Silt deposition in late-glacial lakes of southern British Columbia. American Journal of Science 263: 553-570.

Fulton, R.J., 1969. Glacial Lake History, Southern Interior Plateau, British Columbia. Geological Survey of Canada Paper 69-37.

Fulton, R.J., 1975. Quaternary Geology and Geomorphology, Nicola-Vernon Area, British Columbia (82L W ½ and 92I E ½). Geological Survey of Canada Memoir 380.

Fulton, R.J., and Smith, G.W., 1978. Late Pleistocene stratigraphy of south-central British Columbia. Canadian Journal of Earth Sciences 15: 971-980.

Furbish, D.J., and Andrews, J.T., 1984. The use of hypsometry to indicate long-term stability and response of valley glaciers to changes in mass transfer. Journal of Glaciology 31: 205-213.

Gascoyne, M., Ford, D.C., and Schwarcz, H.P., 1981. Late Pleistocene chronology and paleoclimate of Vancouver Island determined from cave deposits. Canadian Journal of Earth Sciences 18: 1643-1652.

Gilbert, R., 1975. Sedimentation in Lillooet Lake, British Columbia, Canada. Canadian Journal of Earth Sciences 12: 1697-1711.

Gilbert, R., and Desloges, J.R., 1992. The late Quaternary sedimentary record of Stave Lake, southwestern British Columbia. Canadian Journal of Earth Sciences 29: 1997-2006.

Gillespie, A., and Molnar, P., 1994. Asynchronous maximum advances of mountain and continental glaciers. Reviews of Geophysics 33: 311-364.

Goff, J., 1993. Late Pleistocene and Holocene Sedimentation in Silverhope Valley, British Columbia. Ph.D. thesis, University of Western Ontario, London, ON.

Grigg, L.D., and Whitlock, C., 2002. Patterns and causes of millennial-scale climate change in the Pacific Northwest during Marine Isotope Stages 2 and 3. Quaternary Science Reviews 21: 2067-2083.

Halliday, W.E.D., and Brown, A.W.A., 1943. The distribution of some important forest trees in Canada. Ecology 33: 31-41.

Harper, J.T., 1992. The Dynamic Response of Glacier Termini to Climatic Variation during the Period 1940-1990 on Mount Baker Washington. M.S. thesis, Western Washington University, Bellingham, WA.

Haugerud, R.A., 1985. Geology of the Hozameen Group and the Ross Lake Shear Zone, Maselpanik Area, North Cascades, Southwestern British Columbia. Ph.D. thesis, University of Washington, Seattle, WA.

Haugerud, R.A., Brown, E.H., Tabor, R.W., Kriens, B.J., and McGroder, M.F., 1994. Late Cretaceous and early Tertiary orogeny in the North Cascades. In: Swanson, D.A., and Haugerud, R.A. (eds.), Geologic Field Trips in the Pacific Northwest. University of Washington Department of Geological Sciences, Seattle, WA, 2: 2E1-2E51.

Haynes, V.M., 1977. The modification of valley patterns by ice sheet activity. Geografiska Annaler 59A: 195-207.

Heine, J.T., 1998. Extent, timing and climatic implications of glacier advances, Mount Rainier, Washington, U.S.A. at the Pleistocene Holocene transition. Quaternary Science Reviews 17: 1139-1148.

Heller, P.L., 1980. Multiple ice flow directions during the Fraser Glaciation in the lower Skagit River drainage, North Cascade Range, Washington. Arctic and Alpine Research 12: 299-308.

Heusser, C.J., 1974. Quaternary vegetation, climate, and glaciation of the Hoh River Valley, Washington. Geological Society of America Bulletin 85: 1547-1560.

Heusser, C.J., 1977. Quaternary palynology of the Pacific Slope of Washington. Quaternary Research 8: 282-306.

Heusser, C.J., 1978. Palynology of Quaternary deposits of the lower Bogachiel River area, Olympic Peninsula, Washington. Canadian Journal of Earth Sciences 15: 1568-1578.

Heusser, C.J., 1983. Vegetational history of the northwestern United States including Alaska. In: Porter, S.C. (ed.), Late-Quaternary Environments, Vol. 1, The Late Pleistocene. University of Minnesota Press, Minneapolis, MN, pp. 239-258.

Heusser, C.J., and Heusser, L.E., 1980. Sequence of pumiceous tephra layers and the late Quaternary environmental record near Mount St. Helens. Science 210: 1007-1009.

Heusser, C.J., and Igarashi, Y., 1994. Quaternary migration pattern of *Selaginella selaginoides* in the North Pacific. Arctic and Alpine Research 26: 187-192.

Heusser, C.J., and Peteet, D.M., 1988. Spores of *Lycopodium* and *Selaginella* of North Pacific America. Canadian Journal of Botany 66: 508-525.

Hicock, S.R., and Armstrong, J.E., 1981. Coquitlam Drift: A pre-Vashon Fraser glacial formation in the Fraser Lowland, British Columbia. Canadian Journal of Earth Sciences 18: 1443-1451.

Hicock, S.R., and Lian, O.B., 1995. The Sisters Creek Formation: Pleistocene sediments representing a nonglacial interval in southwestern British Columbia at about 18 ka. Canadian Journal of Earth Sciences 32: 758-767.

Hicock, S.R., Hebda, R.J., and Armstrong, J.E., 1982. Lag of the Fraser glacial maximum in the Pacific Northwest: Pollen and macrofossil evidence from western Fraser Lowland, B.C. Canadian Journal of Earth Sciences 19: 2288-2296.

Hicock, S.R., Lian, O.B., and Mathewes, R.W., 1999. 'Bond cycles' recorded in terrestrial Pleistocene sediments of southwestern British Columbia, Canada. Journal of Quaternary Science 14: 443-449.

Hildreth, W., Fierstein, J., and Lanphere, M., 2003. Eruptive history and geochronology of the Mount Baker volcanic field, Washington. Geological Society of America Bulletin 115: 729-764.

Hitchcock, C.L., and Cronquist, A., 1973. Flora of the Pacific Northwest. University of Washington Press, Seattle, WA.

Hodge, S.M., 1974. Variations in sliding of a temperate glacier. Journal of Glaciology 13: 349-369.

Hodge, S.M., Trabant, D.C., Krimmel, R.M., Heinrichs, T.A., March, R.S., and Josberger, E.G., 1997. Climate variations and changes in mass of three glaciers in western North America. Journal of Climate 11: 2161-2179.

Holmes, A., 1965. Principles of Physical Geology. Thomas Nelson Ltd., London.

Hurley, T.M., 1996. Late-glacial Equilibrium-line Altitudes of Glaciers in the Southern North Cascade Range, Washington. M.Sc. thesis, University of Washington, Seattle, WA.

Isarin, R.F.B., and Bohncke, S.J.P., 1999. Mean July temperatures during the Younger Dryas in Northwestern and Central Europe as inferred from climate indicator plant species. Quaternary Research 51: 158-173.

Johnson, S.Y., 1984. Stratigraphy, age and paleogeography of the Eocene Chuckanut Formation, northwest Washington. Canadian Journal of Earth Sciences 21: 92-106.

Kansky, J., 1963. Structure of Transportation Networks: Relationships Between Network Geometry and Regional Characteristics. University of Chicago, Department of Geography Research Paper 84.

Kaufman, D.S., Porter, S.C., and Gillespie, A.R., 2004. Quaternary alpine glaciation in Alaska, the Pacific Northwest, Sierra Nevada and Hawaii. In: Gillespie, A.R., Porter, S.C., and Atwater, B.F. (eds.), The Quaternary Period in the United States. Elsevier Developments in Quaternary Science 1: 77-103.

Kerr, F.A., 1936. Quaternary glaciation in the Coast Range, northern British Columbia and Alaska. Journal of Geology 44: 681-700.

Kovanen, D.J., and Easterbrook, D.J., 2001. Late Pleistocene, post-Vashon, alpine glaciation of the Nooksack drainage, North Cascades, Washington. Geological Society of America Bulletin 113: 247-288.

Kovanen, D.J., and Slaymaker, O., 2005. Fluctuations of the Deming Glacier and theoretical equilibrium line altitudes during the Late Pleistocene and early Holocene on Mount Baker, Washington, USA. Boreas 34: 157-175.

Krajina, V.J., 1970. Ecology of Forest Trees in British Columbia. University of British Columbia, Department of Botany, Ecology of Western North America 2.

Krajina, V.J., Klinka, K., and Worrall, J., 1982. Distribution and Ecological Characteristics of Trees and Shrubs in British Columbia. University of British Columbia, Faculty of Forestry, Vancouver, BC.

LaBonte, J., 1998. Terrestrial Riparian Arthropod Investigations in the Big Beaver Creek Research Natural Area, North Cascades National Park Service Complex, 1995-1996: Part II, Coleoptera. U.S. Department of Interior, National Park Service, Technical Report NPS/NRNOCA/NRTR/98-02.

Lian, O.B., Mathewes, R.W., and Hicock, S.R., 2001. Paleo-environmental reconstruction of the Port Moody interstade, a nonglacial interval in southwestern British Columbia at about 18,000 ^{14}C yr B.P. Canadian Journal of Earth Sciences 38: 943-952.

Licciardi, J.M., Clark, P.U., Brook, E.J., Pierce, K.L., Kurz, M.D., Elmore, D., and Sharma, P., 2001. Cosmogenic ^{3}He and ^{10}Be chronologies of the late Pinedale Northern Yellowstone ice cap, Montana. Geology 29: 1095-1098.

Linton, D.L., 1967. Divide elimination by glacial erosion. In: Wright, Jr., H.E., and Osburn, W.H. (eds.), Arctic and Alpine Environments (Proceedings 7th INQUA Congress). Indiana University Press, Indianapolis, IN, pp. 241-248.

Locke, W.W., 1990. Late Pleistocene glaciers and the climate of western Montana, U.S.A. Arctic and Alpine Research 22: 1-13.

Mackin, J.H., 1941. Glacial geology of the Snoqualmie-Cedar area, Washington. Journal of Geology 49: 449-481.

Mann, D.H., and Hamilton, T.D., 1995. Late Pleistocene and Holocene paleoenvironments of the North Pacific coast. Quaternary Science Reviews 14: 449-471.

Mathewes, R.W., 1993. Evidence for Younger Dryas-age cooling on the North Pacific Coast of America. Quaternary Science Reviews 12: 321-331.

Mathews, W.H., 1944. Glacial lakes and ice retreat in south-central British Columbia. Royal Society of Canada Transactions, Series 3, 38: 39-57.

Mathews, W.H., 1964. Potassium-argon age determinations of Cenozoic volcanic rocks from British Columbia. Geological Society of America Bulletin 75: 465-468.

Mathews, W.H., 1968. Geomorphology of Lightning Creek valley, Manning Park, southwest B.C. Syesis 1: 65-78.

Mathews, W.H., 1991. Development of Cordilleran landscapes during the Quaternary. In: Fulton, R.J. (ed.), Quaternary Geology of Canada and Greenland. Geological Survey of Canada, Geology of North America K-1: 32-44.

McKee, 1972. Cascadia: The Geologic Evolution of the Pacific Northwest. McGraw Hill, New York, NY.

Meier, M.F., and Post, A.F., 1962. Recent variations in mass net budgets of glaciers in western North America. International Association of Scientific Hydrology Publication 58: 63-77.

Meyer, G.A., Fawcett, P.J., and Locke, W.W., 2003. Late Pleistocene equilibrium line altitudes, atmospheric circulation, and timing of mountain glacier advances in the interior northwestern United States. 16th INQUA Congress, Program with Abstracts, p. 73.

Mickelson, D.M., and Colgan, P.M., 2004. The southern limit of the Laurentide Ice Sheet. In: Gillespie, A.R., Porter, S.C., and Atwater, B.F. (eds.), The Quaternary Period in the United States. Elsevier Developments in Quaternary Science 1: 1-16.

Miller, R.F., Morgan, A.V., and Hicock, S.R., 1985. Pre-Vashon fossil Coleoptera of Fraser age from the Fraser Lowland, British Columbia. Canadian Journal of Earth Sciences 22: 498-505.

Minore, D., 1979. Comparative Autecological Characteristics of Northwestern Tree Species – A Literature Review. U.S. Forest Service, Pacific Northwest Forest and Range Experiment Station, General Technical Report PNW-87.

Mullineaux, D.R., 1986. Summary of pre-1980 tephra-fall deposits from Mount St. Helens, Washington State, USA. Bulletin of Volcanology 48: 17-26.

Nelson, R.E., and Coope, G.R., 1982. A late Pleistocene insect fauna from Seattle, Washington. American Quaternary Association Abstracts with Program, p. 146.

Ohmura, A., Kasser, P., and Funk, M., 1992. Climate at the equilibrium line of glaciers. Journal of Glaciology 38: 397-411.

Osmaston, H., 2005. Estimates of glacier equilibrium line altitudes by the Area x Altitude, the Area x Altitude Balance Ratio and the Area x Altitude Balance Index methods and their validation. Quaternary International 138-139: 22-31.

Osmaston, H., 2006. Should Quaternary sea-level changes be used to correct glacier ELAs, vegetation belt altitudes and sea level temperatures for inferring climate changes? Quaternary Research 65: 244-251.

Ovenshire, A.T., 1970. Observations on iceberg rafting in Glacier Bay, Alaska, and identification of ice-rafted deposits. Geological Society of America Bulletin 81: 891-894.

Paterson, W.S.B., 1981. The Physics of Glaciers. Pergamon Press, Oxford.

Pelto, M.S., and Riedel, J.L., 2001. Spatial and temporal variations in annual balance of North Cascades glaciers, Washington. Hydrological Processes 15: 3461-3472.

Penck, A., 1905. Glacial features in the surface of the Alps. Journal of Geology 13: 1-19.

Peterson, E.B., Peterson, N.M., Weetman, G.F., and Martin, P.J., 1997. Ecology and Management of Sitka Spruce, Emphasizing Its Natural Range in British Columbia. University of British Columbia Press, Vancouver, BC.

Pierce, K.L., 1979. History and Dynamics of Glaciation in the Northern Yellowstone National Park Area. U.S. Geological Survey Professional Paper 729-F.

Pierce, K.L., Obradovich, J.D., and Friedman, I., 1976. Obsidian hydration dating and correlation of Bull Lake and Pinedale glaciations near West Yellowstone, Montana. Geological Society of America Bulletin 37: 703-710.

Pisias, N.G., Mix, A.C., and Heusser, L., 2001. Millennial scale climate variability of the northeast Pacific Ocean and northwest North America based on radiolarian and pollen. Quaternary Science Reviews 20: 1561-1576.

Porter, S.C., 1975. Equilibrium line altitudes of late Quaternary glaciers in the Southern Alps, New Zealand. Quaternary Research 5: 27-47.

Porter, S.C., 1976. Pleistocene glaciation in the southern part of the North Cascade Range, Washington. Geological Society of America Bulletin 87: 61-75.

Porter, S.C., 1977. Present and past glaciation threshold in the Cascade Range, Washington, U.S.A.: Topographic and climatic controls, and paleoclimatic implications. Journal of Glaciology 18: 101-116.

Porter, S.C., 1986. Pattern and forcing of northern hemisphere glacier variations during the last millennium. Quaternary Research 26: 27-48.

Porter, S.C., 2001. Snowline depression in the tropics during the last glaciation. Quaternary Science Reviews 20: 1067-1091.

Porter, S.C., and Swanson, T., 1998. Radiocarbon age constraints on rates of advance and retreat of the Puget lobe of the Cordilleran Ice Sheet during the last glaciation. Quaternary Research 50: 205-213.

Porter, S.C., Pierce, K.L., and Hamilton, T.D., 1983. Late Wisconsin mountain glaciation in the Western United States. In: Porter, S.C. (ed.), Late-Quaternary Environments, Vol. 1, The Late Pleistocene. University of Minnesota Press, Minneapolis, MN, pp. 71-111.

Post, A., Richardson, D., Tangborn, W., and Rosselot, F.L., 1971. Inventory of Glaciers in the North Cascades, Washington. U.S. Geological Survey Professional Paper 705-A.

Pringle, P.T., 1993. Roadside Geology of Mount St. Helens National Volcanic Monument and Vicinity. Washington Department of Natural Resources, Olympia, WA.

Reasoner, M.A., Osborn, G., and Rutter, N.W., 1994. Age of the Crowfoot advance in the Canadian Rocky Mountains: A glacial event coeval with the Younger Dryas oscillation. Geology 22: 439-442.

Reiners, P.W., Ehlers, T.A., Garner, J.I., Mitchell, S.G., Montgomery, D.R., Vance, J.A., and Nicolescu, S., 2002. Late Miocene erosion and uplift of Washington Cascade Range. Geological Society of America Bulletin 31: 767-770.

Reiners, P.W., Ehlers, T.A., Mitchell, S.G., and Montgomery, D.R., 2003. (U-Th)/He thermochronology and orogeny of the Washington Cascades. Geological Society of America, Abstracts with Program 126-9: 307.

Riedel, J.L., 1987. Chronology of Late Neoglacial Glacier Recession in the Cascade Range and the Deposition of a Recent Esker in the North Cascade Mountains, Washington. M.S. thesis, University of Wisconsin, Madison, WI.

Riedel, J.L., and Burrows, R., 2003. Glacier mass balance monitoring at North Cascades and Mount Rainier National Parks, Washington. Geological Society of America, Abstracts with Programs 34: 132.

Riedel, J.L., and Haugerud, R.H., 1994. Glacial rearrangement of drainage in the northern North Cascade Range, Washington. Geological Society of America Abstracts with Program 26: 7.

Riedel, J.L., Haugerud, R.A., and Clague, J.J., 2007. Geomorphology of a Cordilleran Ice Sheet drainage network through breached divides in the North Cascades Mountains of Washington and British Columbia. Geomorphology, in press.

Ruddiman, W.F., and Wright, Jr., H.E., 1987. Introduction. In: Ruddiman, W.F., and Wright, Jr., H.E. (eds.), North America and Adjacent Oceans during the Last Deglaciation. Geological Society of America, Geology of North America K3: 1-12.

Ryder, J.M., 1989. Glacial history of the southern Okanagan Range, British Columbia. Canadian Quaternary Association Program with Abstracts 34: A116.

Saunders, I.R., Clague, J.J., and Roberts, M.C., 1987. Deglaciation of Chilliwack River valley, British Columbia. Canadian Journal of Earth Sciences 24: 915-923.

Scoggan, H.J., 1978. The Flora of Canada, Part 3. Canada National Museum of Natural Sciences Publication in Botany 7.

Scott, K.M., Tucker, D., and McGeehin, J., 2003. Island of fire in a sea of ice – The growth of Mount Baker volcano and the Fraser Glaciation in the North Cascades. 16th INQUA Congress, Reno, NV, Programs with Abstracts: 51-9.

Seuss, E., 1888. The Face of the Earth 2. Clarendon Press, Oxford, pp. 326-345 [translated by Sollas, H.B.C., 1906].

Stansell, N.D., Polissar, P.J., and Abbott, M.B., 2007. Last glacial maximum equilibrium line altitude and paleo-temperature reconstructions for Cordillera de Mérida, Venezuelan Andes. Quaternary Research, in press.

Stuiver, M., and Reimer, P.J., 1993. Extended ^{14}C data base and revised CALIB 3.0 ^{14}C age calibration program. Radiocarbon 35: 215-230.

Stuiver, M., Grootes, P.M., and Braziunas, T.F., 1995. The GISP2 $\delta^{18}O$ climate record of the past 16,500 years and the role of the sun, ocean, and volcanoes. Quaternary Research 44: 341-354.

Sturchio, N.C., Pierce, K.L., Morrell, M.T., and Sorey, M.L., 1994. Uranium-series ages of travertines and timing of the last glaciation in the northern Yellowstone area, Wyoming-Montana. Quaternary Research 41: 265-277.

Sudworth, G.B., 1967. Forest Trees of the Pacific Slope. Dover Publications, Toronto, ON.

Sugden, D.E., and John, B.S., 1976. Glaciers and Landscape. E. Arnold Press, London.

Swanson, T.W., and Porter, S.C., 1997. Cosmogenic isotope ages of moraines in the southeastern North Cascade Range. Pacific Northwest Friends of the Pleistocene Field Excursion Guidebook, 18 p.

Tabor, R.W., and Haugerud, R.A., 1999. Geology of the North Cascades: A Mountain Mosaic. The Mountaineers, Seattle, WA.

Tabor, R.W., Haugerud, R.A., Miller, R.B., Brown, E.H., and Babcock, R.S., 1989. Accreted terranes of the North Cascades, Washington. 28th International Geological Congress, Washington, D.C., Field Trip Guidebook T307.

Tabor, R.W., Haugerud, R.A., Hildreth, W., and Brown, E.H., 2003. Geologic Map of the Mount Baker 30-by-60-Minute Quadrangle, Washington. U.S. Geological Survey Geologic Investigations Series I-2660.

Tangborn, W.F., 1980. Two models for estimating the climate-glacier relationships in the North Cascades, Washington. Journal of Glaciology 25: 3-21.

Telka, A., Ward, B.C., and Mathewes, R.W., 2003. Plant and insect macrofossil evidence of Port Moody interstade in eastern Fraser Lowland, Chehalis watershed, southwestern British Columbia. CANQUA-CGRG Conference Program and Abstracts 139.

Thackray, G.D., 1999. Pacific moisture delivery and the variability of mountain glacier chronologies in western North America. Geological Society of America Abstracts with Programs 31(4): A58.

Thackray, G.D., 2001. Extensive early and middle Wisconsin glaciation on the western Olympic Peninsula, Washington, and the variability of Pacific moisture delivery to the northwestern United States. Quaternary Research 55: 257-70.

Thompson, R.S., Anderson, K.H., and Bartlein, P.J., 1999. Atlas of Relations between Climatic Parameters and Distributions of Important Trees and Shrubs in North America – Introduction and Conifers. U.S. Geological Survey Professional Paper 1650-A.

Thompson, R.S., Shafer, S.L., Strickland, L.E., Van de Water, P.K., and Anderson, K.H., 2004. Quaternary vegetation and climate change in the western United States: Developments, perspectives, and prospects. In: Gillespie, A.R., Porter, S.C., and Atwater, B.F. (eds.), The Quaternary Period in the United States. Elsevier, Amsterdam, pp. 403-427.

Thorarinsson, S., 1939. The ice dammed lakes of Iceland with a particular reference to their values as indicators of glacial oscillations. Geografiska Annaler 21: 216-242.

Thorson, R.M., 1980. Ice-Sheet glaciation of the Puget Lowland, Washington, during the Vashon stade. Quaternary Research 13: 303-321.

Tipper, H.W., 1971. Glacial Geomorphology and Pleistocene History of Central British Columbia. Geological Survey of Canada Bulletin 196.

Tribe, S., 2002. Geomorphic evidence for Tertiary drainage networks in southern Coast Mountains, British Columbia. Geological Survey of Canada Current Research 2002-A13: 1-8.

Tucker, D.S., 2004. Geology and Eruptive History of the Hannegan Caldera, North Cascades, Washington. M.S. thesis, Western Washington University, Bellingham, WA.

Tyron, A.F., 1949. Spores of the genus *Selaginella* in North America north of Mexico. Annals of the Missouri Botanical Garden 36: 413-431.

Waitt, Jr., R.B., 1971. Geomorphology and Glacial Geology of the Methow Drainage Basin, Eastern North Cascade Range, Washington. Ph.D. thesis, University of Washington, Seattle, WA.

Waitt, Jr., R.B., 1975. Late Pleistocene alpine glaciers and the Cordilleran Ice Sheet at Washington Pass, North Cascade Range, Washington. Arctic and Alpine Research 7: 25-32.

Waitt, Jr., R.B., 1977. Evolution of glaciated topography of upper Skagit drainage basin, Washington. Arctic and Alpine Research 9: 183-192.

Waitt, Jr., R.B., 1979. Rockslide-avalanche across a distributary lobe of the Cordilleran Ice Sheet in the Pasayten Valley, Northern Washington. Arctic and Alpine Research 11: 33-40.

Waitt, Jr., R.B., and Thorson, R.M., 1983. The Cordilleran Ice Sheet in Washington, Idaho, and Montana. In: Porter, S.C. (ed.), Late-Quaternary Environments of the United States, Vol. 1, The Late Pleistocene. University of Minnesota Press, Minneapolis, MN, pp. 54-70.

Waitt, Jr., R.B., Yount, J.C., and Davis, P.T., 1982. Regional significance of an early Holocene moraine in Enchantment Lakes basin, North Cascade Range, Washington. Quaternary Research 17: 191-210.

Ward, B.C., and Thomson, B., 2004. Late Pleistocene stratigraphy and chronology of lower Chehalis River Valley, southwestern BC: Evidence for a restricted Coquitlam Stade. Canadian Journal of Earth Sciences 41: 881-895.

Wardle, P., 1974. Alpine treelines. In: Ives, J.D., and Barry, R.G. (eds.), Arctic and Alpine Environments. Mehuen & Co., London, pp. 371-402.

Waters, A., 1939. Resurrected erosion surface in central Washington. Geological Society of America Bulletin 50: 638-659.

Whitlock, C., 1992. Vegetational climatic history of the Pacific Northwest during the last 20,000 years: Implications for understanding present-day diversity. The Northwest Environmental Journal 8: 5-28.

Willis, B., 1888. Changes in River Courses in Washington Territory Due to Glaciation. U.S. Geological Survey Bulletin 40: 474-87.

Zernitz, E.R., 1932. Drainage patterns and their significance. Journal of Geology 40: 498-521.